University of Southampton

Investigations of the last step in biotin biosynthesis, the conversion of dethiobiotin to biotin

by
Tillmann Ziegert

A thesis presented for the degree of
Doctor of Philopsophy

Department of Chemistry
University of Southampton
UK

May 2003

Memorandum

This thesis is an account of original research performed by the author in the Department of Chemistry, University of Southampton, between November 1999 and November 2002. Where findings of other works have been used, due reference has been given.

UNIVERSITY OF SOUTHAMPTON

ABSTRACT

FACULTY OF SCIENCE

DEPARTMENT OF CHEMISTRY

Doctor of Philosophy

Investigations of the last step in biotin biosynthesis, the conversion of dethiobiotin to biotin

by Tillmann Ziegert

Biotin synthase (BioB) is an iron-sulphur cluster containing protein that participates in the last step in the biosynthesis of biotin, the conversion of dethiobiotin (DTB) to biotin. Thus far, catalytic activity in vitro has not been reported for biotin synthase. To investigate the mechanism of biotin formation in more detail and to identify potential bottlenecks, several strategies for purifying BioB were investigated, to yield highly purified BioB. A radiochemical and a HPLC based method were developed to assay in vitro biotin formation. The products of the isc gene cluster involved in iron-sulphur cluster assembly, IscS, IscU, IscA, Hsc20, Hsc66 and Fdx, were expressed and purified to homogeneity. No beneficial effects on in vitro biotin formation were found, although it was shown that the optimal concentration of exogenous iron and sulphide is essential for biotin synthase activity. Furthermore, potential inhibitors of BioB activity were assessed. Sinefungin, S-adenosylhomocysteine and biotin were each found to have a weak inhibitory effect on biotin formation, but complete inhibition was only observed when 5'-deoxyadenosine (DOA) and methionine, the products of the reductive cleavage of S-adenosylmethionine, were both added to the standard assay. The concentration of these products in the in vitro assay is close to the IC_{50}, thus presenting a potential bottleneck. The complete inhibition of BioB activity was reversed by the addition of the enzyme PFS, which was found to cleave DOA into 5'-deoxyribose and adenine. However, even after the addition of PFS, no catalytic activity was observed. The identification of this protein co-factor is a major step forward in obtaining a catalytic system for biotin formation. Consequently, various plasmids were constructed encoding genes, deemed essential or helpful for biotin formation in vitro or in vivo.

LIST OF CONTENTS

Chapter Four: Investigation of *in vitro* biotin formation

Chapter Five: Purification and investigation of *isc* gene cluster products

Chapter Six: Inhibition of biotin synthase activity *in vitro*

Chapter Seven: Construction of plasmids encoding essential protein co-factors

Chapter Eight: Experimental Methods

Acknowledgements

I would like to gratefully acknowledge the help, support and advice I received from my supervisor Dr. Peter Roach during my PhD work at the University of Southampton.

Working on a multifaceted project was not easy, but Peter's ideas, know-how and encouragement made the work on the BioB project worthwhile. Pondering scientific questions at the cross-section of biochemistry and chemistry as well as having comments and discussion about contemporary European culture was always instructive and enjoyable.

I would like to particularly thank Peter for his extensive proofreading of this thesis and advice on how to improve the scientific English and the contents of the thesis.

Many thanks to my sweet wife, Qun Yang, for her continuous support and encouragement.

Abbreviations

(v/v)	volume for volume ratio
(w/v)	weight for volume ration
aRR	anaerobic ribonucleotide reductase
Abs	Absorption
ADP	adenosine diphosphate
ATP	adenosine triphosphate
BioB	biotin synthase
bp	base pair
BSA	bovine serum albumin
^{14}C-biotin	biotin radiolabelled with ^{14}C-carbon
CoA	Co-enzyme A
2D	two-dimensional
Da	Dalton
p-DACA	p-dimethylaminocinnamaldehyde
DAPA	7,8-diaminopelargonic acid
DMSO	dimethyl sulfoxide
DNA	deoxyribonucleic acid
DOA	5'-deoxyadenosine
DTB	dethiobiotin
^{14}C-DTB	DTB radiolabelled with ^{14}C-carbon
DTBS	dethiobiotin synthethase
DTT	dithiothreitol
E. coli	*Escherichia coli*
EDTA	ethylendiamintetraacetic acid
ESI-MS	electrospray ionisation mass spectrometry
FAD	flavin adenine dinucleotide
Fdr	flavodoxin reductase
Fdx	ferredoxin
Fe-S cluster	iron-sulphur cluster
FF	Fast Flow
FldA	flavodoxin
FMN	flavin mononucleotide

FPLC	fast protein liquid chromatography
g	gram
HIC	hydrophobic interaction
His_6	polyhistidine tag (6 histidine)
HPLC	high performance liquid chromatography
IC_{50}	concentration of inhibitor at which biotin formation is halved
IMPACT	intein mediated purification with affinity chitin-binding tag
IPTG	isopropyl-β-D-thiogalactoside
isc	iron sulphur cluster
KAPA	7-keto-8-aminopelargonic acid
kDa	kilo daltons
K_m	Michaelis constant
LipA	lipoic acid synthase
Load	material applied to a chromatographic column
MetK	SAM synthetase
mg	milligram
min.	minutes
M_r	molecular weight
MW	molecular weight
MWCO	molecular weight cut off
NADPH	β-nicotinamide adenine dinucleotide phosphate
NMR	nuclear magentic resonance spectroscopy
OD_{600}	optical density at 600 nm
p.	page
P_i	inorganic phosphate
PAGE	polyacrylamide gel electrophoresis
PCR	Polymerase Chain Reaction
PEI	polyethyleneimine
PFS	5'-methythioadenosine/S-adenosylhomocysteine nucleosidase
pKH	plasmid constructed by Dr. K. Hewitson
PLP	pyridoxal 5´-phosphate
pND	plasmid constructed by Nicola Davis
PFL	pyruvate-formate lyase
pTZ	plasmid constructed by the author

RBS	ribosome binding site
rpm	revolutions per minute
RT	room temperature
s	substrate concentration
SAM	S-adenoslylmethionine
SAH	S-adenosylhomocysteine
SDS	sodium dodecyl sulphate
SDS-PAGE	socium dodecyl sulphate-polyacrylamide gel electrophoresis
TEMED	N,N,N',N'-tetramethylethylendiamine
TLC	thin layer chromatography
TPP	thiamine pyrophosphate
Tris	tris(hydroxymethylethyl)aminomethane
v	velocity
UV	ultraviolet

Terms used:

σ represents the standard deviation for the values of a whole series.

[HPLC\Results\ ...] refers to the name of the HPLC file in which the data for this experiment are stored. The folder "HPLC" is on a hard disk, which is supporting material for this thesis.

Chapter One: Introduction

1.1 The Discovery of Biotin

Biotin **1** was discovered as an essential nutrient at the beginning of the 20th century. It was first isolated as a constituent of "bios", an unknown mixture of three compounds required for optimal growth of yeast, which was present in egg yolk. Bios I was identified as myo-inositol, Bios IIA as pantothenic acid. Bios IIB was isolated in crystalline form as its methylester and named biotin (1,2). Rats fed on a diet of raw egg white as the sole source of their amino acids, developed severe dermatitis, followed by hair loss a few weeks later (3). These symptoms were eradicated by treatment with an unknown heat stable factor, from yeast or liver, which was named vitamin H (from the German, skin = die Haut) (4,5). Vitamin H and Biotin were later found to be the same molecule (6). The correct chemical structure was elucidated several years later (7-9) and subsequently the chemical synthesis was achieved by Folkers and co-workers (10,11).

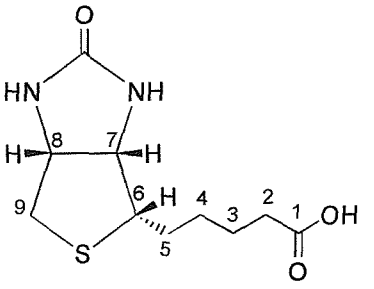

1

Figure 1.1 The structure of biotin (numbering scheme)

1.2 Biochemical functions of biotin

Deficiency of biotin is rare, but biotin is an essential co-factor for carboxylase-catalysed reactions that are involved in vital metabolic pathways such as gluconeogenesis, fatty acid synthesis and amino acid catabolism (12). Biotin is covalently attached to the ε-amino side chain of an active site lysine residue by the enzyme biotin protein ligase, also known as BirA (13). Biotin is first activated by the formation of its acyl-adenylate, bound to BirA, and then attached to ε-Lysine (Scheme 1.1) (14).

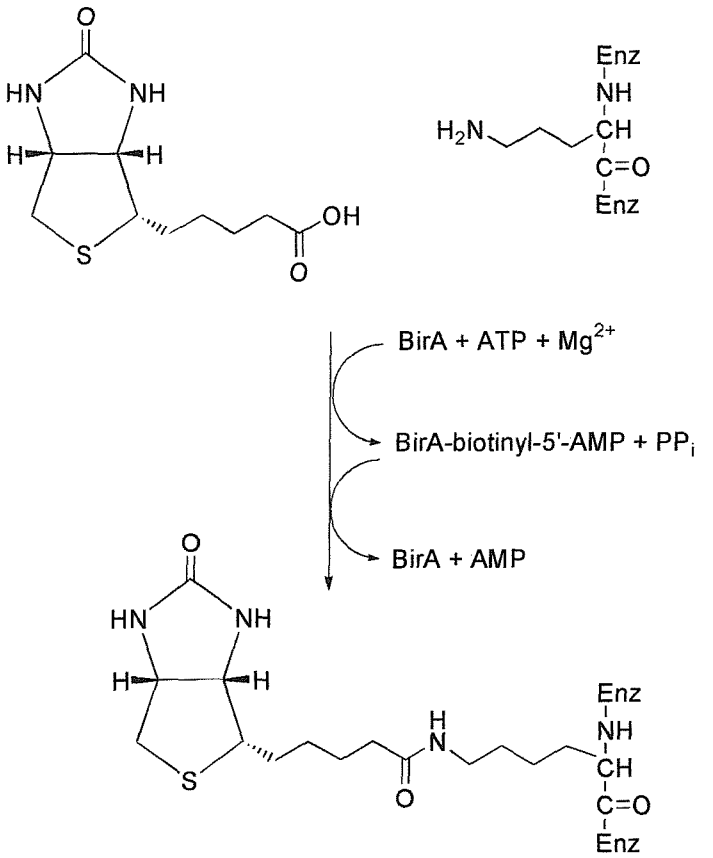

Scheme 1.1 BirA mechanism

Two biotin-dependent enzymes are depicted in Figure 1.2. These enzymes use acetyl CoA **2** or pyruvate **3** and bicarbonate as substrates, but also requires adenosine triphosphate (ATP), which is converted to adenosine monophosphate (AMP) and pyrophophate (PP), and biotin as a co-factor.

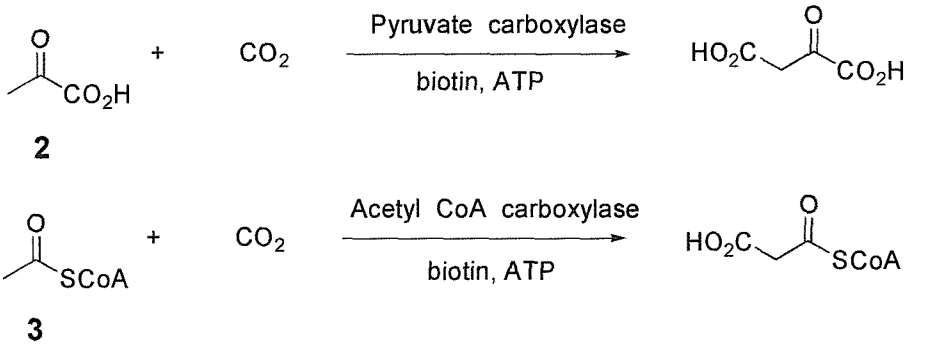

2

3

Figure 1.2 Biotin-dependent enzymes

ATP is used to activate bicarbonate by formation of an acyl phosphate intermediate, known as carbamoyl phosphate **4**. Labelling studies suggested N-carboxy-biotin **5** as intermediate in the reaction (15) (Scheme 1.2).

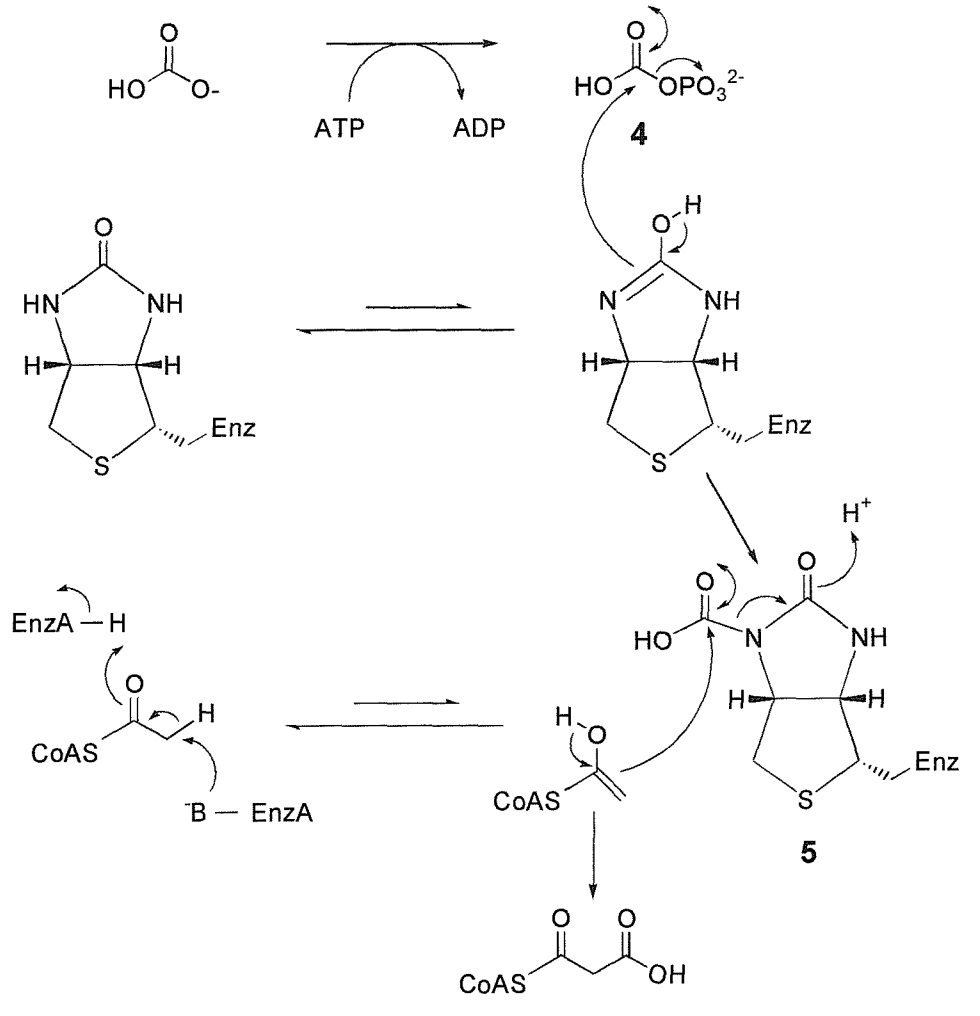

Scheme 1.2: Mechanism for biotin-dependent carboxylation [adapted from (15)].

Biotin as a co-factor is also involved in decarboxylase and transcarboxylase reactions. The underlying mechanism with N-carboxy-biotin **5** as intermediate in the reaction is similiar.

1.3 The biotin biosynthetic pathway

The biosynthetic pathways of biotin have been studied in detail in *Escherichia coli* (16,17), *Bacillus sphaericus* (18), *Bacillus subtilis* (19), *Saccharomyces cerevisia* (20) and higher plants (21). In *E. coli* the genes that encode the biosynthetic enzymes are located in two divergently transcribed operons, controlled by a single operator that interacts with the BirA repressor (22,23). Complexed with its co-repressor, biotinyl-5'-AMP, BirA functions as a repressor by binding to an operator site that overlaps the promotors for divergent *bio*A and *bio*BCDF operons (22) (Figure 1.3). BirA catalyses adenylation of biotin, thereby synthesising its own co-repressor. BirA also catalyses the transfer of the biotin portion of biotinyl-5'-AMP to the ε-amino group of a specific lysine residue of an enzyme (Section 1.2).

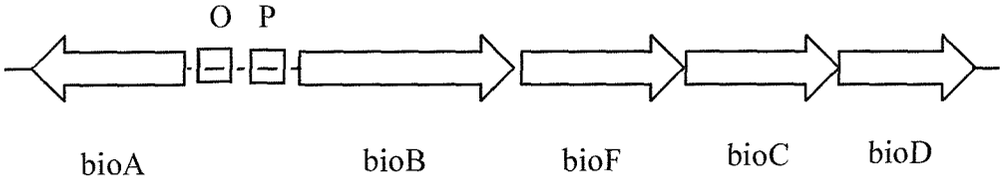

Figure 1.3: The biotin biosynthetic operon of *E. coli.* (O = operator, P = promotor)

In *Bacillus sphaericus*, the genes are located in two separate, unlinked operons (18). The early steps of the pathway, those involved in the synthesis of pimeloyl-CoA are less well understood. *Bacillus sphaericus* contains an enzyme, pimeloyl synthetase (*bio*W) that converts pimelic acid to pimeloyl-CoA (18,24). *E. coli* lacks this enzyme and cannot use pimelic acid as an intermediate in biotin synthesis (18,25,26). Preliminary results with BioH suggest a role as CoA donor to a pimelyl-ACP, releasing pimeloyl-CoA (144). Studies of BioC have been hindered by solubility problems. Scheme 1.3 depicts the biotin biosynthetic pathway.

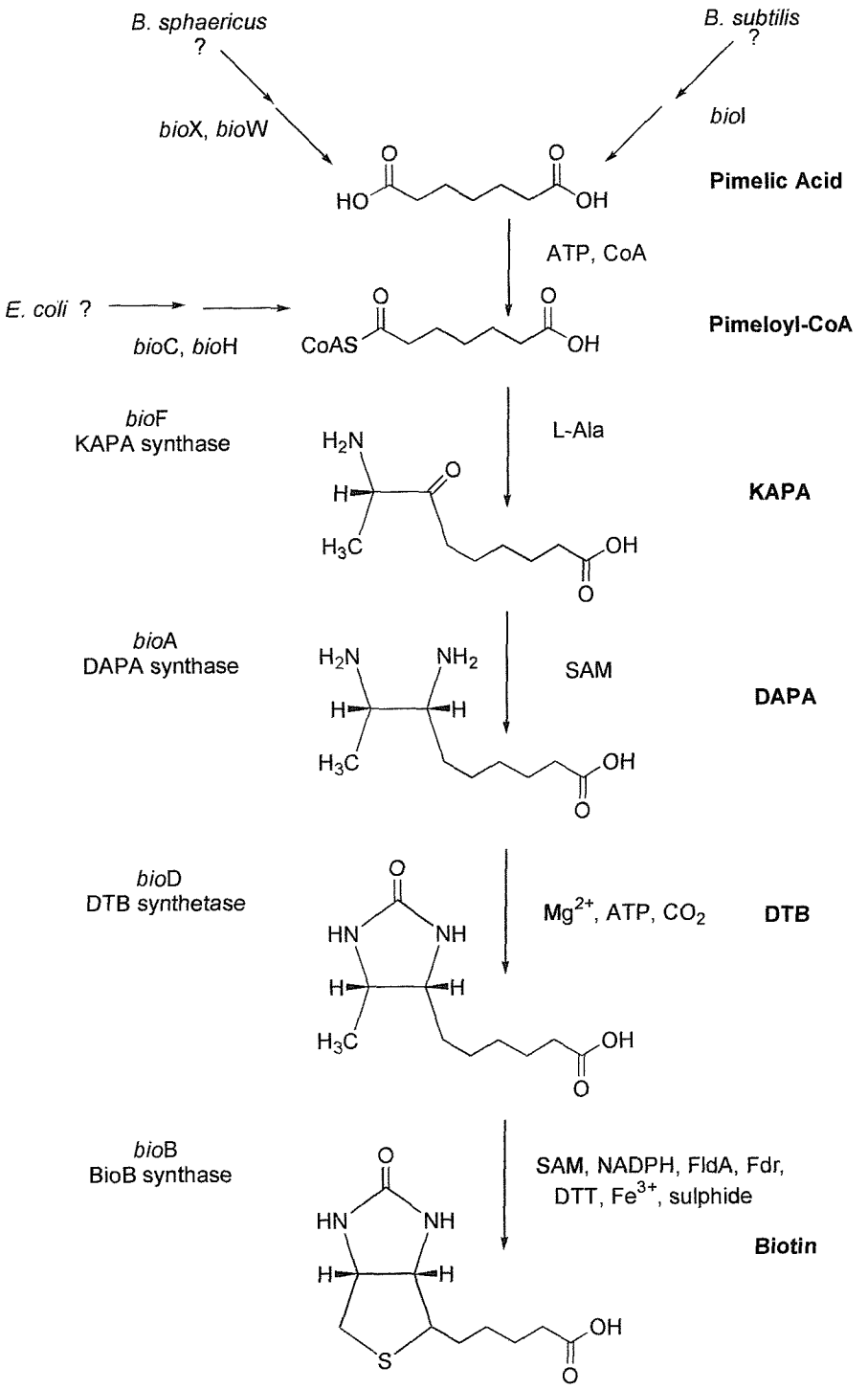

Scheme 1.3: Biotin biosynthetic pathway

(KAPA, 7-keto-8-aminopelargonic acid; PLP, pyridoxal 5′-phosphate; DAPA, 7,8-diaminopelargonic acid)

7-Keto-8-amino pelargonic acid synthase (KAPA synthase)

KAPA synthase is a homodimeric, pyridoxal phosphate (PLP)-dependent enzyme that catalyses the first committed step of the pathway (Figure 1.4). The monomeric enzyme subunit has a molecular mass of about 42 kDa. The crystal structure of KAPA synthase from *E. coli* was determined in the apo- and holoform (27) and potent inhibitors have been synthesised (28). Essential steps of this mechanism (29,30) are the formation of an external aldimine **6** between PLP and the substrate, L-alanine (Scheme 1.4). Deprotonation of the aldimine leads to a quinonoid intermediate, which then attacks the thioester carbonyl of pimeloyl-CoA **7**. Release of HSCoA produces a β-ketoacid aldimine **8**, which after decarboxylation is converted into the product **9** (Scheme 1.5).

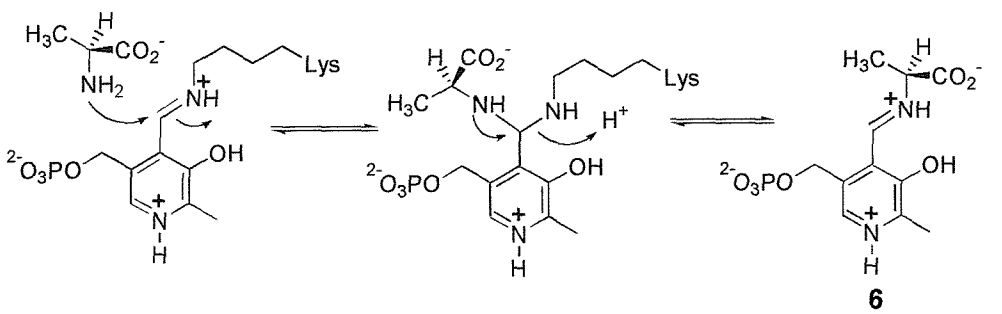

Scheme 1.4: Formation of an external aldimine between PLP and L-alanine.

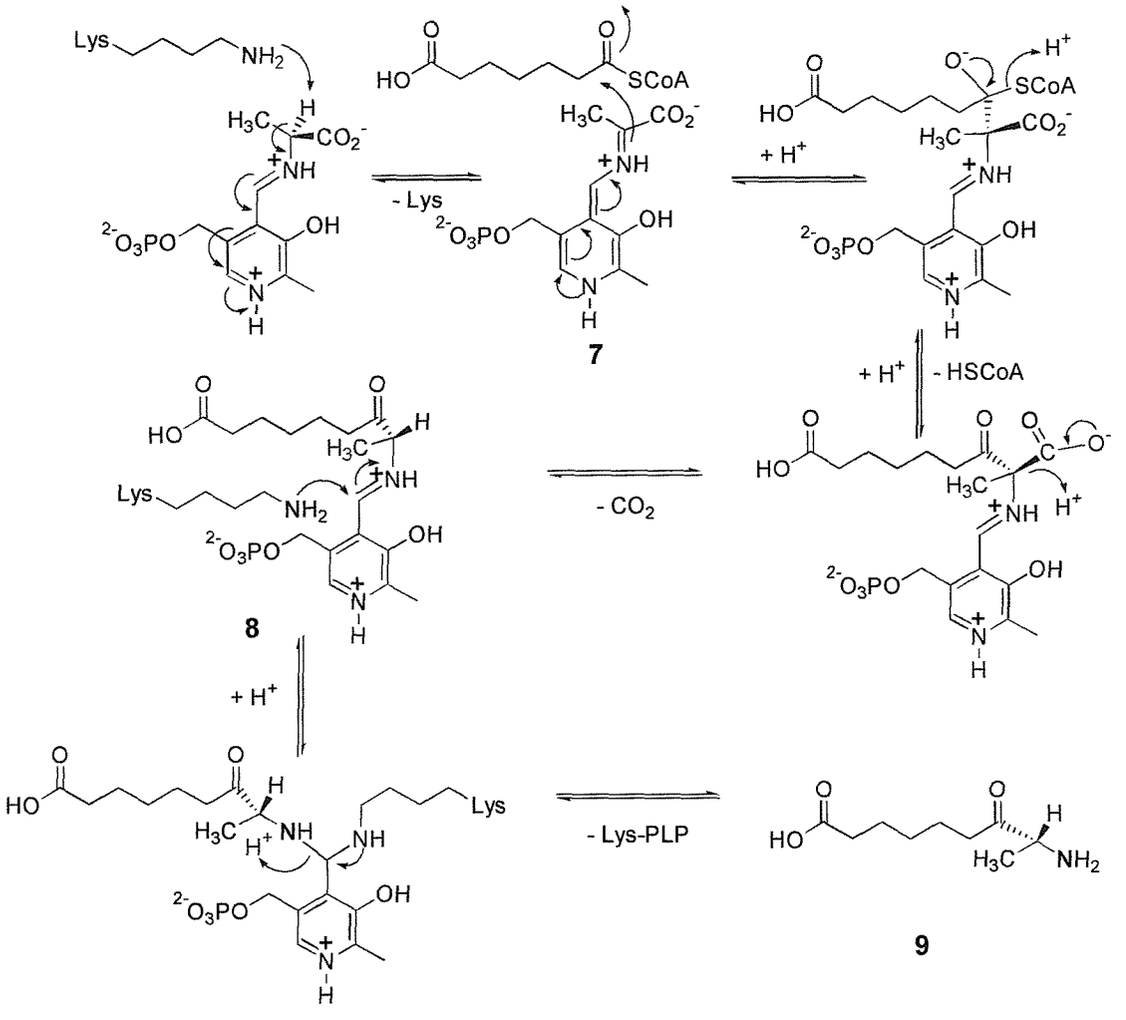

Scheme 1.5: Formation of KAPA

7,8- Diaminopelargonic acid synthase (DAPA synthase)

DAPA synthase is a homodimeric, pyridoxal phosphate-dependent enzyme with a molecular mass of 94 kDa that catalyses the second step of the pathway (Figure 1.4) (31,32). The crystal structure of DAPA synthase from *E. coli* was determined in the apo- and holoform (33). Unusually, the enzyme uses SAM as amino group donor (31). The overall structure of DAPA synthase appears to be very similar to the structure of KAPA synthase. As there is a weak homology in the amino acid sequence, it was suggested that the two enzymes might be evolutionarily related, and are possibly derived from a common ancestor (17). The formation of DAPA proceeds by a classical pyridoxal

phosphate dependent transaminase mechanism. The external aldimine is formed through the reaction of SAM with PLP.

Dethiobiotin synthetase (DTBS)

DTBS is a homodimer, with a subunit molecular mass of 24 kDa. The crystal structure for complexes of DTBS with nucleotides, substrates and substrate analogs from *E. coli* was determined (34-38). The enzyme catalyses the ATP-dependent formation of DTB from DAPA and CO_2 (Scheme 1.6) (39). The first step of the reaction is the formation of a DAPA carbamate **10** at N7 (38,40,41). In the second step a reaction intermediate is formed by transfer of the γ–phosphoryl group from ATP to a carbamate oxygen **11**. The final step involves a nucleophilic attack of the N8 nitrogen onto the carbonyl oxygen of the carbamate, with subsequent release of the phosphate group and formation of the ureido ring of DTB **12**.

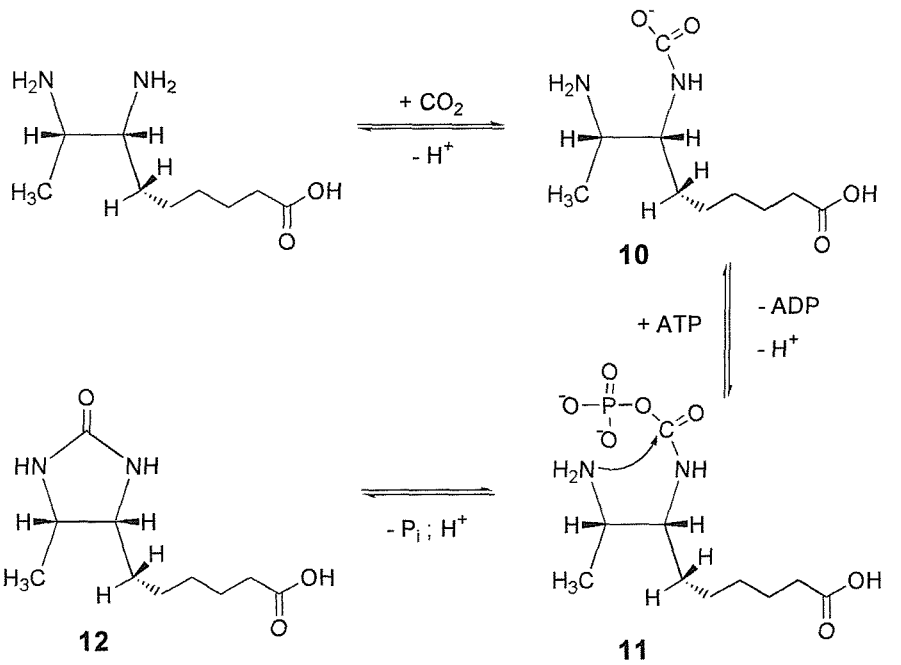

Scheme 1.6: Formation of DTB

Biotin synthase (BioB)

BioB participates in the final step of biotin biosynthesis, the conversion of DTB to biotin, in which a sulphur atom is inserted between the unactivated methyl and C-6 methylene group of DTB to form the tetrahydrothiophene ring of biotin (Scheme 1.3) (42,43). The mechanism of C-S bond formation has been a matter of much debate. Two hypotheses, based on hydroxylation or desaturation at either C6 or C9, were considered by analogy to known enzymatic pathways, but excluded on the basis of labelling studies. They account for the carbons to be functionalised by the involvement of hydroxylated (44) or unsaturated (45-47) intermediates. Possible reaction intermediates for the conversion of DTB to biotin were synthesised (Figure 1.4) and tested for their ability to allow growth of biotin auxotrophs.

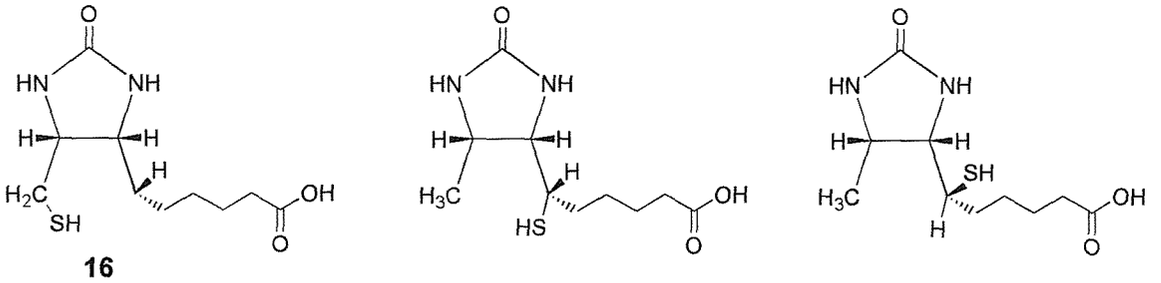

Figure 1.4: Possible reaction intermediates for the last step in the biosynthesis of biotin

Baxter *et al.* found that 9-mercaptodethiobiotin **16** could not support the growth of an *E. coli* biotin auxotroph (48). However, transformation of the biotin auxotroph with a plasmid encoding *bio*B enabled growth. Thus, it was proposed that 9-mercaptodethiobiotin was an intermediate in biotin formation, but could not substitute for biotin. Investigations into *Bacillus sphaericus* biotin auxotrophs yielded similar results (49). A radiolabelled intermediate was isolated from lavender cell cultures with the same retention time, assessed by HPLC, as 9-mercaptodethiobioitin **16** (50). Subsequent work by Shaw *et al.*, demonstrated the isolation of an intermediate from an *in vitro* assay system using *E. coli* cell-free lysate and *E. coli* BioB that could be labelled from ^{14}C-DTB and ^{35}S cystine and could be converted to biotin (51). However, the structure of this intermediate could not be established due to the low amounts of the compound formed. In summary, these results show that 9-mercaptodethiobioitin **16** can be converted into biotin

and may be an intermediate in the conversion of DTB to biotin. Since hydroxylation has been excluded, **16** is probably formed by a direct sulphur insertion. Studies of the *in vivo* conversion of DTB labeled with a chiral methyl group lead to racemisation at C9 (52). This evidence is consistent with the hypothesis that the sulphur transfer occurs *via* a radical mechanism. Further evidence for a radical mechanism came from the *in vitro* requirement of at least two mols of SAM per mol of biotin to achieve maximal activity (51,53). It is likely that SAM **13** is undergoing reductive cleavage to generate methionine **14** and a 5'-deoxyadenosyl radical **15** (Scheme 1.7).

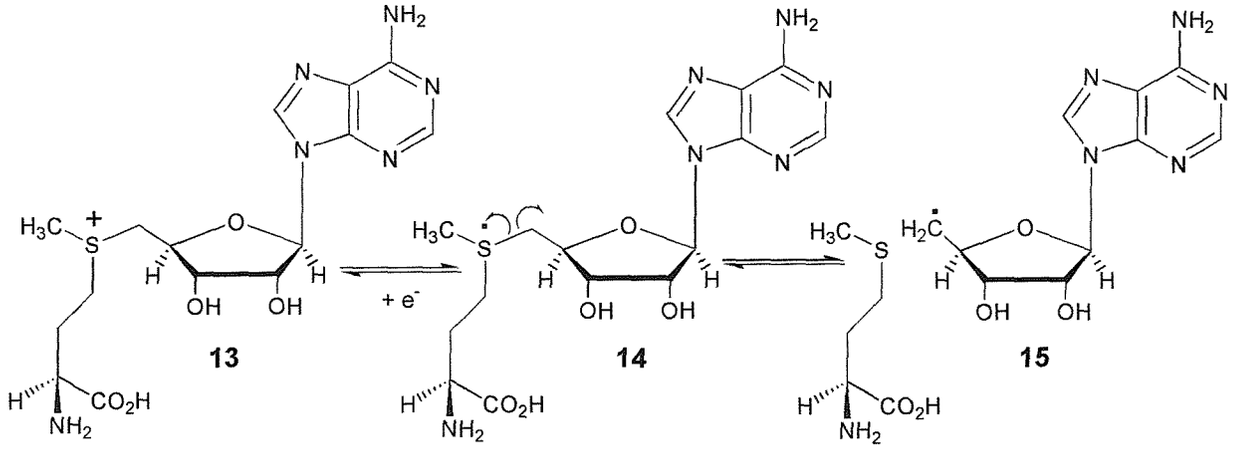

Scheme 1.7: Reductive cleavage of SAM

The primary 5'-deoxyadenosyl radical **15** is highly reactive and can abstract hydrogen from the C6 carbon of DTB, which quenches with a sulphur donor. A second 5'-deoxyadenosyl radical **15** abstracts hydrogen from the C9 carbon of DTB, which leads to tetrahydrothiophene ring formation (Scheme 1.8).
According to the above hypothesis, replacing hydrogen with deuterium at the C6 and C9 position of DTB would lead to deuterium labelled 5'-deoxyadenosine. Escallettes *et al.* synthesized deuterium labelled DTB analogues and investigated deuterium incorporation into DOA (54). Their results were not completely unequivocal, but consistent with the above hypotheses, and they argued against the possibility of a protein bound radical. Additional evidence was found for the removal of the *pro*S hydrogen from the C6 carbon

of DTB, which had already been suggested (45). This suggests that BioB could belong to the Radical SAM superfamily (55), which has recently been discovered by *in silico* sequence analysis. The family includes Fe-S cluster containing enzymes that catalyse the reductive cleavage of SAM and use the resultant free radicals during catalysis (42,43). Examples include the anaerobic ribonucleotide reductase activating enzyme (56) and pyruvate formate lyase-activating enzyme (57) that use a combination of a Fe-S cluster and SAM to generate an essential protein-bound glycyl radical. In addition, BioB contains a sequence motif encompassing three cysteine residues, the cysteine box, which is also found in SAM-dependent enzymes containing Fe-S cluster. The proximal source of the reducing electrons could thus be the $[4Fe\text{-}4S]^{2+/1+}$ cluster of biotin synthase, which is maintained in a reduced state by NADPH, FldA, Fdr (43) and/or mioC (58) (Scheme 1.8).

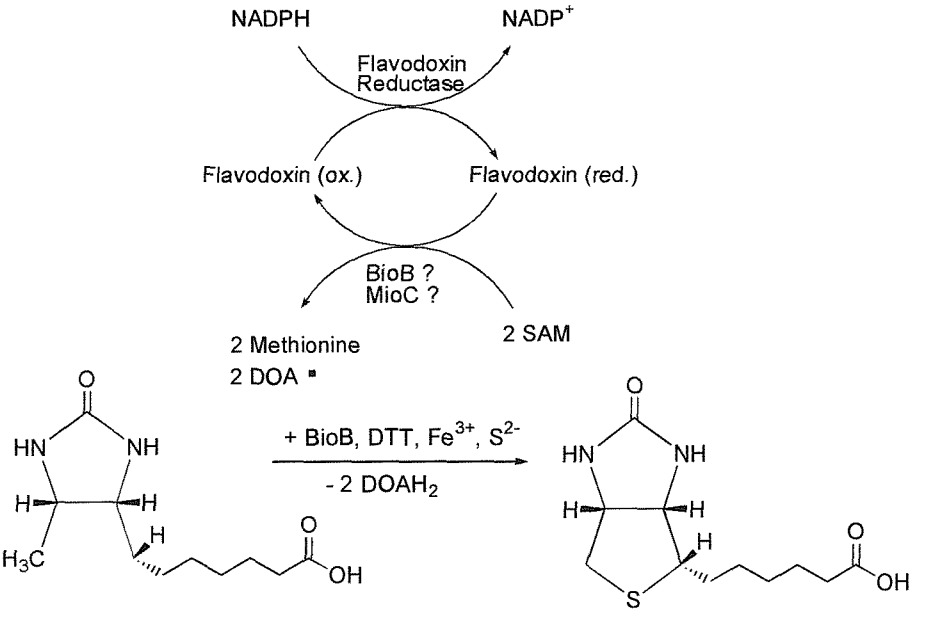

Scheme 1.8: Working model for the conversion of DTB to biotin

The origin of the sulphur incorporated in biotin has been the focus of a number of studies. Recent work provides evidence that the sulphur is donated by biotin synthase itself (59,60), in fact by the Fe-S cluster of BioB (59). This could explain the failure to obtain *in vitro* activity with mutants, in which the cysteine residues in the conserved cysteine box were mutated to serine or threonine (61) or alanine (62). The sequence of BioB with

the eight cysteine residues highlighted is depicted in Figure 1.5. As a result the altered iron-sulphur cluster of mutated BioB is unable to participate in biotin formation. If BioB behaves as a reagent rather than a catalyst, this could also explain the limited, stoichiometric turnover reported *in vitro*. Another possible interpretation for the mutagenesis results is that the iron-sulphur cluster of BioB cannot deliver the electrons necessary for the reductive cleavage of SAM, as it is not properly assembled. As isolated under aerobic condition, biotin synthase is a homodimer and contains close to one [2Fe-2S] cluster per subunit. Upon anaerobic incubation with Fe^{3+} and sulphide, it was proposed that either one $[4Fe\text{-}4S]^{2+/+}$ clusters and one $[2Fe\text{-}2S]^{2+}$ cluster is reconstituted per monomer (63,64) or a $[4Fe\text{-}4S]^{2+/1+}$ cluster per monomer (65). Ugulava *et al.* provided spectroscopic evidence identifying the $[2Fe\text{-}2S]^{2+}$ cluster necessary for sulphur transfer (Scheme 1.9).

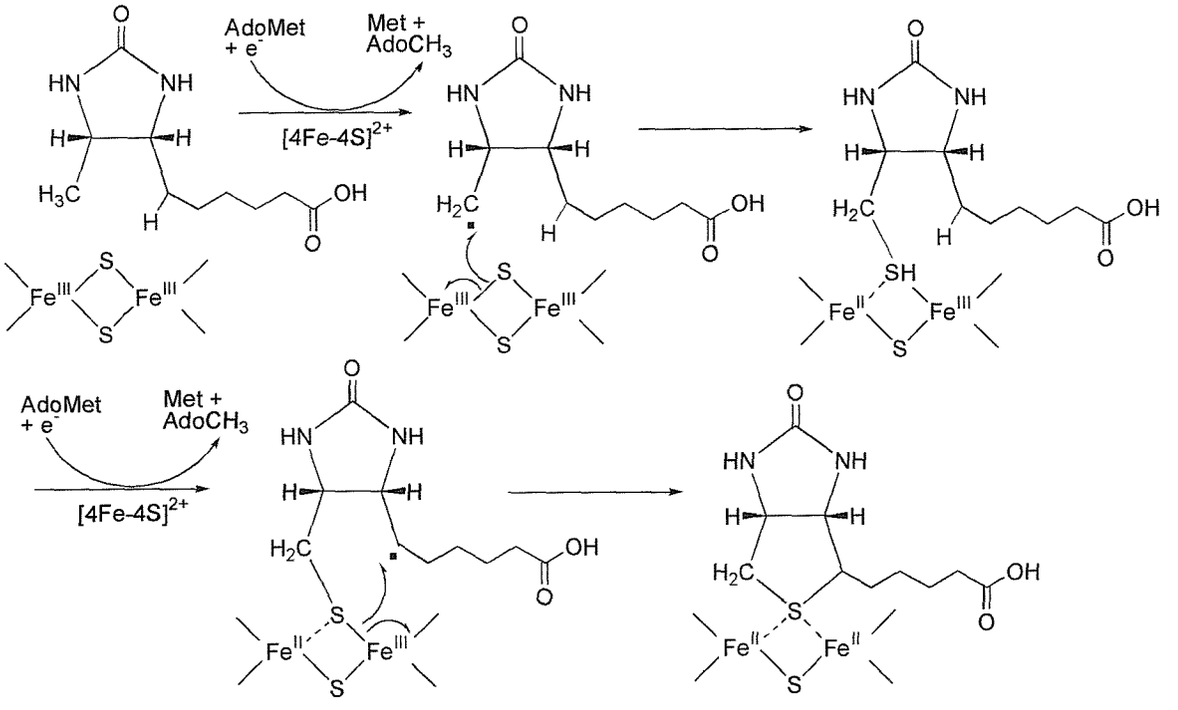

Scheme 1.9: Proposed mechanism for the oxidative insertion of sulphide into dethiobiotin from the $[2Fe\text{-}2S]^{2+}$ cluster in BioB [adapted from (63)]. A cubane [4Fe-4S] cluster would follow the same mechanism and maintain one [2Fe-2S] cluster. The sequence of BioB with the eight cysteine residues highlighted is depicted in Figure 1.5.

```
        10          20          30          40          50          60
         |           |           |           |           |           |
MAHRPRWTLS QVTELFEKPL LDLLFEAQQV HRQHFDPRQV QVSTLLSIKT GACPEDCKYC

        70          80          90         100         110         120
         |           |           |           |           |           |
PQSSRYKTGL EAERLMEVEQ VLESARKAKA AGSTRFCMGA AWKNPHERDM PYLEQMVQGV

       130         140         150         160         170         180
         |           |           |           |           |           |
KAMGLEACMT LGTLSESQAQ RLANAGLDYY NHNLDTSPEF YGNIITTRTY QERLDTLEKV

       190         200         210         220         230         240
         |           |           |           |           |           |
RDAGIKVCSG GIVGLGETVK DRAGLLLQLA NLPTPPESVP INMLVKVKGT PLADNDDVDA

       250         260         270         280         290         300
         |           |           |           |           |           |
FDFIRTIAVA RIMMPTSYVR LSAGREQMNE QTQAMCFMAG ANSIFYGCKL LTTPNPEEDK

       310         320         330         340
         |           |           |           |
DLQLFRKLGL NPQQTAVLAG DNEQQQRLEQ ALMTPDTDEY YNAAAL
```

Figure 1.5: BioB sequence; length: 346 AA; MW: 38648 Da. Eight cysteine residues, potential sites for iron-sulphur cluster assembly, are highlighted in red.

Such mechanism could explain the low *in vitro* activity of biotin synthase. After the transfer of sulphur to biotin the iron-sulphur cluster becomes depleted of sulphur. To proceed with the next catalytic cycle, sulphide would have to be replaced. In this thesis, the limiting factors for biotin synthase activity *in vitro* were investigated.

1.4 Fermentative production of biotin

In recent years many research groups, industrial and academic, have become interested in the production of biotin by fermentation. This process is potentially cheaper and environmentally friendlier than the synthetic multi-step procedures. It is generally accepted that a commercially viable fermentative process will require cells able to produce more than 1 g/L/day (66). Wild type *E. coli* cells produce approximately 10 to 15 ng/l of biotin (67), as isolated from the growth media. To increase the level of biotin formation *in vivo*, several methods have been utilized. De-repressed *E. coli* cells, lacking BirA, excrete approximately 5 to 15 µg/l (68). Mutants resistant to threonine analogues,

which maintained a plasmid containing part or whole of a biotin operon were able to excrete approximately 930 mg/l/82 h (69). This effect was explained in terms of modification to the methionine metabolism, enhancing the supplying system of SAM. However, the dramatic increase could only be achieved by maintaining the cells in a complex fermentation medium, which would make downstream fermentative processing more expensive. Overexpression of the *E. coli bio* operon in *E. coli* by both wild type and artificial promotors (70) and manipulation of the *E. coli* operon by re-organisation of the *bio* operon into one transcriptional unit (66) led to the production of approximately 30 mg/l/d of biotin. Thus far, the fermentative production of biotin in *E. coli* and other microorgainsms has not been sufficient for commercialisation. The bottleneck in the fermentative production is proposed to be the last step in the biosynthesis of biotin, the conversion of DTB to biotin. The metabolic pathway towards DTB could be readily engineered by overcoming the KAPA to DAPA bottleneck using a lysine-utilizing DAPA aminotransferase to give an increase in the DTB concentration, little of which was converted into biotin (71). In this thesis, the last step in the biosynthesis of biotin in which BioB participates, was investigated in detail to identify possible limitations for the *in vivo* application.

1.5 SAM dependent enzymes

A novel protein superfamily with over 600 members was discovered by iterative profile searches and analysed using bioinformatics and visualization methods (55). The common mechanistic feature of these enzymes is that they generate a 5'-deoxyadenosyl radical by reductively cleaving SAM (Scheme 1.7; p. 10). The electron necessary for the reductive cleavage might be provided by the $[4Fe\text{-}4S]^{2+/1+}$ cluster bound to the protein or a protein co-factor. Although more experimental evidence is needed to support the notion of a Radical SAM superfamily, it will help guide laboratory efforts to characterize and identify group members. As these enzymes share some mechanistic details with biotin synthase, selected examples are reviewed below, highlighting the parallels with the biotin forming reaction.

Anaerobic ribonucleotide reductase (aRR)

The synthesis of deoxyribonucleotides in *E. coli*, essential for DNA synthesis, under anaerobic conditions is carried out by a class III ribonucleotide reductase (72,73) (Figure 1.6).

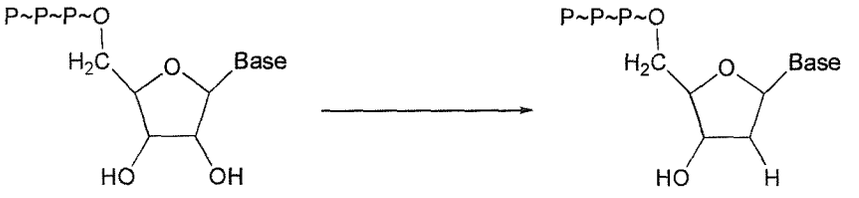

Figure 1.6: The reduction of a ribonucleotide to a deoxynucleotide.

Anaerobic ribonucleotide reductase has a $\alpha_2\beta_2$ tetrametric structure (74). The small β subunit with molecular weight of 17.5 kDa (75) contains a [2Fe-2S] cluster that can be anaerobically reconstituted by either dithionite or deazaflavin to $[4Fe\text{-}4S]^{2+/1+}$ cluster (74,76). The iron-sulphur cluster can be maintained in its reduced state by a redox chain providing electrons including NADPH, FldA and Fdr (77,78). The reduced $[4Fe\text{-}4S]^{2+/1+}$ cluster is proposed to reductively cleave SAM to methionine and a reactive 5'-deoxyadenosyl radical. The latter is thought to abstract a hydrogen atom from a specific glycine residue, Gly 681, on the 80 kDa α protein (79,80). In turn, the glycyl radical is thought to function in hydrogen abstraction from a cysteine residue located close to the bound substrate (81). The resulting thiyl radical may then remove the 3' hydrogen atom from the ribose and initiate the reaction (82) leading to the deoxyribonucleotide, the mechanism of which is not fully understood.

Pyruvate Formase Lyase (PFL)

PFL is a key enzyme of the anaerobic glucose fermentation in *E. coli* and other microorganisms, catalysing the CoA-dependent cleavage of pyruvate to acetyl-CoA **17** and formate **18** (Figure 1.7) (83).

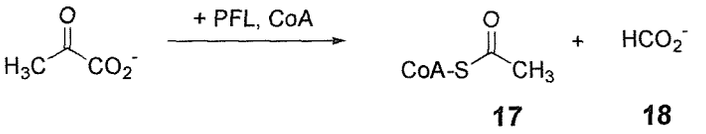

Figure 1.7: CoA-dependent cleavage of pyruvate

The enzyme is a homodimeric protein of 170 kDa, which occurs in both an inactive (PFL_i) and active (PFL_a) form (84,85). The switch from PFL_i to PFL_a is controlled by the Pyruvate-Formate Lyase Activating Enzyme (PFL AE). *In vitro* activity requires a reduced flavin and further low molecular weight compounds such as SAM, Fe^{2+}, DTT and pyruvate as positive allosteric effector (86). A stable glycyl radical at glycine 734 on PFL_a effects the rearrangement of pyruvate to formate (83,87,88). This active site radical is formed through the abstraction of the pro*S* hydrogen by a 5'-deoxyadenosyl radical. The radical is formed by the reductive cleavage of SAM into a 5' deoxyadenosyl radical and methionine by the $[4Fe\text{-}4S]^{2+/1+}$ cluster of PFL AE, which, in turn, is maintained in its reduced state by flavodoxin (89). Although PFL is dimeric, only one of the two possible Gly 734 residues is converted to a glycyl radical (90). Based on the crystal structure of PFL showing the position of the active site residues relative to the bound substrate molecule, a mechanism was proposed that is shown in Scheme 1.10.

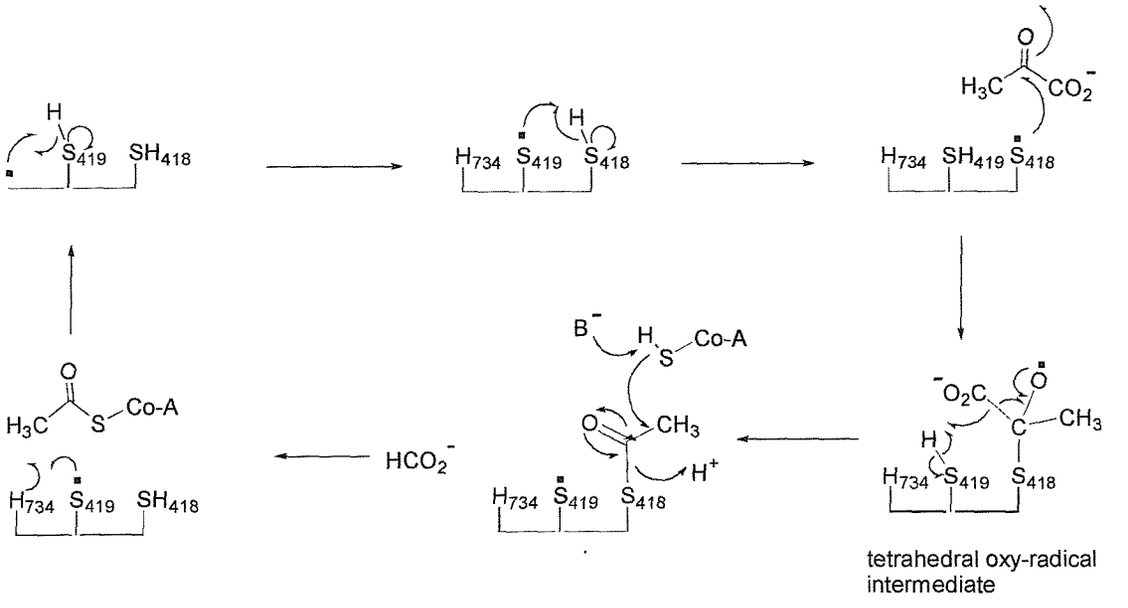

Scheme 1.10: The conversion of pyruvate to acetyl-CoA and formate catalysed by PFL.

Lipoic synthase (LipA)

Lipoic acid **25** is an essential co-factor for all α-ketoacid dehydrogenase complexes. In *E.coli*, octanoic acid **24** is a precursor in the biosynthesis of lipoic acid (Figure 1.8). Sulphur is inserted into lipoic acid in a reaction in which LipA participates (91,92).

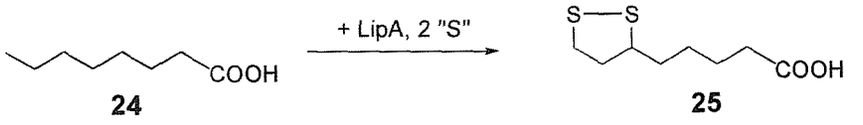

24 **25**

Figure 1.8: LipA participates in the conversion of octanoic acid to lipoic acid.

LipA has been overexpressed in *E. coli* and purified from the soluble fraction (93) and insoluble aggregates that were subsequently refolded and reconstituted with ferrous iron and sulphide (94). LipA contains a sequence motif encompassing three cysteine residues, the cysteine box (94), which is also found in SAM-dependent enzymes containing Fe-S cluster. Subsequently it could be shown that LipA contains a [4Fe-4S] cluster (65,92-94). Investigation of the conversion of octanoic acid to lipoic acid was hindered by the absence of a functional *in vitro* assay. Miller *et al.* assayed lipoate or lipoyl formation using *E. coli* lipoate-protein ligase (LplA) or lipoyl-[acyl-carrier-protein]-protein-*N*-lipoyltransferase (LipB), respectively, to lipolyate apo-pyruvate dehydrogenase complex (apo-PDC) (95). When suitably reduced LipA was incubated with octanoyl-ACP, LipB, apo-PDC, and SAM, the formation of lipoylated PDC was observed. This was assayed spectrophotometrically via reduction of NAD^+ in the presence of pyruvate, CoA, TPP, and cysteine, was formed (92). These results suggest that LipA belongs to the group of enzymes that use the reductive cleavage of SAM as source for generation of radicals that includes aRR, PFL and BioB. However, it has to be noted that the measured turnover was extremely low (0.01 mol product/ 1 mol of LipA polypeptide). The optimisation of the *in vitro* reaction conditions and identification of small- or large molecular weight factors, will be necessary to further the understanding of the biosynthesis of lipoic acid.

Chapter Two: Purification of *E. coli* biotin synthase (BioB)

2.1 Purification of BioB from pKH200/BL-21(DE3)

In order to conduct biochemical studies on BioB it was necessary to obtain large quantities of the purified enzyme. The plasmid pKH200 (Figure 2.1) was a kind gift from Dr. K. Hewitson (Oxford University). It encodes the *bio*B gene under the control of the strong T7 promotor (pET24d(+), Novagen) inducible with IPTG. The plasmid was transformed into BL-21 (DE3) (Stratagene) which encodes T7 RNA polymerase.

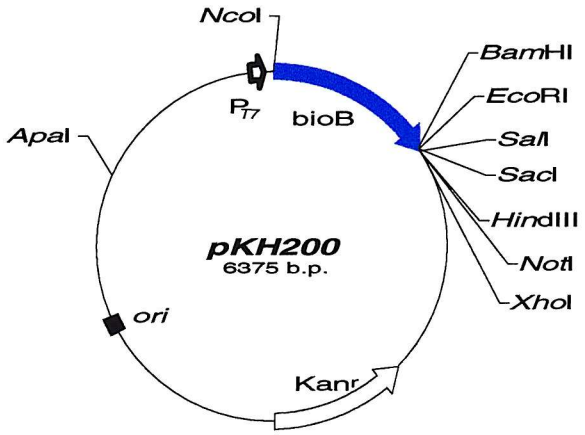

Figure 2.1: Plasmid map of pKH200 with prominent restriction sites

Large-scale fermentations (3 X 25 l) carried out by Dr. P. Roach afforded 300 g of cells expressing BioB at about 10-15% of total cell protein and an optimised purification protocol was followed (96). A 35 % ammonium sulphate cut was followed by HIC chromatography (Figure 2.2). After the fractions containing BioB were pooled, the protein sample was further purified by gel filtration chromatography (Figure 2.3 and 2.4).

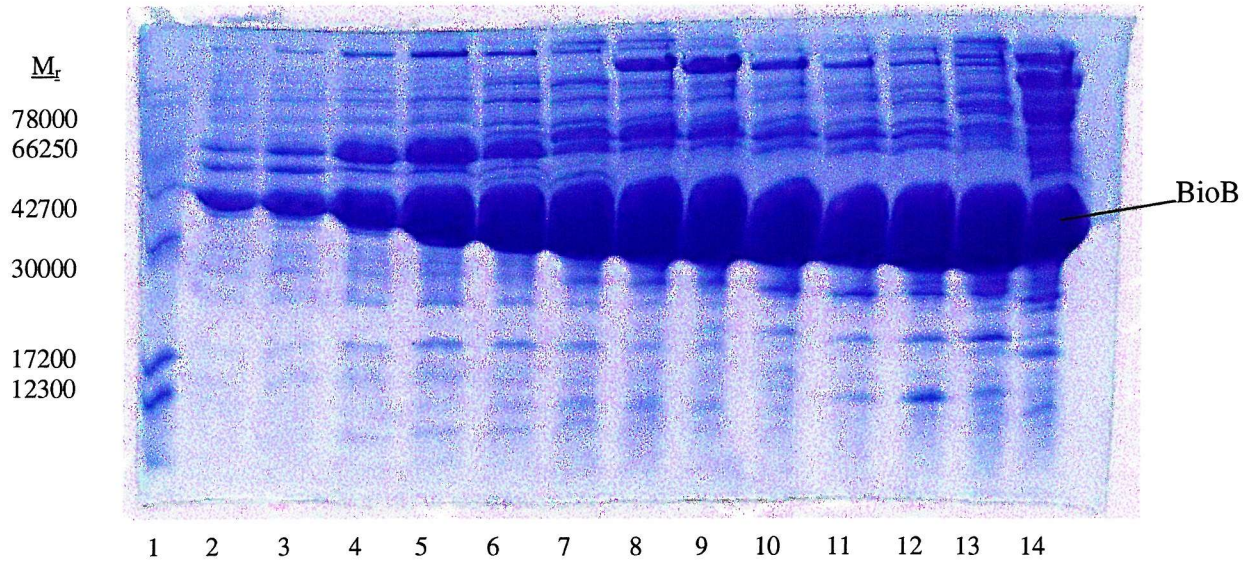

Figure 2.2: Coomassie Blue stained 15 % SDS-PAGE gel. (1) Molecular weight markers, (2) – (14) BioB containing fractions eluting from the HIC column. Fractions (8) to (14) were applied to the S-200 column.

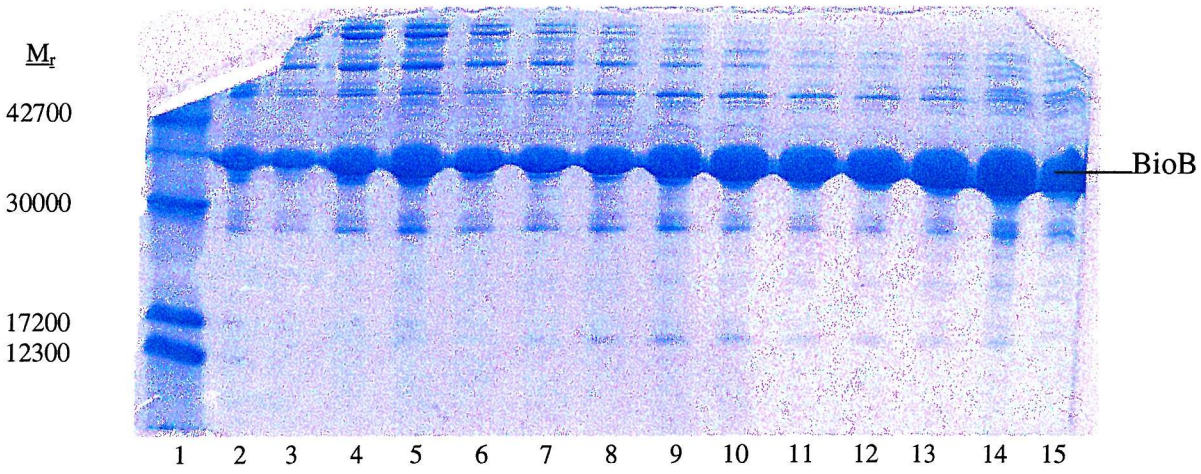

Figure 2.3: Coomassie Blue stained 15 % SDS-PAGE gel showing the fractions eluting from the gel filtration column. (1) Molecular weight markers, (2) – (15) BioB containing fractions. fractions (11) to (15) were pooled and used for further purification.

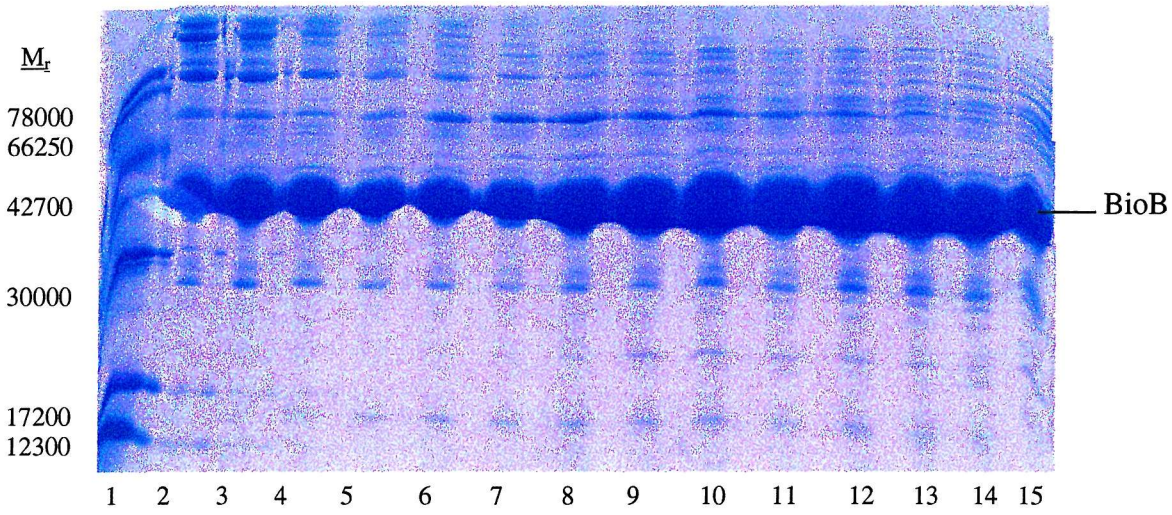

Figure 2.4: Coomassie Blue stained 15 % SDS-PAGE gel. (1) Molecular weight markers, (2) – (15) BioB containing fractions. Fractions (9) to (14) were pooled and used for further purification.

BioB of medium purity, as judged by SDS-PAGE, was produced by this procedure. This was deemed insufficient for rigorous biochemical investigations, although the yield was sufficient with 570 mg final protein (50 g cell paste).

Therefore, potential improvements were investigated to increase the purity of the final protein sample. Most purification parameters remained the same but the 35 % final concentration of ammonium sulphate was reduced to 30 % for the initial precipitation step (Figure 2.5 and 2.6).

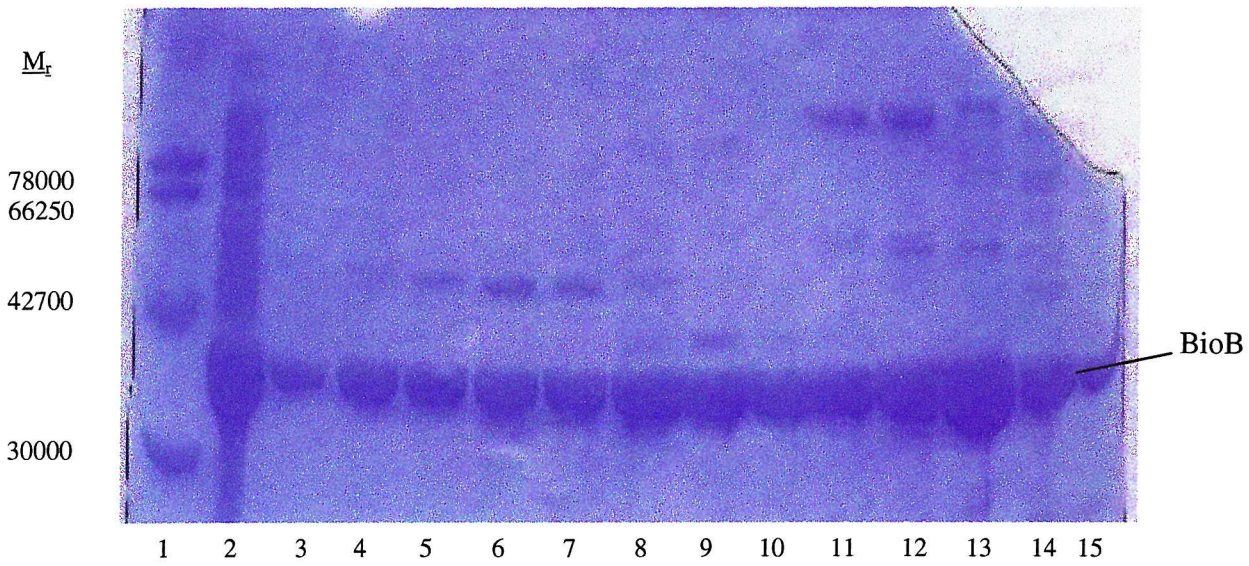

Figure 2.5: 15 % SDS-PAGE gel of the HIC column (an extended gradient to allow better resolution of high molecular weight components). (1) Molecular weight markers, (2) Load, (3) – (15) BioB containing fractions. Fraction (4) to (10) were applied to the gel filtration column.

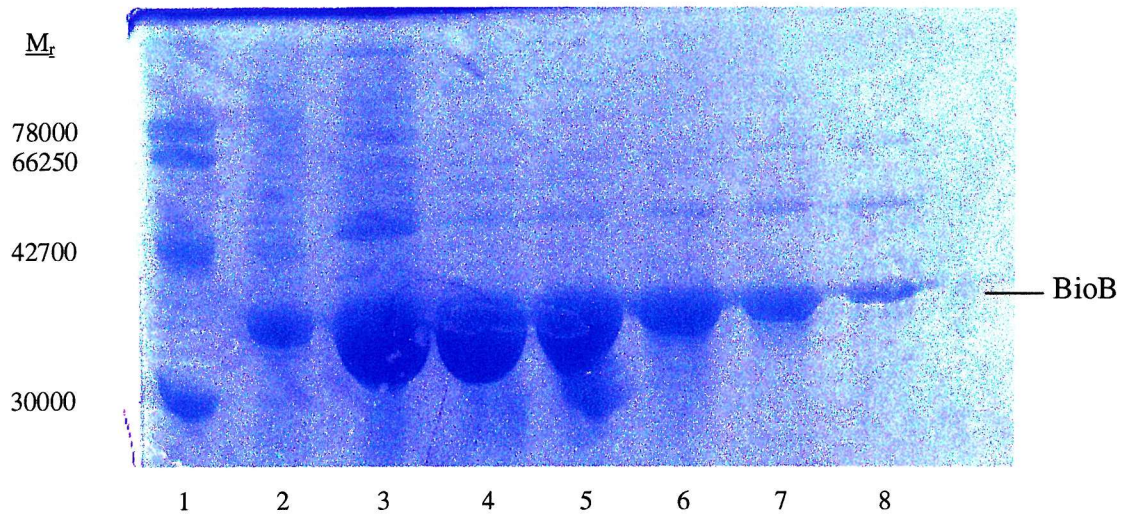

Figure 2.6: Gel filtration chromatography. (1) Molecular weight markers, (2) Load, (3) – (8) BioB containing fractions. Fraction 4 and 5 were pooled and used for biochemical investigations.

With this procedure BioB of higher purity, as judged by SDS-PAGE, was obtained, although it lowered the final yield of purified BioB to 110 mg.

Screening a range of dye affinity media (Section 8.2.1), which do not mimic a specific co-facor but have a complex, hydrophobic structure, BioB was found to bind to the Brown Reactive 10 resin (Sigma), which was subsequently used to further purify BioB (Figure 2.7).

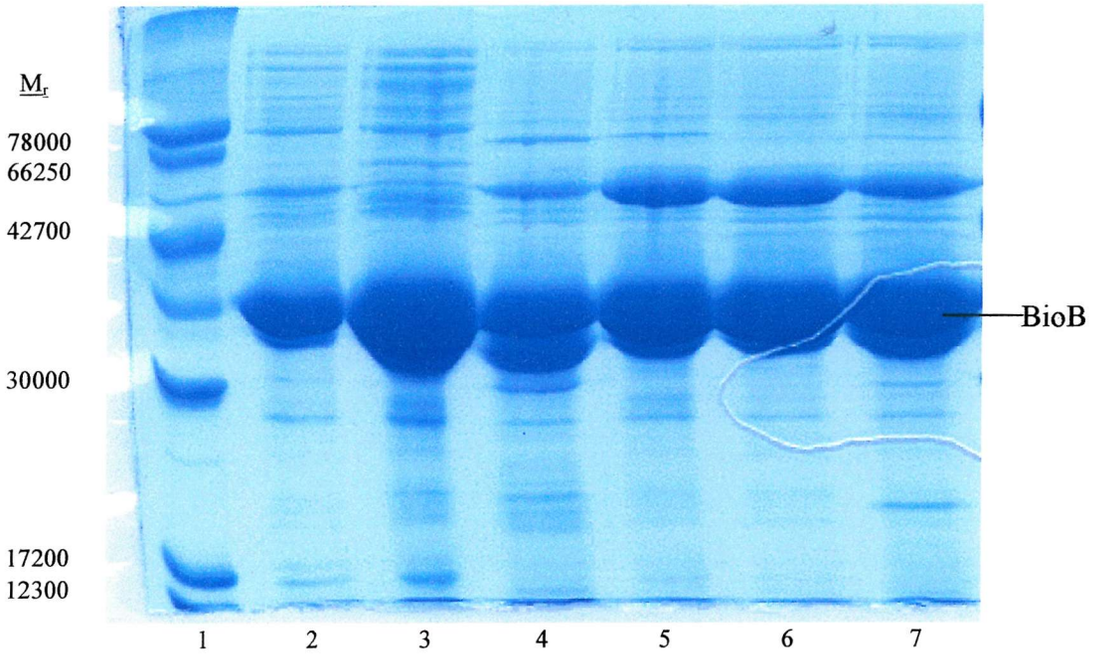

Figure 2.7: Coomassie Blue stained 15 % SDS-PAGE gel of the Brown Reactive 10 column fractions. (1) Molecular weight markers, (2) flow through, (3) – (7) BioB containing fractions.

As can be seen in Figure 2.7, fractions eluting from the Brown Reactive 10 column contained a co-eluting impurity at ~50 kDa. This impurity has a stronger affinity to the Brown Reactive 10 resin than BioB, as it is significantly depleted in the flow through. The flow through was thus reapplied to the Brown Reactive 10 column and bound protein eluted isocratically with high salt (Figure 2.8).

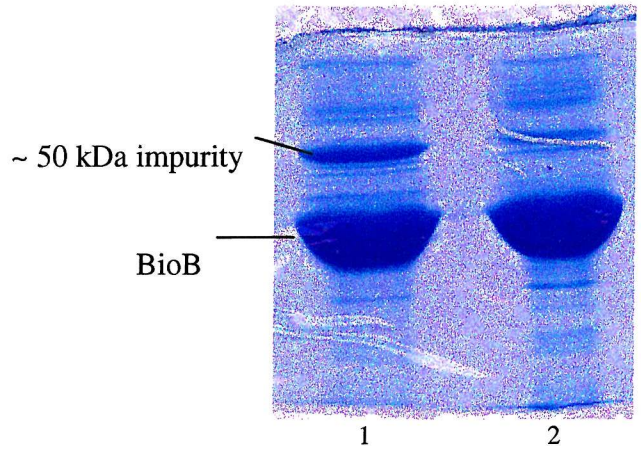

Figure 2.8: Coomassie Blue stained 15 % SDS-PAGE gel of (1) pooled fractions 4 to 7 (Figure 2.7), (2) reapplied flow through eluted with high salt.

This last purification step yielded BioB of highest purity, as judged by SDS-PAGE, a significant improvement to previous protocols. The BioB containing fractions obtained in the first purification procedure (35 % ammonium sulphate cut) were thus pooled and applied to the Brown Reactive 10 column. The flow through was collected and reapplied (Figure 2.9).

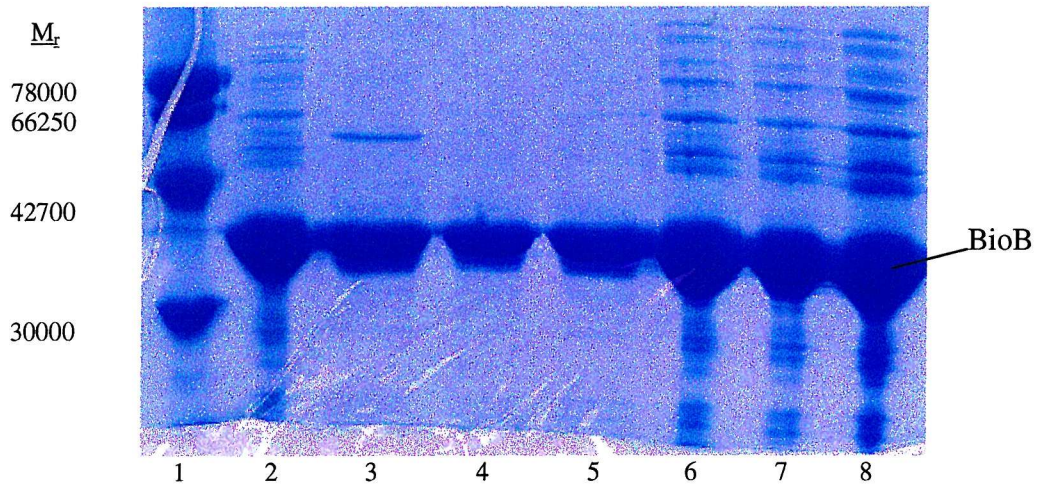

Figure 2.9: (1) Molecular weight markers, (2) Load, (3-5) BioB containing fractions for a three step purification were desalted and stored at - 80°C, (6-8) flow through after each of the three purification steps, (6) and (7) were reapplied.

Through this purification scheme BioB of highest purity, as judged by SDS-PAGE, was obtained. The drawbacks of this purification are that it is laborious and low yielding. Thus, other ways of purifying BioB were investigated that make use of affinity tags to allow a one step purification of BioB.

2.2 Purification of BioB from p12:bioB/Bl-21(DE3)

IMPACT (Intein Mediated Purification with an Affinity Chitin-binding Tag, BioLabs, New England) is a protein purification system (97), which utilizes the inducible self-cleavage activity of a protein-splicing element (named Intein) to separate the target protein from the affinity tag. A schematic representation of the IMPACT system is given in Figure 2.10.

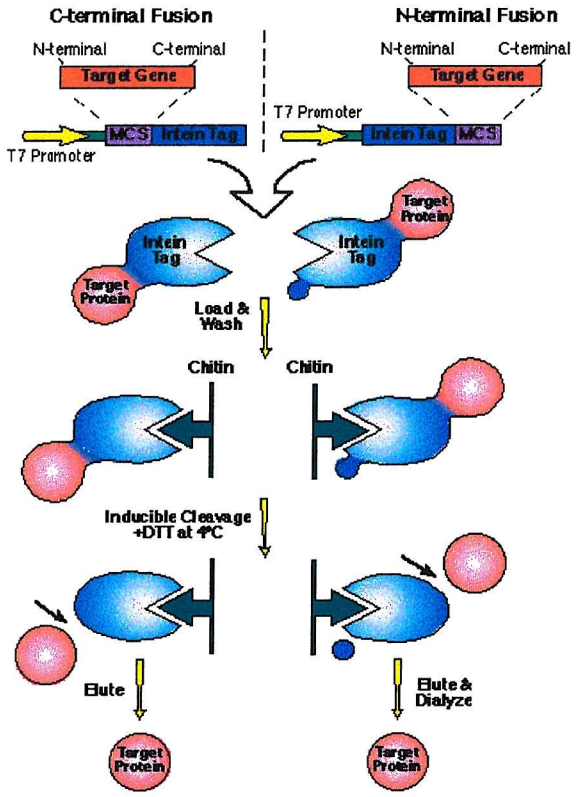

Figure 2.10: Protein purification using the IMPACT system (BioLabs, New England)

The gene for the target protein is first subcloned into the vector of choice. Induction of expression results in the overexpression of a fusion protein. There are four different plasmids provided with the IMPACT system, a kind gift of Dr. K. Hewitson (Oxford University). They differ in their restriction sites and the usage of N-terminal or C-terminal fusions. The plasmid p12 (Figure 2.11) was chosen because of its convenient restriction sites. The *bioB* gene could therefore be restricted out from pTZ204 (Section 7.4) on a NdeI/EcoRI fragment. The construction of the plasmid p12:bioB is shown in Figure 2.11.

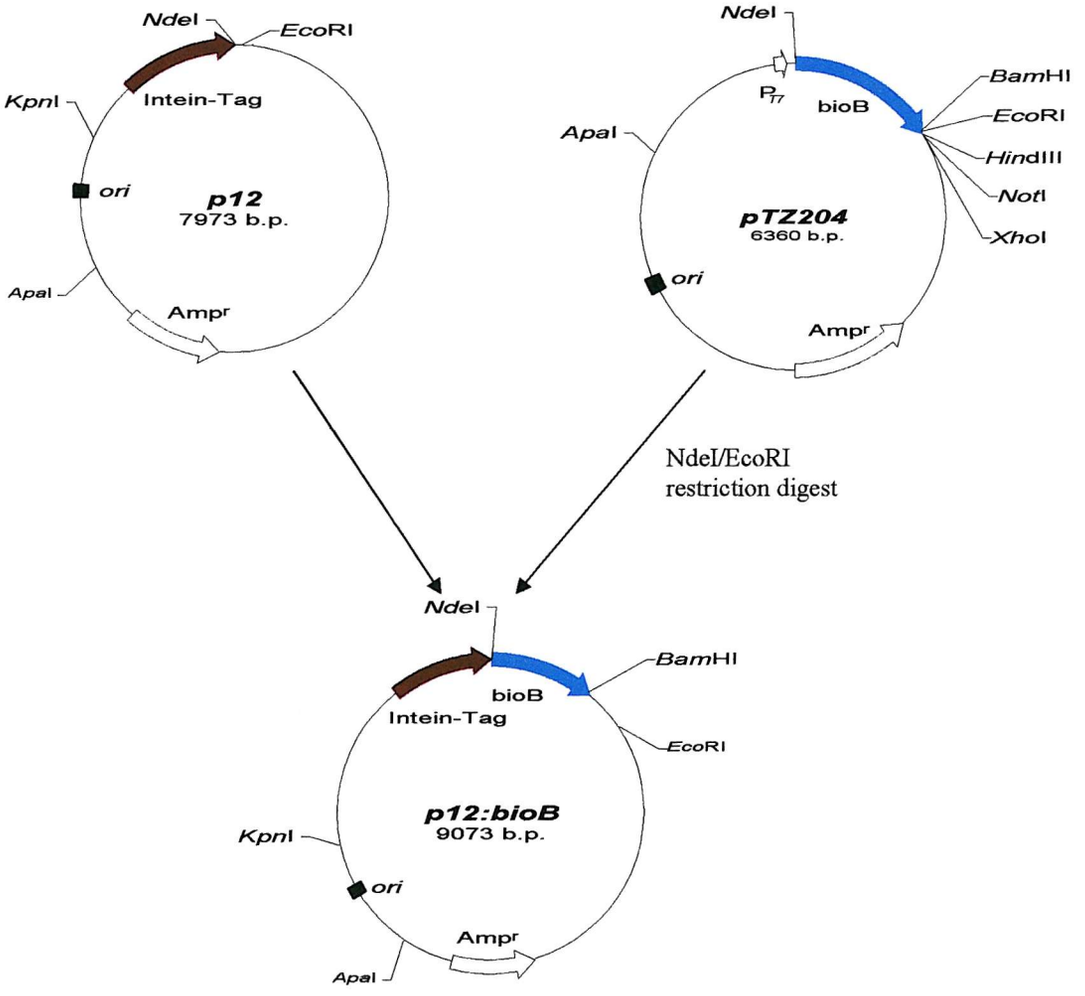

Figure 2.11: Construction of p12/bioB

A digestion of p12:bioB with several restriction enzymes is shown in Figure 2.12.

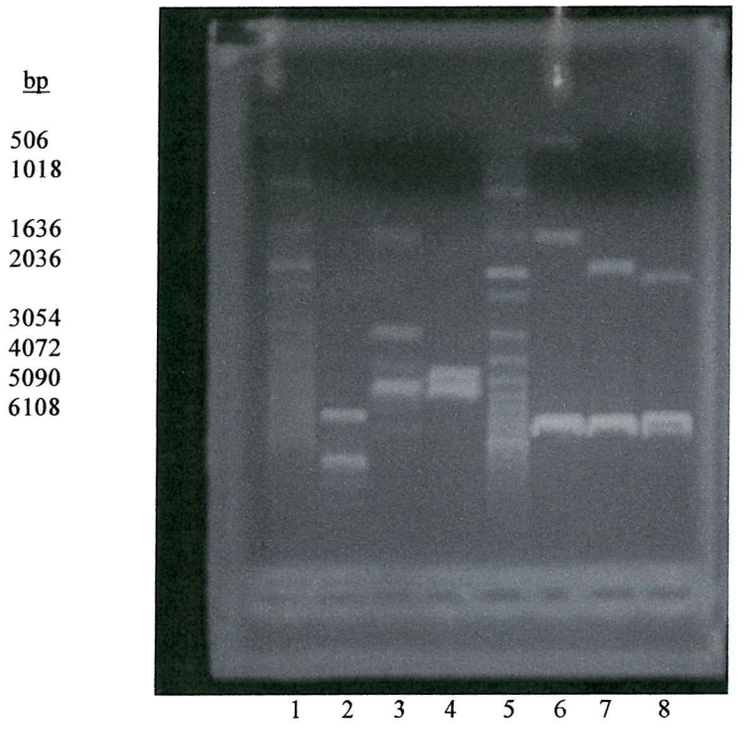

Figure 2.12: Restriction digestion of p12/bioB, (1) Marker, (2) Plasmid, (3) ApaI/BamHI, (4) ApaI/EcoRI, (5) Marker, (6) NdeI/BamHI, (7) NdeI/EcoRI, (8) NdeI/KpnI

Cells were grown under conventional conditions, the cell-free lysate was applied to a Chitin affinity column (BioLabs, New England). The top of the resin turned brownish, indicating bound BioB. Protein bound to the chitin medium was incubated overnight in the presence of DTT to induce cleavage (97) (Figure 2.13).

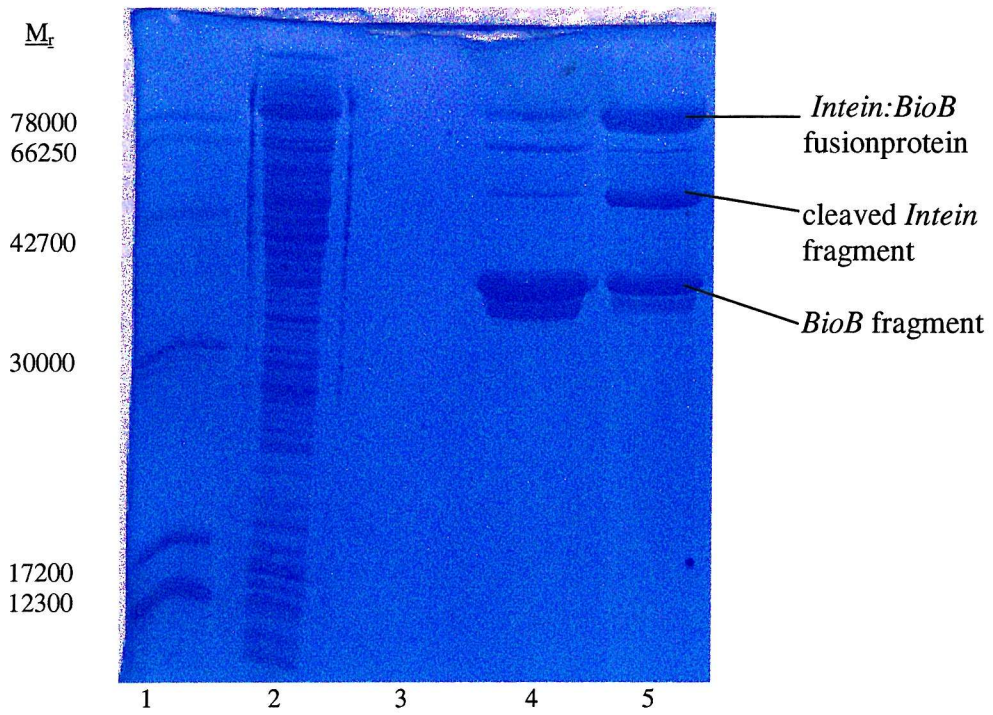

Figure 2.13: Coomassie Blue stained 15 % SDS-PAGE. (1) Molecular weight markers, (2) Load, (4) pooled fractions eluted from the Chitin affinity column after overnight incubation in 30 mM DTT, (5) 10 µl Chitin resin mixed with SDS loading buffer

As can be seen in Figure 2.14, the binding of the fusion protein, cleavage and subsequent elution of BioB from the Chitin affinity column was successful. However, the yield was extremely low (5 g of cell paste gave 4 mg of purified BioB), the purity of BioB was less than outstanding and a significant quantity of fusion protein remained still bound to the Chitin resin. The purification was therefore scaled-up and optimized, but on a larger scale, the easily compressed Chitin resin proved problematic and did not result in BioB of higher purity or higher yield.

2.3 Purification of BioB from pet6H:bioB/BL-21(DE3)

The plasmid pet6H:bioB (61) (Figure 2.14) was a kind gift from Dr. D. Campopiano (University of Edinburgh). It was transformed into BL-21(DE3), and BioB was expressed with an N-terminal polyhistidine tag, which allowed purification using nickel chelating chromatography (Figure 2.15).

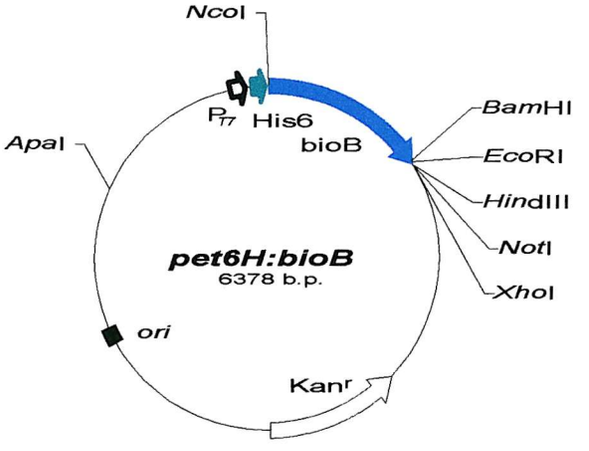

Figure 2.14: Plasmid map of pet6H:bioB with prominent restriction sites

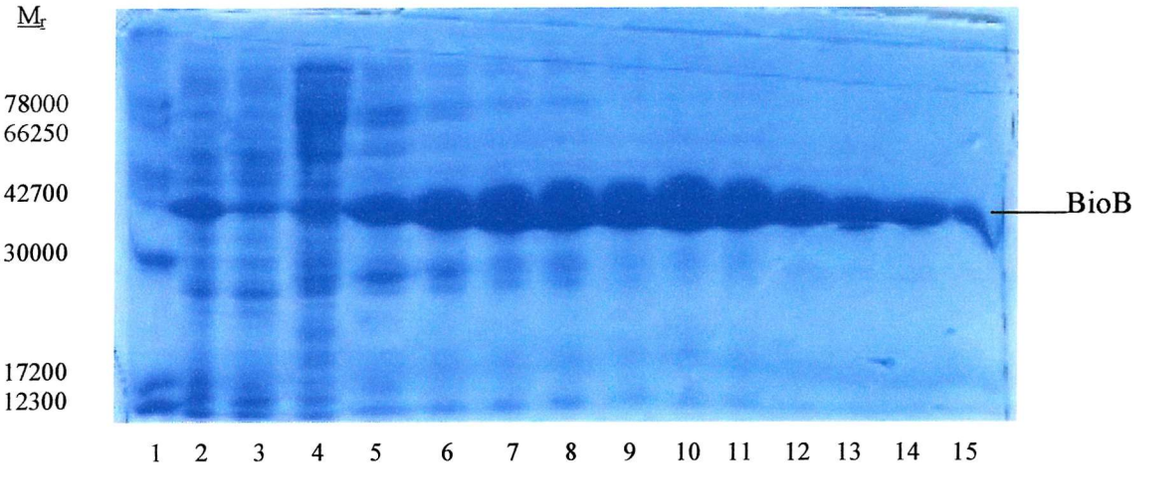

Figure 2.15: Coomassie Blue stained 15 % SDS-PAGE gel of the nickel chelating affinity column. (1) Molecular weight markers, (2) Load, (3) flow through, (4) – (15) BioB containing fractions. Fraction 9 to 15 were desalted, concentrated (Method I) and used for biochemical investigations.

The purification was further optimised by increasing the initial imidazole concentration resulting in BioB of even higher purity (Figure 2.16).

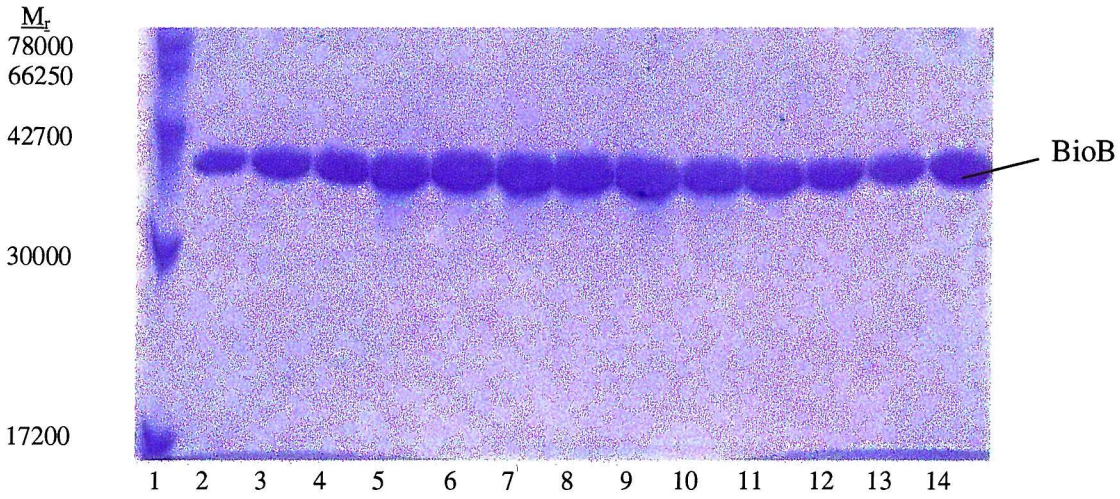

Figure 2.16: (1) Molecular weight markers, (2) – (14) BioB containing fractions. Fraction 4 to 14 were desalted and concentrated (Method II) and used for biochemical investigations.

The purification of BioB from pet6H:bioB/BL-21(DE3) yielded extremely pure His_6-BioB. The purification is quick, reliable and high yielding and is the method of choice for preparation of BioB used for *in vitro* investigation and biochemical studies.

2.4 The iron content of BioB

The amount of iron and sulphur bound to active BioB is still a matter of debate (63-65,94,98). BioB purified under anaerobic condition contains approximately 1.5 mol Fe/ mol BioB (Table 2.1).

Date	04/03/01	12/02/02
Sample	BioB (Figure 2.9)	His_6-BioB (Figure 2.17)
Fe mol / BioB monomer mol	1.24	1.41

Table 2.1: Iron content of aerobic purified BioB

It has been observed that different reconstitution conditions give BioB with a [4Fe-4S] cluster (94) or one [4Fe-4S] cluster and one [2Fe-2S] cluster (63). In our hands it was found that the iron content of reconstituted BioB varied considerably depending on the reconstitution method used (Section 8.2.4.1; p. 128) and thus far no method was found to reproducibly form a single iron-sulphur cluster (Table 2.2).

Date	01/03/01	06/03/01	12/03/01	13/03/01	21/02/02
Sample	BioB	BioB	BioB	BioB	His_6-BioB
Reconstitution method	I	II	I	II	III
Fe mol / BioB monomer mol	4.4	3.57	6.3	6.0	5.56

Table 2.2: Iron content of reconstituted BioB

Figure 2.17 shows the UV/visible spectrum of BioB from an aerobic purification and after anaerobic reconstitution. A change in the spectrum between 400 to 600 nm is observed. The observed maxima at ~ 450 nm and ~ 410 nm could be consistent with the presence of a $[2Fe\text{-}2S]^{2+}$ cluster and a $[4Fe\text{-}4S]^{2+}$ cluster (63). However, it has to be noted that UV/visible spectroscopy gave highly variable results probably due to a difference in sample preparation, oxygen and protein concentration. An assignment of iron-sulphur cluster states would require more vigorous analytical investigations, which were not available.

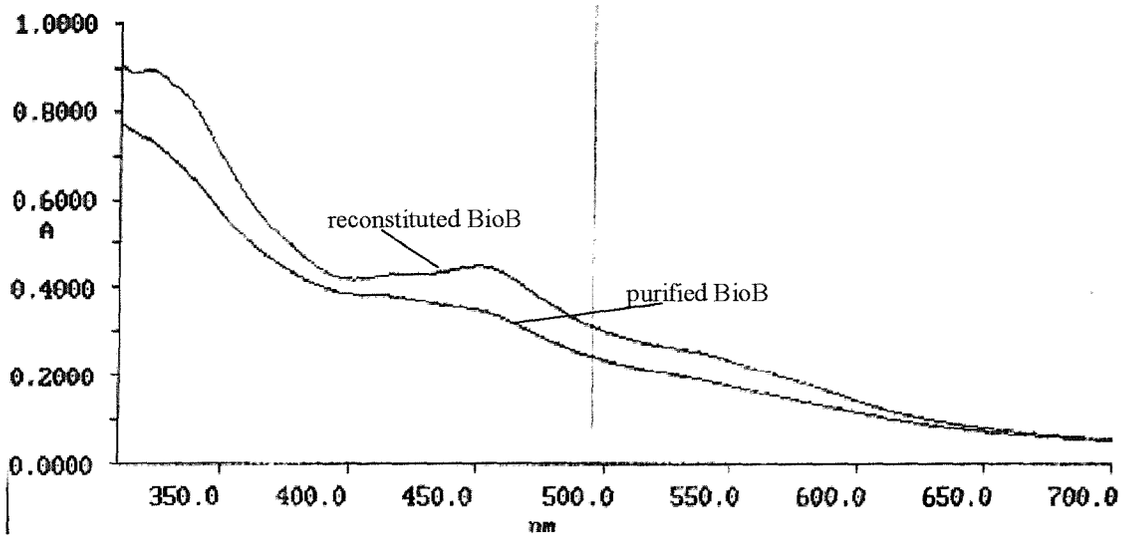

Figure 2.17: UV/visible spectrum of BioB from an aerobic purification and after anaerobic reconstitution.

2.5 Summary

Several protocols were used to purify BioB from pKH200/BL-21(DE3). Using dye affinity chromatography as the last step increases the purity by binding BioB specifically and removing a ~ 50 kDa impurity. This purification procedure can be used if BioB without an affinity-tag is needed. Intein mediated purification of a fusion protein with an affinity Chitin-binding tag is possible but is low yielding and was therefore not pursued.

The purification of His_6-BioB gave routinely 150 mg BioB of highest purity from ~ 30 g of cell paste, or 400 mg BioB of highest purity from ~ 60 g of cell paste. Thus it was the method of choice for the purification of enzyme for the *in vitro* assay.

Reconstituted BioB varied in the final amount of protein bound iron present, due to a number of factors such as the original iron and sulphide content and reconstitution conditions. In addition, the sulphide concentration was difficult to estimate (wet Na_2S as standard solution) and the inaccuracy of the Bradford assay or alternatives in estimation the protein concentration made an exact distinction or assignment of different iron-sulphur cluster forms difficult. However, for experiments assaying the *in vitro* activity of BioB, this was less of a problem, as the empirically determined optimum of the iron and sulphide to BioB ratio was used throughout (Section 4.4).

Chapter Three: Investigation of two *in vitro* systems to assay biotin formation

3.1 Introduction

Catalytic activity *in vitro* has not thus far been reported for the conversion of dethiobiotin (DTB) to biotin (43,63). This led to the hypothesis that some components, which might include proteins or small molecules, are missing *in vitro* (43,63) or alternatively that it is impossible to achieve a high degree of catalytic turnover because of the intrinsic constraints of the reaction, i.e biotin synthase is a reagent. To investigate if it is possible to lift the constraints of the last step in the biosynthesis of biotin *in vitro*, two assay systems were investigated.

The key practical requirement for investigating the limitation of biotin production is a good assay for biotin, DTB and other components. There are three assays that have been used to measure the activity of biotin synthase.. The first is a microbiological assay that utilises either *E. coli* KS302Δ*bio* or *Lactobacillus plantarum* (99,100). Both of these organisms lack the biotin operon and thus are biotin auxotroph. The second, based on a radiochemical method, measures ^{14}C-DTB to ^{14}C-biotin conversion by autoradiography (43). The third assay detects biotin formation by HPLC (63). Thus, biological, radiochemical and chromatographic assays had been reported in the literature. Each of the three assay methods was investigated. After an initial investigation of a biological assay using *Lactobacillus plantarum*, it was rapidly discarded, as it proved highly unreliable and laborious. Radiochemical (Section 3.2) and chromatographic (Section 3.3) assays were investigated in detail.

3.2 Radiochemical method for biotin detection *in vitro*

Birch *et al.* developed a radiochemical method using ^{14}C-DTB for the measurement of biotin synthase activity *in vitro* (43). ^{14}C-DTB was enzymatically synthesised using dethiobiotin synthase (DTBS).

3.2.1 Construction of pET11a:bioD

The *bioD* gene encoding DTBS was amplified from genomic DNA of *E. coli* using appropriate primers (Section 8.3.1). Construction of the plasmid followed Method D (Section 8.7.3). The PCR product was digested and inserted into the pET11a(+) vector (Novagen) and transformed into BL-21(DE3). The obtained plasmid was designated pET11a:bioD (Figure 3.1).

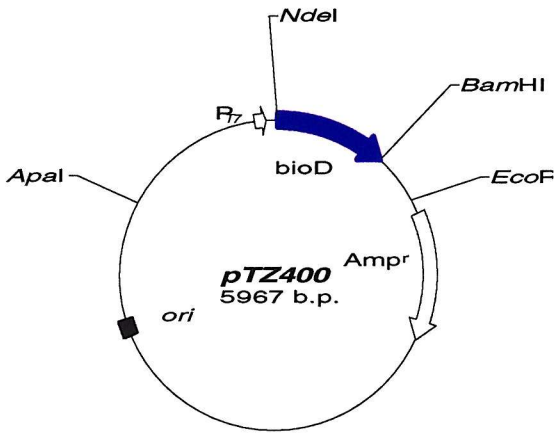

Figure 3.1: Plasmid map of pET11a:bioD including prominent restriction sites

The resulting plasmid was checked by DNA gel electrophoresis and restriction digestion (Figure 3.2).

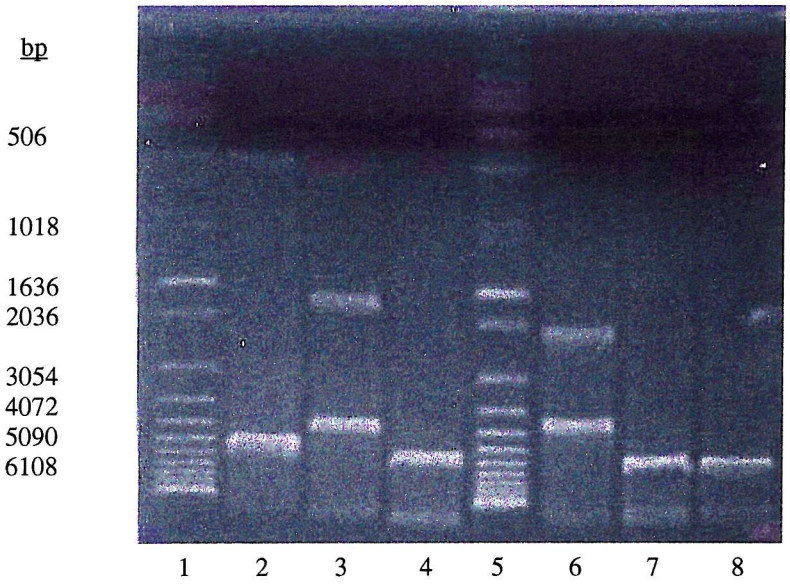

Figure 3.2: Restriction digestion of pET11a:*bioD*, (1) Marker, (2) NdeI/BamHI, (3) ApaI/BamHI, (4) NdeI, (5) Marker, (6) NdeI/EcoRI, (7) EcoRI, (8) ApaI.

3.2.2 Purification of *E. coli* dethiobiotin synthetase (DTBS)

DTBS was purified using anion exchange chromatography (Figure 3.3) and gel filtration chromatography (Figure 3.4).

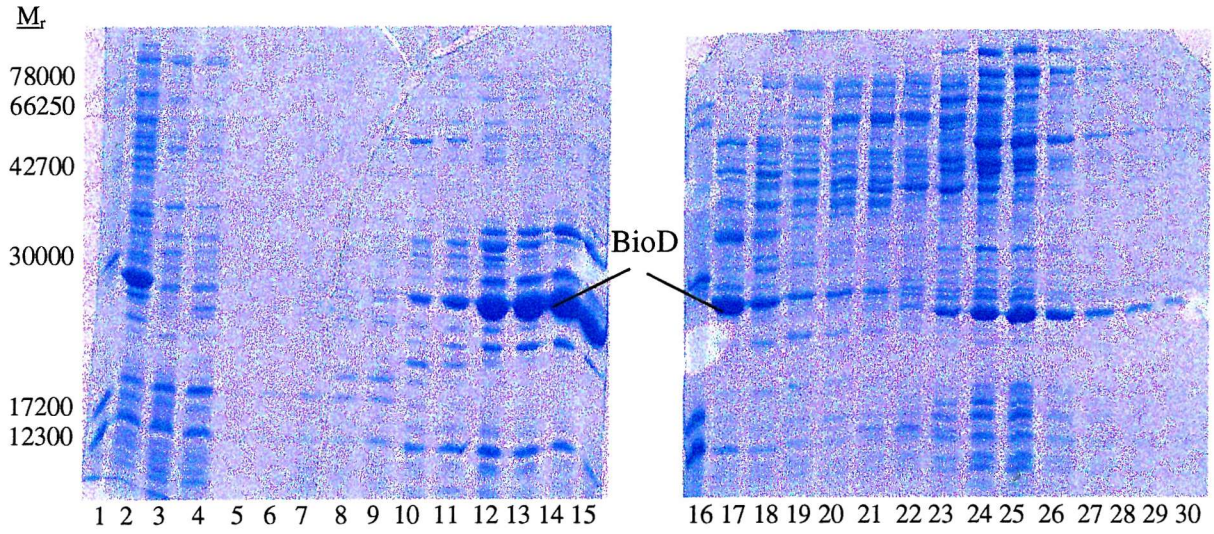

Figure 3.3: Coomassie Blue stained 15 % SDS-PAGE gel. (1), (16) Molecular weight markers, (2) Load, (3), (4) flow through, (5) – (30) fractions eluting from the anion exchange column. Fraction (12) – (15), (17) were pooled and submitted to gel filtration chromatography.

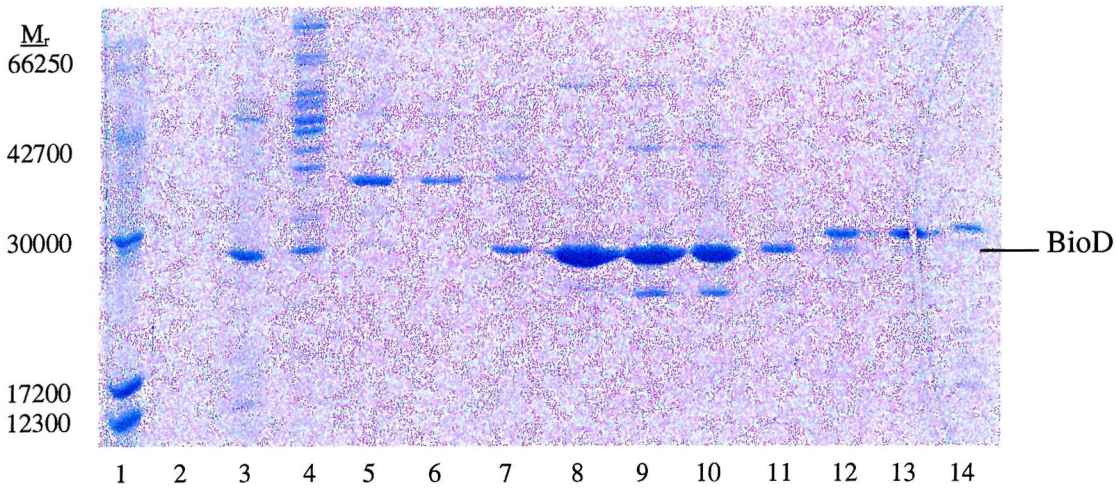

Figure 3.4: (1) Molecular weight markers, (2) – (14) fractions eluting from the gel filtration column, (8) – (10) were pooled and used for ^{14}C-DTB synthesis.

3.2.3 Enzymatic synthesis of ^{14}C-DTB

The protocol for ^{14}C-DTB synthesis (Section 8.3.4) was kindly provided by Dr. K. Hewitson (Oxford University). The radiochemical yield was low (20 and 35 %). However, ^{14}C-DTB could be used for the *in vitro* assay, so the protocol was not further optimised which might allow for a higher yield.

3.2.4 Initial *in vitro* assay for biotin formation

Birch *et al.* developed an *in vitro* assay system for the last step of the biosynthesis of biotin (43). In this assay a cell-free extract from an *E. coli* strain containing a cloned *bioB* gene is incubated with ^{14}C-DTB. Several low- and high molecular weight compounds were identified as being required for biotin formation (Table 3.1). After purification on a solid phase extraction column, ^{14}C-DTB and ^{14}C-biotin were separated by TLC and detected by autoradiography.

Compound	**Final Conc.**	**Compound**	**Final Conc.**
E. coli lysate	~ 20 mg/ml	Fe(II)-Gluconate	500 µM
E. coli lysate (overexpressing BioB)	~ 20 mg/ml	^{14}C-DTB (57 mCi/mmol)	5 µM
Asparagine	9.3 mM	Buffer	50 mM Hepes pH: 7.5
TPP	250 µM	**Time**	1 hour
NADPH	250 µM	**Anaerobic**	No
Cysteine	500 µM	**Volume**	250 µl
DTT	250 µM	**Termination**	250 µl 12.5% TCA
SAM	230 µM	**Detection**	Autoradiography (^{14}C-DTB/^{14}C-biotin)

Table 3.1: *In vitro* assay conditions as described by Birch *et al.* (43)

The above conditions were used for initial assays with pKH200/BL-21(DE3) and BL-21(DE3) lysate to establish a functioning assay (Figure 3.5). As can be seen in Figure 3.6, the enzymatic synthesis of ^{14}C-DTB was successful (Lane 1) and the incubation of ^{14}C-DTB with the necessary co-factors lead to biotin formation (Lane 2). Measurement of the ^{14}C-DTB and ^{14}C-biotin amount was possible by scraping the TLC plate and scintillation counting of the material. This gave 840 pmol for ^{14}C-DTB and 130 pmol for ^{14}C-biotin. The amount of BioB used in this experiment was estimated as 10 nmol, suggesting low turnover (1.3 %).

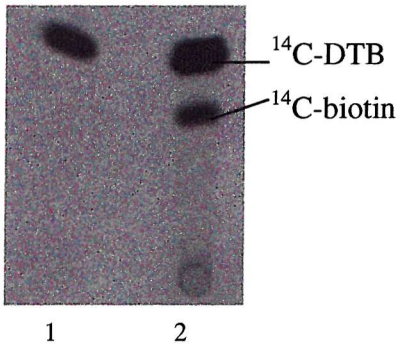

Figure 3.5: ^{14}C-DTB to ^{14}C-biotin conversion using reaction conditions from Table 3.1

3.3 Detection of biotin formation *in vitro* by HPLC

Ugulava *et al.* rationalised and simplified the reaction conditions for the last step in the biosynthesis of biotin (63) (Table 3.2). This made it possible to use HPLC to separate the low molecular weight compounds and detect biotin and DTB in the assay mixture by using a UV/Vis detector at 200 nm.

Compound	**Final Conc.**	SAM	500 µM
BioB	30 µM	DTB	200 µM
DTT	10 mM	Buffer	50 mM Tris-HCl pH 7.5, 10 mM KCl
$FeCl_3$	200 µM	**Time**	3 hours
Na_2S	200 µM	**Anaerobic**	Yes
NADPH	1 mM	**Volume**	0.2 – 2 ml
Fdr	4 µM	**Termination**	10 – 100 µl sat. sodium actetate, pH 4
FldA	10 µM	**Detection**	200 nm by RP-HPLC

Table 3.2: *In vitro* assay conditions as described by Ugulava *et al.* (63)

Separation and detection of biotin and DTB by HPLC

The absorbance at 200 and 254 nm was recorded and peaks integrated with Gilson Unipoint software. 10 to 200 µM biotin could be readily detected at 200 nm and the biotin peak is well resolved from the DTB peak (Figure 3.6).

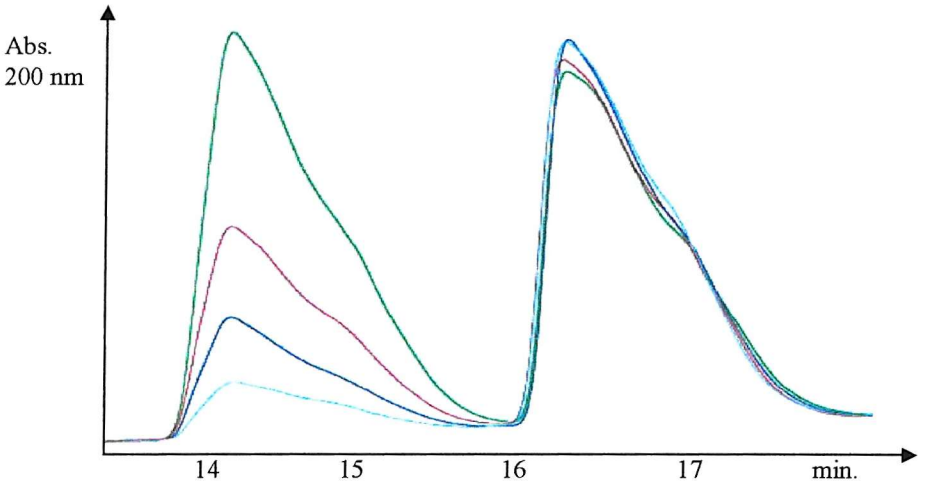

Figure 3.6: Separation of biotin (R_t, 14.5 min.) and DTB (16.5 min.) standards. Concentration of biotin 25, 50, 100 and 200 µM; DTB concentration: 200 µM; [Method I; HPLC\Results\dtb.biotin1\2-6]. The scale is relative to the absorbance of other co-factors as shown in Figure 4.12 (p. 51).

Biotin and DTB were separated under various conditions (Section 8.3.6). Solutions of biotin and DTB of known concentrations were analyzed and this data was used to prepare a calibration curve (Section 8.3.7). This assay could also be used to measure the biotin and DTB present in whole assays. Protein components were removed by either acid precipitation or the usage of MWCO membrane filter.

Figure 3.7 shows biotin formation in a typical standard mixture as given in Table 3.2.

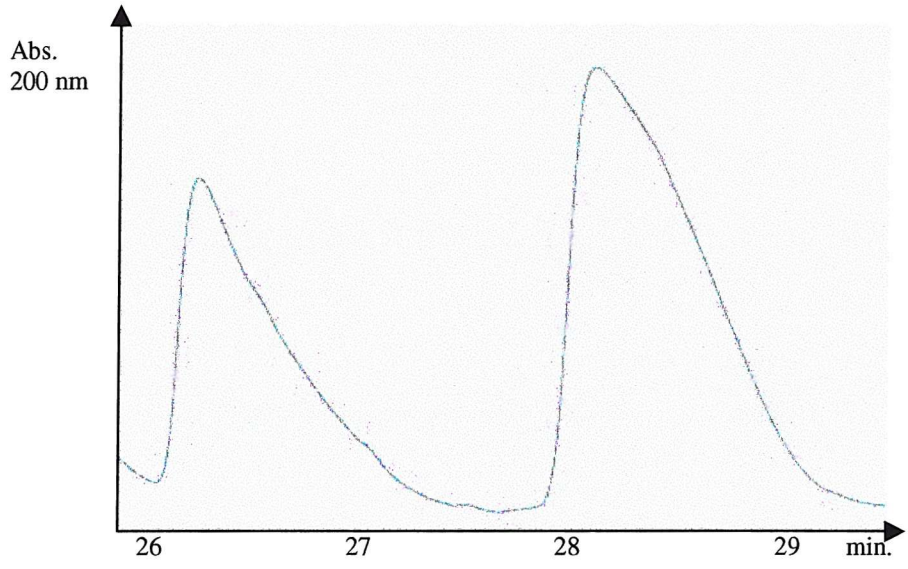

Figure 3.7: Separation of biotin (Rt, 26.5 min.) and DTB (28.5 min.) from other low molecular weight compounds after *in vitro* biotin formation. Calculated concentration of original sample: 40 µM biotin, 150 µM DTB. [Method III; HPLC\Results\inh8\RP2.004\2]

3.3.1 ^{14}C-DTB to ^{14}C-biotin conversion

The *in vitro* conditions proposed by Ugulava *et al.* (Table 3.2) simplified the assay in comparison to the radiochemical assay of Birch *et al.* (Table 3.1). ^{14}C-DTB to ^{14}C-biotin conversion was investigated with the reaction conditions proposed by Ugulava *et al.* (Figure 3.8).

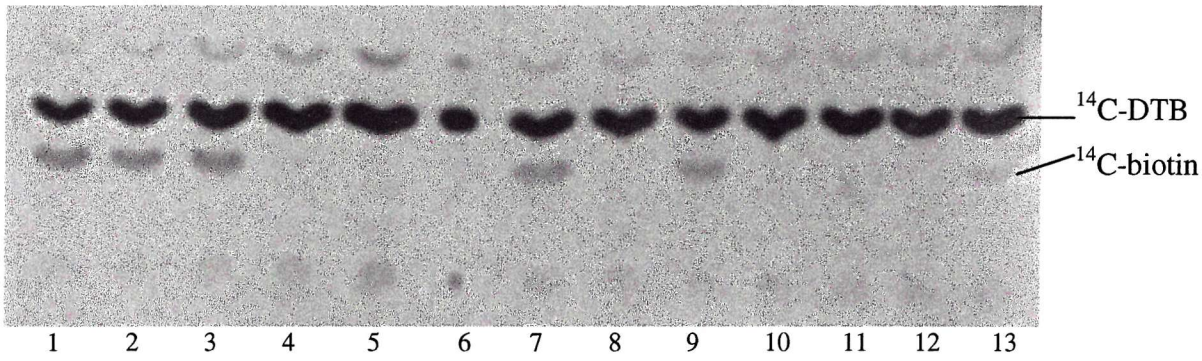

Figure 3.9: Autoradiography of *in vitro* assays: (1) to (3): 100 µl ,150 µl, 250 µl final assay volume, (4) minus Fe^{3+}, (5) minus DTT, (6) ^{14}C-DTB standard, (7) SAM 250 µM, (8) minus SAM, (9) NADPH 500 µM, (10) minus NADPH, (11) minus flavodoxin, (12) minus flavodoxin reductase, (13) minus sulphide.

3.4 Summary

Two *in vitro* systems have been used to investigate the last step in the biosynthesis of biotin the conversion of DTB to biotin. In the assay by Birch *et al.* (43) a cell-free extract from an *E. coli* strain containing a cloned *bio*B gene is incubated with ^{14}C-DTB. There are several drawbacks to the radiochemical method. Quantification of ^{14}C-biotin is difficult and erroneous and the assay is laborious and hazardous. However, investigating this assay system Birch *et al.* were able to identify essential protein components for *in vitro* formation of biotin (43,58). It also led to the discovery of a labeled intermediate generated during the last step in the biosynthesis of biotin in *E. coli* (51).

Ugulava *et al.* (63) simplified the assay conditions. Instead of cell-free lysate, purified protein components were used. This made it possible to use HPLC to separate the low molecular weight compounds and detect biotin and DTB in the assay mixture at 200 nm. Investigating this assay, Ugulava *et al.* could follow the spectroscopic changes occurring within the iron-sulphur cluster of BioB during turnover and could get more detailed information about the iron-sulphur cluster redox state of BioB.

Chapter Four: Investigation of *in vitro* biotin formation

4.1 Introduction

The two assay system described in Chapter Three were used to investigate biotin formation *in vitro*. The assay conditions were modified to optimise turnover of DTB into biotin.

4.2 Time course of biotin formation

With the HPLC based assay and the detection of biotin and DTB at 200 nm, it was possible to obtain more accurate quantitative data on the conversion of DTB into biotin in the range of 10 – 200 μM final concentration. Figure 4.1 shows a time course formation of biotin over a period of 210 min.

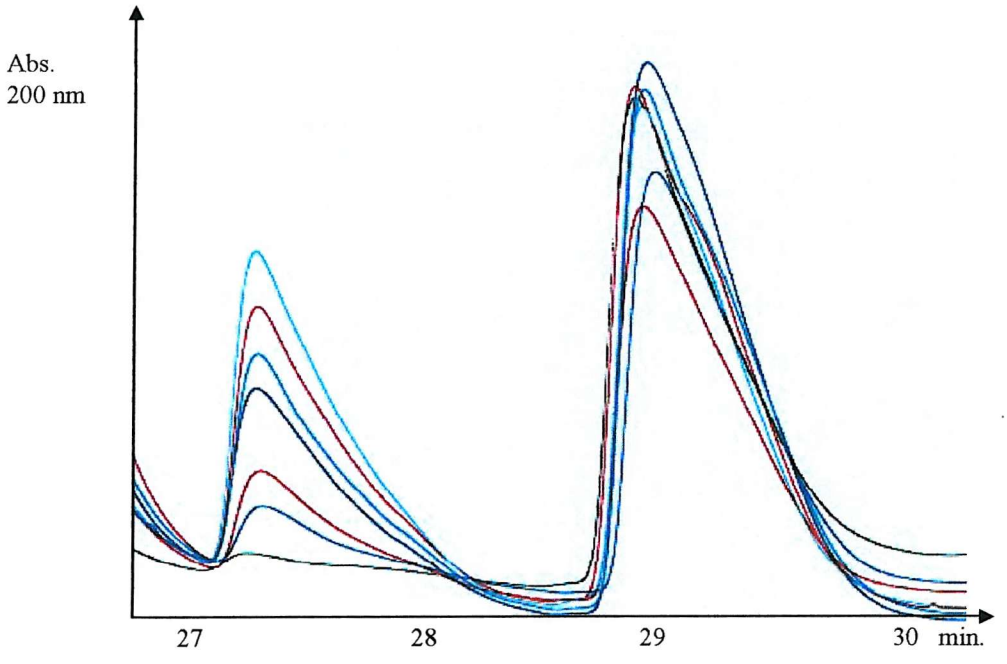

Figure 4.1: HPLC traces for the time course assay, Biotin (R_t, 27.5 min.) and DTB (R_t, 29.3 min.). Time points were 0, 30, 60, 90, 120, 180, and 210 min.; [Method III; HPLC\Results\time.co-fact\RP2.001\2,3,5,8,10,12,16]. The scale is relative to the absorbance of other co-factors as shown in Figure 4.12 (p. 51).

The calculated values can be found in Table 4.1.

Time (min.)	Biotin I (Area) *10^5	Biotin II (Area) *10^5	DTB I (Area) *10^5	DTB II (Area) *10^5	Biotin I [µM]	Biotin II [µM]	DTB I [µM]	DTB II [µM]
0	0.14	0.26	11.18	11.55	0.00	0.00	88.28	91.40
30	1.07	1.61	10.70	9.98	1.21	3.56	84.24	78.18
60	1.91	2.80	9.44	11.77	4.88	8.81	73.63	93.31
90	3.79	4.09	13.18	14.16	13.14	14.48	105.19	113.45
120	4.48	4.85	13.59	13.08	16.19	17.79	108.62	104.35
150	5.65	4.98	12.77	12.33	21.33	18.36	101.68	97.97
180	6.76	6.17	12.42	10.99	26.19	23.61	98.75	86.71
210	7.25	6.72	12.48	11.73	28.33	26.00	99.29	92.90
240	7.15	7.28	13.09	10.98	27.90	28.48	104.40	86.61

Table 4.1: Values for the time course experiment, I and II represent duplicate assays.

Figure 4.2 plots biotin formation versus time for the values found in Figure 4.1 (calculated in Table 4.1).

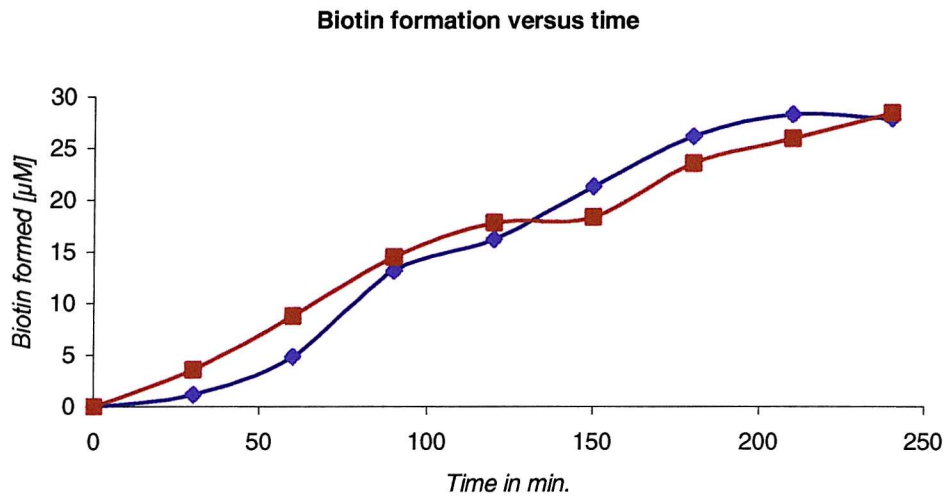

Figure 4.2: Time course experiment for biotin formation (σ: 0.98).

Biotin increased gradually over time. After a period of three to four hours ~ 30 µM biotin were formed, which correlates roughly to one mol of biotin formed per mol of BioB present in the assay.

4.3 DOA formation *in vitro* and stoichiometry of its use

The use of MWCO membrane filter improved the chromatography of the small molecule components at the end of the assay period (Section 4.6). Figure 4.3 shows DOA formation over a period of 240 min. The distorted peak shape might be due to the use of a gentle gradient in this separation method.

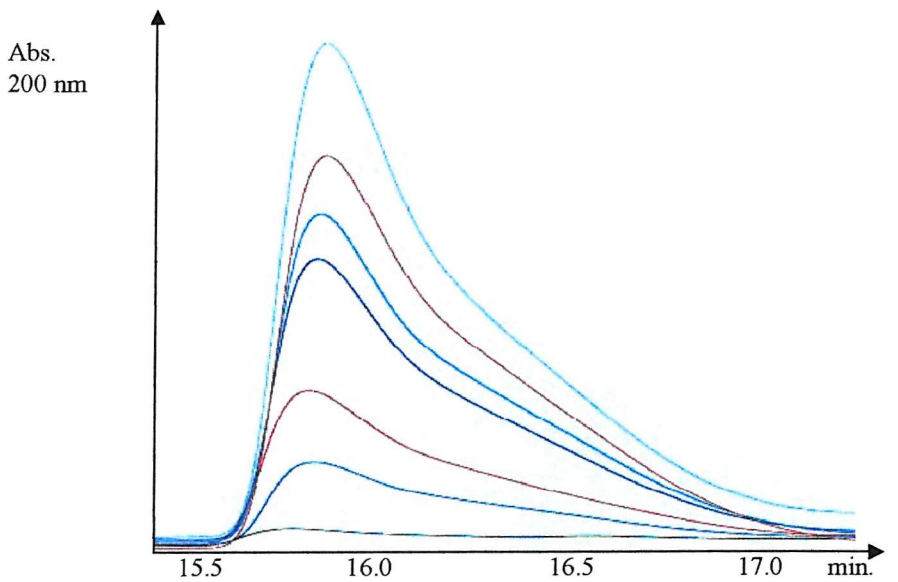

Figure 4.3: HPLC traces for the time course assay, DOA (Rt, 16.0 min.), Time points were 0, 30, 60, 90, 120, 180 and 210 min. [Method III; HPLC\Results\time.co-fact\RP2.001\2,3,5,8,10,12,16]. The scale is relative to the absorbance of other co-factors as shown in Figure 4.12 (p. 51).

DOA peaks were integrated, the calculated values can be found in Table 4.2.

Time (min.)	DOA I (Area) *10^5	DOA II (Area) *10^5	DOA I [µM]	DOA II [µM]
5	1.56	1.59	5.20	5.22
30	10.78	13.37	15.92	18.94
60	19.71	22.73	26.33	29.84
90	39.64	38.92	49.53	48.68
120	43.94	45.16	54.53	55.95
150	52.54	51.76	64.54	63.63
180	59.66	56.20	72.83	68.80
210	62.10	63.70	75.67	77.54
240	57.12	67.75	91.08	82.25

Table 4.2: Values for the time course experiment, I and II represent duplicate assays.

A plot of DOA formation versus time for two duplicate experiments is depicted in Figure 4.4.

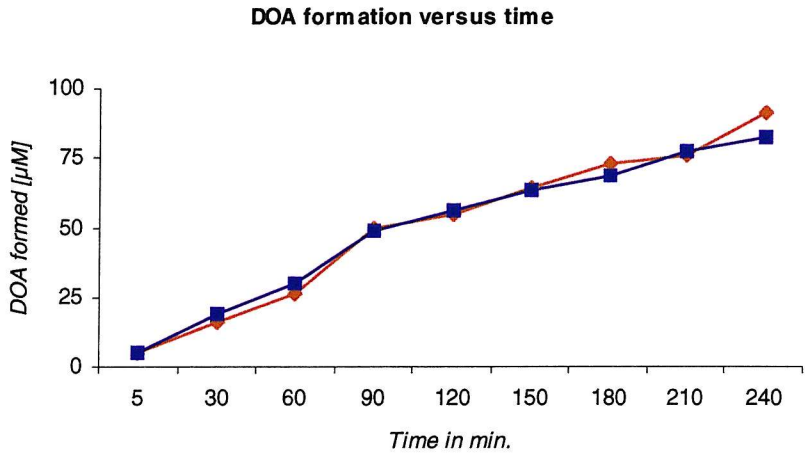

Figure 4.4: Time course experiment for DOA formation (σ: 0.97).

In Figure 4.5 the amount of DOA and biotin formed is plotted versus time to investigate the stoichiometry of biotin versus DOA formation.

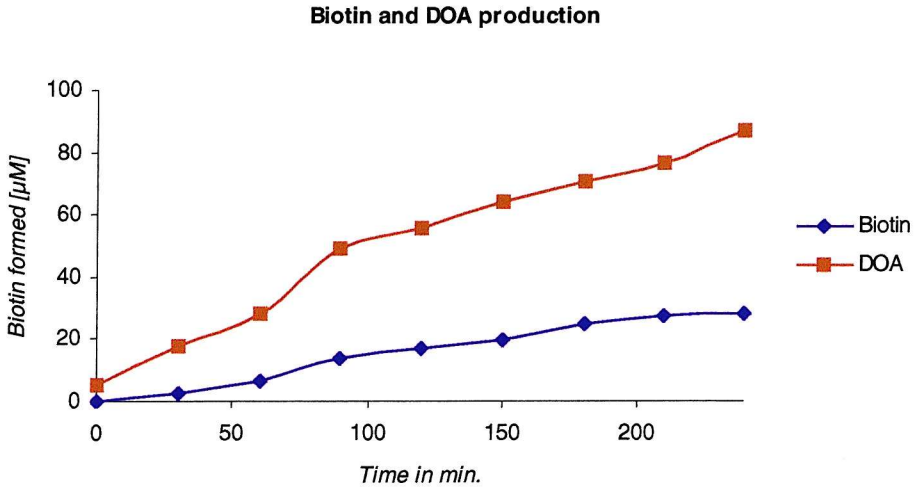

Figure 4.5: DOA and biotin formation versus time, each curve represents the average of two duplicate assays.

Table 4.3 calculates the ratio of formed biotin and DOA.

Time (min.)	Biotin (µM)	DOA [µM]	Ratio (Biotin/DOA)
0	0.00	5.21	
30	2.38	17.43	
60	6.84	28.08	4.10
90	13.81	49.10	3.56
120	16.99	55.24	3.25
150	19.84	64.08	3.23
180	24.90	70.82	2.84
210	27.16	76.60	2.82
240	28.19	86.67	3.07

Table 4.3: The ratio of biotin to DOA formation. Values represent the average of duplicate experiments.

Shaw *et al.* quantified the methionine formed *in vitro* and found a close to 2:1 ratio per mol biotin formed after a period of 30 min (51). After this initial period the ratio was closer to 3:1. They suggested that one molecule of SAM might be used for the conversion of DTB to the intermediate and two molecules for the conversion of the intermediate to biotin, or vice versa. This could explain the 3:1 ratio (mol DOA per mol biotin) found by Guianvarc'h *et al.* (53). In the above assay the DOA to biotin ratio is initially closer to 4:1. However, DOA is not formed in the absence of DTB but is formed in the standard assay (Figure 4.6).

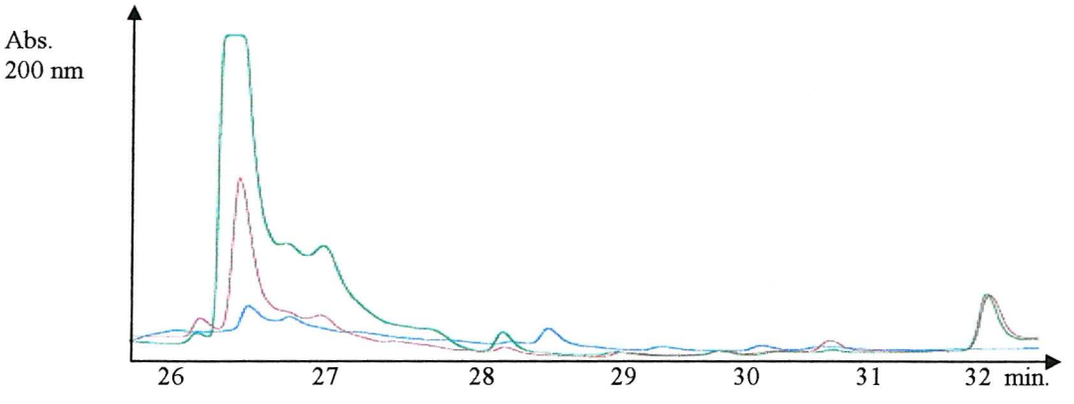

Figure 4.6: HPLC traces for DOA formation in the absence of DTB, DOA (Rt, 26.5 min.); standard assay (Biotin R_t: 30.6 min.; 12 µM), standard assay without DTB, standard assay plus 400 µM DOA and 400 µM methionine (Section 6.6); [Method III; HPLC\Results\added\rp210\4,5,7]. The scale is relative to the absorbance of other co-factors as shown in Figure 4.12 (p. 51).

4.4 Effect of iron and sulphide *in vitro*

The reaction mixture optimised by Ugulava *et al.* includes all essential compounds to convert DTB into biotin (63). The rationale for these assay conditions is that first BioB is reconstituted containing one $[4Fe\text{-}4S]^{2+/1+}$ cluster and one [2Fe-2S] per monomer (incubation of DTT, Fe^{3+}, S^{2-}, BioB for 10 min.), followed by generation of the DOA radical (incubation with SAM, NADPH, FldA and Fdr for 10 min.). The conversion starts with the addition of DTB. Ugulava *et al.* suggested that BioB is only capable of participating in the conversion if each BioB monomer contains one $[4Fe\text{-}4S]^{2+/1+}$ cluster and one [2Fe-2S] for a total of six iron and six sulphur per polypeptide chain. BioB with a lower or higher amount of iron and sulphide should not be able to participate in the reaction effectively. In Figure 4.7 the amount of iron added to the assay was varied to investigate this hypothesis.

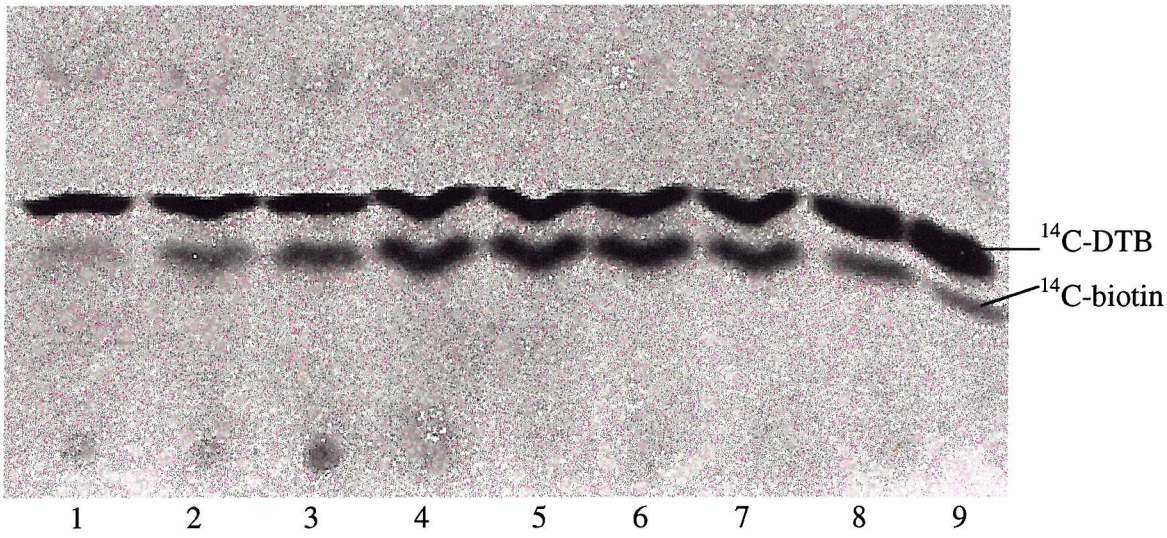

Figure 4.7: Autoradiography of *in vitro* assays (Assay conditions as in Table 3.2): Increase in Fe^{3+} concentration, constant sulphide concentration: 200 µM, (1) 0 µM, (2) 12,5 µM, (3) 25 µM, (4) 50 µM, (5) 100 µM, (6) 200 µM, (7) 400 µM, (8) 800 µM, (9) 1,6 mM.

The amount of iron added *in vitro* in the assay has a strong effect on biotin formation. As the BioB concentration is 40 µM, the peak activity would be expected to be approximately 240 µM. The hypothesis that the active species in the conversion of DTB

to biotin is BioB's $[4Fe\text{-}4S]^{2+/1+}$/[2Fe-2S] cluster is thus feasible. Table 4.4 shows the results for the effect of iron *in vitro* found by using the HPLC based detection of biotin.

Fe [µM]	Biotin I (Area) $*10^5$	Biotin II (Area) $*10^5$	Biotin I [µM]	Biotin II [µM]
0	0.38	0.24	0	0
37.5	3.67	3.75	12.61	12.99
75	4.47	4.67	16.12	16.99
150	4.60	4.47	16.69	16.12
225	5.16	5.12	19.18	19.00
300	4.91	4.80	18.06	17.57
375	3.47	3.74	11.74	12.94
450	3.55	3.68	12.09	12.65

Table 4.4: Values for Figure 4.8, I and II represent duplicate assays; [Method II; HPLC\Results\added\RP21\5 - 22].

Figure 4.8 plots the biotin formation versus iron concentration.

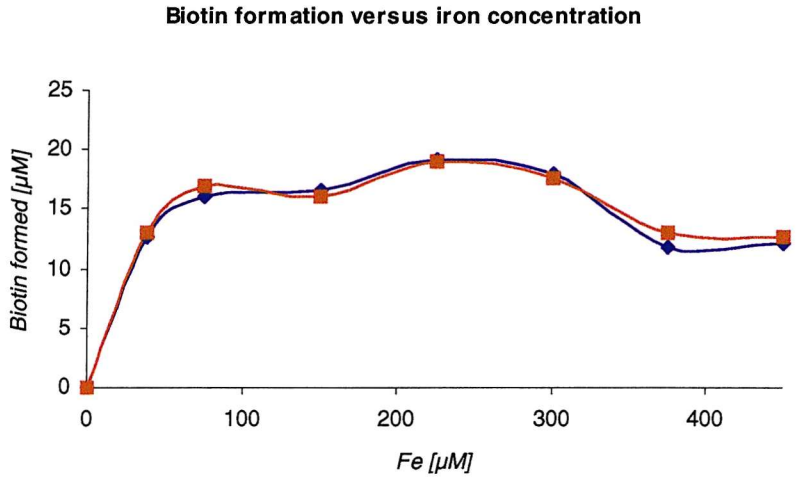

Figure 4.8: Effect of increased iron concentration on biotin formation (σ: 0.26).

These results give a better quantitative measurement and are consistent with the above results found using the radiochemical method.

The effect of an increasing sulphide concentration was investigated (Figure 4.9).

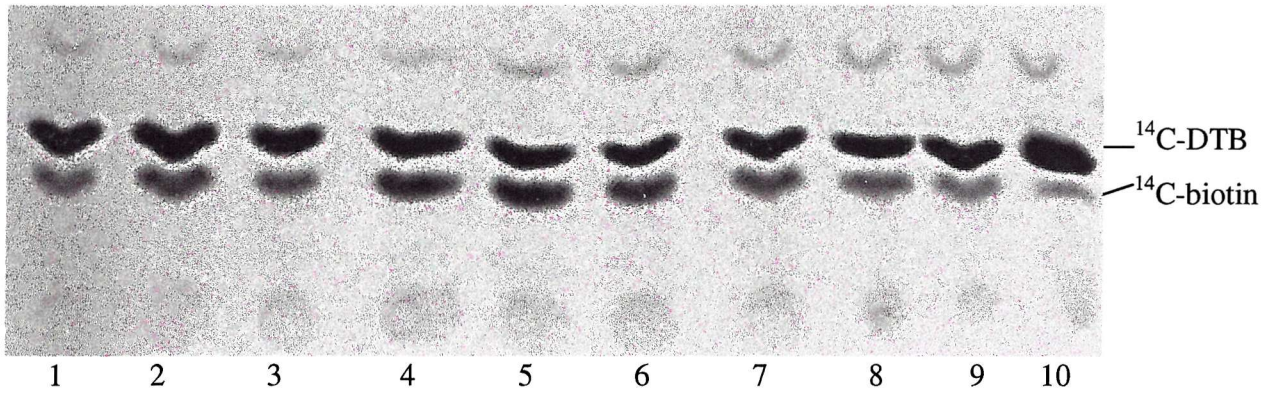

Figure 4.9: Autoradiography of *in vitro* assays (Assay conditions as in Table 3.2; 72 hours exposure to photographic film): Increase in sulphide concentration, constant Fe^{3+} concentration of 200 µM, (1) 0 µM, (2) 12,5 µM, (3) 25 µM, (4) 50 µM, (5) 100 µM, (6) 200 µM, (7) 400 µM, (8) 800 µM, (9) 1.6 mM, (10) 3.2 mM.

The effect of exogenous sulphide on biotin formation is not as pronounced as the effect of iron. Less exogenous sulphide is required for optimal activity.

4.4.1 Timed addition of iron and sulphide *in vitro*

If BioB is unable to participate in the conversion of DTB to biotin after one reaction cycle because the iron-sulphur cluster is depleted in sulphur (Section 1.3), the addition of exogenous sulphur and iron *in vitro*, in addition to the iron and sulphide present for reconstitution, might enhance biotin formation. Table 4.5 and 4.6 show the results for this experiment.

Addition of iron and sulphide	Biotin I (Area) $*10^5$	Biotin II (Area) $*10^5$	Biotin I [µM]	Biotin II [µM]
2.5 eq. Fe	5.51	6.12	20.7	23.4
5 eq. Fe	5.00	5.50	18.4	20.7
2.5 eq. S	6.39	5.84	24.6	22.2
5 eq. S	6.29	5.77	24.1	21.8
2.5 eq. FeS	5.48	5.86	20.6	22.3
5 eq. FeS	6.64	6.03	25.7	23.0
standard assay	5.28	5.22	19.7	19.4

Table 4.5: Values for iron and sulphide addition at 30 min.; see Table 4.6 for details.

Addition of iron and sulphide	Biotin I (Area) $*10^5$	Biotin II (Area) $*10^5$	Biotin I [µM]	Biotin II [µM]
2.5 eq. Fe	6.41	6.63	24.6	25.6
5 eq. Fe	6.39	6.25	24.6	24.0
2.5 eq. S	6.65	6.56	25.7	25.3
5 eq. S	7.02	6.63	27.3	25.6
2.5 eq. FeS	6.77	6.46	26.2	24.9
5 eq. FeS	6.66	6.26	25.7	24.0
standard assay	7.11	6.71	27.7	26.0

Table 4.6: Values for iron and sulphur addition at 90 min., the assays were halted after 180 min.; I and II represent duplicate assays; eq: equivalent amount of iron and or sulphur added in regards to the BioB concentration, (30 µM); standard assay: no further addition of iron and sulphide; [Method II; HPLC\ Results\ added\ RP2.001\ 1-35; HPLC\Analysis\fe.sulfer1].

An equivalent amount of iron and sulphur was added in regards to the BioB concentration at 30 or 90 min. to provide exogenous iron and sulphide for the reconstitution of the iron-sulphur cluster of BioB, with the aim of increasing biotin formation. Slight increases in biotin formation were observed (Table 4.5).

4.5 Effect of asparagine, MioC, TPP and unlabeled DTB *in vitro*

Birch *et al.* (43) reported a vital role for MioC, TPP and asparagines in the turnover of biotin synthase. The influence of these compounds was therefore further investigated (Figure 4.10). As a low turnover of ^{14}C-DTB was observed for BioB in the standard assay, unlabeled DTB was added. The enzyme active sites might not be fully saturated and thus optimal activity for BioB is not observed. If a potential co-factor that enhances biotin formation is added in the presence of unlabeled DTB, a significant decrease in ^{14}C-DTB should be observed (Figure 4.10).

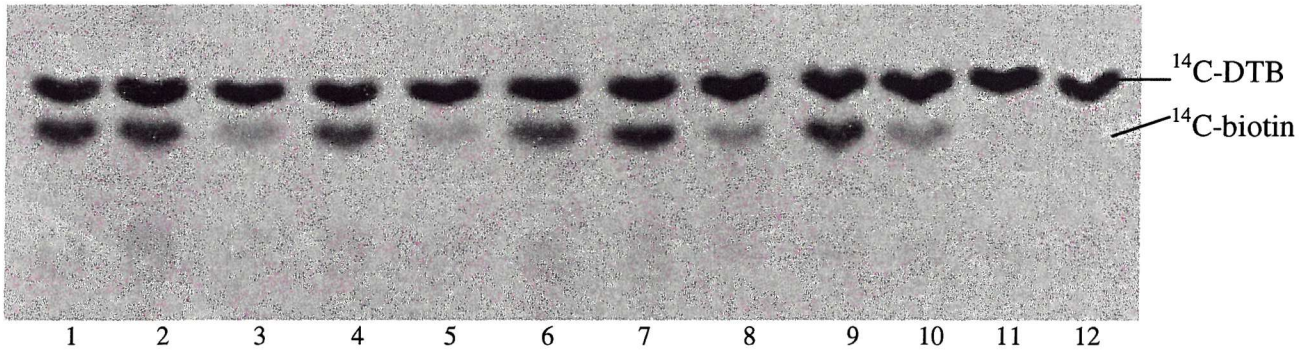

Figure 4.10: Autoradiography of *in vitro* assays (Assay conditions as in Table 3.2 plus 5 µM ^{14}C-DTB instead of 200 µM DTB; p. 37); (1) standard assay, (2) standard assay plus 2.5 µM ^{14}C-DTB, (3) standard assay plus 20 µM unlabeled DTB, (4) Fe^{3+} for Fe^{2+}, (5) Fe^{3+} for Fe^{2+} plus 20 µM unlabeled DTB, (6) standard assay, (7) standard assay plus 9.3 mM asparagine, (8) as (3) plus 9.3 mM asparagine, (9) standard assay plus 10 µM MioC, (10) as (3) plus 10 µM MioC, (11) standard assay minus BioB, (12) standard assay minus co-factors.

The addition of unlabeled DTB did not increase biotin formation. Furthermore, none of these potential co-factors greatly enhanced the biotin forming ability. This differs from the results found by Birch *et al.* (43). Further experiments were conducted (Table 4.7).

Sample	Biotin I (Area) $*10^5$	Biotin II (Area) $*10^5$	Biotin I [µM]	Biotin II [µM]
1	4.75	4.92	17.37	18.10
2	4.61	5.42	16.77	20.32
3	5.22	6.58	19.42	25.38
4	5.88	6.32	22.33	24.27
5	5.13	5.41	19.03	20.25
6	5.28	5.51	19.71	20.70
7	6.77	7.06	26.23	27.50
8	6.52	6.58	25.14	25.41
9	5.07	5.32	18.76	19.86

Table 4.7: see Figure 4.11 for details; I and II represent duplicate assays; [Method II; HPLC\Results\mioC.tpp\1-18].

Figure 4.11 shows the results found in Table 4.7.

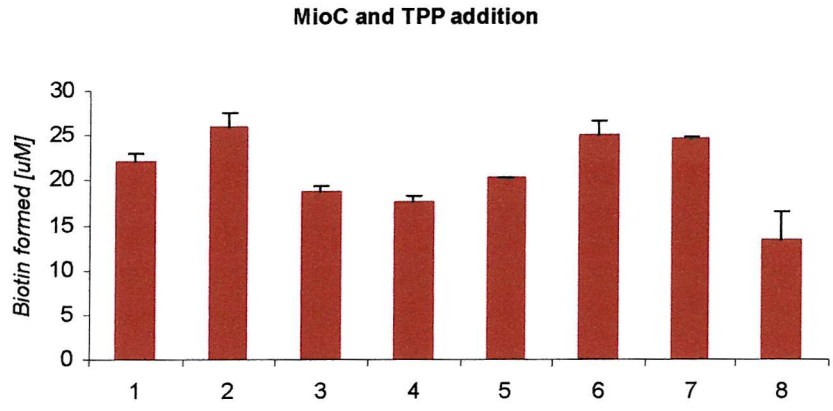

Figure 4.11: Addition of co-factors *in vitro*; (1) standard assay plus 15 µM MioC, (2) standard assay plus 30 µM MioC, (3) standard assay plus 150 µM TPP, (4) standard assay plus 300 µM TPP, (5) standard assay plus 15 µM MioC and 150 µM TPP, (6) assay plus 30 µM MioC and 150 µM TPP, (7) assay plus 30 µM MioC and 300 µM TPP, (8) standard assay.

The results of these assays did not suggest a strong effect of MioC and TPP on biotin formation *in vitro*. This is supported by the findings of Ugulava *et al.* (63), although it has to be noted that the assay conditions used by Birch *et al.* differed, as they used cell-free lysate instead of purified proteins.

4.6 Separation of small co-factors by HPLC

The use of MWCO membrane filter for sample preparation allowed a separation of hydrophobic from polar small molecular weight compounds (Figure 4.12). Peaks were assigned by the retention time of standards and comparison of TLC analysis of collected peaks and standard samples. This was an improvement over the method of Ugulava *et al.*, where the acid added to precipitate the proteins masked the peaks from more polar components. The use of MWCO membrane filters to remove the proteins from assay mixtures allowed the direct injection of the remaining low molecular weight components onto a RP-HPLC column.

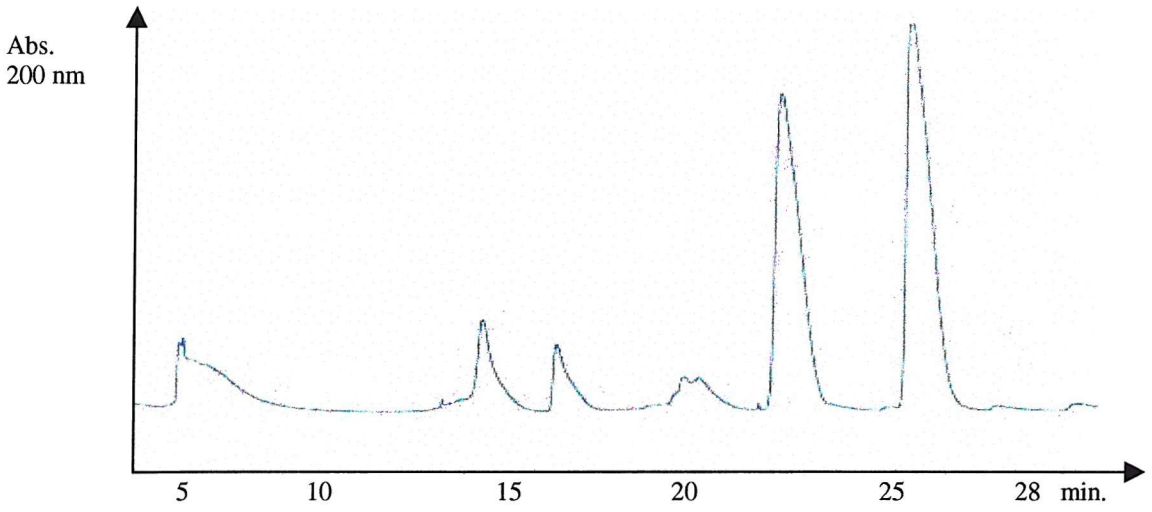

Figure 4.12: HPLC traces for separation of small molecular weight compounds; *in vitro* assay after 180 min.; [Method III; HPLC\ Results\time.course1\RP1.009\17]. Peaks are identified in Figure 4.13, 4.14 and Section 8.4 (p. 136).

4.6.1 DTT is present in the oxidized and reduced state *in vitro*

DTT is a potent reducing agent and with 10 mM final concentration present at a high concentration in the *in vitro* assay. Figure 4.13 shows the absorbance at 200 nm for 0 and 180 min. respectively.

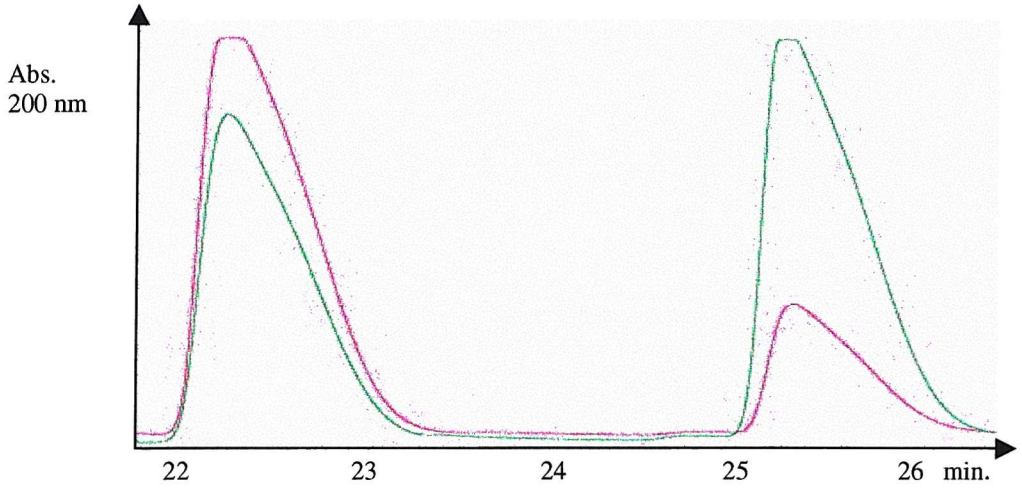

Figure 4.13: HPLC traces for separation of oxidised (R_t: 25 min.) and reduced (R_t: 22 min.) DTT; *in vitro* assay after 0 and 180 min.; [Method III; HPLC\ Results\time.course1\RP1.009\17].

4.6.2 Adenine is present *in vitro*

The adenine concentration *in vitro* increases with time in a reaction that appears to be unrelated to biotin formation (Figure 4.14).

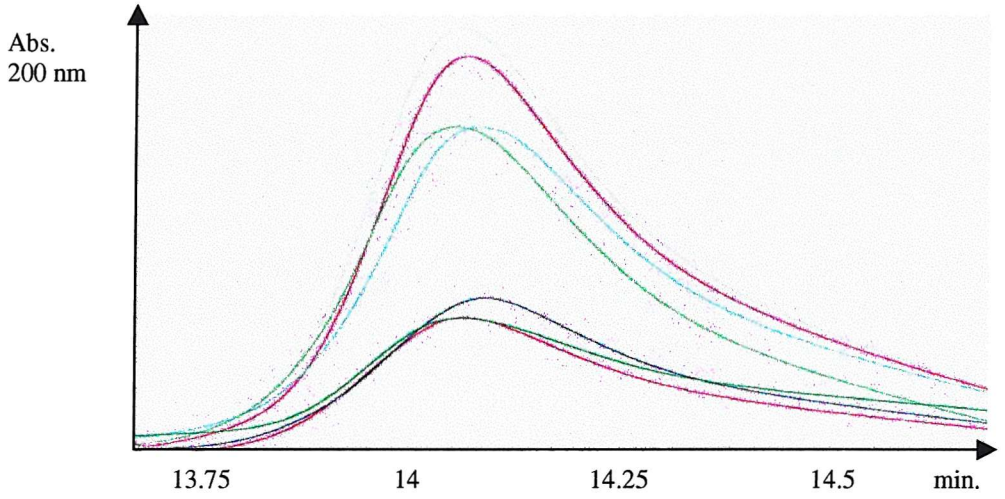

Figure 4.14: Adenine formation *in vitro* at 0, 30, 60, 90, 120, 150 and 180 min.; [Method II; HPLC\ Results\time.course1\RP1.009\17].

The amount of adenine formed is non-linear (Figure 4.14) with time and presumably derives from the hydrolysis of SAM (Figure 4.15, Scheme 4.1).

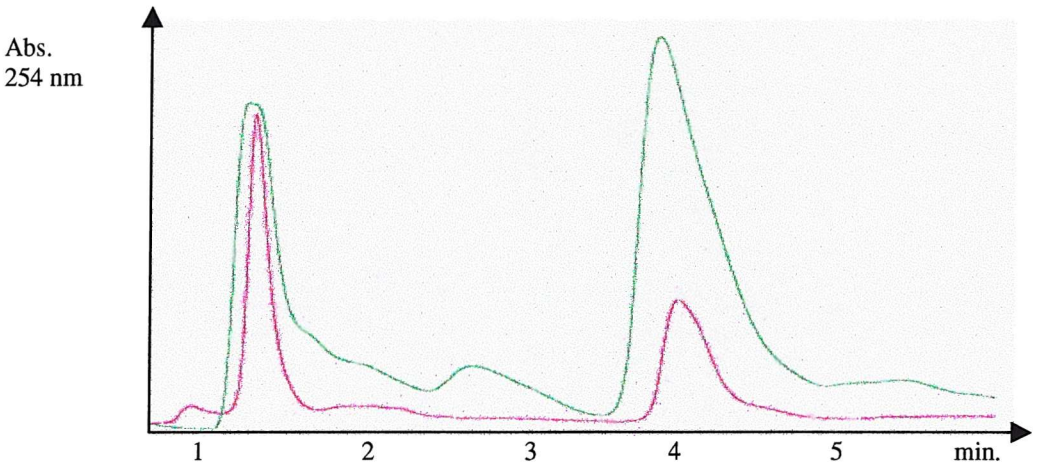

Figure 4.15: Adenine formation through SAM hydrolysis. SAM standard after 180 min., standard assay plus 250 µM adenine after 180 min.; [Method III; HPLC\ Results\added\rp210\9\rp2\2].

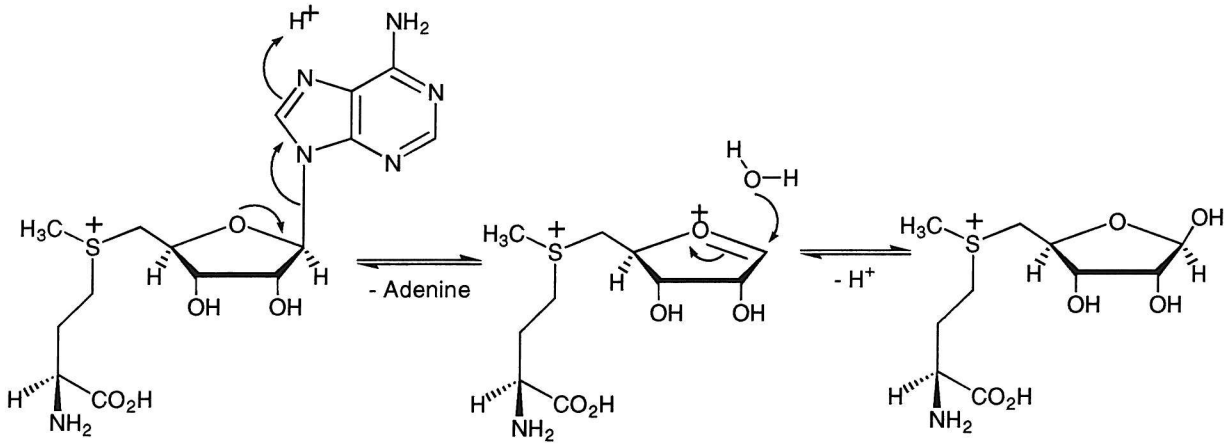

Scheme 4.1: Possible reaction for the hydrolysis of SAM, the formation of adenine **1**.

4.6.3 Biotin, DTB and DOA are present *in vitro*

Biotin, DTB and DOA could be detected by TLC (Section 8.4; p. 136)

4.6.4 FMN and FAD are present *in vitro*

In some experiments, acid precipitation is used to remove proteins. Acid precipitation of FldA and Fdr causes the release of the bound co-factors FMN and FAD respectively (Figure 4.16), which are both absorbing at 200 and 254 nm. Although the retention times are quite close to those for DTB and biotin, they can be differentiated, as DTB and biotin do not absorb at 254 nm (Figure 4.16).

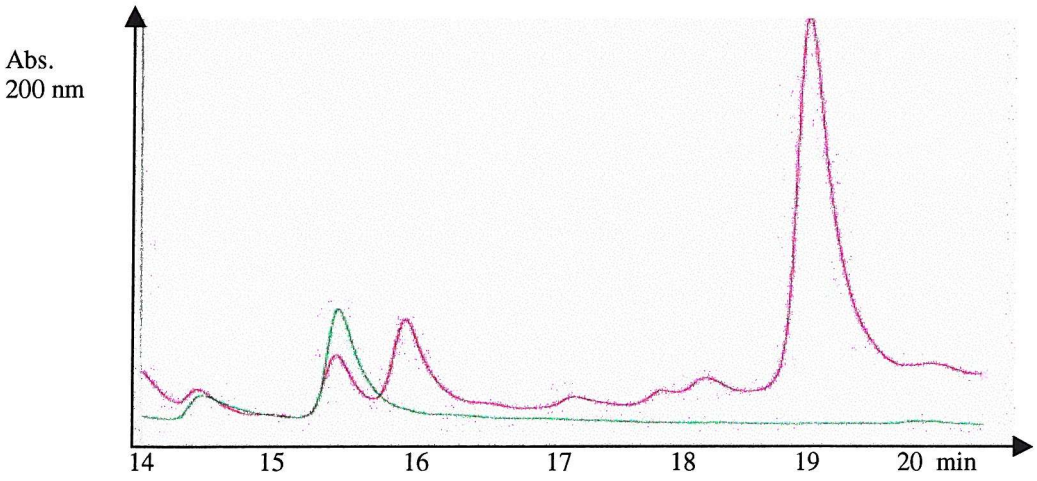

Figure 4.16: FAD (14.5 min.) and FMN (15.5 min.) separation from biotin (16 min.) and DTB (19 min.) (200 and 254 nm); [Method III; HPLC\Results\added\rp27\3].

Method III gave a good separation of FMN, FAD, biotin and DTB. However, great care has to be taken using acid precipitation to separate FMN from biotin. The amount of biotin formed *in vitro* will otherwise be overestimated. The alternative method preparation using MWCO membrane filters did not result in a release of bound co-factors (Figure 4.17).

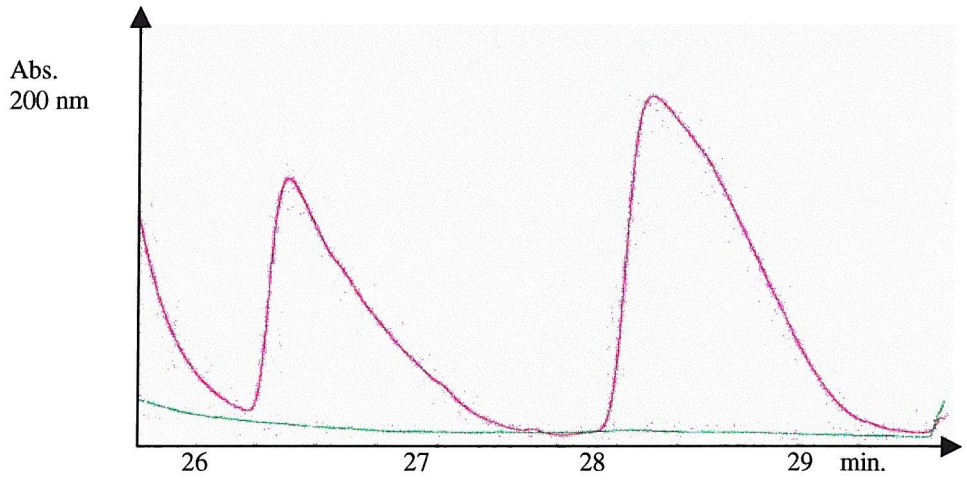

Figure 4.17: Sample preparation with MWCO (200 and 254 nm). Biotin (26.5 min.) and DTB (28.5 min.) with no absorbance at 254 nm. [Method III; HPLC\Results\inh8\RP2.004\2].

4.7 Summaries and Conclusions

Time course of biotin formation: Biotin formation could be observed in a time dependent manner, with approximately 1 mol of biotin is formed per mol of BioB monomer after roughly 180 min. The formation of biotin has been characterised by Jarret *et al.* using two first order rate constant (63). This was not reproduced in our experiment. Ugulava *et al.* investigated biotin formation at several time points and found that it proceeded with two phases with apparent first order rate constants over 2 h at 37 °C. Our results suggest a cautious approach for the calculation of the reaction rates for the *in vitro* assay. The average error is high (σ: 0.3 – 1.4) and assay results differ from experiment to experiment, which could be due to several reasons such as changes in the anaerobic environment, instable co-factors and variation in protein concentration. It would be tempting to investigate the effect of small molecules or protein co-factors on the rate constant *in vitro*, but at this stage the results may be misleading and inconsistent. Thus,

investigating the endpoint of biotin formation *in vitro* should provide data, which will be consistent among various research groups.

DOA formation *in vitro* and stoichiometry of its use: DOA formation could be observed in a time dependent manner. If two radical reactions were required by BioB, one to activate the methyl carbon and a second to activate the methylene carbon, this would be consistent with the use of two molecules of SAM per molecule of biotin formed. Shaw *et al.* quantified the formed methionine *in vitro* and found a close to 2:1 ratio per mol biotin formed after a period of 30 min (51). After this initial period the ratio was closer to 3:1. The conversion of DTB to biotin could proceed through formation of an intermediate that thus far has not been isolated and characterized. The intermediate was proposed to be 9-mercaptodethiobiotin (50). However, the intermediate isolated by Shaw *et al.* differed in its R_f value from 9-mercaptodethiobiotin. Shaw *et al.* argued that it is possible that one molecule of SAM is used for the conversion of DTB to the intermediate and two molecules for the conversion of the intermediate to biotin, or vice versa. This could explain the 3:1 ratio (mol DOA per mol biotin) found by Guianvarc'h *et al.* (53). In the above assay the DOA to biotin ratio is initially closer to 4:1 and DOA is not formed in the absence of DTB but is formed in the standard assay. A possible explanation for this could be the presence of an additional mol of intermediate or a different kind of intermediate, which could be converted into biotin or might be lost for biotin formation due to an alternative pathway. This hypothesis is consistent with the fact that routinely 40 to 70 µM DTB cannot be accounted for at the end point of the assay (Table 4.1; p. 41). After the activation of the methyl carbon, DTB might react with an unknown compound to give an unknown intermediate that cannot be converted to biotin. Recently, Fontecave *et al.* proposed that only one mol of SAM per mol of biotin is used (143). They found that BioB could bind PLP and potentially form a protein-bound persulphide by desulphuration of free cysteine, providing an oxidizing equivalent. The inconsistency with the above results is difficult to explain. Further experiments will need to compare results obtained by using similar assay conditions.

Effect of iron and sulphide *in vitro:* Ugulava *et al.* reconstituted BioB containing various iron-sulphur cluster and found that only BioB with one $[4Fe\text{-}4S]^{2+}$ cluster and one $[2Fe\text{-}2S]^{2+}$ cluster efficiently participated in biotin formation (63). Consistent with these findings, the *in vitro* peak activity was found to require a total of six iron and six sulphur

per polypeptide chain, both with the radiochemical method and detection of biotin formation by HPLC. However, iron and sulphide had to be added to the assay mixture to achieve optimal activity. If anaerobically reconstituted BioB was added, without any exogenous iron and sulphide present, the measurement of biotin formation became inaccurate and irreproducible (data not shown), probably due to difficulties in determining the exact nature of the iron-sulphur cluster present *in situ*. Thus, for experiments assaying the *in vitro* activity of BioB the empirically determined optimum was used throughout. The effect of exogenous sulphide on biotin formation is not as pronounced as the effect of iron. Less exogenous sulphide is required for optimal activity. This is interesting as it suggest that an excess of iron is more important for biotin formation, although a sulphur transfer is reportedly occurring into biotin from BioB (60,101). The addition of extra iron and sulphur at various time points throughout the assay did not lead to an increase in biotin formation. It may be necessary for the sulphur to be provided as a persulphide such as that formed by IscS, a cysteine desulphurase (Chapter 5). However, other findings (Chapter 6) suggested that the depletion of BioB in iron and sulphur is not the principle reason for reproducible activity (63).

Effect of asparagine, MioC, TPP and unlabeled DTB *in vitro:* The addition of extra asparagine, MioC, TPP and unlabeled DTB did not have a positive effect on biotin formation. This is supported by the findings of Ugulava *et al.* (63). However, it has to be noted that the assay conditions used by Birch *et al.* differed from the optimised protocol (63), as cell-free lysate was used instead of purified proteins. In addition, it has to be noted that no catalytic activity for biotin synthase has thus far been reported. Hence it is still possible, that these co-factors might be required to achieve catalytic activity.

Separation of small co-factors by HPLC: The use of MWCO membrane filters allowed the identification by TLC and HPLC of essential hydrophobic compounds *in vitro* apart from DOA, DTB and biotin (Figure 4.12). At the start of the reaction DTT is mostly in its reduced state. In the course of the reaction the amount of DTT in its oxidised state increase gradually. The adenine concentration *in vitro* increases with time in a reaction that appears to be unrelated to biotin formation and is probably due to the hydrolysis of SAM. With this optimized separation procedure, it might be possible to identify labeled or unlabeled reaction intermediates and follow the transfer of hydrogen from DTB to DOA, as previous results have given ambiguous results (54).

Chapter Five: Purification and investigation of *isc* gene cluster products

5.1 Introduction

Iron-sulphur clusters are ubiquitous in nature and are found in numerous proteins that have important redox, catalytic, or regulatory properties (102,103). The pathway of Fe-S cluster synthesis has been outlined in the work of Dean and his collaborators (104), who have focused on the synthesis of Fe-S clusters required for N_2 fixation by *Acetobacter vinelandii*. It was known for some time (105) that cysteine is the original source of sulphide required for cluster formation. By analysis of the structure of the genes involved it was shown that a pyridoxal-phosphate-containing enzyme, a cysteine desulphurase, NifS, is the key enzyme in providing the sulphur in a reactive form. By incubating NifS with a second protein, NifU, in the presence of additional iron, a preliminary iron-sulphur cluster is formed on NifU (106). Homologs of *nif*S and *nif*U, which code for proteins less specialized than the Nif proteins are widely distributed in prokaryotes and eukaryotes (107-110). In *E. coli* the *isc* gene cluster (*i*ron *s*ulphur *c*luster) was identified, which includes *isc*S and *isc*U, homolog to *nif*S and *nif*U respectively (Scheme 5.1).

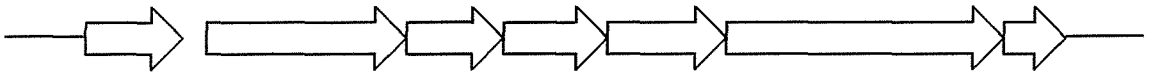

Scheme 5.1: The *isc* operon of *E.coli*

IscS is also a pyridoxal-phosphate containing, cysteine desulphurase. X-ray crystal structures of two members of this general class of enzyme have been published (111,112), and the active site structures are in good agreement with previous mechanistic proposals involving an active site cysteine persulphide intermediate (104). IscU can serve as a scaffold for the assembly of a [2Fe-2S] or [4Fe-4S] cluster (113). In addition, IscA, was identified and found to assemble a [2Fe-2S] cluster (114,115). IscR (*i*ron-*s*ulphur *c*luster *r*egulator) is encoded by an ORF located immediately upstream of genes coding for the *E. coli* Fe-S cluster assembly proteins, IscS, IscU, and IscA. Analysis of IscR by electron paramagnetic resonance showed that the anaerobically isolated protein contains a

[2Fe-2S]$^{1+}$ cluster, which is important for its regulatory function (116). In *E. coli* the *isc*SUA genes are located adjacent to the *hsc*A, *hsc*B and *fdx* genes and are probably co-transcribed (117). The products of these genes, Hsc20, Hsc66 and Fdx, might play an important role in iron sulphur cluster assembly, as they show sequence similiarity to the DnaK and DnaJ system, which act as chaperon and co-chaperone (118) and have been shown to interact with IscU (119).

It was proposed that the iron-sulphur cluster of BioB is depleted in sulphur after one reaction cycle (Section 1.3). The addition of extra iron and sulphide at various time points did not lead to an increase in biotin formation (Section 4.4.1). One possible explanation for this failure might be that the sulphur has to be provided as a protein bound persulphide such as that formed by IscS in the presence of other protein co-factors. Thus, the *isc* gene cluster products might increase the active form of BioB to allow higher turnover of DTB. IscS, IscU, IscA, Hsc20, Hsc66 and ferredoxin from *E. coli* were purified to homogeneity to investigate this hypothesis.

5.2 Purification of IscS from pET24a:IscS/BL-21(DE3)

The plasmid pET24d:IscS was constructed by Dr. P. Roach (Figure 5.1).

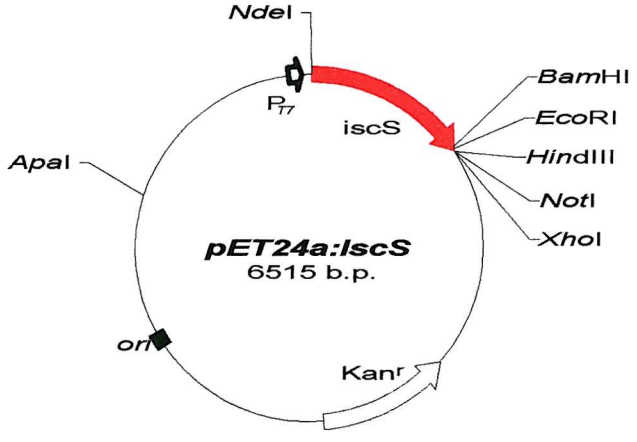

Figure 5.1: Plasmid map of pET24a:IscS with prominent restriction sites

IscS was purified to high purity, as judged by SDS-PAGE, using anion exchange and gel filtration chromatography (Figure 5.2 and 5.3).

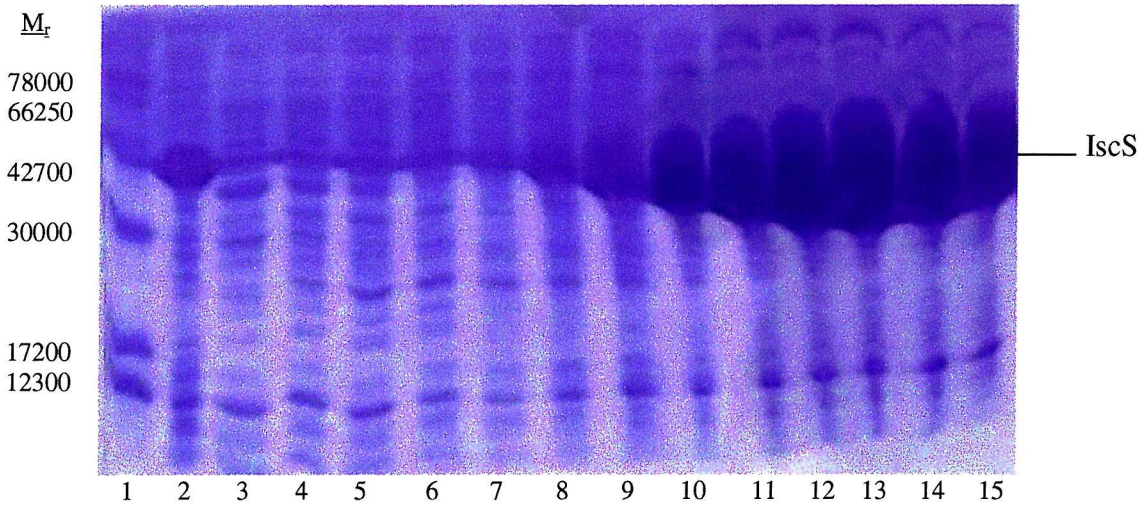

Figure 5.2: Coomassie Blue stained 15 % SDS-PAGE gel of the anion exchange column. (1) Molecular weight markers, (2) Load, (3) flow through, (4) – (15) IscS containing fractions. Fraction (9) to (15) were pooled and submitted to gel filtration chromatography.

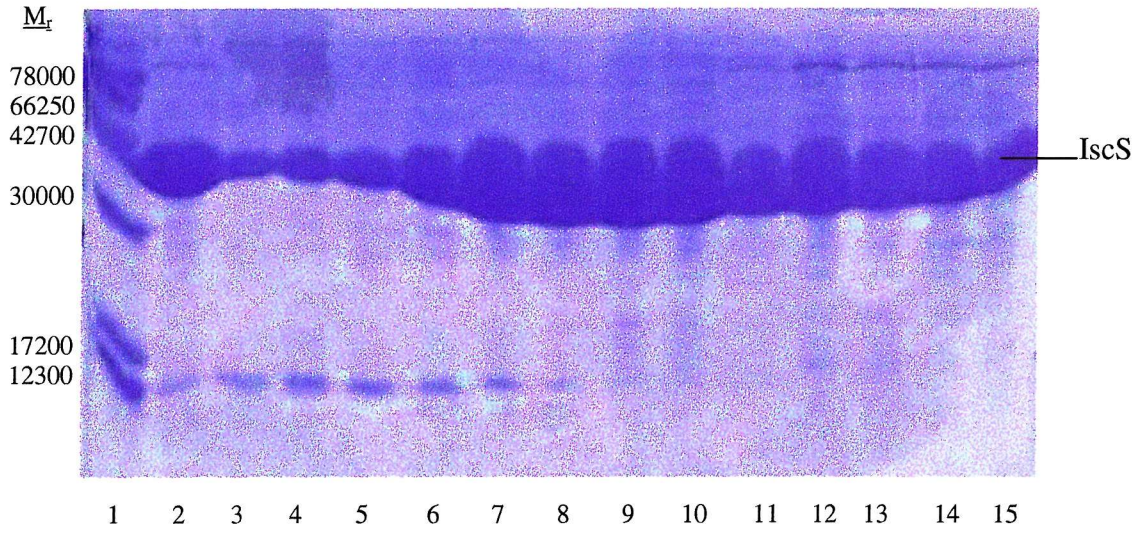

Figure 5.3: Gel filtration chromatography. (1) Molecular weight markers, (2) Load, (3) – (15) IscS containing fractions. Fraction (7) and (11) were pooled and submitted to HIC chromatography.

IscS purification could be further improved by using Blue Sepahrose dye affinity chromatography (Figure 5.4 and 5.5).

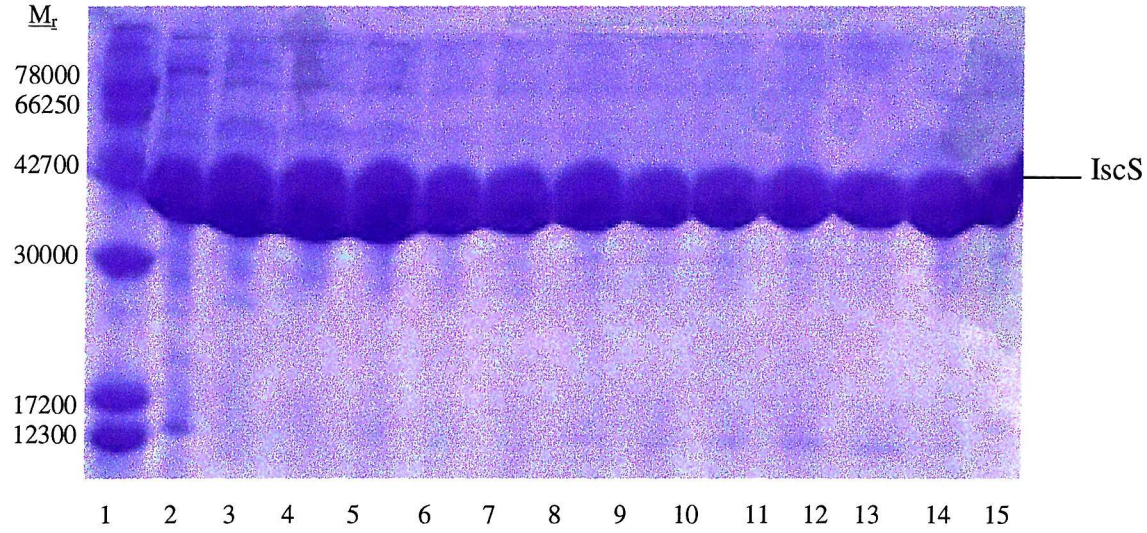

Figure 5.4: Dye affinity chromatography. (1) Molecular weight markers, (2) Load, (3) – (15) IscS containing fractions. Fraction (5) and (14) were pooled and submitted to gel filtration chromatography.

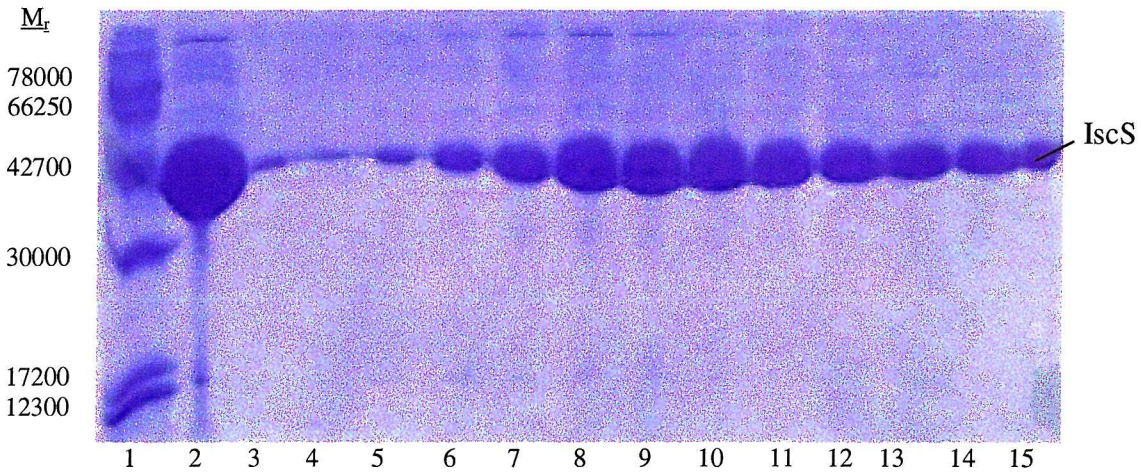

Figure 5.5: Coomassie Blue stained 15 % SDS-PAGE gel of the gel filtration column. (1) Molecular weight markers, (2) Load, (3) – (15) IscS containing fractions eluting. Fraction (9) to (15) were pooled and used biochemical investigations.

IscS containing fractions were bright yellow due to the pyridoxal-phosphate co-factor. Coloured fractions containing IscS were pooled and used for biochemical investigations. 40 g of cell paste yielded 450 mg of highly pure IscS, as judged by SDS-PAGE, after the first two steps. Further steps lowered the yield to 150 mg of IscS of greater purity, as judged by SDS-PAGE.

ESI-MS for purified IscS

Multiple charged IscS was observed by ESI-MS and the molecular weight (MW) was determined to be 45083.4 (Figure 5.6). The calculated molecular weight of IscS from the amino acid sequence is 45089.5. This mass difference is reasonable, as the accuracy of the instrumentation is 0.2 %.

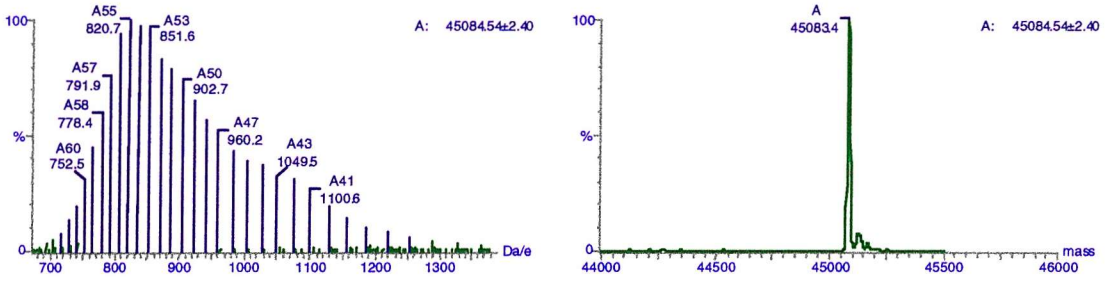

Figure 5.6: ESI-MS for IscS

5.3 Purification of IscU from pET24a:IscU/BL-21(DE3)

The plasmid pET24a:IscU was constructed by Dr. P. Roach (Figure 5.7).

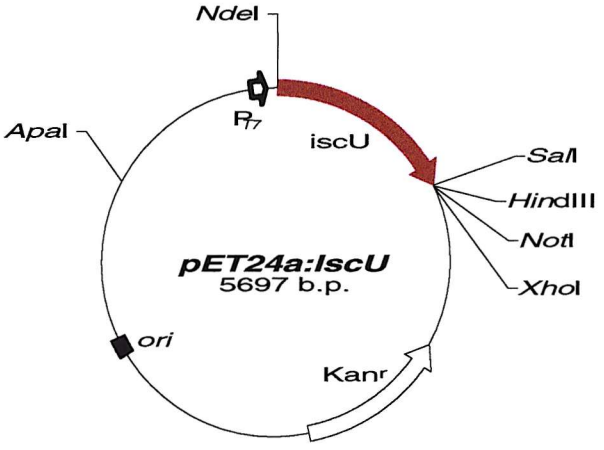

Figure 5.7: Plasmid map of pET24a:IscU with prominent restriction sites

IscU of high purity, as judged by SDS-PAGE, was purified using anion exchange and gel filtration chromatography (Figure 5.8).

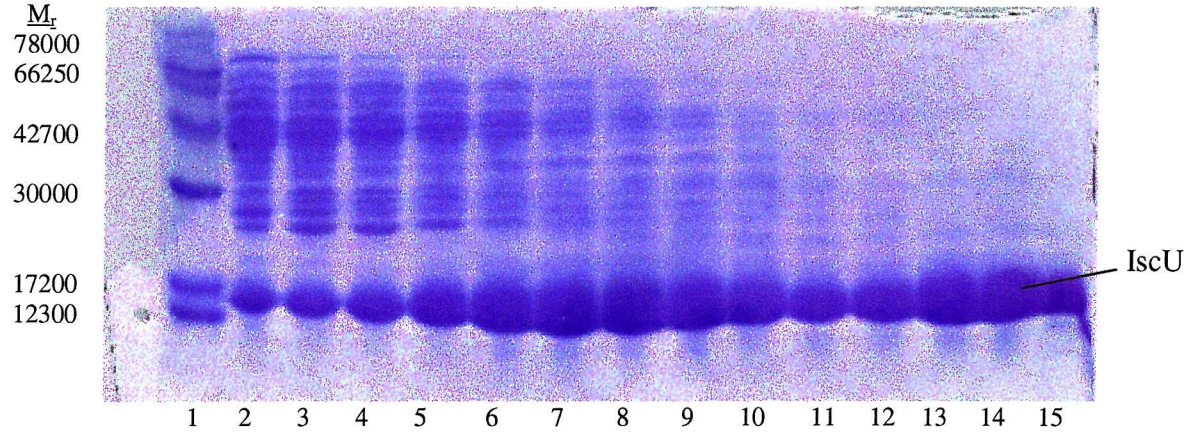

Figure 5.8: Coomassie Blue stained 15 % SDS-PAGE gel of the gel filtration column. (1) Molecular weight markers, (2) Load, (3) – (15) IscU containing fractions. Fraction (10) to (15) were pooled and used for biochemical investigations.

Fractions containing IscU were of slight red colour due to iron and sulphide bound to IscU. The iron concentration was at ~ 1.1 mol per mol of IscU monomer. 30 g of cell paste yielded 210 mg of purified IscU.

ESI-MS for purified IscU

Multiple charged IscU was observed by ESI-MS and the molecular weight (MW) was determined to be 13708.1 (Figure 5.9). The calculated molecular weight of IscU from the amino acid sequence is 13717.4. This is within the expected error (0.2%).

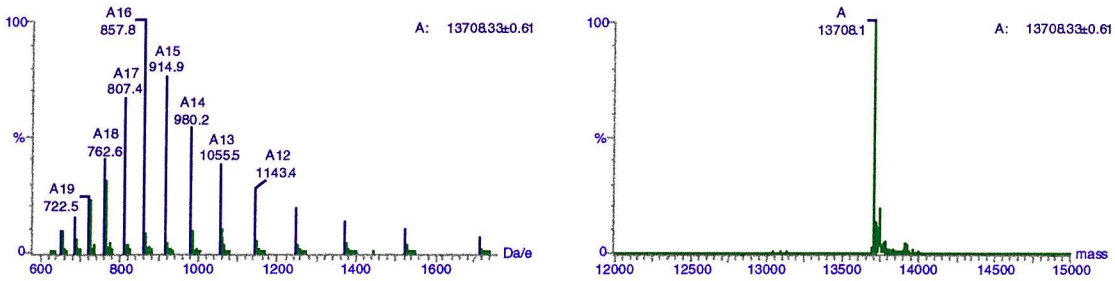

Figure 5.9: ESI-MS for IscU

5.4 Purification of His_6-IscA from pQiscA-55 /BL-21(DE3)

The plasmid pQiscA-55 in *E. coli* M15(pREP4) was a kind gift of Dr. S. Ollagnier-de-Choudens (CEA, Grenoble). (Figure 5.10).

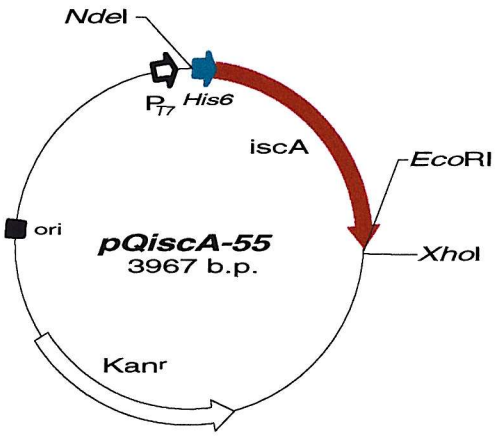

Figure 5.10: Plasmid map of pQiscA-55 with prominent restriction sites

His_6-IscA was purified to high purity, as judged by SDS-PAGE, using nickel chelating chromatography (Figure 5.11 and 5.12).

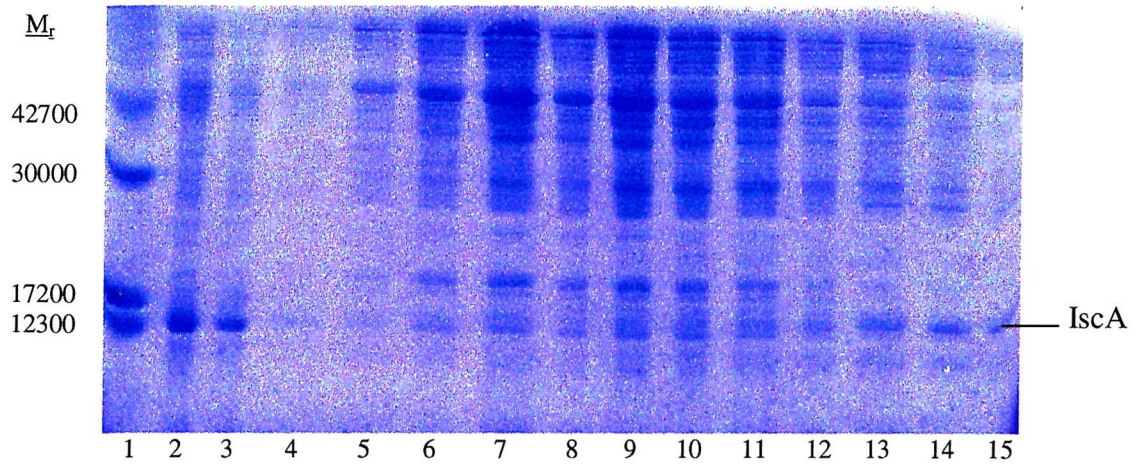

Figure 5.11: Coomassie Blue stained 15 % SDS-PAGE gel of the nickel chelating column. (1) Molecular weight markers, (2) Load, (3) flow through, (4) – (15) BL-21 (DE3) proteins bound unspecifically to the nickel column.

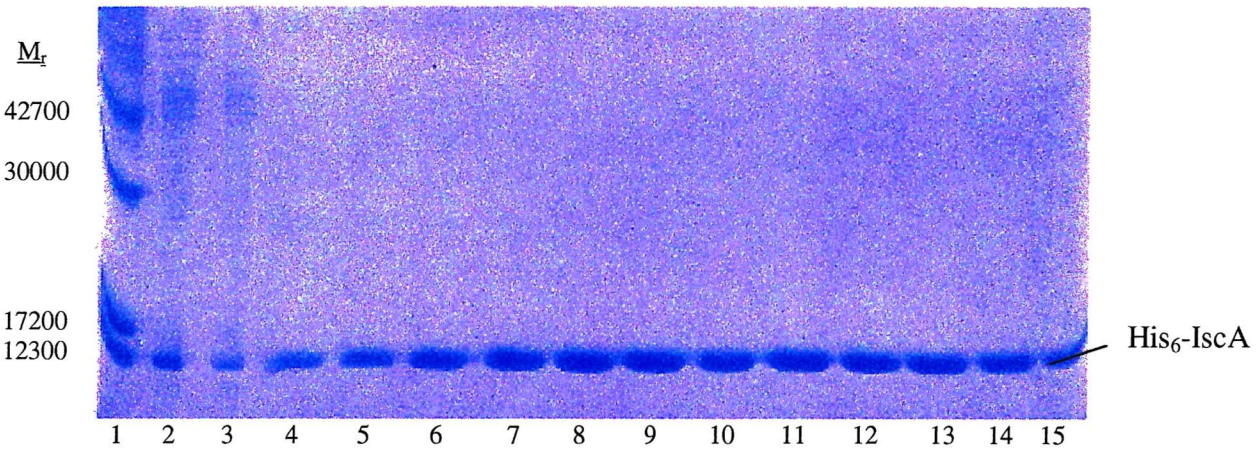

Figure 5.12: Coomassie Blue stained 15 % SDS-PAGE gel of the nickel-chelating column. (1) Molecular weight markers, (2) Load, (3) flow through, (4) – (15) fractions containing His_6-IscA. Fraction (6) to (15) were pooled and used for biochemical investigations.

Fractions containing His_6-IscA were of slight red colour due to iron and sulphide bound to His_6-IscA. The iron concentration was at ~ 0.8 mol per mol of His_6-IscA monomer.

ESI-MS for purified IscA-His_6

Multiple charged His_6-IscA was observed by ESI-MS and the molecular weight (MW) was determined to be 12812.4 (Figure 5.13). The calculated molecular weight of IscA-His_6 from the amino acid sequence is 12828.42. The mass difference could be explained by the formation of metal adducts (i.e. Na^+).

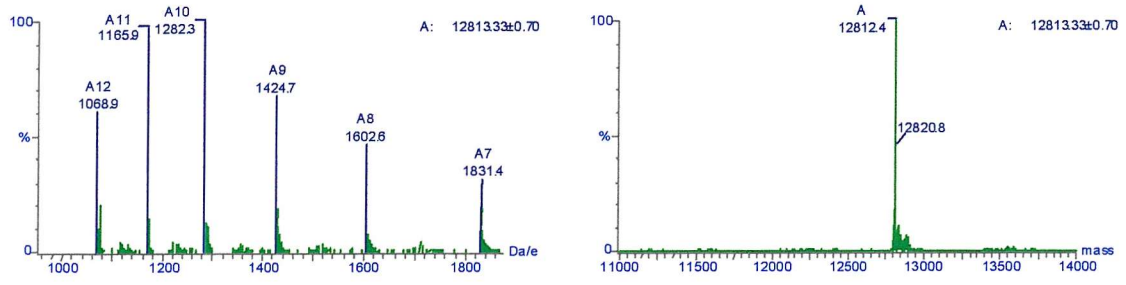

Figure 5.13: ESI-MS for His_6-IscA

5.5 Purification of Hsc66, Hsc20 and ferredoxin from pET24d:HscF/BL-21(DE3)

The plasmid pET24d:HscF was constructed by subcloning a NcoI/XhoI fragment containing *hsc*A, *hsc*B and *fdx* from pMK300, a kind gift from Dr. M. Kriek, into pET24d(+) (Figure 5.14).

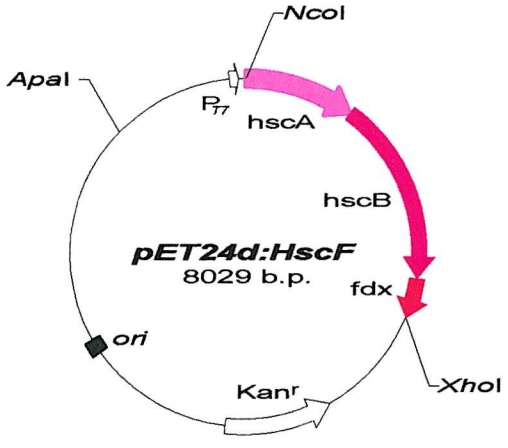

Figure 5.14: Plasmid map of pET24d:IscS with prominent restriction sites

The construct was effective in high-level expression of Hsc66 and Hsc20 in *E.coli* (BL-21 (DE3) strain) (Figure 5.15).

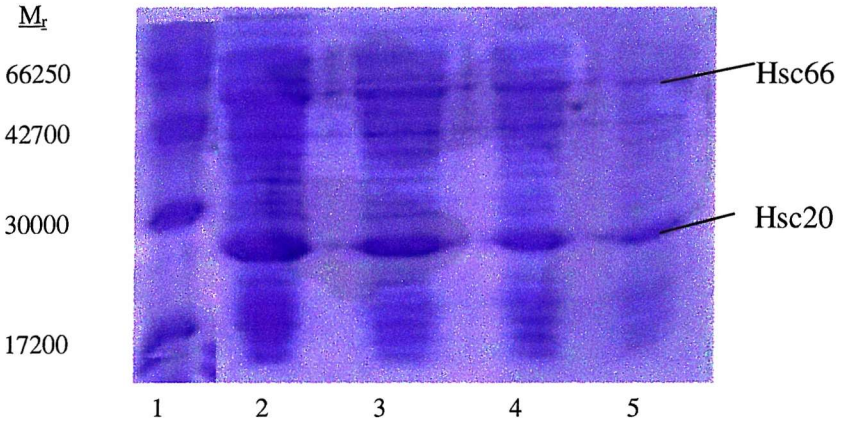

Figure 5.15: SDS-Page analysis of pET24d:HscF. (1) Molecular weight markers, (2) 25 µg of crude lysate, (3) 12,5 µg of crude lysate, (4) 6 µg of crude lysate, (5) 3 µg of crude lysate.

The proteins were initially purified by anion exchange chromatography (Figure 5.16). Hsc20 could be readily purified using gel filtration chromatography (Figure 5.17), whereas Hsc66 required an additional step using HIC chromatography (5.18). Ferredoxin could be purified using gel filtration chromatography (5.19).

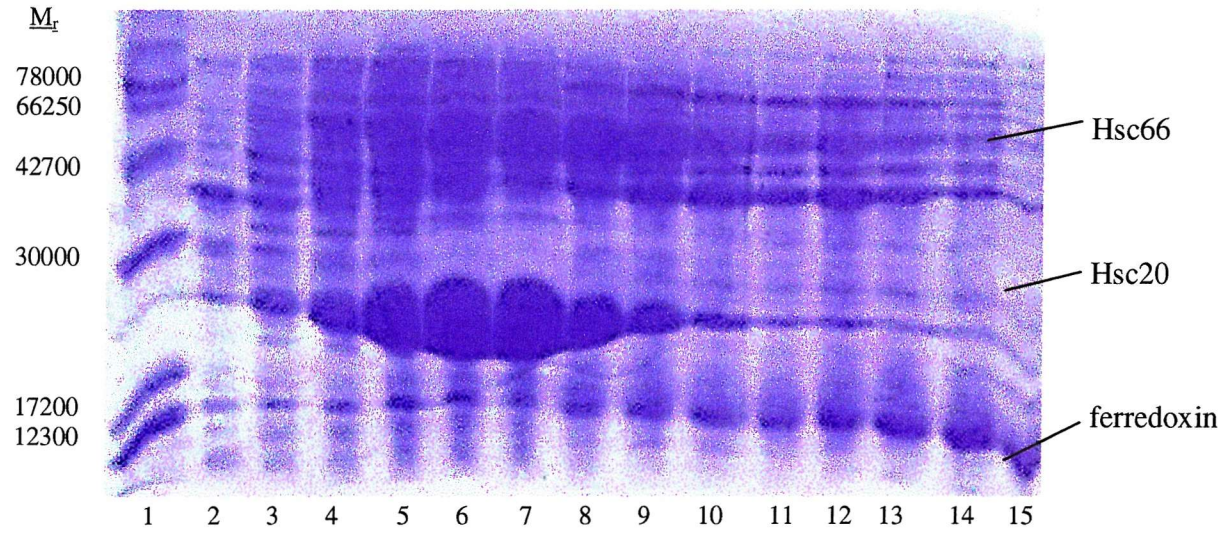

Figure 5.16: Coomassie Blue stained 15 % SDS-PAGE gel of the anion exchange column. (1) Molecular weight markers, (2) Load, (3) – (15) Fractions eluting from the anion exchange column. Fraction (4) to (10), containing Hsc66 and Hsc20, and fraction (11) to (15), containing ferredoxin, were pooled and further purified by gel filtration chromatography.

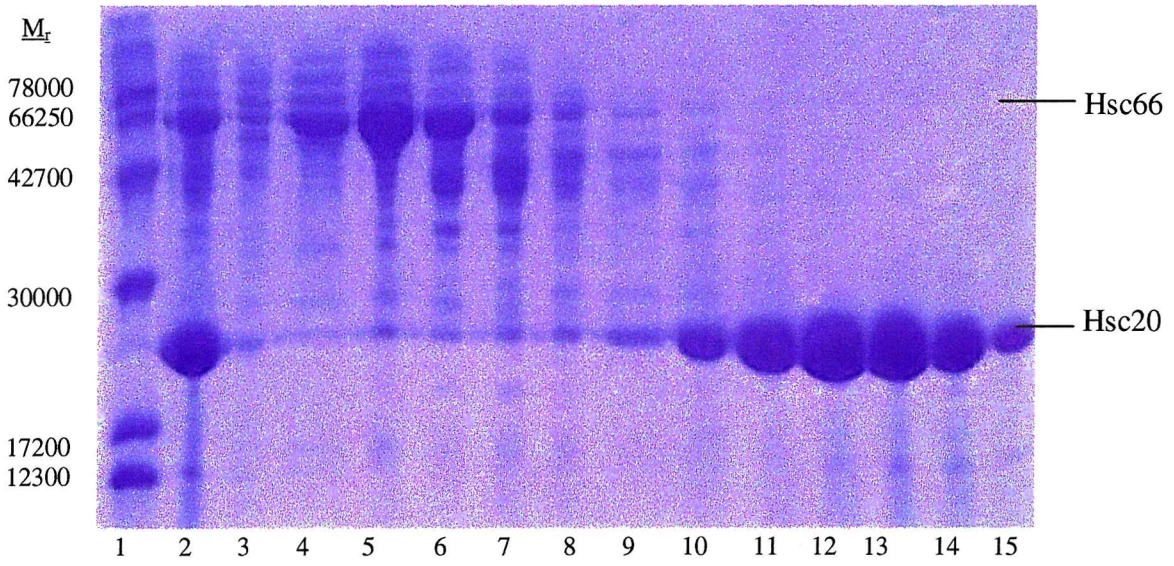

Figure 5.17: Gel filtration chromatography. (1) Molecular weight markers, (2) Load, (3) – (15). Fractions eluting from the gel filtration column. Fraction (4) to (7), containing Hsc66 were pooled and submitted to HIC chromatography. Fraction (11) to (15), containing Hsc20, were pooled and used for biochemical investigations.

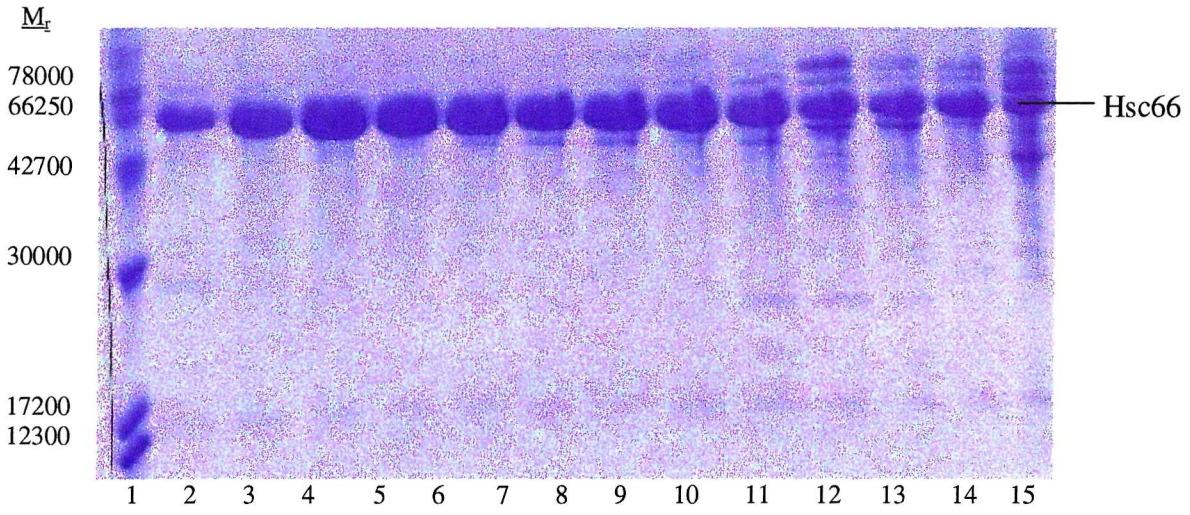

Figure 5.18: Coomassie Blue stained 15 % SDS-PAGE gel of the HIC column. (1) Molecular weight markers, (2) – (15) Fractions containing Hsc66. Fraction (3), (4) and (5) were desalted and used for biochemical investigations.

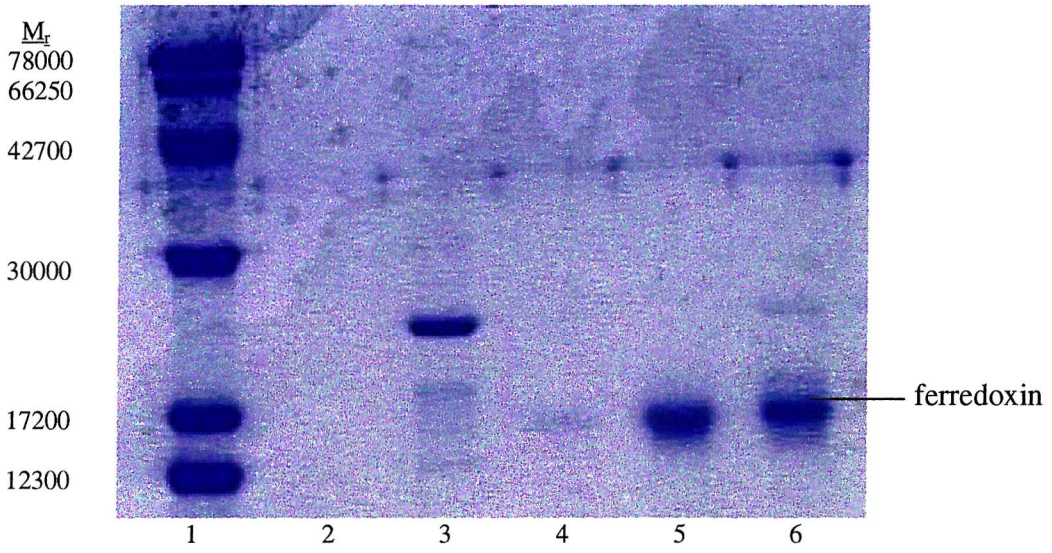

Figure 5.19: Gel filtration chromatography. (1) Molecular weight markers, (2) – (6). Fractions eluting from the gel filtration column. Fraction (5) and (6), containing ferredoxin, were pooled and used for biochemical investigations.

Hsc20, Hsc66 and ferredoxin could be readily purified from pET24d:HscF/BL-21(DE3). From 40 g of cell paste it was typical to obtain 500 mg of highly purified Hsc20, 150 mg of highly purified Hsc66 and 20 mg of medium purified ferredoxin. Purity was judged by SDS-PAGE.

ESI-MS for purified Hsc20, Hsc66 and ferredoxin

Multiple charged Hsc20, Hsc66 and ferredoxin were observed by ESI-MS and the molecular weight (MW) was determined to be 20125.8 for Hsc20 (Figure 5.20), 65536.0 (Figure 5.21) for Hsc66 and 12194.7 for ferredoxin (Figure 5.22). The calculated molecular weight from the amino acid sequence is 20006.52 for Hsc20, 65521.24 for Hsc66 and 12199 for ferredoxin. This is within the expected error (0.2%). The experimental mass found for ferredoxin is in good correlation to its theoretical mass.

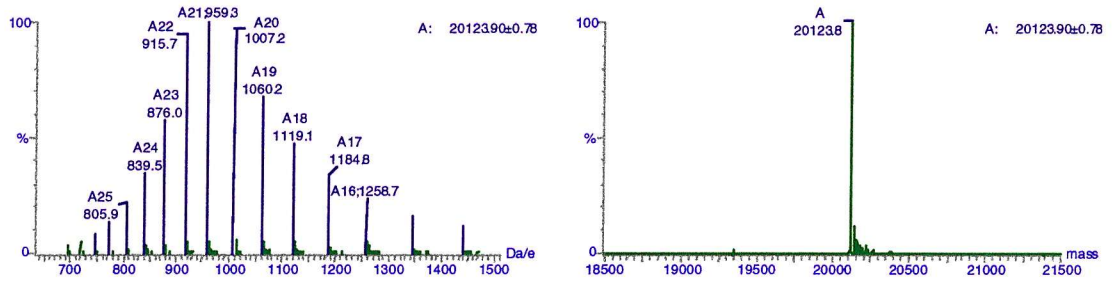

Figure 5.20: ESI-MS for Hsc20

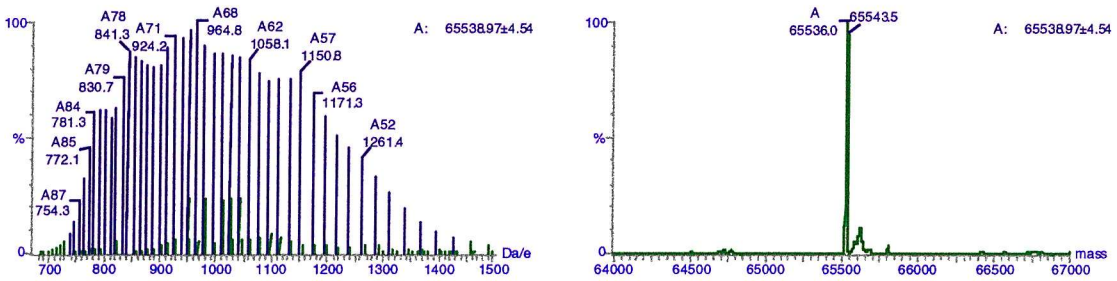

Figure 5.21: ESI-MS for Hsc66

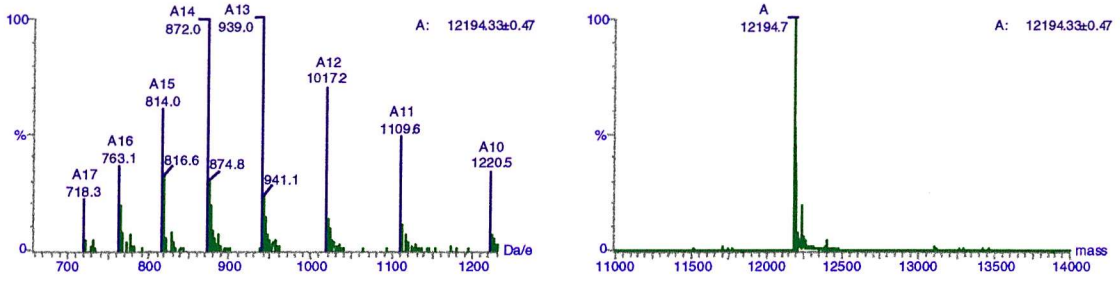

Figure 5.22: ESI-MS for ferredoxin

5.6 Effect of IscS on biotin formation *in vitro*

IscS forms a protein bound persulphide by desulphurising cysteine to give alanine (Scheme 5.1).

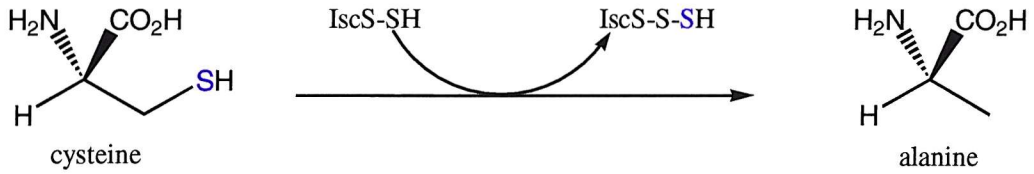

Scheme 5.1: IscS is a cysteine desulphurase

It was investigated if this protein bound persulphide can substitute for sulphide in the standard assay (Table 5.1, Figure 5.23).

IscS [µM]	Biotin I (Area) $*10^5$	Biotin II (Area) $*10^5$	Biotin I [µM]	Biotin II [µM]
0	1.49	1.75	4.44	3.57
0.5	8.12	8.51	32.16	33.89
1	8.41	7.92	33.41	31.30
2.5	7.35	7.69	28.78	30.29
5	6.92	7.03	26.90	27.37
10	7.14	7.09	27.87	27.63
15	7.33	7.29	28.68	28.51
20	7.00	7.17	27.22	27.98

Table 5.1: Values for Figure 5.23; I and II represent duplicate assays; [Method IV; HPLC\Results\IscS.U.Cys1\RP1.004\1-18].

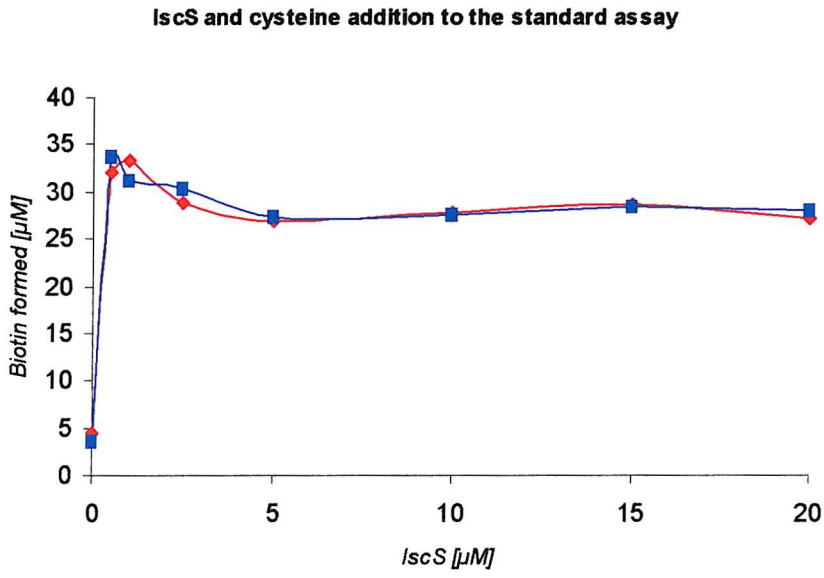

Figure 5.23: IscS and cysteine addition to the standard assay (σ: 0.47).

IscS and cysteine can mobilise the sulphur required for biotin formation (Section 4.4). In our hands there is no notable increase in biotin formation (101) but IscS and cysteine can replace inorganic sulphide (Table 5.2, Figure 5.24).

Sample ID	Biotin I (Area) $*10^5$	Biotin II (Area) $*10^5$	Biotin I [µM]	Biotin II [µM]
standard assay	8.68	8.54	34.62	34.01
addition of 0.5 µM IscS and 500 µM cysteine	8.12	8.51	32.16	33.89

Table 5.2: values for Figure 5.24; I and II represent duplicate assays; [Method IV; HPLC\Results\IscS.U.Cys1\RP1.004\1-18].

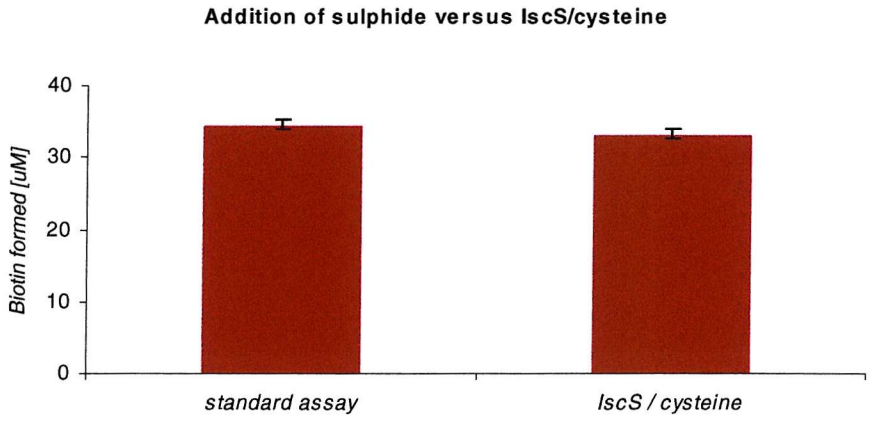

Figure 5.24: Comparison of inorganic sulphide and IscS/cysteine addition

5.7 Effect of IscU on biotin formation *in vitro*

IscU can assemble a [2Fe-2S] and a [4Fe-4S] cluster depending on the reconstitution conditions (113). An effect on biotin formation was investigated (Table 5.3, Figure 5.25).

IscU [µM]	Biotin I (Area) $*10^5$	Biotin II (Area) $*10^5$	Biotin I [µM]	Biotin II [µM]
0	6.25	6.30	23.94	24.15
0.5	6.49	6.12	25.01	23.38
1	6.58	6.52	25.40	25.15
2.5	6.42	6.45	24.70	24.85
5	7.82	7.07	30.84	27.53
10	7.15	7.24	27.90	28.29
15	7.29	7.16	28.49	27.94
20	7.16	6.59	27.94	25.45

Table 5.3: Values for Figure 5.25; I and II represent duplicate assays; [Method IV; HPLC\Results\IscS.U.Cys1\RP1.004\19-36].

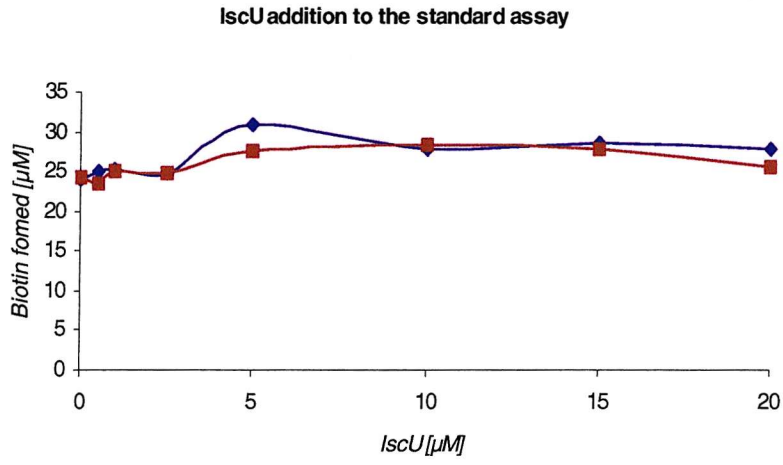

Figure 5.25: IscU addition to the standard assay (σ: 0.56).

IscU failed to show no significant effect on biotin formation.

5.8 Addition of IscS, cysteine and IscU to the standard assay

IscU alone had no significant effect on biotin formation. It might require the IscS/cysteine dependant assembly of a [2Fe-2S] or [4Fe-4S] cluster (113) to participate in the reassembly (Section 5.1) of the iron-sulphur cluster of BioB (Table 5.3, Figure 5.26).

Sample ID	Biotin I (Area) $*10^5$	Biotin II (Area) $*10^5$	Biotin I [µM]	Biotin II [µM]
1	6.10	6.29	23.27	24.12
2	5.25	4.98	19.55	18.39
3	6.66	6.32	25.77	24.24
4	4.86	4.41	20.48	22.62
5	1.79	1.88	18.36	15.89
6	2.10	1.91	17.84	15.86
7	5.46	5.95	4.37	4.77
8	4.98	4.41	5.74	4.91
9	2.14	2.17	5.92	6.05

Table 5.3: see Figure 5.26 for details; I and II represent duplicate assays; [Method IV; HPLC\Results\IscS.U.Cys\RP1.005\1-18].

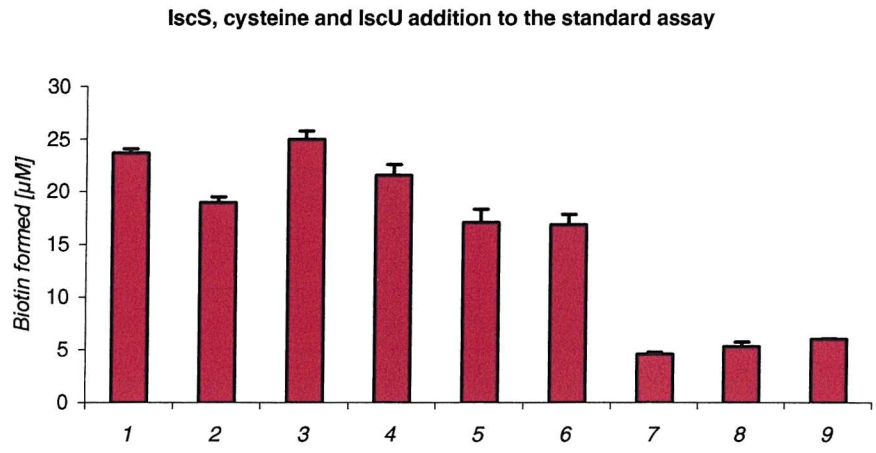

Figure 5.26: IscS, cysteine and IscU addition to the standard assay. Standard assay (Table 3.2, no inorganic sulphide present) plus (1) 0.5 µM IscS and 500 µM L-cysteine, (2) 10 µM IscU, 0.5 µM IscS, 500 µM L-cysteine and 50 µM Fe^{3+} after reconstitution of the [4Fe-4S] cluster of IscU, (3) 10 µM IscU, 0.5 µM IscS and 500 µM L-cysteine, (4) 0.25 µM IscS and 250 µM L-cysteine, (5) 5 µM IscU, 0.25 µM IscS, 250 µM L-cysteine and 25 µM Fe^{3+} after reconstitution of the [4Fe-4S] cluster of IscU; (6) standard assay; standard assay plus (7) 500 µM L-cysteine, (8) 0.5 µM IscS; (9) standard assay minus BioB.

Combined addition of IscS, cysteine and IscU failed to show a significant effect on biotin formation. IscU containing a [4Fe-4S] cluster did not assist in the reassembly of BioB to give an active form of BioB, able to participate in an additional turnover of DTB. This could be explained by the absence of additional protein co-factors.

5.9 Addition of IscA, Hsc20, Hsc66 and ferredoxin to the standard assay

IscA can assemble a [2Fe-2S] cluster (115,120), which could reassemble the [2Fe-2S] cluster of BioB (63) that might be depleted in sulphur after one turnover (Section 1.3.3). Ferredoxin contains a [2Fe-2S] cluster (121). Hsc20 and Hsc66 are chaperones (118,122), which might assist iron-sulphur cluster proteins in assembling an iron-sulphur cluster. Their effect on biotin formation was investigated (Table 5.4, Figure 5.27).

Sample ID	Biotin I (Area) $*10^5$	Biotin II (Area) $*10^5$	Biotin I [µM]	Biotin II [µM]
1	5.92	5.57	22.51	20.95
2	6.32	5.78	24.28	21.89
3	6.21	6.41	23.77	24.65
4	6.96	6.73	27.06	26.06
5	5.40	5.76	20.23	21.82
6	5.86	6.13	22.23	23.42
7	5.53	5.76	20.78	21.78
8	6.28	6.31	24.07	24.23
9	6.99	6.89	27.19	26.74
10	7.26	7.26	28.37	28.38

Table 5.4: see Figure 5.27 for details; I and II represent duplicate assays; [Method II; HPLC\Results\HscA.B1\RP1.005\1-18].

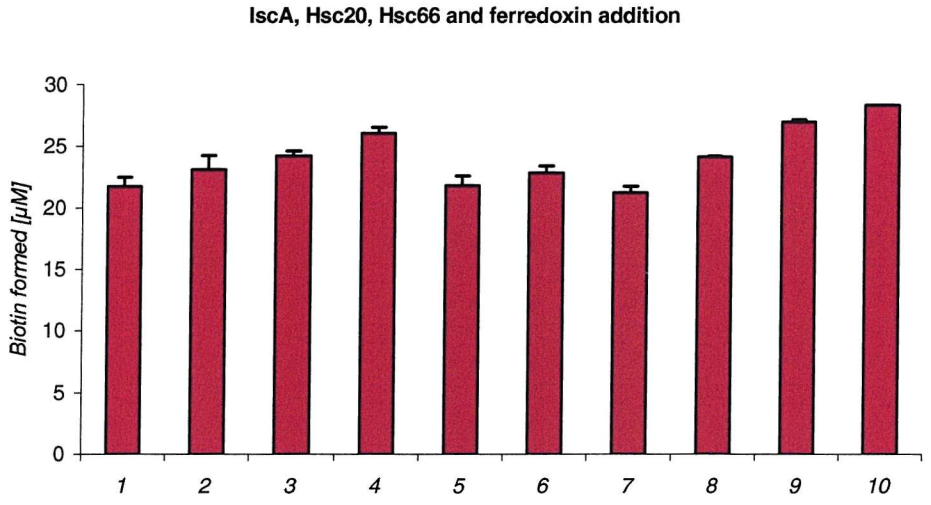

Figure 5.27: IscA, Hsc20, Hsc66 and Fdx addition to the standard assay. Standard assay (Table 3.2, 0.5 µM IscS/500 µM L-cysteine) plus (1) 10 µM IscA, 20 µM Hsc20, 10 µM Hsc66, 400 µM ATP, 10 µM Fdx, 10 µM IscU, (2) 10 µM IscA, 20 µM Hsc20, 10 µM Hsc66, 400 µM ATP, (3) 10 µM Hsc66, (4) 20 µM Hsc20, (5) 10 µM IscA, (6) 10 µM Fdx, (7) 400 µM ATP, (8) standard assay, (9) 10 µM IscA, 20 µM Hsc20, 10 µM Hsc66, 400 µM ATP, 10 µM Fdx, 10 µM IscU (incubation time: 300 min.), (10) standard assay (incubation time 300 min.).

None of the added protein co-factor showed a significant effect on biotin formation.

5.10 Summary and Conclusion

The *isc* gene cluster products, which participate in iron-sulphur cluster assembly, IscS, IscU, IscA, HscA, HscB and Fdx could be readily purified to high purity by overexpression from various plasmids. IscS, a cysteine desulphurase, can substitute for inorganic sulphide in the standard assay in the presence of cysteine. Hsc20 could reproducibly increase the biotin concentration by 5 to 10 μM. The iron-sulphur cluster of IscU could be reassembled following literature procedures (113), but addition of reconstituted IscU did not enhance biotin formation *in vitro*. The combined addition of the *isc* gene cluster products to the *in vitro* assay, in the presence of ATP and exogenous iron, failed to show a significant effect on biotin formation *in vitro*. A possible explanation is that the *in vitro* conditions are not optimal for iron-sulphur cluster assembly. For example, a reductant, such as dithiothreitol is included in the assay. This reductant is capable of mediating sulphide release from an IscS-associated cysteine persulphide (115), which might affect the iron-sulphur cluster assembly process. New findings in regards to the iron-sulphur cluster assembly might assist in optimising the reaction condition. Different possibilities for iron-sulphur cluster repair and the mobilization of sulphur are being investigated. Ollagnier-de-Choudens *et al.* have recently reported that biotin synthase is a pyridoxal phosphate-dependent cysteine desulphurase (123). However, it may be that mechanisms other than iron-sulphur reassembly may be limiting BioB turnover (Chapter 6).

Chapter Six: Inhibition of biotin synthase activity *in vitro*

6.1 Introduction

It has been suggested (59,60,63,114) that the inability to obtain multiple turnover of biotin *in vitro* is due to the depleted iron-sulphur cluster of BioB. This problem could be addressed by the addition of iron-sulphur cluster biosynthesis proteins to the assay. This hypothesis was investigated by other groups (101,124) and in Chapter 5, but thus far no catalytic activity of biotin synthase has been reported. It was therefore necessary to investigate other potential inhibitory mechanisms.

6.2 An inhibitor might be present in the *in vitro* assay

To investigate mechanism by which BioB stops forming biotin, biotin formation was initiated in a scaled up assay and then halted after 180 min. by removing all the small molecules through dialysis. After the complete removal of small molecules, the remaining protein fraction containing BioB, FldA and Fdr was split into aliquots and then incubated again with all the essential small molecular weight components in an attempt to restore activity. If a small molecular inhibitor was generated in the course of biotin formation, the dialysis step would remove it from the protein mixture. In addition, an additional aliquot of each BioB, FldA and Fdr was added to some assays in an attempt to restore activity (Table 6.1, Figure 6.1).

Sample ID	Biotin I (Area) $*10^5$	Biotin II (Area) $*10^5$	Biotin I [µM]	Biotin II [µM]
1	2.69	2.70	8.33	8.36
2	0.84	0.75	0.22	0.50
3	2.19	2.47	6.14	7.35
4	4.70	4.60	17.14	16.70
5	4.22	4.27	15.05	15.24
6	2.20	2.31	6.15	6.66

Table 6.1: see Figure 6.1 for details; I and II represent duplicate assays; [Method I; HPLC\Results\dialysis1\RP1.002\1-8].

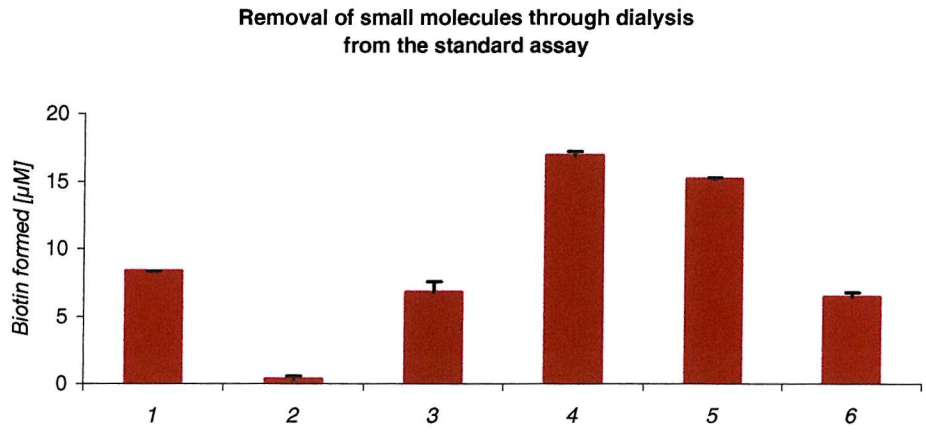

Figure 6.1: Proteins (BioB, Fdr, FldA) from a typical assay mixture were dialysed against buffer for 3 hours. The following were then added to the dialysed proteins and the assays were halted after 90 min.; concentrations of added co-factors can be found in Table 3.2; Addition of (1) small co-factors, (2) no co-factor, (3) small co-factors plus BioB; (4) small co-factors plus BioB, FldA, Fdr, (5) small co-factors plus FldA, (6) small co-factors plus Fdr to the protein fraction after dialysis.

This experiment led to several interesting observations. Re-addition of small co-factors led to a partial recovery of biotin synthase activity (Lane 1). A possible explanation would be that either one or more small co-factors are depleted after 180 min. or that an inhibitor is formed in the assay, which slows down biotin formation. Addition of BioB did not increase biotin formation (Lane 3). This suggests that the amount of BioB is not rate limiting in these assays, rather some other component is limiting and Lane 4 and 5 suggest this component is FldA. We expect FldA to play an important role in biotin formation and this could be due to a need for additional reducing power. The above hypotheses were investigated further.

6.3 Timed addition of small and large molecular weight co-factors

If a co-factor were depleted during the course of biotin formation, biotin formation would be expected to slow down. Thus, all relevant factors were added after approximately one reaction cycle (180 min.) to identify those helpful in restoring or stimulating further activity (Table 6.2, Figure 6.2).

Sample	Biotin I (Area) $*10^5$	Biotin II (Area) $*10^5$	Biotin I [µM]	Biotin II [µM]
1	4.75	4.92	17.37	18.10
2	4.61	5.42	16.77	20.32
3	5.22	6.58	19.42	25.38
4	5.88	6.32	22.33	24.27
5	5.13	5.41	19.03	20.25
6	5.28	5.51	19.71	20.70
7	6.77	7.06	26.23	27.50
8	6.52	6.58	25.14	25.41
9	5.07	5.32	18.76	19.86

Table 6.2: see Figure 6.2 for details; I and II represent duplicate assays; [Method I; HPLC\Results\flavo.3hours1\RP1.006\23-31; RP1.007\1-9].

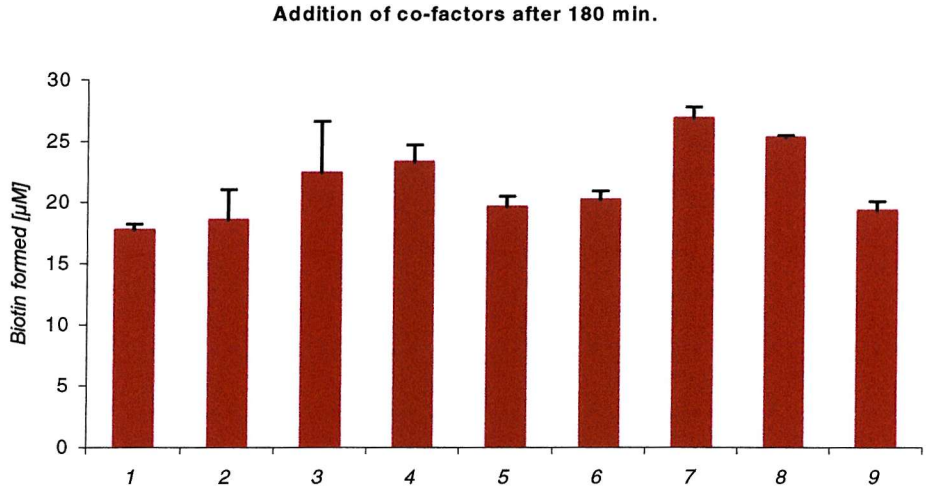

Figure 6.2: Addition of co-factors *in vitro* after 180 min; the amount of co-factors added was equal to the initial amount in the standard assay (Table 3.2); standard assay (1) plus SAM, (2) plus NADPH, (3) plus FldA, (4) plus SAM, NADPH, FldA; standard assay after reconstitution of BioB by adding DTT, iron and sulphide (5) plus SAM, (6) plus NADPH, (7) plus FldA, (8) plus SAM, NADPH, FldA, (9) standard assay.

Addition of extra flavodoxin seemed to increase biotin formation. This could be due to a requirement for additional reducing power towards the end of one reaction cycle, which could have an effect on the maintenance of both the $[4Fe\text{-}4S]^{2+/1+}$ and $[2Fe\text{-}2S]^{2+}$ (63). These findings might be valuable for an *in vivo* application as it identifies the right concentration of FldA as important in the reaction.

SAM and NADPH added after 180 min. did not have a significant effect on biotin formation, which suggest that these co-factors are not depleted after 180 min. in the assay. Furthermore, this result is consistent with the hypothesis that an inhibitor is accumulating during the time of the assay. This hypothesis was thoroughly investigated, as it might have great importance for the *in vivo* production of biotin. If the cellular concentration of an inhibitor increased during fermentation, it might explain the inability of Shaw *et al.* (66) to obtain more than 30 mg/L of biotin by fermentation. On this basis, the effect on biotin formation of a range of substrate analogues and reaction products was investigated.

6.4 Sinefungin and S-adenosylhomocysteine (SAH) inhibition of BioB activity

Sinefungin **1** is a potent inhibitor of SAM decarboxylase, its structure shows homologies to the structure of SAM and thus exhibits competitive inhibition in methyltransferase reactions (125,126). SAH **2** exert significant antiproliferative effects in many cellular systems and is believed to function as growth regulatory molecule (127). It is a co-product and potent feedback inhibitor of SAM dependent methyltransferase reactions (128). The *in vitro* assay systems allow the assessment of potential inhibitory molecules. However, it has to be noted that there are good reasons not to over interpret kinetic data as biotin synthase participates in a complex mechanism, i.e approximately two mol of SAM are used, only a single turnover is observed and quantification of biotin formation can be inaccurate.

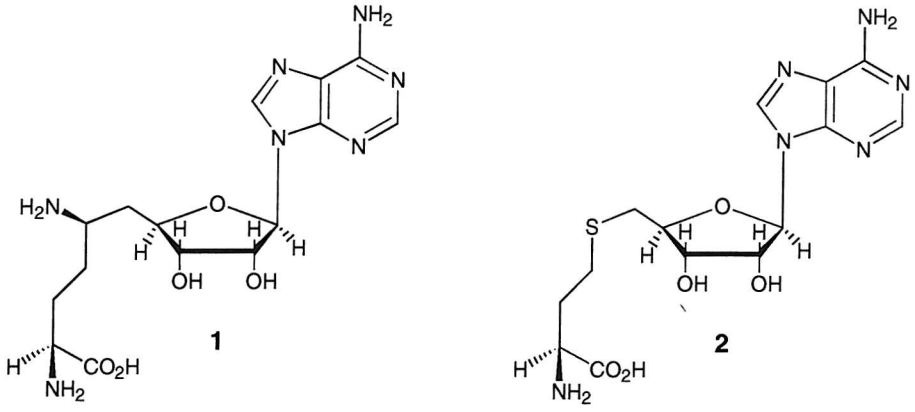

Scheme 6.1: Structures of Sinefungin **1** and SAH **2**.

The inhibition of BioB activity by Sinefungin was first investigated with the radiochemical method (Figure 6.3).

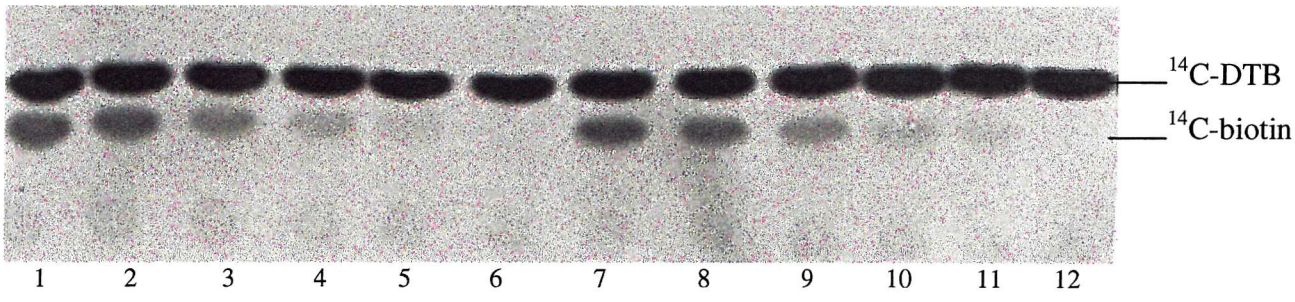

Figure 6.3: Inhibition of BioB activity by Sinefungin; Autoradiography of *in vitro* assays (Assay conditions as in Table 3.1); Sinefungin (1), (7) 0 µM, (2), (8) 250 µM, (3), (9) 500 µM, (4), (10) 750 µM, (5), (11) 1000 µM, (6), (12) 1250 µM.

Sinefungin had an inhibitory effect on BioB activity (IC_{50}: 750 µM), although it should be noted that the IC_{50} was high. This effect was subsequently investigated in greater detail using the HPLC based assay (Table 6.3, Figure 6.4).

Sinefungin [µM]	Biotin I (Area) *10^5	Biotin II (Area) *10^5	Biotin I [µM]	Biotin II [µM]
1500	3.57	4.25	12.20	15.15
1250	3.86	4.30	13.48	15.40
1000	3.76	4.19	13.00	14.89
800	4.25	4.99	15.17	18.44
600	4.58	5.07	16.61	18.76
400	4.88	5.90	17.96	22.43
200	5.33	6.24	19.90	23.91
100	6.25	7.00	23.97	27.24
0	7.02	7.89	27.35	31.16

Table 6.3: values for Figure 6.4; I and II represent duplicate assays; [Method I; HPLC\Results\inh1.2\RP1.004\3-5\ RP1.004\1-6\ RP1.006\1-18].

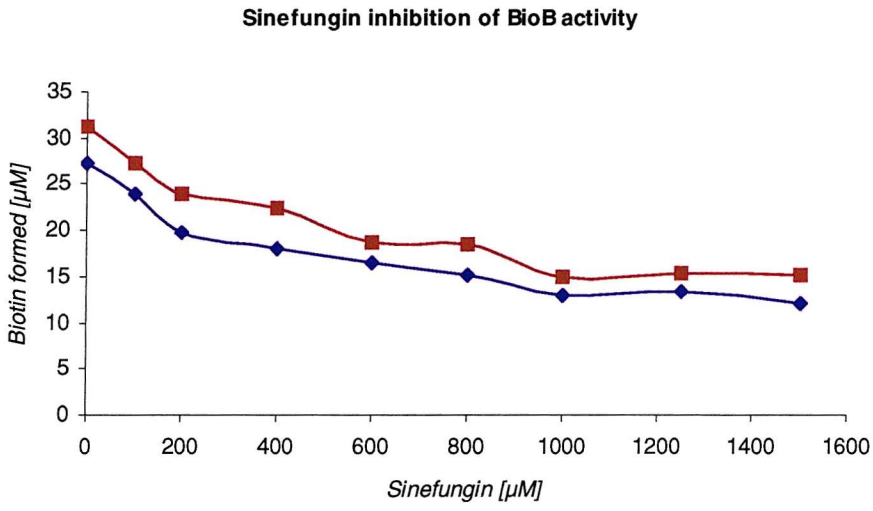

Figure 6.4: Sinefungin inhibition of BioB activity (σ: 1.54).

These experiments corresponded to the results above (IC_{50}: 800 µM). Sinefungin shares common chemical and conformational features with both substrate (SAM) and products (DOA, methionine) of the biotin synthase reaction and might act as a competitive inhibitor.

Further experiments were conducted assessing the inhibitory effect of SAH, another SAM analogue, on BioB activity (Table 6.4, Figure 6.5).

SAH [µM]	Biotin I (Area) $*10^5$	Biotin II (Area) $*10^5$	Biotin I [µM]	Biotin II [µM]
1500	4.37	5.08	15.72	18.83
1000	4.39	5.21	15.78	19.40
600	4.47	5.60	16.11	21.07
300	4.87	5.46	17.87	20.50
160	5.18	5.61	19.26	21.14
30	5.85	6.70	22.18	25.93
10	7.41	8.43	29.06	33.51
0	8.95	9.33	35.82	37.47

Table 6.4: values for Figure 6.5; I and II represent duplicate assays; [Method I; HPLC\Results\inh1.2\RP1.001\1-5\ RP1.003\1\ RP1.006\19-34].

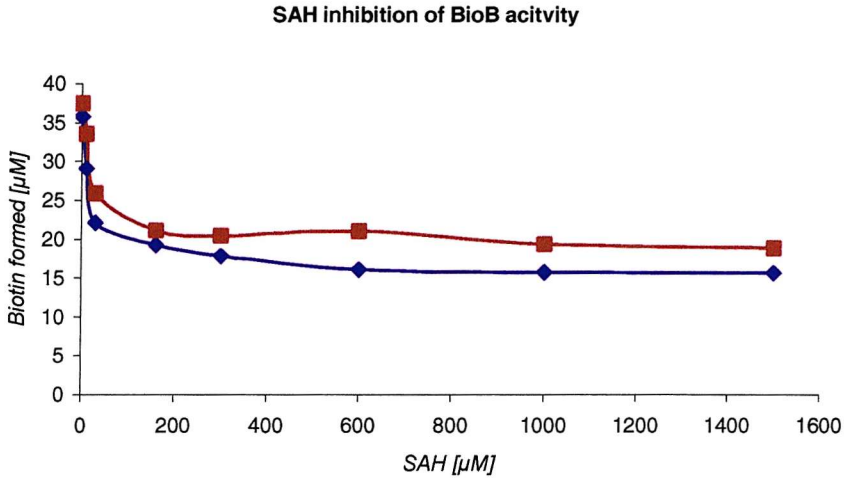

Figure 6.5: SAH inhibition of BioB activity (σ: 1.63).

Inhibition of BioB activity by SAH (IC_{50}: 160 µM) was more effective in comparison to Sinefungin inhibition, although the inhibitory effect leveled after reaching the IC_{50}. It is unlikely that SAH is present in the assay, but it might share increased common chemical and conformational feature with the inhibitor present.

6.5 Biotin inhibition of BioB activity

Biotin production is tightly controlled in cells (68). However, biotin inhibition of BioB activity has thus far not been investigated. As the biotin concentration increases over time in the assay, biotin could be a potential inhibitor (Table 6.5, Figure 6.6).

Biotin [µM]	Biotin I (Area) *10^5	Biotin II (Area) *10^5	Biotin III (Area) *10^5	Biotin IV (Area) *10^5	Biotin I [µM]	Biotin II [µM]	Biotin III [µM]	Biotin IV [µM]
50	14.03	12.49	14.02	13.15	8.12	1.35	8.06	4.25
25	8.63	8.71	8.93	9.19	9.38	9.74	10.72	11.86
15	7.47	6.75	7.66	7.86	14.30	11.13	15.12	16.01
10	6.46	6.47	6.67	6.91	14.86	14.90	15.81	16.85
7.5	6.11	6.24	6.68	6.75	15.84	16.39	18.34	18.62
5	6.10	6.44	6.23	6.58	18.31	19.78	18.86	20.41
2.5	5.39	5.85	6.16	6.09	17.66	19.70	21.04	20.74
1	5.46	5.77	6.10	5.81	19.48	20.85	22.30	21.03
0	5.14	5.66	5.72	5.82	19.09	21.35	21.64	22.07

Table 6.5: values for Figure 6.5; I, II, III and IV represent four fold repeated assays; [Method I; HPLC\Results\biotin.inh\RP1.002\1-45].

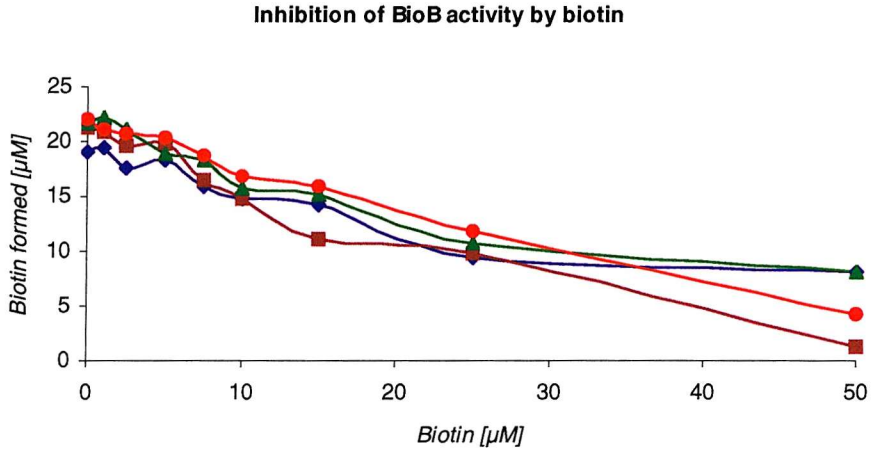

Figure 6.6: Inhibition of BioB activity by biotin (σ: 0.8).

The results of these assays suggested an inhibitory effect of biotin in the assay. However, all the assays investigated biotin formation after 180 min. Investigating biotin formation at earlier time points could detect more efficiently biotin inhibition as the amount of

formed biotin increases faster in the initial phase of the assay (Section 4.2). The assays at a high biotin concentration were difficult to reproduce. The assays were thus repeated at a lower level of biotin and earlier time points (Table 6.6, Figure 6.7).

Time in min.	Biotin I (Area) *10^5	Biotin II (Area) *10^5	Biotin III (Area) *10^5	Biotin IV (Area) *10^5	Biotin I [µM]	Biotin II [µM]	Biotin III [µM]	Biotin IV [µM]
0	1.42	1.73	2.94	3.11	2.73	4.11	0.20	0.17
10	1.87	1.95	3.29	3.30	4.73	5.08	0.94	0.99
20	1.99	2.25	3.70	3.35	5.24	6.39	2.74	1.21
30	1.97	2.23	3.76	3.67	5.16	6.29	3.01	2.63
40	2.17	2.48	3.96	3.86	6.03	7.40	3.91	3.48
50	2.65	2.74	4.10	3.95	8.16	8.53	4.52	3.83

Table 6.6: values for Figure 6.5; I, II, III and IV represent duplicate assays; [Method I; HPLC\Results\biotin.inh2\RP1.003\1-12\ RP1.004,5,6\1-3\ RP1.007\1-10].

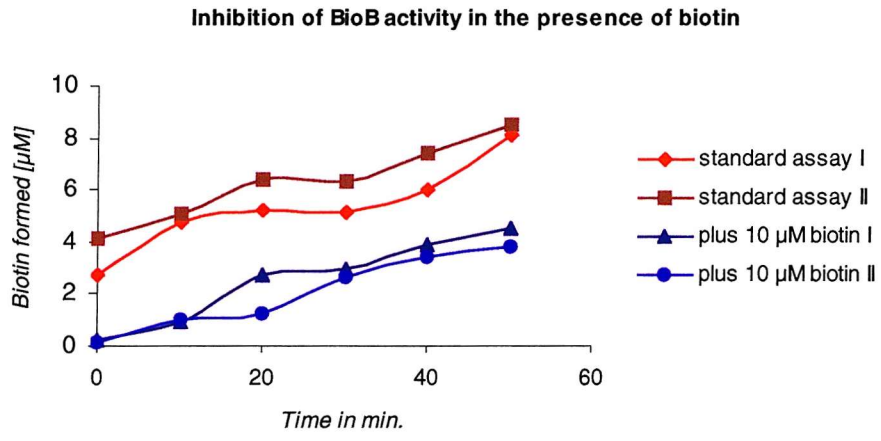

Figure 6.7: Inhibition of BioB activity by biotin (σ: 0.37).

Although biotin is unable to completely inhibit biotin formation, it had an inhibitory effect *in vitro* at a concentration that is reached after approximately 60 min. (Section 4.2). This could be one reason why the biotin formation is slowing down after an initial exponential phase (63). However, other bottlenecks might also exist to hinder multiple turnover.

6.6 DOA and methionine inhibition of BioB activity

5'-deoxyadenosine **3** and methionine **4** are the products of the reductive cleavage of SAM (Section 1.3). *In vitro* the biotin to DOA (or methionine) ratio was suggested to be 1 mol of biotin per 2 mol of DOA (or methionine) (51,53), although in our hands the biotin to DOA ratio generated during DTB turnover was closer to 1 mol of biotin per 3.5 mol of DOA (Section 4.3).

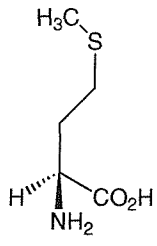

3

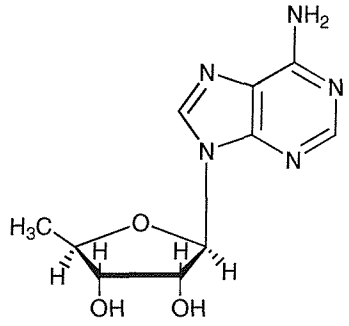

4

Scheme 6.2: 5'-deoxyadenosine and methionine, the products of the reductive cleavage of SAM

As DOA and methionine are present in the assay, they could be potential inhibitors. In addition, the structure of DOA shares chemical and conformational similarities to Sinefungin and SAH (Section 6.3). The inhibitory effect of methionine (Table 6.7, Figure 6.8) and DOA (Table 6.8, Figure 6.9) was investigated.

methionine [µM]	Biotin I (Area) *10^5	Biotin II (Area) *10^5	Biotin I [µM]	Biotin II [µM]
1400	2.87	2.63	9.12	8.05
700	3.09	2.77	10.07	8.66
280	3.49	3.23	11.82	10.67
140	3.73	3.43	12.91	11.55
70	4.19	3.85	14.89	13.40
0	4.55	4.61	16.48	16.73

Table 6.7: values for Figure 6.8; I and II represent duplicate assays; [Method II; HPLC\Results\inh4\RP1.003\1-12].

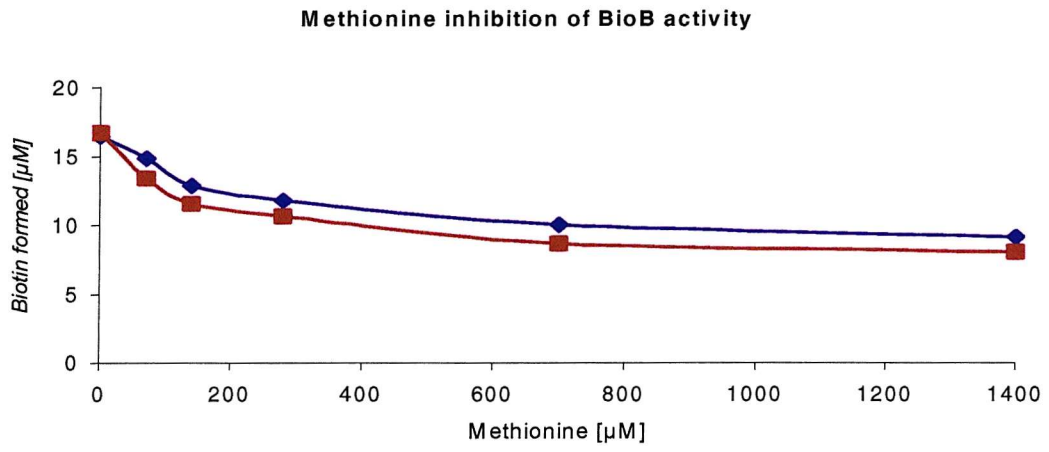

Figure 6.8: Methionine inhibition of BioB activity (σ: 0.56).

DOA [µM]	Biotin I(Area) *10^5	Biotin [µM]
800	2.08	5.66
400	2.41	7.10
160	3.05	9.90
80	3.86	13.44
40	4.30	15.41
0	4.55	16.48

Table 6.8: values for Figure 6.9; [Method II; HPLC\Results\inh4\RP1.002\1-12].

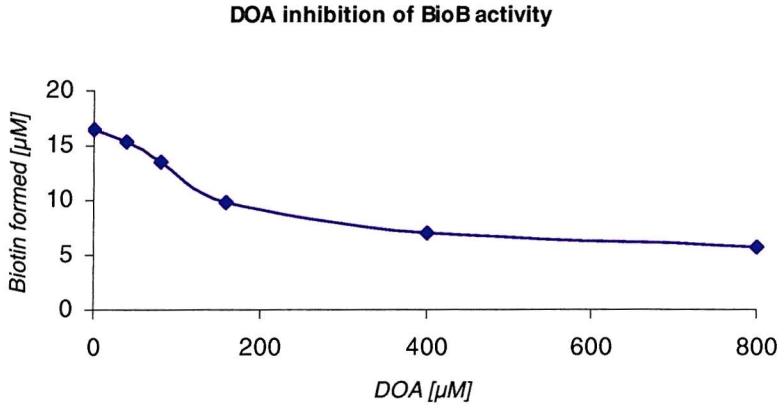

Figure 6.9: DOA inhibition of BioB activity (single assay).

There is a weak inhibitory effect of both methionine (IC_{50}: 700 µM) and DOA (IC_{50}: 400 µM). DOA and methionine are present at lower concentration in the assay and could thus

exert only slight inhibitory effects as an alternative. However, as they are produced in a 1:1 molar ratio, we investigated whether they could act in a synergistic manner.

6.7 Synergistic inhibition of BioB activity by DOA and methionine

As seen above (Section 6.5), DOA and methionine exert inhibitory effects above the concentration typically found in the assay and we examined the effect of adding an equimolar mix of the two compounds at varying concentrations (Table 6.9, Figure 6.10).

DOA/methionine [µM]	Biotin I (Area) $*10^5$	Biotin II (Area) $*10^5$	Biotin I [µM]	Biotin II [µM]
400	0.79	0.71	0.00	0.00
200	1.83	1.77	4.55	4.30
100	2.75	2.90	8.59	9.26
50	3.56	3.57	12.13	12.20
25	3.86	3.88	13.47	13.56
0	4.32	4.55	15.46	16.48

Table 6.9: values for Figure 6.10; I and II represent duplicate assays; [Method IV; HPLC\Results\inh8\RP2.004\1-8].

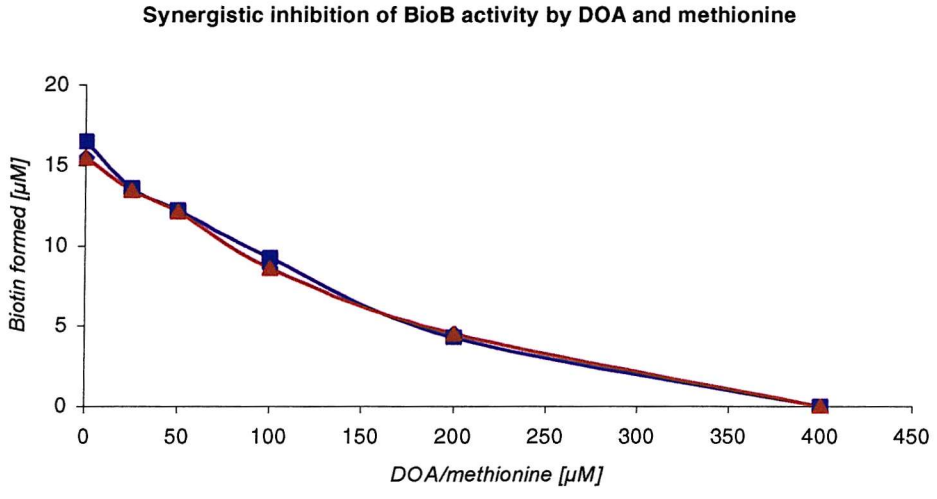

Figure 6.10: Synergistic inhibition of BioB activity by DOA and methionine (σ: 0.17).

Added alone to the assay DOA and methionine have only a slight inhibitory effect. However, if methionine and deoxyadenosine are added together in a 1 to 1 molar ratio

stronger synergistic inhibition occurs. This inhibition (IC_{50}: 150 μM) is exerted at a concentrations to which DOA and methionine accumulate *in vitro*. Interestingly, whilst SAH and sinefungin do not appear to give complete inhibition, even at very high concentration, the addition of an equimolar mix of DOA and methionine leads to complete inhibition of biotin synthase activity. This might suggest that methionine and DOA are binding at the the SAM binding site together at some point in the reaction cycle. Removing DOA or methionine formed *in vitro* during the assay may therefore be a way of achieving multiple turnover of BioB.

6.8 Inhibition of BioB activity is reversed by PFS, the product of the *pfs* gene

The enzyme 5'-methythioadenosine/S-adenosylhomocysteine nucleosidase (PFS) is responsible for cleavage of the glycosidic bond in both 5'-methylthioadenosine (MTA) and S-adenosylhomocysteine **5** to yield both adenine and the corresponding thiopentose (methylribose or S-ribosyl-homocysteine **6**; Scheme 3 and 4) (129,130).

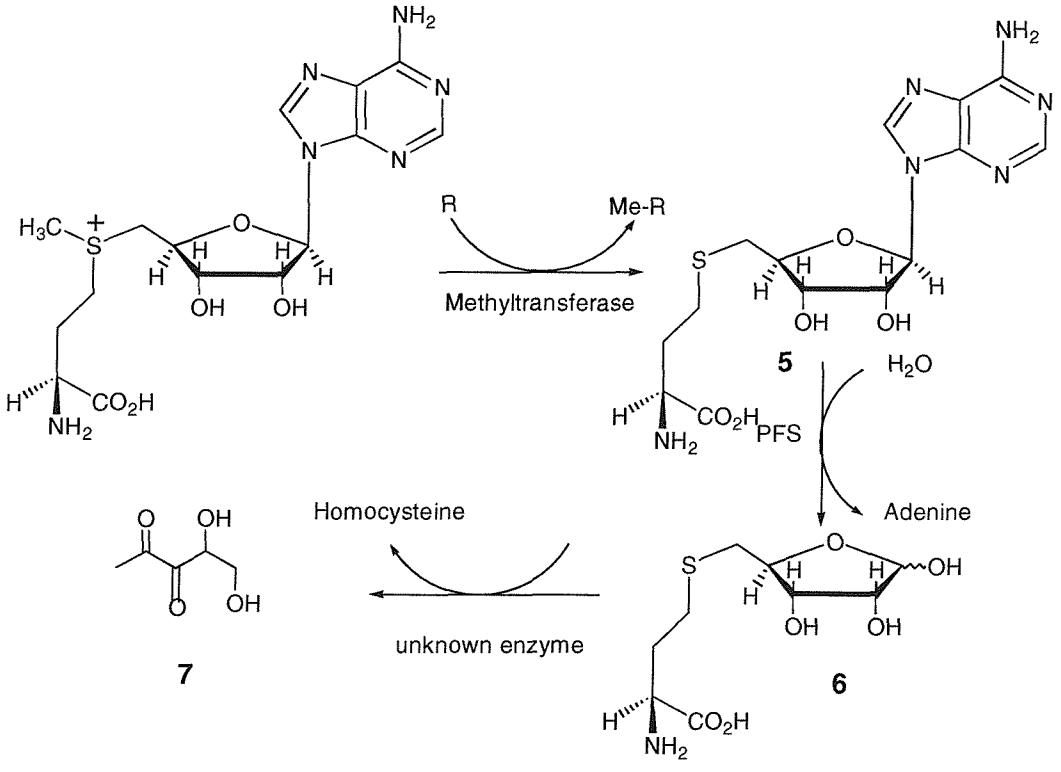

Scheme 3: PFS catalysed cleavage of SAH (see below for details).

A number of methyltransferase enzymes catalyse the transfer of the methyl group from SAM to particular cellular substrates. S-adenosylhomocysteine (SAH) **5** is formed in this process. The PFS nucleosidase subsequently cleaves adenine from SAH forming S-ribosylhomocysteine (SRH) **6**. SRH is converted to homocysteine and 4,5-dihydroxy-2,3-pentanedione **7** by an unknown enzyme.

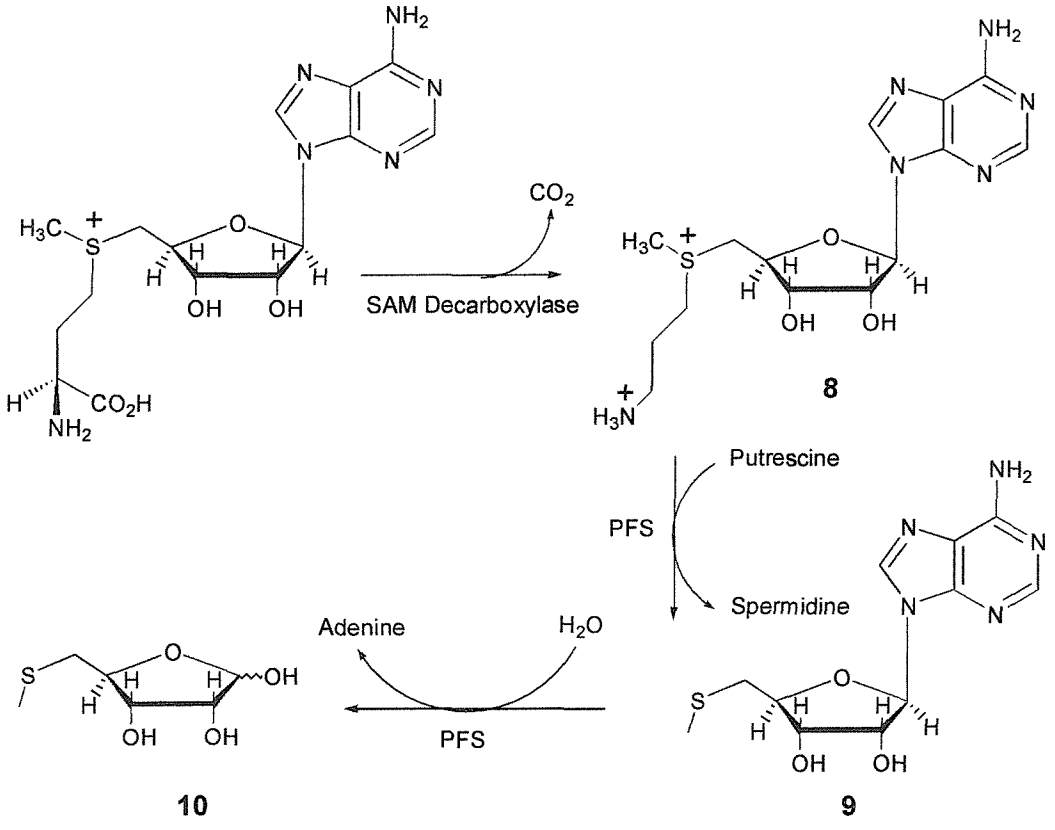

Scheme 4: In two sequential reactions, SAM is decarboxylated to yield **8**, and the aminopropyl moiety is used in the synthesis of polyamines such as spermidine. Methylthioadenosine (MTA) **9** is formed by these reactions. The PFS nucleosidase catalyses the hydrolysis of MTA to form methylthioribose (MTR) **10** and adenine. The subsequent steps in the utilization of MTR are not known.

In experiments to identify proteins that improve biotin biosynthesis, a fraction enriched in Pfs had been isolated (Dr. N. Shaw, personal communication), but the mode of action had not been explained. We speculated that one possible mode of action involves the cleavage

adenine **11** and 5'-deoxyribose **12** (Scheme 5). Knappe *et al.* identified a nucleosidase activity in the cell-free lysate used for investigating pyruvate formate lyase activity (131). This nucleosidase activity lead to the undesired cleavage of DOA into methionine and a compound, which was found to be 5'-deoxyribose. However, the enzyme responsible for the nucleosidase activity was not identified. To investigate the function of PFS, the enzyme was overexpressed in BL-21(DE3) and purified to homogeneity.

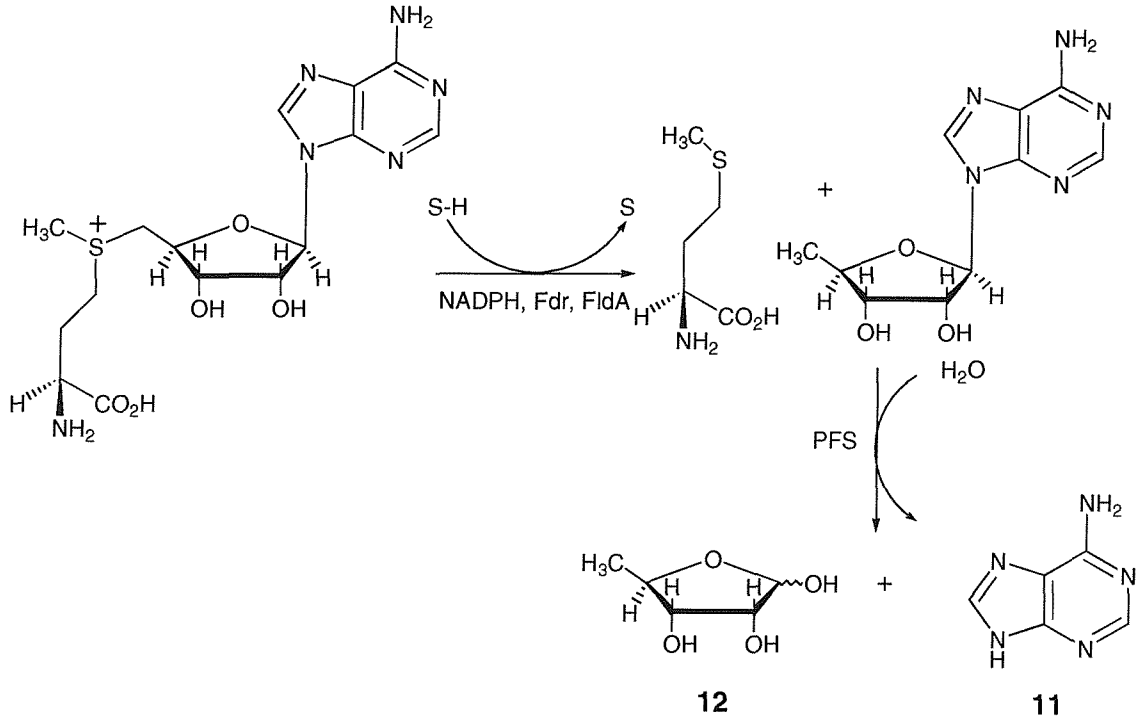

Scheme 5: New mode of action for PFS; the cleavage of DOA into adenine **11** and 5'-deoxyribose **12.** (S-H: reduced substrate, S: oxidised substrate).

6.8.1 Purification of His_6-PFS from pProExHTApfs/BL-21(DE3)

The plasmid pProExHTApfs (Figure 6.11) was a kind gift from Prof. K. Cornell (Oregon Health Science University, Portland). It was transformed into BL-21(DE3). His_6-PFS was expressed with an N-terminal polyhistidine tag and purified using nickel chelating chromatography (Figure 6.12). Comparison of PFS activity with and without an affinity tag, showed no notable difference (130). His_6-PFS was chosen, because of the one-step purification.

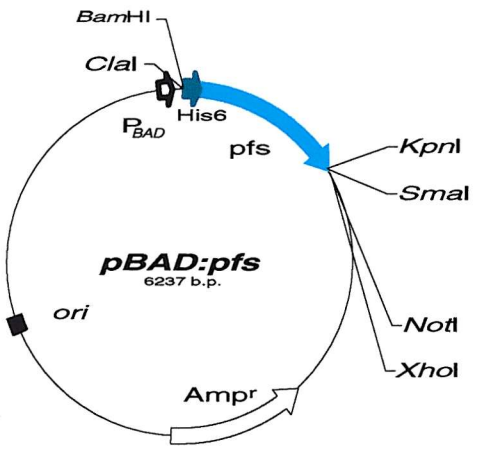

Figure 6.11: Plasmid map of pProExHTApfs with prominent restriction sites

His_6-PFS was purified using nickel chelating chromatography (Figure 6.12).

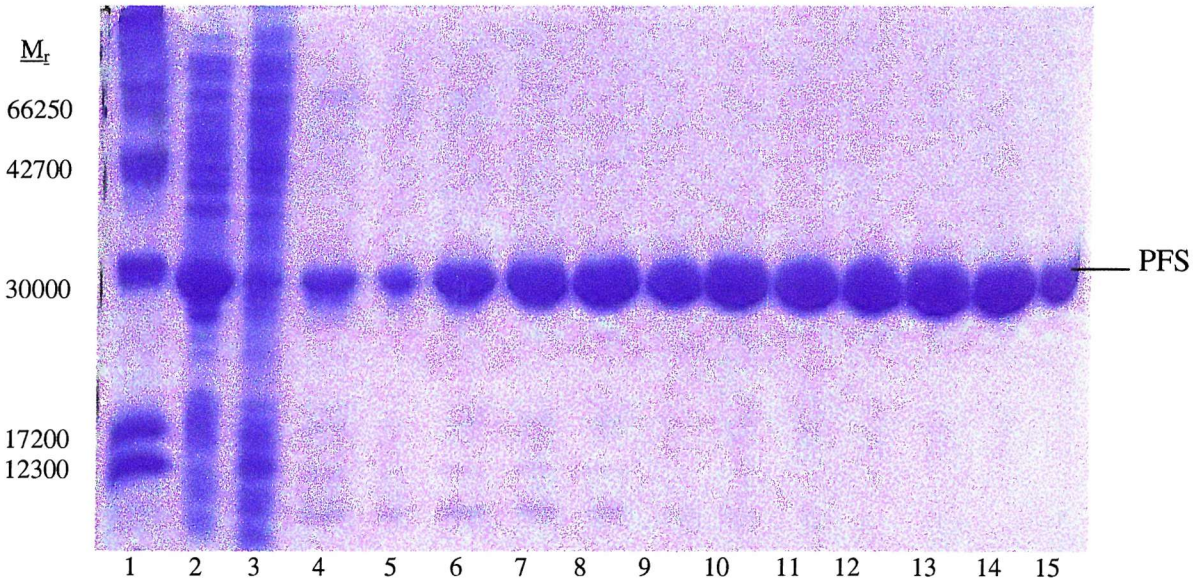

Figure 6.12: Coomassie Blue stained 15 % SDS-PAGE gel of the nickel chelating affinity column. (1) Molecular weight markers, (2) Load, (3) flow through, (4) – (15) His_6-PFS containing fractions. Fraction 8 to 15 were desalted, concentrated (Method II) and used for biochemical investigations.

ESI-MS for purified His_6-PFS

Multiple charged His_6-PFS was observed by ESI-MS and the molecular weight (MW) was determined to be 28008.7 (Figure 6.13). The calculated molecular weight of His_6-PFS from the amino acid sequence is 28159.01 (132). The remaining discrepancy cannot be accounted for.

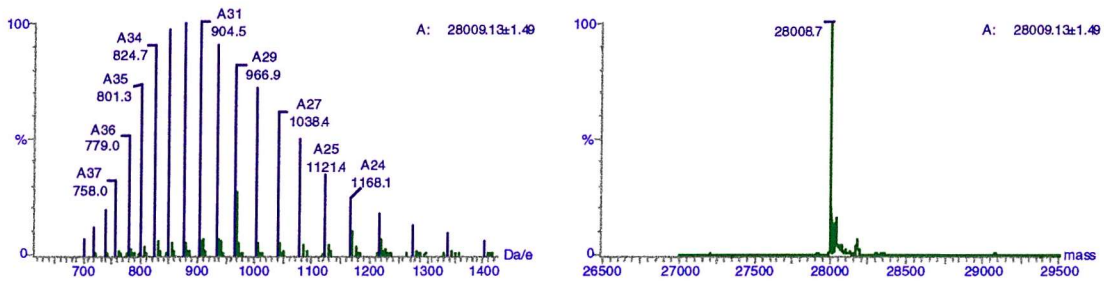

Figure 6.13: ESI-MS for His_6-PFS

6.8.2 PFS addition *in vitro*

To investigate if PFS could cleave DOA and thus reverse the inhibition (Section 6.6), purified His_6-PFS was added to the assay (Figure 6.14 and 6.15).

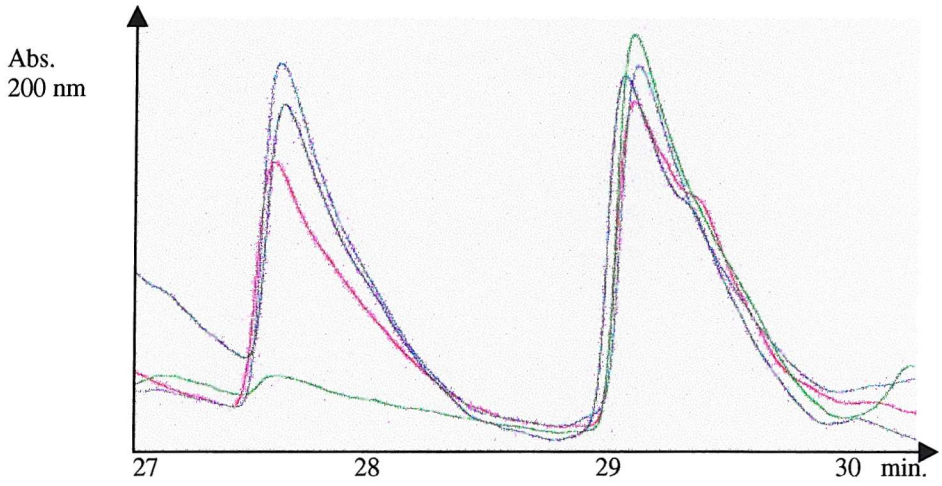

Figure 6.14: Conversion of DTB (R_t, 29.5 min.) to Biotin (R_t, 27.5 min.) in the presence of inhibitor. See Figure 6.12 for concentration; standard assay, plus DOA/methionine, plus PFS, DOA/methionine, plus PFS; [Method IV; HPLC\Results\inh8\RP2.004\ 2,3,6,7].

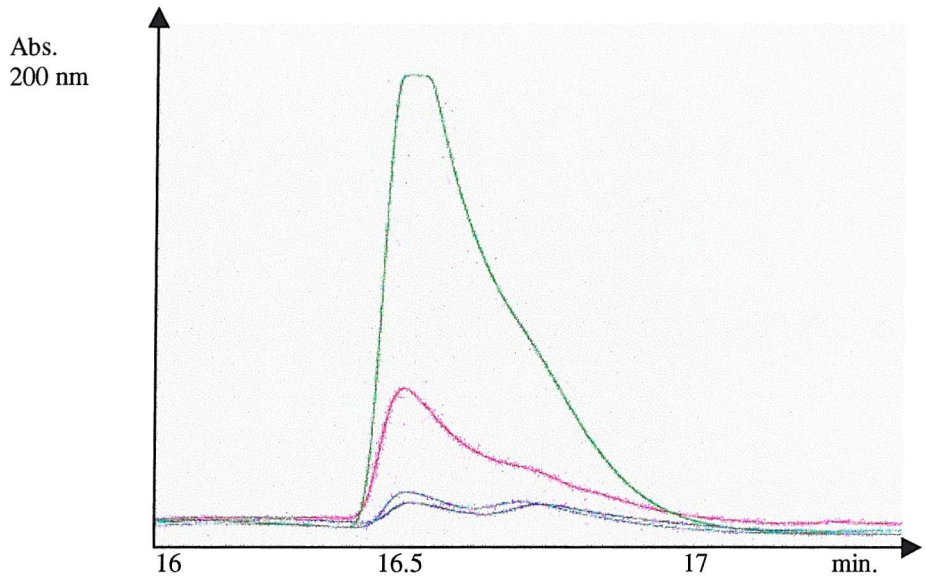

Figure 6.15: DOA concentration (R_t, 16.6 min.) in the assay in the presence and absence of PFS and inhibitors; standard assay, plus 400 µM DOA/methionine, plus 1 µM PFS, 400 µM DOA/methionine, plus 1 µM PFS; [Method IV; HPLC\Results\inh8\RP2.004\2,3,6,7].

The concentration of biotin and DTB were estimated by integrating the peak areas and computing these values with a standard calibration (Table 6.10, 6.16).

Sample ID	Biotin I (Area) *10^5	Biotin II (Area) *10^5	Biotin I [µM]	Biotin II [µM]
1	6.57	7.00	25.35	27.26
2	0.85	0.61	0.24	0.10
3	7.10	6.94	27.69	27.00
4	8.54	8.26	34.01	32.77

Table 6.10: see Figure 6.16 for details; I and II represent duplicate assays; [Method IV; HPLC\Results\inh8\RP2.004\2,3,6,7].

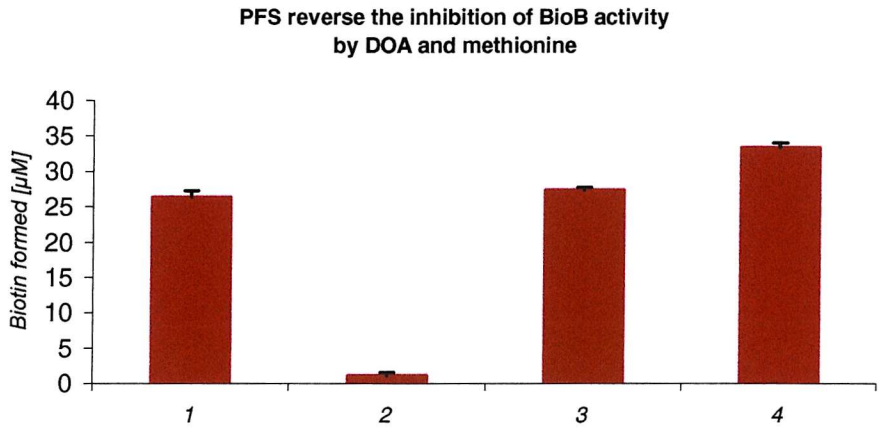

Figure 6.16: PFS, DOA and methionine addition to the standard assay; (1) standard assay; standard assay (2) plus 400 µM methionine and 400 µM DOA, (3) plus 400 µM methionine, 400 µM DOA and 1 µM PFS, (4) plus 1 µM PFS.

Thus the synergistic inhibition by DOA and methionine can be completely reversed by the product of the *pfs* gene, PFS. In fact, the addition of PFS to an assay from the beginning leads to a small but reproducible increase in activity.

6.8.3 PFS catalysed cleavage of DOA, determination of the K_m

DOA cleavage was halted at various time points to investigate the time to achieve optimal turnover (Table 6.11; Figure 6.17).

Time in min.	DOA (Area) $*10^5$	Adenine (Area) $*10^5$	DOA [µM]	Adenine [µM]
1	25.51	85.14	43.10	133.60
2	54.83	71.89	87.61	113.49
4	75.64	49.90	119.18	80.12
8	97.67	36.16	152.62	59.27

Table 6.11: DOA cleavage by PFS at various enzyme concentrations; [Method II; HPLC\Results\added\rp1\11-15].

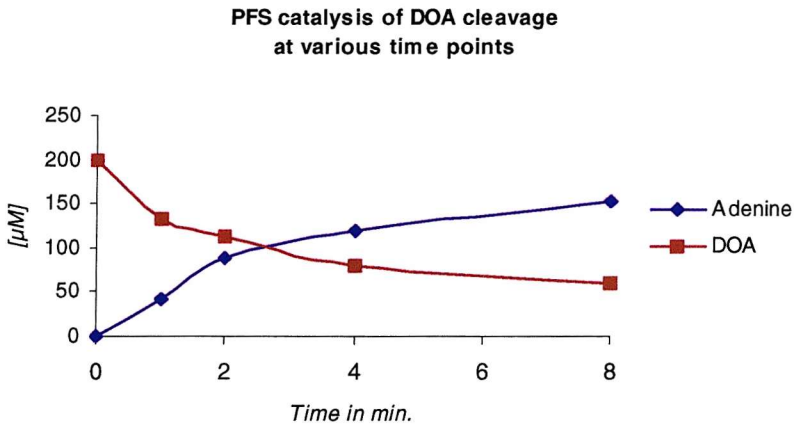

Figure 6.17: DOA cleavage by PFS at time points (DOA: 200 µM, PFS: 1µM).

PFS was added at various concentrations to investigate the cleavage of DOA (Table 6.12, Figure 6.18).

PFS [µM]	DOA (Area) *10^5	Adenine (Area) *10^5	DOA [µM]	Adenine [µM]
10	184.55	5.32	24	321
1	134.39	58.84	39	309
0.1	55.01	162.06	88	250
0.01	22.96	200.45	208	94
0.001	13.07	208.50	284	12

Table 6.12: DOA cleavage by PFS at various enzyme concentrations; [Method II; HPLC\Results\added\1-10].

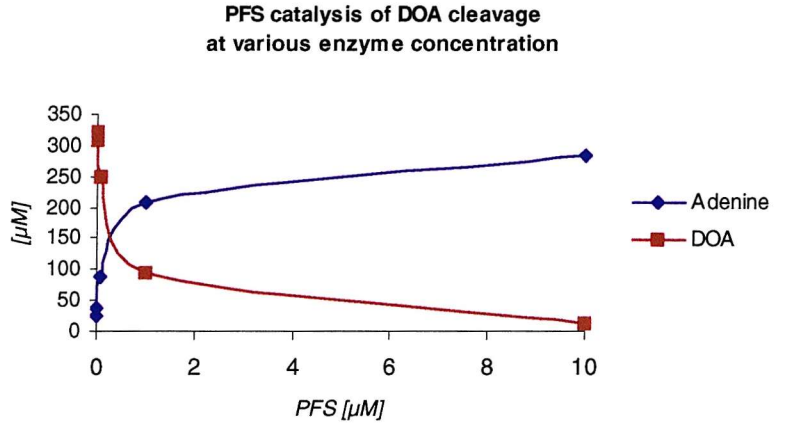

Figure 6.18: DOA cleavage by PFS at various enzyme concentrations (assay was halted after 5 min., DOA: 400 µM).

Using these optimised conditions the K_m for the PFS catalysed cleavage of DOA to adenine and 5'-deoxyribose could be determined by plotting 1/v versus 1/S (Lineweaver-Burk plot; Figure 6.19; Section 8.6.3; p. 143). The K_m of PFS was determined to be 462 μM, indicating a lower affinity of PFS to DOA than to MTA (0.54 μM) and the specific activity was found to be 47 μmol/ min/ mg, which corresponds to reported specific activities of PFS catalysed reactions for analogue substrates (130).

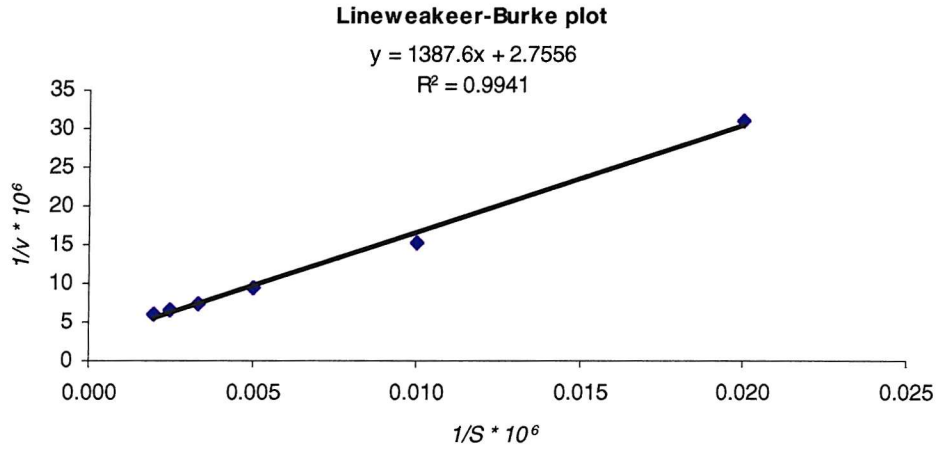

Figure 6.19: Lineweaver-Burk plot for the determination of the K_m of PFS

6.8.4 A new mode of action for PFS

To be completely sure of the products formed by PFS from DOA (Scheme 6), the reaction mixture was investigated by NMR spectroscopy.

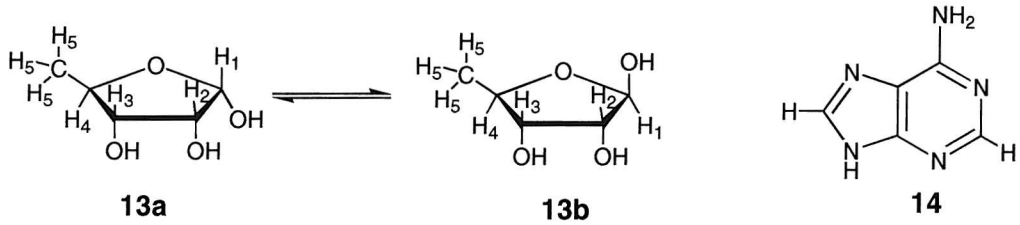

Scheme 6: The products of adenine cleavage: adenine **14** and 5'-deoxyribose. In solution 5'-deoxyribose exist in as α- (**13a**) and β- (**13b**) anomer.

The cleavage of DOA was initiated by the addition of PFS (1 μM) to DOA (1 mM) in H_2O. After 60 min. the reaction was halted by removing the protein fraction with MWCO membrane filters (> 10 kDA, 4 ml, Millipore). The flow through containing the small molecules was freeze dried, resuspended in CD_3OD (0.5 ml) and submitted to NMR spectroscopy and mass spectrometry.

δH (400 MHz, CD_3OD): 8.10 (1H, s, AdH), 7.95 (1H, s, AdH), 5.15 (1H, d, J = 4.51, H_1-α), 4.95 (1H, d, J = 0, H_1-β), 3.95 (2H, m, $H_{2\text{-}4}$-α), 3.80 (3H, m, $H_{2,3,4}$-β), 3.55 (1H, t, J = 6.02, H_3-α), 1.25 (3H, d, J = 8.53, H_5-β), 1.15 (3H, d, J = 6.52, H_5-α).

δC (75.5 MHz, CDE3OD): 154.8 (C), 142.2 (C), 104.2 (C), 98.6 (C), 80.2 (C), 79.9 (C), 78.6 (C), 78.3 (C), 73.2 (C), 21.4 (C), 20.1 (C).

HRMS: m/z ($M+H^+$) 135 and 136
Calculated MW: adenine (135); 5'-deoxyribose (134)

^{1}H-NMR identified the 5'-deoxyribose present in an approximate 1: 1.7 mixture of α- and β-anomer. The data found by NMR spectroscopy and mass spectrometry corresponded with literature reports for 5'-deoxyribose (133).

6.9 Effect of MetK on inhibition of BioB by DOA and MetK

MetK is catalysing the conversion of ATP **15** and methionine to SAM (134,135) (Scheme 5).

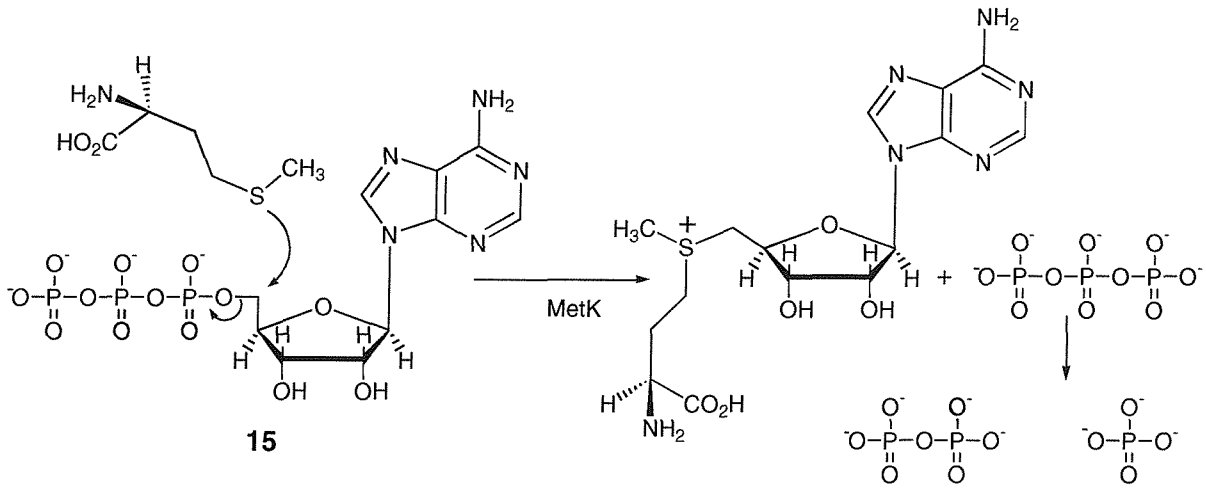

Scheme 5: Biosynthesis of SAM. SAM is synthesised from methionine and ATP **15** by a displacement of triphosphate, which is subsequently hydrolysed to phosphate and pyrophosphate.

As PFS can cleave DOA and thus reverse the inhibition of BioB activity, MetK might exhibit a similar effect on BioB activity in the assay by removing methionine to synthesise SAM. To investigate this hypothesis, MetK was overexpressed in BL-21(DE3) and purified to homogeneity.

6.9.1 Purification of MetK from pK8/BL-21(DE3)

The plasmid pK8 (Figure 6.19) was a kind gift from Prof. G. Markham (Institute for Cancer Research, Philadelphia). MetK was overexpressed in BL-21(DE3).

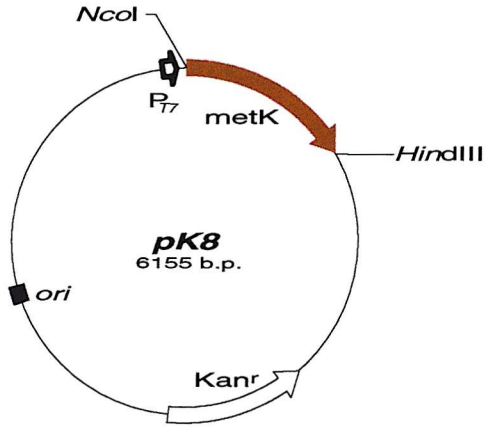

Figure 6.19: Plasmid map of pK8 with prominent restriction sites

MetK was purified using anion exchange and gel filtration chromatography (Figure 6.20 and 6.21). MetK was purified to ~ 80 % purity and used for subsequent *in vitro* studies.

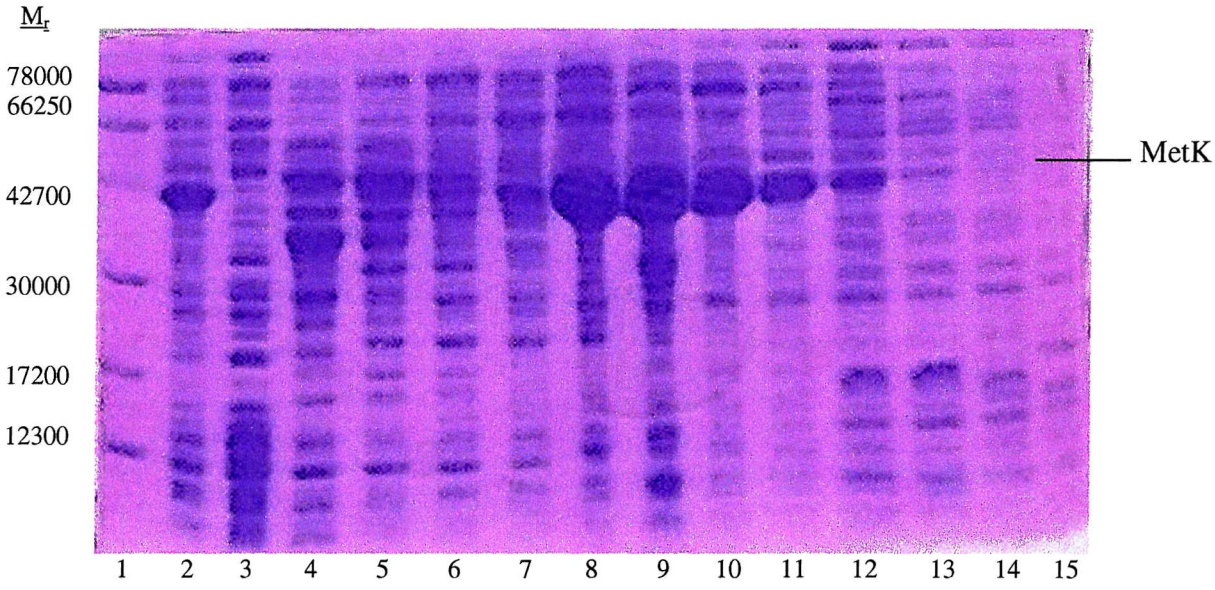

Figure 6.20: Coomassie Blue stained 15 % SDS-PAGE gel of the anion exchange column. (1) Molecular weight markers, (2) Load, (3) flow through, (4) – (15) MetK containing fractions. Fraction 8 to 11 were pooled and further purified by gel filtration chromatography.

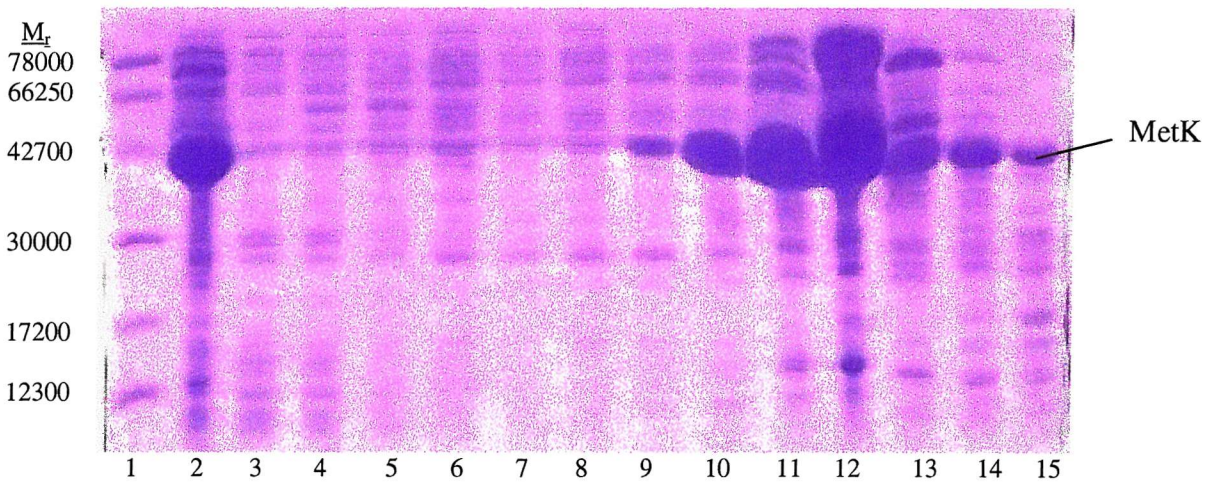

Figure 6.21: Coomassie Blue stained 15 % SDS-PAGE gel of the gel filtration column. (1) Molecular weight markers, (2) Load, (3) – (15) MetK containing fractions. Fractions 10 to 12 were used for biochemical investigations.

ESI-MS for purified MetK

Multiple charged MetK was observed by ESI-MS and the molecular weight (MW) was determined to be 41795.8 (Figure 6.22). The calculated molecular weight of MetK from the amino acid sequence is 41820.43. The mass difference may be due to protein bound Na^+ (MW: 23).

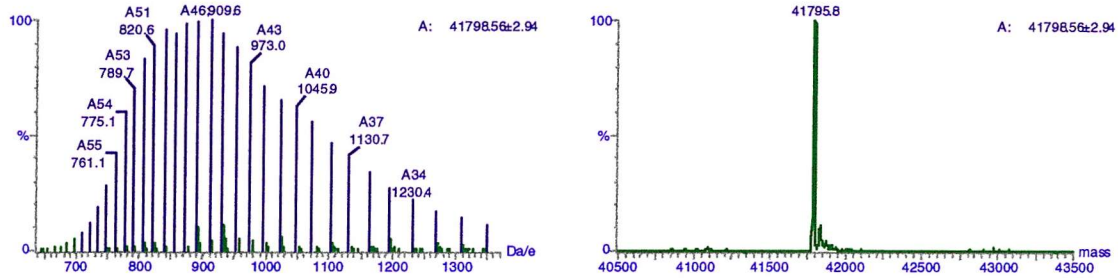

Figure 6.22: ESI-MS for MetK

6.9.2 Effect of MetK on inhibition of BioB activity

MetK and ATP were added to the assay in the presence of DOA and methionine (Table 6.13, Figure 6.23).

Sample ID	Biotin I (Area) $*10^5$	Biotin II (Area) $*10^5$	Biotin I [µM]	Biotin II [µM]
1	1.11	1.67	1.4	3.8
2	1.71	1.57	4.0	3.4
3	4.32	4.55	16.36	15.68

Table 6.13: see Figure 6.23 for details; I and II represent duplicate assays; [Method V; HPLC\Results\added\rp210\11-18].

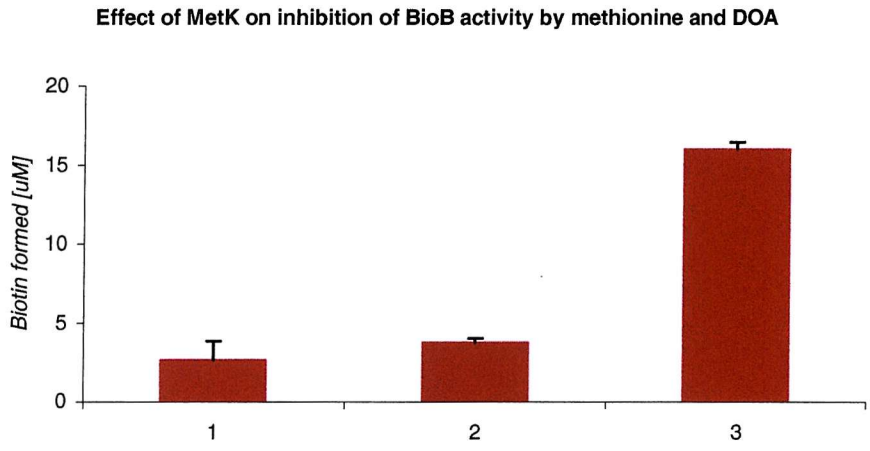

Figure 6.23: Effect of MetK on the inhibition of BioB activity. (1) standard assay plus 400 µM DOA and 400 µM methionine, (2) standard assay plus 400 µM DOA, 400 µM methionine, 10 µM MetK and 400 µM ATP, (3) standard assay.

MetK was unable to reverse the inhibition, which could be due to several factors. As was shown above (Section 6.5), methionine has a much higher IC_{50} in comparison to DOA. Thus, removing methionine is likely to have a less pronounced effect. The *in vitro* conditions, optimised for BioB activity, might be unfavourable for MetK to synthesise SAM. In a detailed study of Metk, successful enzymatic synthesis of SAM was only achieved by using reducing agents, organic solvents or denaturing agents (136). An additional effect might be the high concentration of SAM in the assay, which

allosterically inhibits MetK activity. A possible alternative to *E. coli* MetK would be the use of yeast SAM synthetase, encoded by the *sam2* gene, which does not exhibit substrate inhibition.

6.10 Summary and Conclusion

BioB participates in the last step of the biosynthesis of biotin. Thus far, no catalytic activity *in vitro* has been reported. An experiment which removed the small molecules from the assay, allowed us to show that the proteins were able to produce more biotin when the small molecules were removed and fresh substrates and co-factors were introduced. We thus speculated that an inhibitor may be present and possible inhibitors were proposed and investigated. Inhibition of biotin synthase activity by SAH was more effective in comparison to sinefungin inhibition, although the inhibitory effect levelled after reaching the IC_{50}. As no catalytic biotin forming system is available, it is difficult to assess their inhibitory profile. Although biotin is unable to completely inhibit biotin formation, it had an inhibitory effect *in vitro* at a concentration that is reached after approximately 60 min. Effective inhibition occurred when DOA and methionine, the products of the reductive cleavage of SAM, were added. At a concentration of 400 µM of both DOA and methionine, biotin formation halted almost completely. This synergistic inhibition of BioB activity by DOA and methionine was reversed by PFS, the product of the *pfs* gene, through cleavage of 5'-deoxyadenosine into adenine and 5'-deoxyribose. It was thus suggested, that the enzyme present in cell-free lysate and responsible for the cleavage of 5'-deoxyadenosine into adenine and 5'-deoxyribose (131), was PFS.

The identification of a further protein co-factor for the biotin formation *in vitro* is a major step forward in obtaining a catalytic system for biotin formation. It was found that at least one other protein co-factor was having a beneficial effect on biotin formation *in vitro* (Dr. N. Shaw, personal communication). The addition of MetK did not reverse the inhibition of biotin synthase activity, possibly because the *in vitro* conditions are unfavourable for MetK to utilise methionine in the synthesis of SAM. An alternative to *E. coli* MetK would be the use of yeast SAM synthetase, encoded by the *sam*2 gene, which does not exhibit substrate inhibition. It is noteworthy, that PFS is unrelated to iron-sulphur cluster assembly. There is a strong research focus on the state of iron-sulphur cluster of BioB

and iron-sulphur cluster assembly, but other mechanism could be involved in biotin formation. The addition of exogenous iron, sulphide or the products of the *isc* gene cluster did not, with the exception of IscS, show a strong effect on biotin formation (Chapter Five). The finding that PFS could reverse the synergistic inhibition of BioB activity by DOA and methionine might have some major implication for the fermentative production of biotin. Shaw *et al.* could produce 30 mg/L of biotin per day. This would result in an approximate cellular concentration of approximately 500 μM DOA, if other mechanisms of DOA salvage are discounted. Biotin formation halted almost completely at this concentration *in vitro*, which might explain the inability of various research groups to increase the biotin formation *in vivo*. We therefore suggest that the biotin produced *in vivo* might increase considerably if possible inhibitors, such as DOA, are removed by the overexpression of PFS

The inhibitors of biotin synthase activity might assist in obtaining BioB in crystalline form. The growth of BioB crystals might be facilitated by the addition of co-factors, which bind tightly to BioB but are not turned over. Preliminary experiments did not enable the growth of BioB crystals (data not shown). However, in the presence of some detergents BioB kept its reddish colour, a possible indication for iron-sulphur cluster stability. The other prerequisite for obtaining BioB in crystalline form, namely obtaining BioB of highest purity, was achieved as described in Chapter Two. Further studies will need to focus on characterizing and maintaining holo-BioB during screening for the optimal crystallization conditions.

Chapter Seven: Construction of plasmids encoding essential protein co-factors

7.1 Introduction

High-level fermentative production of biotin (1 g/L/day) has thus far been unsuccessful (Section 1.4). To conduct future *in vivo* experiments and apply *in vitro* findings *in vivo* plasmids were constructed encoding various genes, deemed essential or helpful for biotin formation *in vitro* or *in vivo* (Chapter 4,5,6).

7.2 General cloning strategy

The PCR reaction is a well-established technique to amplify a gene of choice from DNA (137). Various DNA polymerases are commercially available. For PCR amplifications *Taq* DNA polymerase (Promega) and *Pfu* DNA polymerase (Stratagene) were used. *Taq* DNA polymerase is very reliable in our hands and adds a single deoxyadenosine, in a template-independent fashion, to the 3' ends of the amplified fragments, which is advantageous for downstream subcloning methods. *Pfu* DNA polymerase is less reliable in our hands but it has a 5'-3' proofreading activity, which lowers the error rate about 10 fold in comparison to *Taq* DNA polymerase.

IscS and IscU have been successfully cloned and overexpressed within this lab by Dr. P. Roach. The plasmid of choice was a pET vector (Novagen) due to the high expression levels of soluble protein reported for its use. The pET24a(+) vector is approximately 5.3 kb in size, encodes kanamycin resistance and contains a T7 promotor as dominant characteristics for high level of protein expression. Protein expression is induced by the addition of isopropyl-β,D-thiogalactoside (IPTG). Usually difficulties had been encountered with the direct subcloning of genes into the pET24a(+) (Method A; Section 8.7.3). This problem can be resolved by first inserting the DNA fragment into the pGEM-T vector (Promega) and then excising the gene with the appropriate restriction enzymes (Method B; Section 8.7.3). The pGEM-T vector has a 3' terminal thymidine added to both ends. These single 3'-T overhangs at the insertion site prevent recircularization of the vector and provides a compatible overhang for PCR products generated by *Taq* DNA polymerase.

Experiments had shown that 5' biotinylated primer could facilitate cloning (Method C; Section 8.7.3). By the addition of streptavidin, a protein that binds strongly to biotin, it was possible to assay the extent of restriction enzyme cleavage. Direct digestion of the PCR fragment, followed by addition of streptavidin gave retarded, undigested PCR product and non-retarded, digested PCR product. This strategy requires 5' biotinylated primers. A further way of subcloning was the use of the pBAD-TOPO vector (Method D; Section 8.7.3). The pBAD-TOPO vector has topoisomerase I added after the recognition sequence 5'-CCCTT in one strand. Topoisomerase I cleaves the phosphodiester backbone to form a covalent bond between the 3' phosphate of the cleaved strand and a tyrosyl residue of topoisomerase I. The phospho-tyrosyl bond between the plasmid and enzyme can subsequently be attacked by the 5' hydroxyl of the PCR fragment, reversing the reaction, releasing topoisomerase and inserting the PCR fragment into the vector. As *Pfu* DNA polymerase does not provide a compatible overhang for the pGEM-T and pBAD-TOPO vector, each PCR product was A-tailed with *Taq* DNA polymerase before subcloning into the vector of choice.

7.3 Construction of pTZ100

The plasmid pTZ100 encodes the biotin operon genes (Section 1.3) in a pET24d-derived plasmid. Primers were designed for the PCR amplification of *bio*BFD and *bio*A (Section 8.7.2). An NdeI restriction site was incorporated at the 5' terminus and a HindIII restriction site at the 3' end of *bio*BFD. A HindIII was incorporated at the 5' terminus and a EcoRI restriction site at the 3' end of *bio*A. Construction of the plasmid followed initially Method A, but as problems were encountered Method B was preferred (Section 8.73). After insertion of *bio*BFD into the pGEM-T vector restriction digestion and sequencing showed that the NdeI and the BamHI restriction sites were not present. The reason for this remains unclear. Primers were designed for the PCR of a *Start* fragment and an *End* fragment to restore the restriction sites (Section 8.7.2). A NruI restriction site was incorporated at the 3' end of the *Start* fragment. An AgeI was incorporated at the 5' terminus of the *End* fragment. Forward and reverse primer were the same used for the amplification of *bio*BFD. The construction of pTZ100 is depicted in Figure 7.1a and 7.1b.

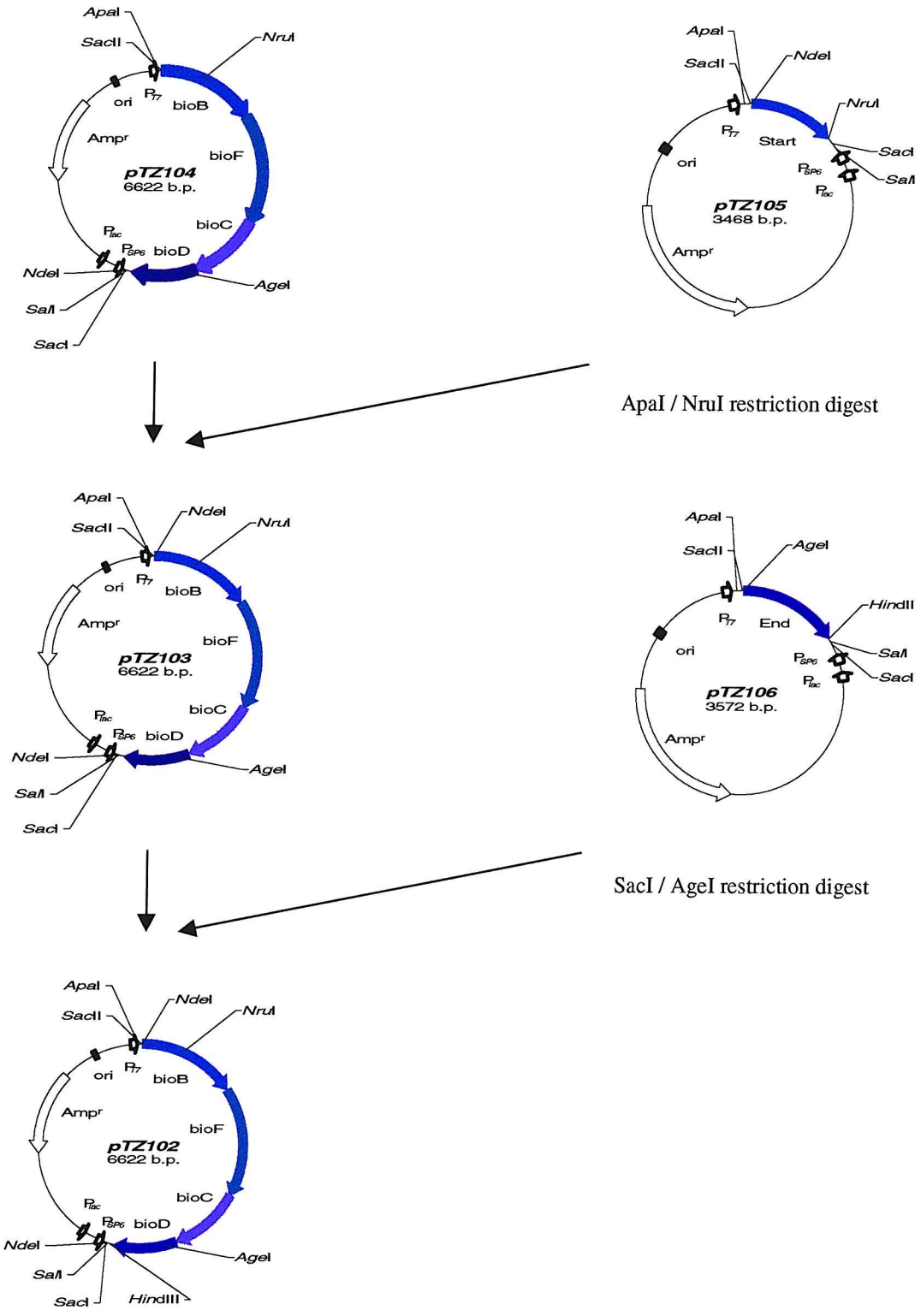

Figure 7.1a: The construction of pTZ100 (repair of the end and start sequence).

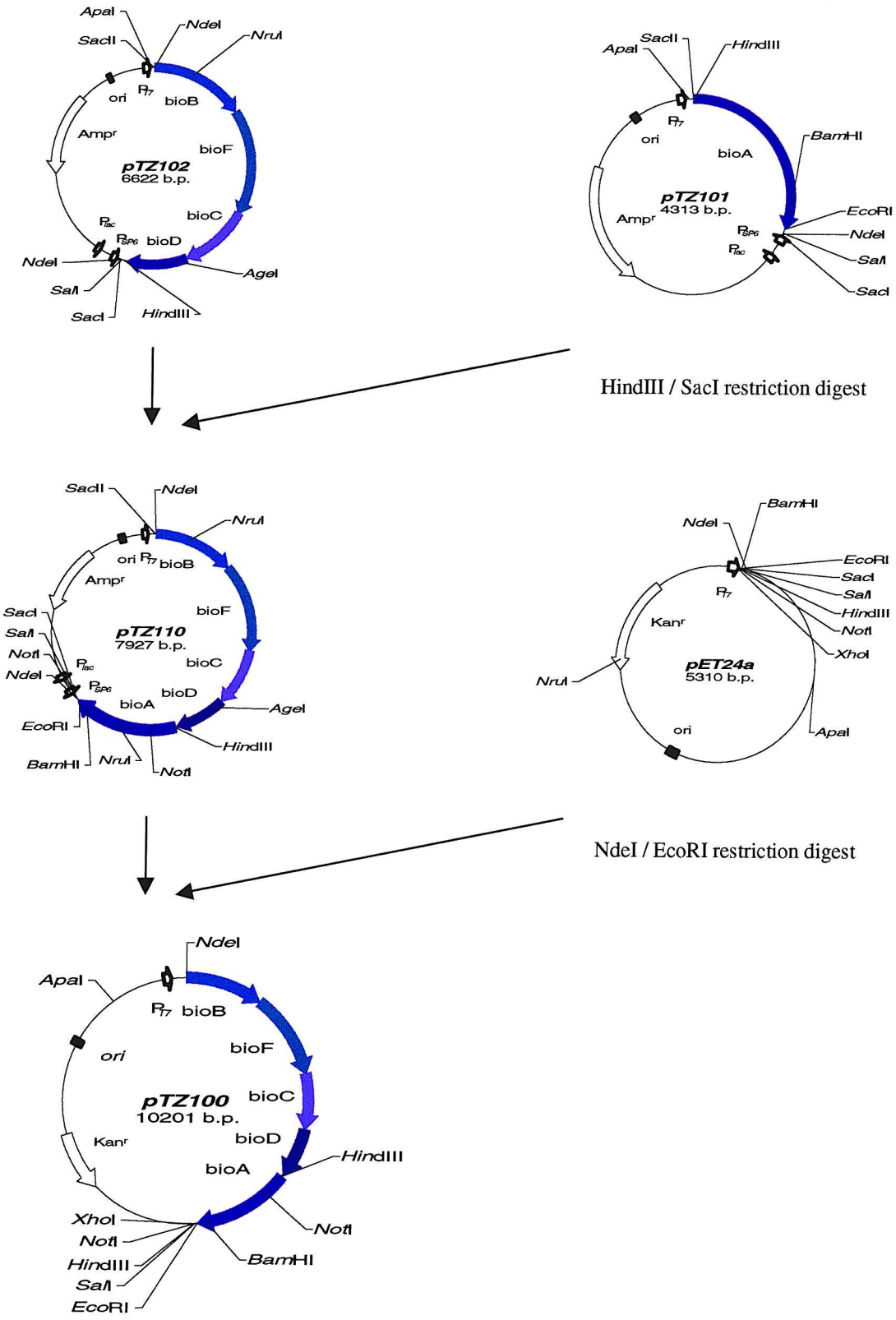

Figure 7.1b: The construction of pTZ100 (insertion of *bio*A).

The resulting plasmid was checked by DNA gel electrophoresis and restriction digestion (Figure 7.2).

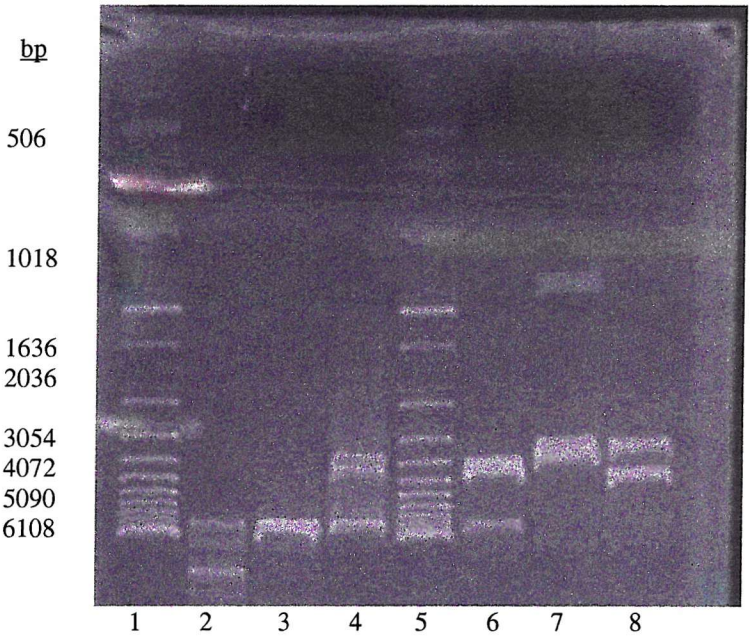

Figure 7.2: Restriction digestion of pTZ100, (1) Marker, (2) uncut plasmid, (3) NdeI, (4) NdeI/BamHI, (5) Marker, (6) NdeI/XhoI, (7) ApaI/HindIII, (8) ApaI/BamHI.

7.4 Construction of pTZ200

The plasmid pTZ200 encodes *bio*B, *mio*C, *fld*A, *fpr*. Primers were designed for the PCR amplification (Section 8.7.2). A BamHI restriction site was incorporated at the 5' terminus and a KpnI restriction site at the 3' end of *mioC*. A KpnI restriction site was incorporated at the 5' terminus and a SacI restriction site at the 3' end of *fpr*. A KpnI restriction site was incorporated at the 5' terminus and a NotI restriction site at the 3' end of *fld*A. A NdeI restriction site was incorporated at the 5' terminus and a BamHI restriction site at the 3' end of *bio*B. Each primer incorporated an artificial ribosome-binding site (RBS; AAG GAG) that is situated -9 bp from the ATG start codon of the next gene. This strategy was adopted to enhance the expression level of genes, which are not placed immediately after the promotor and the associated RBS of the pET vector. A region rich in guanine and cytosine was incorporated at each 5' terminus and at each 3' end of the primer to increase the binding of the primer to the DNA template. Construction

of the plasmid followed Method B (Section 8.73). The construction of pTZ200 is depicted in Figure 7.3a and 7.3b.

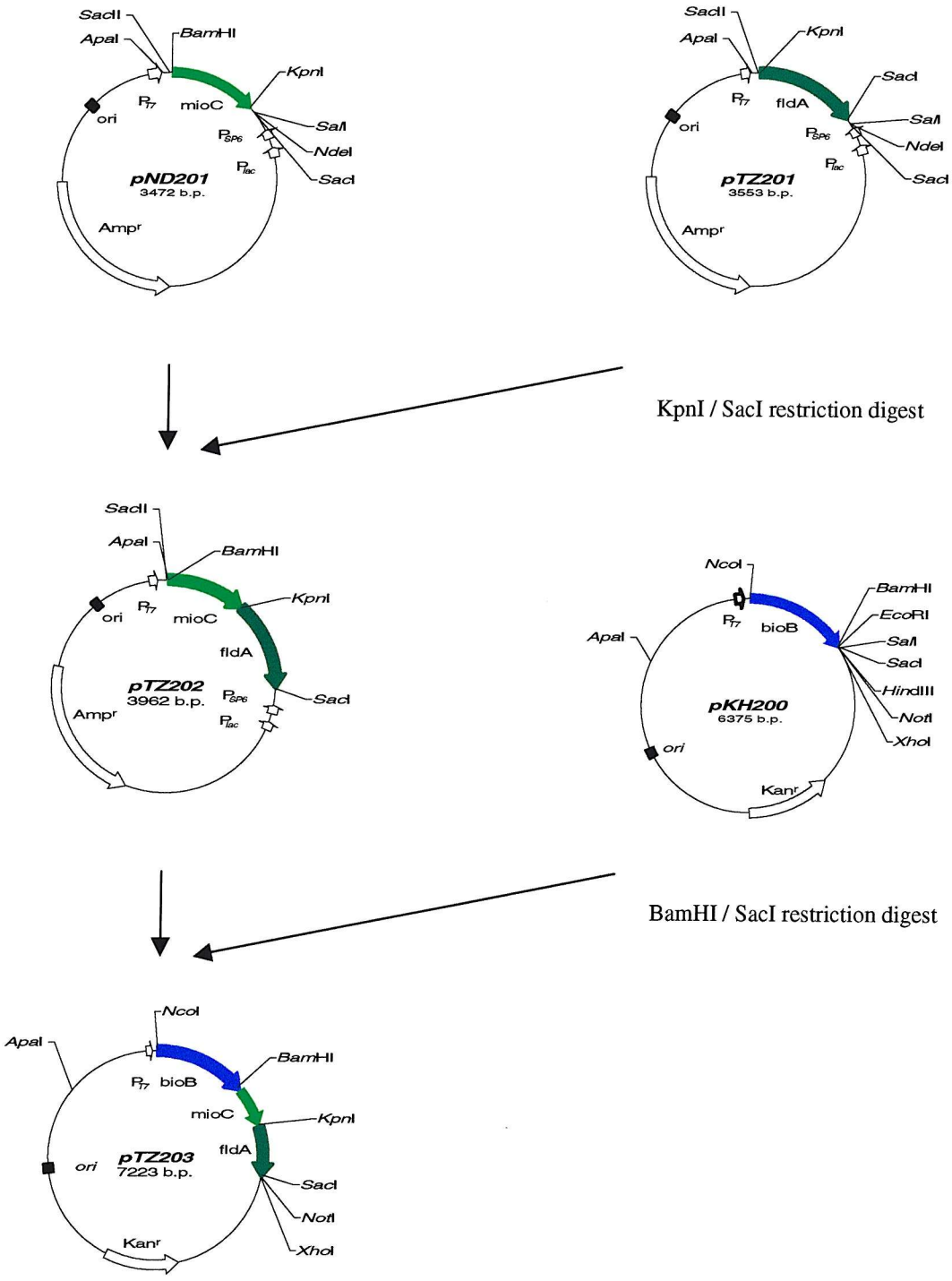

Figure 7.3a: The construction of pTZ200 (no RBS site downstream of *bio*B).

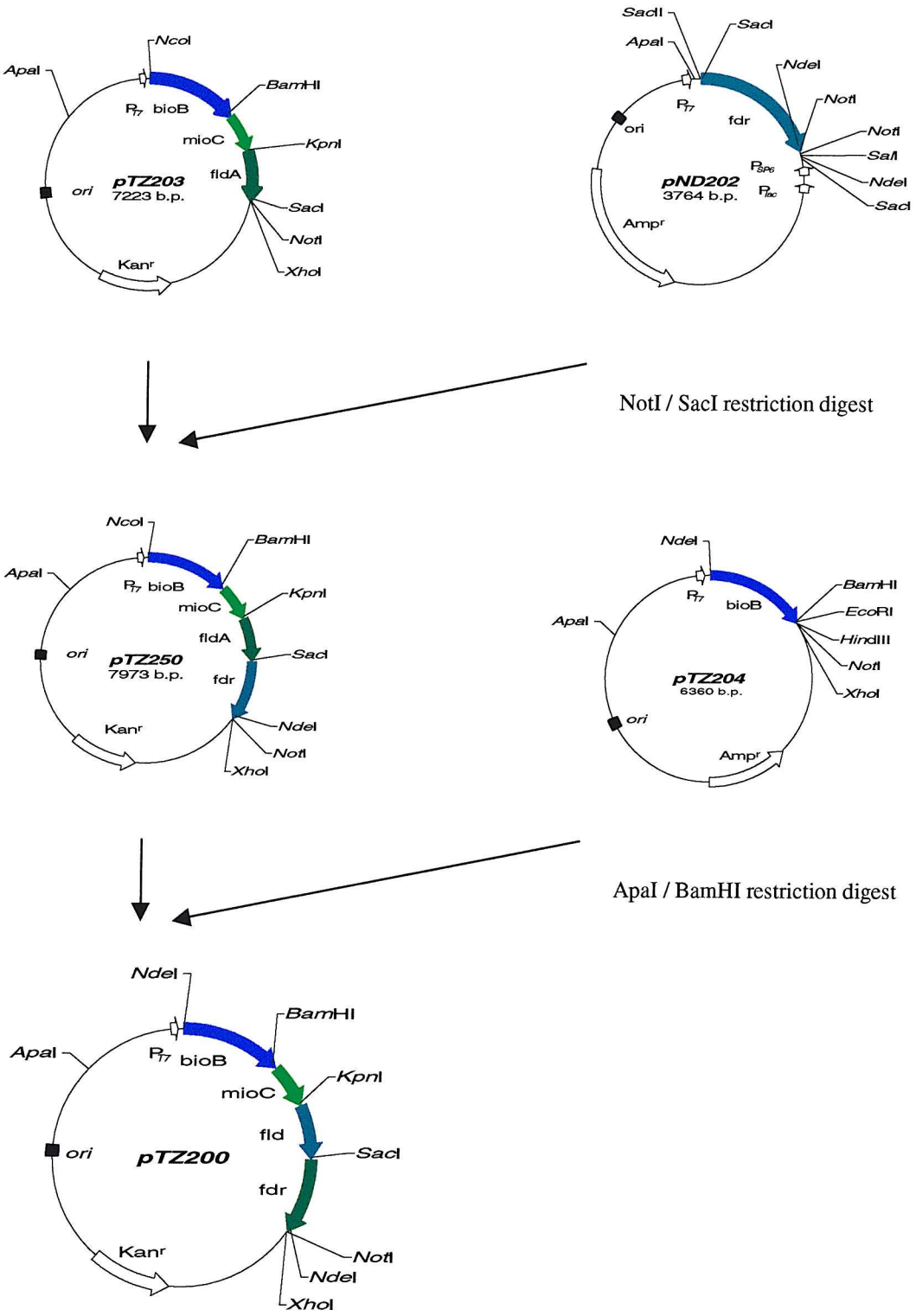

Figure 7.3b: The construction of pTZ200 (RBS site downstream of *bio*B).

The resulting plasmid was checked by DNA gel electrophoresis and restriction digestion (Figure 7.4).

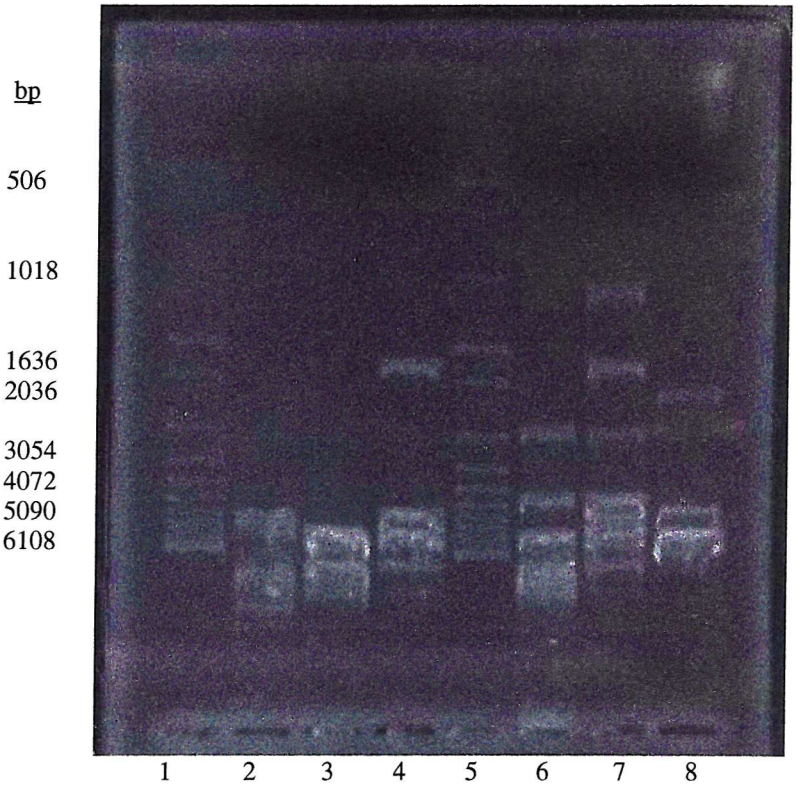

Figure 7.4: Restriction digestion of pTZ200, (1) Marker, (2) uncut plasmid, (3) BamHI, (4) BamHI/NotI, (5) Marker, (6) NdeI, (7) NdeI/BamHI, (8) ApaI/BamHI.

7.5 Construction of pTZ300

The plasmid pTZ300 encodes the *isc* operon genes (Section 5.1). Primers were designed (Section 8.7.2). A NdeI restriction site was incorporated at the 5' terminus and a BamHI restriction site at the 3' end of the *iscR*SUA genes. A BamHI restriction site was incorporated at the 5' terminus and a NotI restriction site at the 3' end of the *hsc*66, *hsc*20 and *fdx* genes. Each reverse primer incorporated an artificial ribosome binding site (RBS; AAG GAG) -9 bp from the ATG start sequence of the next gene. Construction of the plasmid followed Method B (Section 8.73). The construction of pTZ300 is depicted in Figure 7.5a and 7.5b.

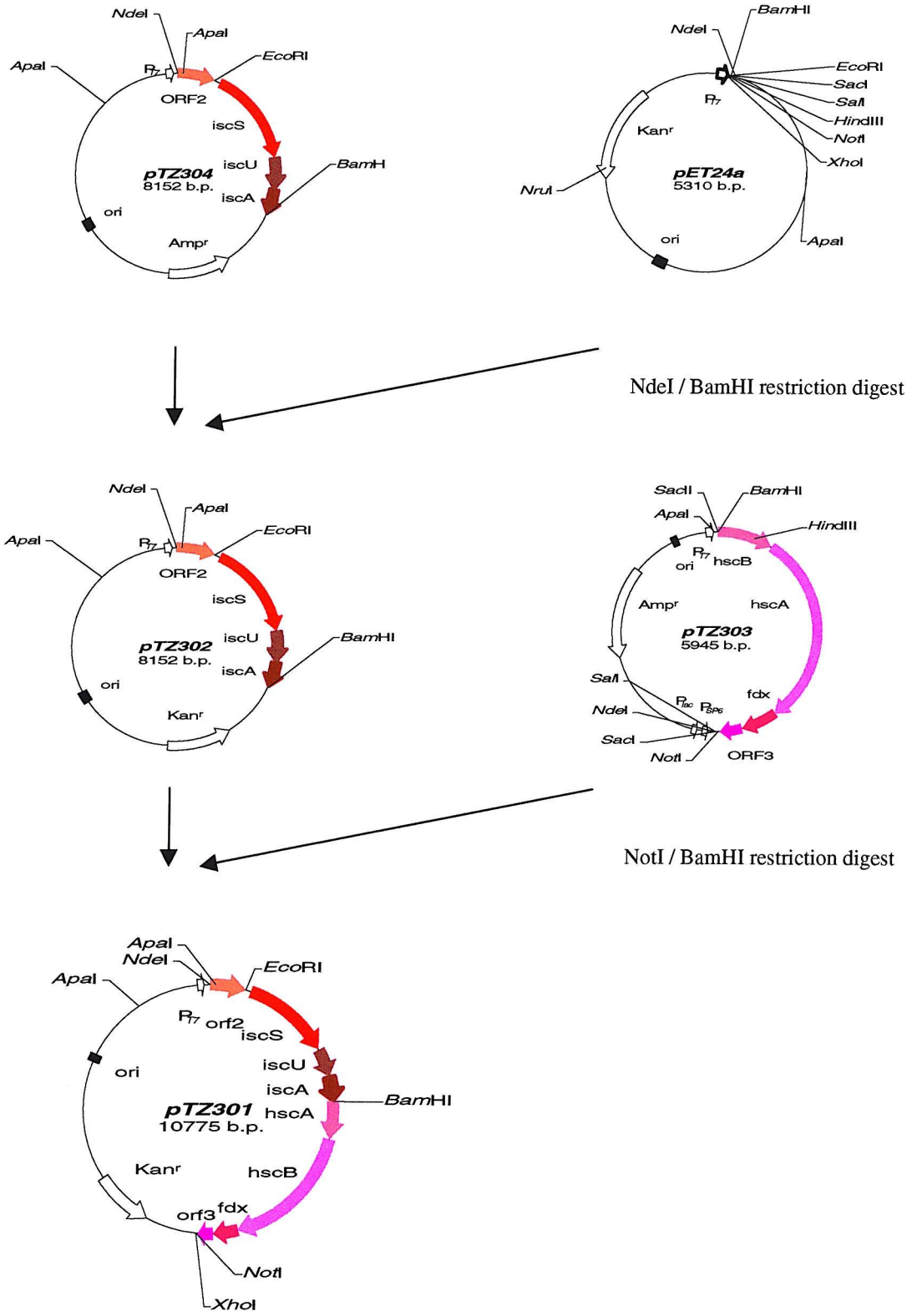

Figure 7.5a: The construction of pTZ300 (construction of a plasmid encoding Kan^r).

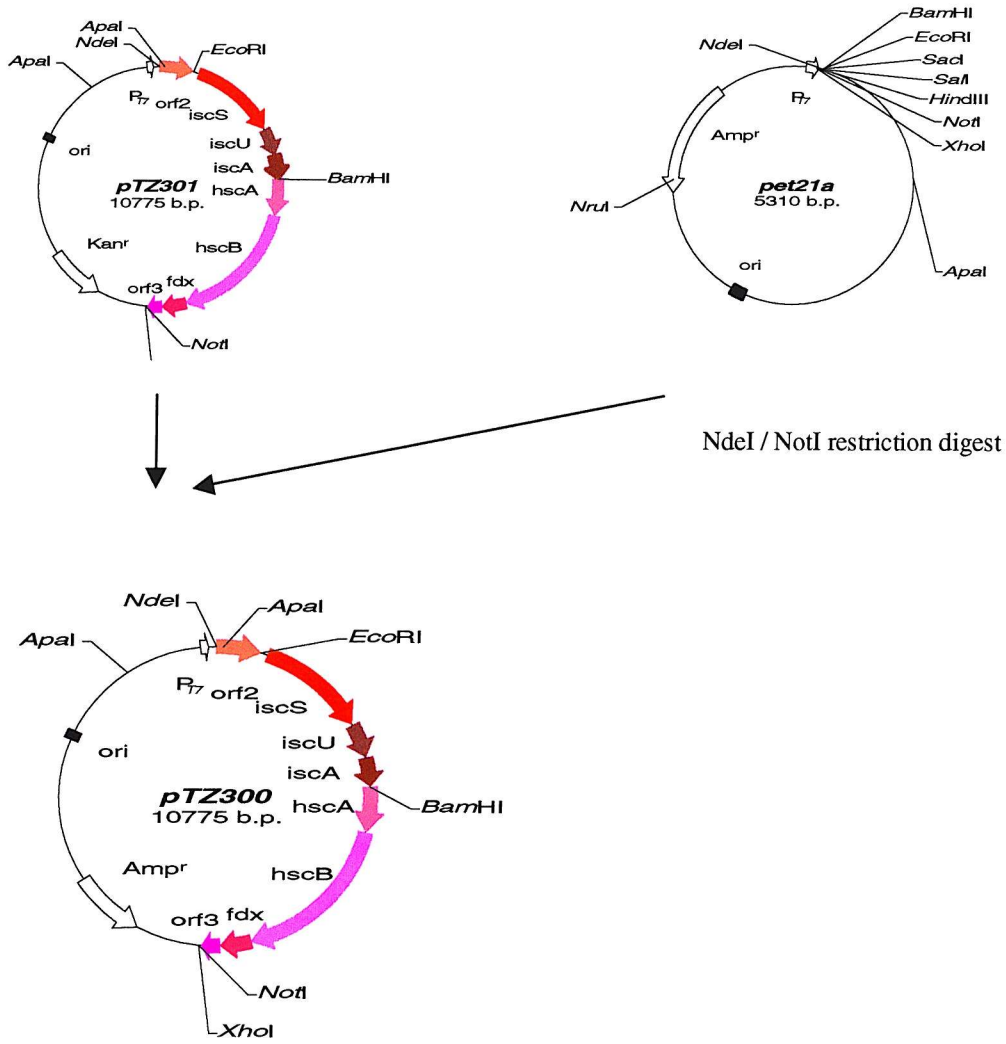

Figure 7.5b: The construction of pTZ300 (construction of a plasmid encoding Amp^r).

The resulting plasmid was checked by DNA gel electrophoresis and restriction digestion (Figure 7.6).

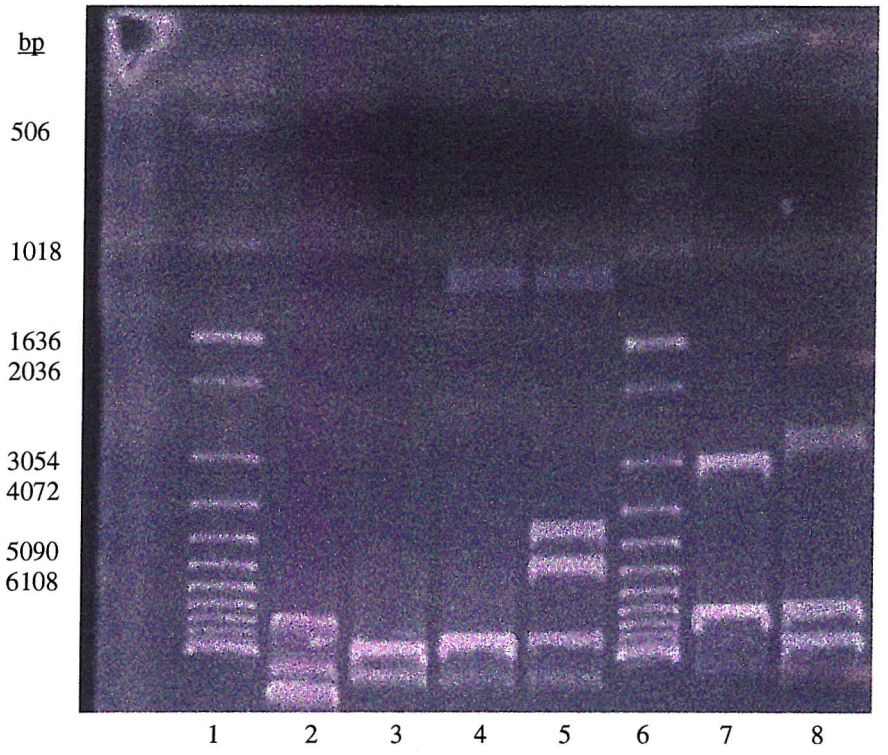

Figure 7.6: Restriction digestion of pTZ300, (1) Marker, (2) uncut plasmid, (3) NotI, (4) ApaI, (5) ApaI/NotI, (6) Marker, (7) BamHI/XhoI, (8) HindII/NotI.

7.6 Construction of pBO88-1+pfs

The plasmid pBO88-1 was a kind gift from Dr. N. Shaw (Lonza AG). It encodes the biotin operon and the gene *fld*A. All the gene products are expressed at a high level in *E. coli* (Dr. N. Shaw, personal communication). The gene *fld*A was replaced by *pfs* to allow high level expression of PFS. Primers were designed (Section 8.7.2). BamHI and ClaI restriction sites were incorporated at the 5' terminus and KpnI and SmaI restriction sites at the 3' end of the *pfs* genes. Construction of the plasmid followed Method D (Section 8.73). The construction of pBO88-1+pfs is depicted in Figure 7.7.

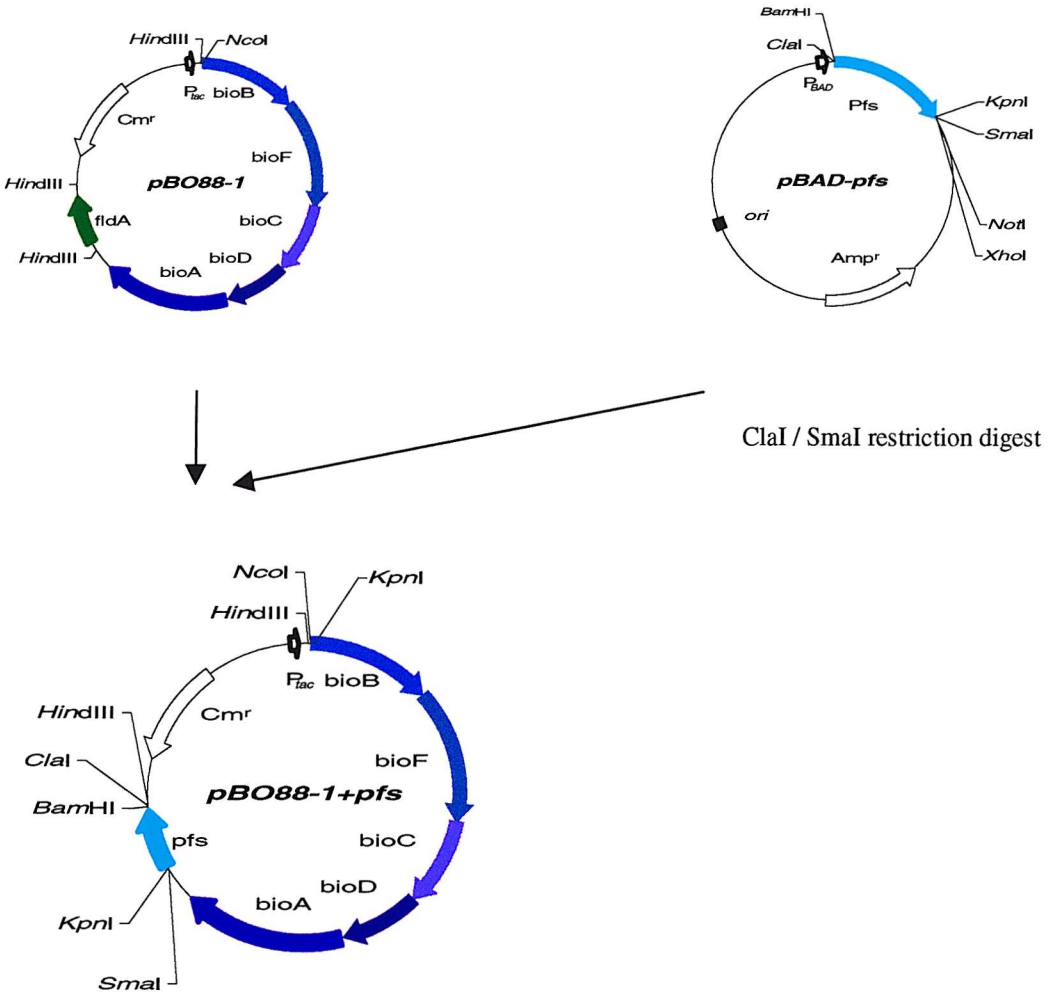

Figure 7.7: The construction of pBO88-1+pfs.

The resulting plasmid was checked by DNA gel electrophoresis and restriction digestion (Figure 7.8).

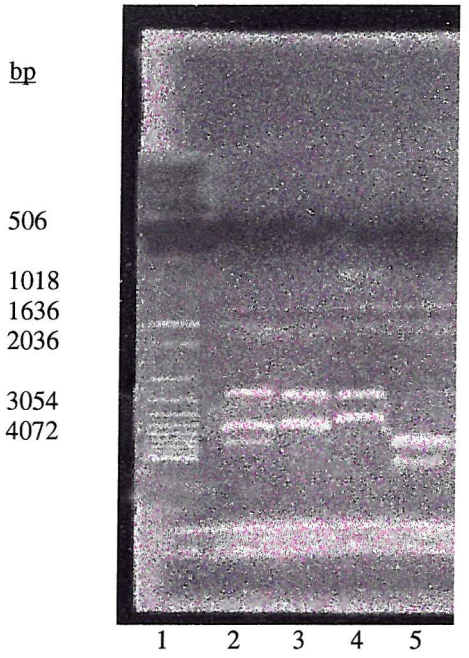

Figure 7.8: Restriction digestion of pBO88-1plus pfs, (1) Marker, (2) HindIII, (3) KpnI, (4) KpnI/SmaI, (5) uncut plasmid.

7.7 Summary and Conclusion

Various plasmids were constructed encoding genes, deemed essential or helpful for biotin formation *in vitro* or *in vivo* (Chapter 4,5,6). An *in vivo* application will require a reliable way of detecting and measuring biotin *in vivo*. The microbiological method is routinely used for this purpose but an initial investigation of a biological assay using *Lactobacillus plantarum*, proved it to be highly unreliable and laborious. Other method of detecting biotin are complicated by the highly complex nature of the growth medium, making a reliable and quick detection of biotin challenging. The extraction of biotin from growth medium with agarose bound streptavidin, a protein that binds strongly to biotin, in combination with HPLC analysis was unsuccessful (data not shown).

As multiple protein co-factors at various concentrations are essential for biotin formation *in vitro*, it would be advantageous to determine their cellular expression level in *vivo*. This will require more advanced analytical techniques such as 2D protein gels or overexpression of plasmid-encoded proteins in mini-cells (66). In addition, future investigations could explore ways of controlling the cellular expression levels of protein

co-factors, such as rearranging the genes on a plasmid, use of various promoters (T7, pBAD, *tac*) and integrating essential genes into the genomic DNA. This could include an investigation into how transcriptional relates to translational expression. Although these studies might yield valuable insights into fundamental techniques for metabolic engineering, they are long-term studies and will require a substantial amount of resources.

Based on the *in vitro* findings presented in this work a more rational approach towards the metabolic engineering of a microorganism to overproduce biotin can be devised. This would take into consideration the effect of PFS on the synergistic inhibition of biotin synthase activity by DOA and methionine, as well as the important function of FldA and Fdr and the optimal concentration of iron and sulphide in relation to the BioB concentration.

Chapter Eight: Experimental Methods

8.1 General Experimental methods

Materials

Electrophoresis grade agarose was obtained from Bio-Rad. Acrylamide/bis-acrylamide stock solution was from Anachem. Bacto Tryptone, Yeast Extract and Bacto Agar, for culture media, were purchase from Oxoid and Difco. *Taq* DNA polymerase and restriction enzymes were obtained from Promega, *Pfu* DNA polymerase was obtained from Stratagene. Molecular weight markers for DNA electrophoresis and for SDS-PAGE were from BDH. All other chemicals used were of the highest quality available and purchased from either Aldrich, Sigma, Fluka or Advocado. SAM was a kind gift from BASF (Stuttgart, Germany), Sinefungin was a generous gift from Prof. J. Baldwin (Oxford University), DAPA, DTB, pimelic acid were a kind gift from Dr. N. Shaw (Lonza AG, Switzerland).

Buffers used for protein purification

If not otherwise stated, the following buffers were used:

Buffer A: Tris-HCl buffer (50 mM, pH 8.1)

Buffer B: Tris-HCl buffer (50 mM, pH 8.1) plus $(NH_4)_2SO_4$ (1M)

Buffer C: Tris-HCl buffer (50 mM, pH 8.1) plus NaCl (1 M)

Buffer D: Tris-HCl buffer (50 mM, pH 8.1) plus imidazole (0.5) and NaCl (0.5 M)

Centrifugation

Samples were centrifuged at 4°C in a Avant J-25 centrifuge (Beckman) centrifuge. For sample less than 1.5 ml, a microCentrifugette 4214 (ALC) was used at room temperature or 4°C (11,000 g).

Determination of pH

Measurements of pH were performed using a Mettler Delta 340 pH meter connected to a Mettler Toledo Inlab 413 Combination Electrode. This was calibrated at pH 4.0 to 7.0 or pH 7.0 to 10.0 before use and stored in 3 M postassium chloride.

Bacterial cell cultures

Fermentation was carried out in an Innova 4400 Incubator Shaker (New Brunswick Scientific) or in an Innova 4230 Refrigerated Incubator Shaker (New Brunswick Scientific) on 100 ml or 1 l scales. Resulting cell pellets were collected by centrifugation and stored at - 80°C.

Mass spectrometry

ESI-MS was performed on a VG Platform single quadrupole mass spectrometer configured for open access operation (OAMS). The data were acquired using continuum format to allow observation of multiple charge envelopes. An external standard was used for calibration and all subsequent spectra were calibrated using this standard.

External calibration for ESI-MS

Multiple charged myoglobin was observed by ESI-MS and the molecular weight (MW) was determined to 16952.4 (Figure 8.1). The calculated molecular weight of myoglobin from the amino acid sequence is 16952.5.

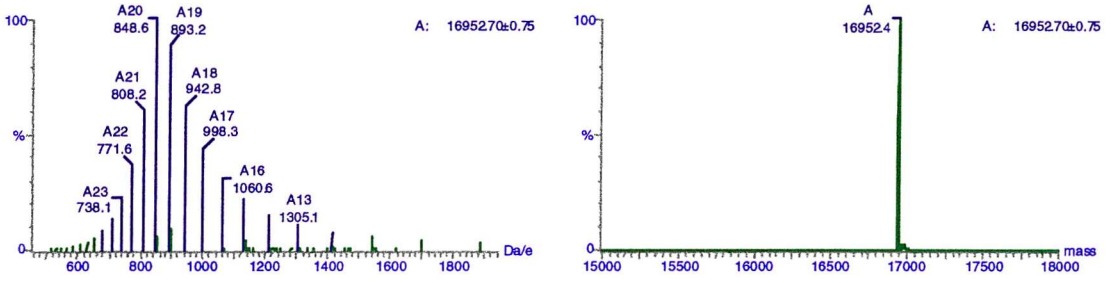

Figure 8.1: ESI-MS for myglobin

Protein concentration determination

Protein concentrations were determined by the method of Bradford (138). Bradford reagent (0.01% (w/v) Coomassie Brilliant Blue G250 in a solution of aqueous phosphoric acid 8.8% (w/v), ethanol 4.75% (v/v), 1 ml) was added to 20 µl of protein sample and incubated at room temperature for approximately 5 minutes before the absorbance at 595

nm was recorded with reference to a blank sample containing Bradford reagent. The sample was diluted if the absorbance exceeded 1.0. Protein concentrations were routinely calculated from a known approximation of bovine serum albumin (1 mg/ml = 1.0). If a more accurate measurement was needed, a calibration curve of bovine serum albumin was constructed.

Oligonucleotide synthesis and sequencing

Sequencing and oligonucleotides synthesis were both carried out by Oswel DNA Service (Boldrewood, Southampton).

Incubations

Bacterial plate cultures were grown at 37°C overnight in an Economy Incubator Size 2 (Gallenkamp). Liquid starter cultures were incubated in an Innova 4400 Incubator Shaker (New Brunswick Scientific) or in an Innova 4230 Refrigerated Incubator Shaker (New Brunswick Scientific overnight at 37°C t and 225 rpm.

Microbiological techniques

Standard sterile techniques were applied throughout the project. Plates were poured and streaked using media and equipment that had been sterilised in a PriorClave autoclave (Priorclave Ltd) at 121°C for 21 min. Solutions of IPTG, antibiotics and other heat labile compounds were filter sterilised through 0.22 μm filter (Millipore).

Growth Media

All growth media was autoclaved in a PriorClave autoclave (Priorclave Ltd.) at 121°C for 21 min. before use.

2xTryptone/Yeast Extract (2xTY)

Per litre:

Bacto tryptone	16 g
Yeast Extract	10 g
NaCl	5 g

Transformation medium

2xYT	100 ml
$MgSO_4$ (1 M)	1 ml
$MgCl_2$ (1 M)	1 ml
Glucose (2 M)	1 ml

Competent cell preparations

Competent cells were prepared using the rubidium chloride method (139). *E. coli* strains used during this investigation had the following genotypes:

BL-21(DE3): [F^- *ompT* *hsd*S_B (r_B-m_B-; *dcm*, *gal*, λ(DE3))]

XL-1 Blue: *rec*A2, *end*A1, *gyr*A96, *thi*-1, *hsd*R17, *sup*E44, *rel*A1, *lac*$^-$ F' [proAB$^+$ *lac*I^q*lac*ZΔM15 Tn*10* (*Tet*^{r})]

E. coli strains denoted DE3 contain a chromosomal copy of the gene for T7 RNA polymerase.

Bacterial cultures were preserved for long-term storage by the addition of 100 µl of 75% glycerol of to 500 µl of cell culture. After gently mixing, the glycerol freezes were stored at - 80°C and were viable for at least one year.

DNA electrophoresis gels and solutions

50X running buffer solution, 50X TAE

Per litre:

Tris	242 g
Glacial acetic acid	57.1 ml
0.5 M EDTA	100 ml

Adjusted to pH 8.0 with HCl

Electrophoresis gel, 1% (w/v)

Per gel:

Agarose	0.4 g
1 X TAE buffer	40 ml

The solution was heated at top power rating in a Sharp Compact microwave oven until the agarose had dissolved, poured and allowed to solidify at 4°C for 5 min.

5X Gel electrophoresis sample loading buffer

Glycerol	30% (v/v)
Bromophenol blue	0.25% (w/v)

Electrophoresis gel stain

Ethidium bromide	~10 µg/ml in H_2O

Sodium Dodecyl Sulphate Poly Acrylamide Gel Electrophoresis (SDS-PAGE)

The purity of proteins eluting from FPLC columns and cell lysate expression levels were analysed according to the method of Laemmli (140). Proteins were separated with a Bio-Rad Mini Protean II System at constant voltage (200 V) using a Power Pac 3000 (Bio-Rad).

10X running buffer solution

Per litre:

Tris	30 g
Glycine	144 g
SDS	10 g

Separating gel, 15 %

30% (w/v) acrylamide/1.034% (w/v) bisacrylamide stock solution	2.08 ml
1.5 M Tris-HCl (pH 8.8)	1.25 ml
10% SDS	50 µl
Milli-Q water	1.57 ml
Ammonium persulphate, 10% (w/v)	50 µl
TEMED	4 µl

Stacking gel, 3.0%

30% (w/v) acrylamide/1.034% (w/v) bisacrylamide stock solution	0.5 ml
50 mM Tris-HCl (pH 6.8)	500 µl
10% SDS	50 µl
Milli-Q water	1.57 ml
Ammonium persulphate, 10% (w/v)	50 µl
TEMED	5µl

The freshly prepared ammonium persulphate and the TEMED were added just prior to pouring the gels.

2 X SDS-PAGE sample loading buffer

Tris-HCl	0.65 M
Bromophenol Blue	0.01% (w/v)
SDS	10% (w/v)
Glycerol	50% (v/v)
β-Mercaptoethanol	1.0% (v/v)

SDS-PAGE gel stain (aqueous)

Acetic acid	10% (v/v)
Methanol	50% (v/v)
Coomassie Brilliant Blue	0.25% (w/v)

SDS-PAGE gel destain (aqueous)

Acetic acid	10% (v/v)
Methanol	25% (v/v)

Purification of proteins

Protein purification was carried out using a Pharmacia-LKB fast performance liquid chromatography (FPLC) unit equipped with various columns. All columns used were packed manually by the author. The resins were purchased from Pharmacia.

8.2 Experimental for Chapter Two

8.2.1 Purification of BioB from pKH200/BL-21(DE3)

Resuspension and Lysis of cell paste

Method 1: A typical protein preparation involved the resuspension of 30 g of cell paste in lysis buffer (250 ml; 50 mM Tris-HCl, pH 7.5, 30 % glycerol) at 4°C. Lysozyme was added to a final concentration of 1 mg/ml, followed by the addition of benzonase (1U/µl). Cells were sonicated using a Soniprep 150 sonicator (Sanyo) cooled on ice. The sonicated mixture was centrifugated (J-14 rotor) at 4°C, 14,000 rpm for 30 min.

Method 2: A typical protein preparation involved the resuspension of 30 g of cell paste in lysis buffer (250 ml; 50 mM Tris-HCl, pH 7.5, 30 % glycerol) at 4°C. Lysozyme was added to a final concentration of 1 mg/ml followed by sonication using a Soniprep 150 sonicatior (Sanyo) cooled on ice Polyethyleneimine was added to a final concentration of 0.1 % before the sonicated mixture was spun at 4°C, 14,000 rpm (J-14 rotor) for 30 min.

Purification of BioB from pKH200/BL-21(DE3)

A cell-free lysate using 50 g of cell paste was prepared following Method 1 (Section 8.2.1). To the supernatant ammonium sulphate was added to a final concentration of 35% (w/v). An indication of the presence of BioB in the pellet came from the dark red colour due to the iron-sulphur cluster of BioB. After resuspension of the precipitated pellet in buffer A (100 ml, 50 mM Tris-HCl, pH 8.1), an equal volume of ammonium sulphate (0.5 M) in buffer A was added. The protein solution was then applied to a Phenyl Resource column (200 ml; Pharmacia) with a flow rate of 10 ml/min, which had

previously been equilibrated with buffer B (1 M ammonium sulphate added to buffer A) and buffer A. Protein was eluted with a linear gradient of 0 % to 100 % buffer A over five column volumes.

The purest fractions, as judged by SDS-PAGE, were pooled and concentrated by ultafiltration using an Amicon pressure cell with a PM30 membrane to approximately 45 mg/ml. The concentrate, ~ 2 X 7 ml, was applied to a Sepharose 200 column (20 mm ID X 850 mm; Pharmacia) equilibrated with buffer A at 3 ml/min. Protein was eluted isocratically with buffer A at 3 ml/min and eluted from 110 to 230 min. The purest fractions, as judged by SDS-PAGE were combined, concentrated by ultafiltration using an Amicon pressure cell with a PM30 membrane to approximately 50 mg/ml and stored at -80°C.

Dye affinity screening

The binding of BioB to various affinity columns was assessed using the Reactive Dye-Ligand Test Kit (Sigma). This kit contains pre-packed affinity columns (2.5 ml) of various colours, each colour corresponding to a resin with unique separating properties. The resins used to assess the binding of BioB were Reactive Yellow 86 Agarose, Reactive Blue 72 Agarose, Reactive Green 19 Agarose and Reactive Brown 10 Agarose. BioB could be further purified using the Reactive Brown 10 Agarose column.

BioB purification using Reactive Brown 10 resin

The purified fractions from the previous step (30 % ammonium sulphate) were applied to a Brown Reactive 10 column (30 ml; Sigma) at a flow rate of 3 ml/min, which had previously been equilibrated with buffer A and buffer C (1 M NaCl added to buffer A). An increasing gradient of 0 to 100 % of buffer C was used to elute BioB containing fractions. Further purification used 100 % buffer C isocratically to elute bound BioB.

8.2.2 Purification of BioB from p12:bioB/BL-21(DE3)

Construction of p12:bioB

Detailed experimental procedures for the construction of plasmids are given below (Section 8.7).

***In vivo* growth of p12:bioB/BL-21(DE3) and pet6H:bioB/BL-21(DE3)**

DNA (~ 1 μg) of p12:bioB and pet6H:bioB was transformed into chemically competent (Section 8.7) *E. coli* BL-21(DE3) cells (100 μl) by standard protocols (139). From the transformation mixture, 50 μl was spread onto a 2TY/ampicillin (100 μg/ml) plate and incubated at 37°C overnight. A single colony was picked and used to inoculate 2TY medium (~ 100 ml) containing ampicillin (100 μg/ml). After overnight growth at 37°C, the starter culture was used as a 1 % inoculum in 4 X 1.5 L of 2TY medium containing ampicillin (100 μg/ml) in a 5 L baffled flask. The initial growth temperature was 37°C, but when the OD_{600} reached 0.6 - 1, the temperature was decreased to 27°C. Protein overexpression was induced by the addition of IPTG (0.5 mM) and cells harvested after 5 to 6 hours later by centrifugation (14,000 rpm at 4°C for 15 min.). The cell paste was stored at - 80°C until further use. Yields ranged from 15 to 35 g (6 L).

Purification of BioB from p12bioB/BL-21(DE3)

A cell-free lysate was prepared from cell paste (5 g) following Method 1 (Section 8.2.1). The cleared supernatent was applied to a Chitin affinity column (5 ml; BioLabs, New England) at 1 ml/min that had been equilibrated with buffer A (50 mM Tris-HCl, pH 8.1). Protein was eluted after overnight incubation in DTT (30 mM) with a 0 – 100% gradient of buffer C over 3 column volumes at 1 ml/min. The eluting fractions were combined because of low protein content, assessed with the Bradford reagent, and analysed by SDS-PAGE.

8.2.3 Purification of His_6-BioB from pet6H:bioB/BL-21(DE3)

***In vivo* growth of pet6H:bioB/BL-21(DE3)**

Growth of pet6H:bioB/BL-21(DE3) was carried out as described (Section 8.3.2.2). Medium-scale cell culture (5 L) afforded 30 g of cell paste.

Purification of His_6-BioB

A cell-free lysate using of cell paste (30 g) was prepared following Method 1 (Section 8.2.1) using buffer D (25 mM imidazole and 0.5 M NaCl added to buffer A). The protein solution was applied to a Chelating Sepharose column (35 ml; Pharmacia), which was

charged with $NiSO_4$ (0.2 M; 50 ml) and equilibrated with buffer D. Proteins were eluted with a 0 to 50 % gradient of buffer D (buffer A plus 0.5 M imidazole and 0.5 M NaCl) over 10 column volumes at a flow rate of 6 ml/min. Fractions containing His_6-BioB of the highest purity, as judged by SDS-PAGE were desalted and concentrated using Method I or II (Section 8.2.3.3).

Desalting and concentration of His_6-BioB

Method I: Protein fractions eluting from columns were analysed by SDS-PAGE. The purest fractions, as judged by SDS-PAGE, were combined and concentrated using an Amicon pressure cell with a PM30 membrane. Concentrated protein was applied to a Slide-A-Lyzer 10K (Pierce) and dialysed against Tris-HCl buffer (50 mM, pH 8.1) overnight at 4°C. Desalted protein were aliquoted (1 ml) and stored at -80°C.

Method II: Protein fractions eluting from columns were analysed by SDS-PAGE. While SDS-PAGE analysis fractions containing the majority of protein, as judged using the Bradford Reagent, were concentrated individually using a MWCO membrane filter (4 ml, >10K, Millipore) at 8,000 rpm, 4°C. These fractions were then desalted by repeated addition of Tris-HCl buffer (50 mM, pH 8.1). After determination of protein purity by SDS-PAGE, fractions containing pure protein were combined and desalted using a PD-10 desalting column (Pharmacia) according to the manufacturer's instruction. Desalted fractions were stored at -80°C. This method has the advantage of being much quicker than Method I. As some proteins are unstable this is the method of choice to ensure fast desalting and storage at -80°C.

8.2.4 Reconstitution of BioB

8.2.4.1 Reconstitution of BioB under anaerobic conditions

Method I: 80 µl of BioB (highly purified, 40 - 50 mg/ml) were transferred anaerobically to a MWCO membrane filter (0.5 ml, >5K, Millipore) and concentrated to 40 µl to allow for optimal exclusion of iron and sulphide on a Bio-Spin P-6 column (Bio-Rad). The concentrated sample was incubated anaerobically with DTT (5 mM) and a 5-fold molar excess of Na_2S and $FeSO_4$ for 3 hours at 18°C. Excess of precipitated Fe_2S was removed by centrifugation in a picofuge (Stratagene). The supernatant was applied to a Bio-Spin

P-6 column (Bio-Rad) previously equilibrated with buffer A and eluted by centrifugation with a picofuge (Stratagene). 5 – 10 µl were taken to quantify iron aerobically following the method of Fish (Section 8.2.4.2).

Method II: Method II differed from I in that after elution of reconstituted BioB from the Bio-Spin column, the eluate was incubated anaerobically for 30 min. with EDTA (2 mM) to chelate excess iron. The sample was then applied to a Bio-Spin P-6 column (Bio-Rad) previously equilibrated with buffer A and eluted by centrifugation with a picofuge (Stratagene). 5 – 10 µl were taken to quantify iron aerobically following the method of Fish (Section 8.2.4.2).

Method III: This method was used for large-scale preparation of reconstituted BioB. BioB (2.5 ml, highly purified, 20 – 40 mg/ml) were incubated anaerobically with DTT (5 mM) and a 5-fold molar excess of Na_2S and $FeSO_4$ for 3 hours at 18°C in a Falcon tube (15 ml). Reconstituted BioB was separated from excess iron and sulphide by applying the solution (2.5 ml) to a PD-10 column (Pharmacia) previously equilibrated with buffer A. Protein was eluted by applying buffer A (3.5 ml). 5 – 10 µl were taken to quantify iron aerobically following the method of Fish (8.2.4.2).

8.2.4.2 Iron measurement [according to Fish (141)]

Solution A was prepared as follows: Conc. HCl (1 ml) was diluted in H_2O (9 ml) in a Falcon tube (15 ml), $KMnO_4$ (450 µg) were dissolved in H_2O (10 ml) and the solutions combined in a 1:1 ratio. Solution A was prepared fresh each time. Solution B contained the following components: Ferrozine (80 mg), neocuproine (80 mg), ascorbic acid (8.8 g), ammonium acetate (9.7 g) in a final volume of 25 ml. Solution B could be stored at room temperature in the dark. The standard solution was prepared by dissolving $FeSO_4 \cdot H_2O$ (50 mg) in H_2O (10 ml). This gave an iron concentration of 10 mg/ml. After a 100 fold dilution, 100 µl in 10 ml, the final concentration of iron was 100 µg/10 ml or 10 µg/ml. The dilutions were prepared as stated (Table 8.1) in 1.5 ml Eppendorf tubes.

Sample	add buffer (µl)	Add Fe-Standard (10 µg/ml)	Final [Fe] (µg/ml)	Final [Fe] (nmols)
1	600	400	4	70
2	650	350	3.5	61
3	700	300	3	52
4	750	250	2.5	43
5	800	200	2	35
6	850	150	1.5	26
7	900	100	1	17
8	950	50	0.5	9
9	970	30	0.3	5
10	990	10	0.2	2

Table 8.1: Dilution series for iron standards

The samples were diluted in water to 1 ml. 20 µl were taken to measure the protein concentration in the sample. Solution A (0.5 ml) was added. Standards, samples and blanks (1 ml H_2O) were heated in a water-bath at 60°C for 2 hours. Solution B (100 µl, very viscous) was added to initiate development of the chromophore.

The colour reaction reached completion in 15 min. at RT and stayed stable for the next 10 hours. The absorbance was measured at 562 nm. Protein samples were microcentrifugated (14,000 rpm, RT, 5 min.) to remove precipitated protein.

8.3 Experimental for Chapter Three

8.3.1 Enzymatic synthesis of ^{14}C-DTB

Primer design for the amplification of *bio*D

Primers were designed (Table 8.8) and the *bio*D gene amplified by PCR (Section 8.7.1).

Construction of pET11a:bioD

Detailed experimental procedures for the construction of plasmids are given below (Section 8.7).

Overexpression and purification of DTBS

Medium scale cell cultures (Section 8.2.2; 5 L) afforded 25 g of cell paste. Cell-free lysate was prepared following Method 1 (Section 8.2.1). Supernatant was applied to a Q-Sepharose FF column (130 ml; Pharmacia) at a flow rate of 10 ml/min, which had

previously been equilibrated with buffer A. Protein was eluted with a linear gradient of 0 to 100 % of buffer B, fractions containing DTBS were pooled, concentrated concentrated by ultafiltration using an Amicon pressure cell with a PM10 membrane to approximately 50 mg/ml and applied to a Sephadex 75 column (20 mm ID X 850 mm; Pharmacia). The purest fractions, as judged by SDS-PAGE, were combined, concentrated by ultafiltration using an Amicon pressure cell with a PM10 membrane to approximately 50 mg/ml and stored at -80°C.

Enzymatic synthesis of ^{14}C-DTB

Appropriate radiochemical safety procedures were applied throughout. At various points during the synthesis of ^{14}C-DTB, samples (denoted in bold numerical letters) were withdrawn to monitor the reaction and calculate the yield. DAPA sulphate salt was a kind gift from Dr. N. Shaw (Lonza AG, Basel). DAPA sulphate salt (50 mM), ATP (50 mM), $MgSO_4$ (5 mM) and DTT (1 mM) were dissolved in Tris-Hcl buffer (50 mM, pH 8.1). The pH was adjusted with 10 µl aliquots of 1 M NaOH to pH 7.5. This solution was degassed using argon. Purified DTBS was then added to 1 mg/ml followed by $NaH^{14}CO_3$ (25 µCi, 54 mCi/mmol). The reaction mixture was left in a sealed Falcon 15 ml tube at room temperature for three days **1** (Table 8.2 and 8.3).

The reaction was quenched by the addition of 100 µl 10% (v/v) of TCA **2**. Great care was taken to avoid inhalation of $^{14}CO_2$. The precipitated protein was removed by centrifugation at 10,000 rpm for 10 min at room temperature. The supernatant **3** was applied to a disposable C_{18} SPE column that had previously been equilibrated with methanol (1 ml), water (1 ml) and 1 % (v/v) acetic acid (1 ml). The column was then washed with 1% (v/v) acetic acid (2 ml) and water (2 ml) **4** before the ^{14}C-DTB was eluted with methanol (1 ml) **5**. The methanolic fraction was dried under vacuum and the resulting pellet resuspended in water **6**.

Sample ID	V (µl)	cpm	total V (ml)	total cpm	µCi
1	10	53,552	3	16065600	7.24
2	10	80,508	3	24152400	10.88
3	10	66,412	3	19923600	8.97
4	10	35,764	3	10729200	4.83
5	10	36,610	1	3661000	1.65
6	5	294,00	0.5	5880000	2.65

Table 8.2: Sample fractions withdrawn during ^{14}C-DTB synthesis

Sample ID	V (µl)	cpm	total V (ml)	total cpm	µCi
1	7.5	133,446	3	53378400	24.04
2	5	92,000	3	55200000	24.86
3	10	170,000	3	51000000	22.97
4	10	25,035	3	7510500	3.38
5	5	179,376	1	35875200	16.16
6	5	401,030	0.25	20051500	9.03

Table 8.3: Sample fractions withdrawn during ^{14}C-DTB synthesis

8.3.2 Isolation and detection of ^{14}C-DTB and ^{14}C-biotin

After incubation with the appropriate co-factors for 3 hours at 37°C, the reaction was quenched by the addition of TCA (10 µl of 50 % (v/v)). Precipitated protein was removed by centrifugation at 12,000 rpm for 5 min. at RT. The resulting supernatant was applied to a disposable C_{18} SPE column that had previously been equilibrated with methanol (1 ml), water (1 ml) and 1 % (v/v) acetic acid (1 ml). The column was then washed with 1% (v/v) acetic acid (2 ml) and water (2 ml) before the ^{14}C-DTB was eluted with methanol (0.5 ml). The methanolic fraction was dried under vacuum before resuspension in 25 µl of methanol/water/acetic acid (65/25/10), which had 1 mg of unlabeled biotin and DTB added to it as internal standard. TLC plates (AMGAM SIL 6; Macherey-Nagel) were developed with chloroform/methanol/formic acid (17/3/0.2). The unlabeled biotin and

DTB could be visualised with p-DACA (142). TLC plates were exposed overnight to Hyperfilm-βmax (Amersham) in a Hypercassette (18 X 24 cm; Amersham) and processed with developer (CEATANK), fixer (CEAFIX; both CEA, Sweden) and Milli-Q H_2O.

8.3.3 Detection of biotin formation *in vitro* by HPLC

Methods used to detect biotin formation *in vitro* by HPLC

The solvent system, C_{18} columns and sample preparation were adapted to the needs of the particular assay. In the following a detailed description of each method is given. The method used for an *in vitro* assay will be stated.

General: Each method will state the solvent system, C_{18} columns and sample preparation used. Each assay was measured on a Gilson System Workcenter, including 321 pumps, UV/VIS-155 detector and a 234 Gilson Autoinjector equipped with a Tray 36. The UV/VIS-155 detector was set to 200 and 254 nm to detect small molecular weight compounds. Sample (200 µl) was applied through loop (500 µl) for each run. Each method included at the end of the separation an equilibration step of 5 to 10 min. 70 % organic solvent and 5 to 15 min. 95 % aqueous solvent to equilibrate the column for the next run.

Method I: Small molecular weight compounds were isolated from the assay mixture by precipitating the protein with TCA (10 µl of 50 % (v/v)) and were separated on an analytical Purescil column (5 µ C18, 120 Å, 4.6 X 150 mm; Millipore). An initial isocratic step of 95 % solvent A (10 mM PO_4^{3-}) for 5 min. was followed by linear gradient of solvent B (acetonitrile) over 30 min. to 70 % at a flow rate of 1 ml/min.

Method II: Small molecular weight compounds were isolated from the assay mixture by precipitating the protein with TFA (10 µl of 50 % (v/v)) and were separated on an analytical Purescil column (5 µ C_{18}, 120 Å, 4.6 X 150 mm; Millipore). An initial isocratic step of 95 % solvent A (1 % TFA/H_2O) for 5 min. was followed by a linear gradient of solvent B (1 % TFA/acetonitrile) over 30 min. to 70 % at a flow rate of 1 ml/min.

Method III: Small molecular weight compounds were isolated from the assay mixture with MWCO membrane filter (Millipore) and were separated on an analytical Phenomenx column (5 μ $C_{18,}$ Prodigy 5, 4.6 X 250 mm; Millipore). An initial isocratic step of 95 % solvent A (10 mM PO_4^{3-}) for 10 min. was followed by a linear gradient of solvent B (acetonitrile) over 45 min. to 70 % at a flow rate of 1 ml/min.

Method IV: Small molecular weight compounds were isolated from the assay mixture with MWCO membrane filter (Millipore) and were separated on an analytical Phenomenx column (5 μ $C_{18,}$ Prodigy 5, 4.6 X 250 mm; Millipore). An initial isocratic step of 95 % solvent A (1 % TFA/H_2O) for 10 min. was followed by a linear gradient of solvent B (1 % TFA/acetonitrile) over 45 min. to 70 % at a flow rate of 1 ml/min.

Method V: Small molecular weight compounds were isolated from the assay mixture by precipitating the protein with TFA (10 μl of 50 % (v/v)) and were separated on an analytical Phenomenx column (5 μ $C_{18,}$ Prodigy 5, 4.6 X 250 mm; Millipore). An initial isocratic step of 95 % solvent A (1 % TFA/H_2O) for 5 min. was followed by a linear gradient of solvent B (1 % TFA/acetonitrile) over 30 min. to 70 % at a flow rate of 1 ml/min.

Method VI: Small molecular weight compounds were isolated from the assay mixture with MWCO membrane filter and were separated on a Semiprep Zorbax column (9.4 X 250 mm; Du Pont Instruments). An initial isocratic step of 95 % solvent A (1 % TFA/H_2O) for 10 min. was followed by a linear gradient of solvent B (1 % TFA/acetonitrile) over 45 min. to 70 % at a flow rate of 2 ml/min.

Standard curves for biotin and DTB

Biotin and DTB (1mg) were dissolved in buffer A (1 ml). Serial standard solution for the concentration range of interest were prepared and analysed by HPLC. A standard curve for the measurement of unknown concentration was calculated using linear regression (Figure 8.3 and 8.4).

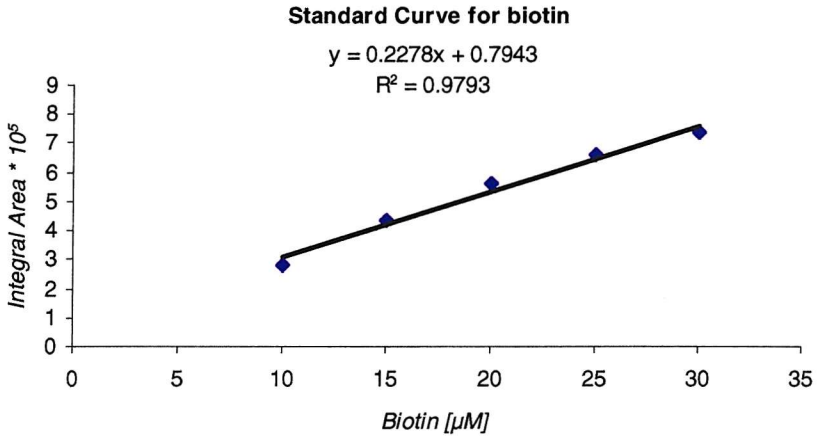

Figure 8.3: Standard curve for biotin at 200 nm (σ: 0.12). [Method I; HPLC\Results\stan.biotin\1-8].

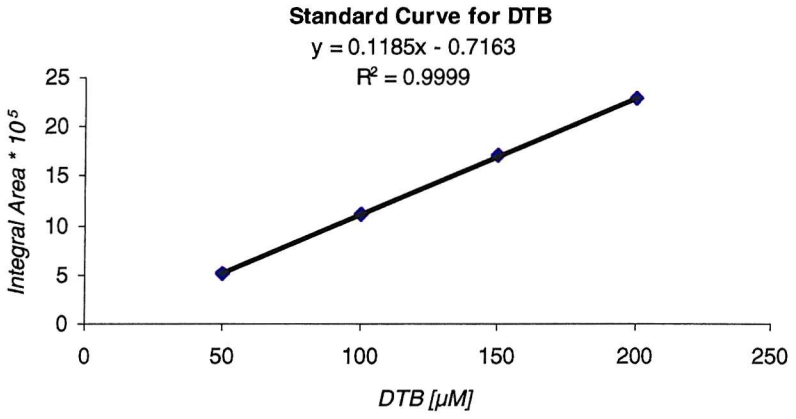

Figure 8.4: Standard curve for DTB at 200 nm (σ: 0.09). [Method I; HPLC\Results\added\rp21\1-4\rp212\1-5].

Purification of FldA, Fdr and MioC

FldA, Fdr and MioC were prepared by Robert Wood (see quarterly reports for details). The plasmids pNADP$^+$, pFLAV and pMIO were kindly provided by Dr. K. Hewitson (Oxford University). They were transformed into BL-21(DE3) (Section 8.2.2).

8.4 Experimental for Chapter Four

The methods used for the separation and quantification of the small molecules are given above (Section 8.3.5 and 8.3.6).

Standard curves DOA (254 nm)

DOA (1 mg) was dissolved in buffer A (1 ml). Serial standard solution for the concentration range of interest were prepared and analysed by HPLC. A standard curve for the measurement of unknown concentration was calculated using linear regression (Figure 8.5).

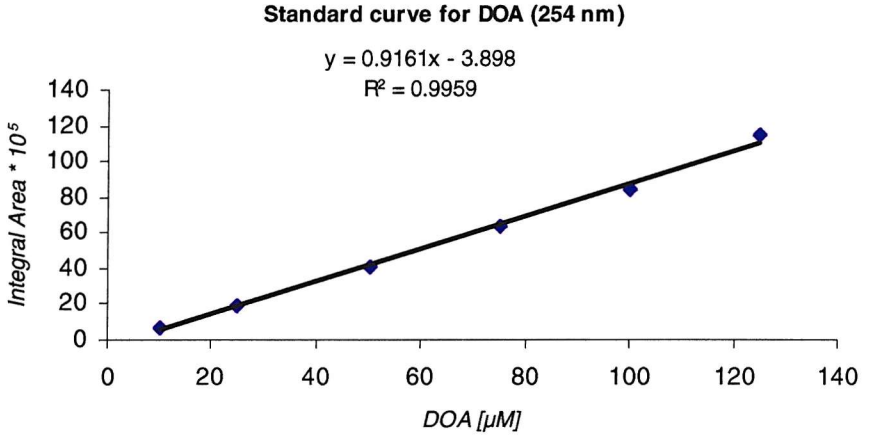

Figure 8.5: Standard curve for DOA recorded at 254 nm (σ: 0.15). [Method I; HPLC\Results\doa.stan\9-13].

Isolation and analysis of small molecules

The assay volume was scaled up to 5 ml (total volume). After 180 min. the protein components were removed using MWCO membrane filter (>10K, 4 ml, Millipore) and the 3.5 ml flow through containing the small molecules was freeze dried overnight using a Modulyo freeze dryer (0°C, 10^{-2} mbar; Edwards). The resulting pellet was resuspended in Tris-HCl buffer (250 µl, 50 mM, pH 8.1). Small molecules were separated by HPLC (Method VI) and collected according to their retention times. The solvent of the pooled fractions (1 to 3.5 ml) was evaporated using a Jouan RC 10.22 rotary evaporator (Welch). The resulting pellets were resuspended in methanol (50 µl, 50 % (v/v)) and analyzed by TLC (silica: AMGAM SIL 6; Macherey-Nagel).

DTT is present in the oxidized and reduced state *in vitro*

The peaks at 22 and 25.5 min. were collected, solvent evaporated and resuspended in methanol and analyzed by TLC. TLC (silica, H_20/methanol (30/70), visualized with $KMnO^{4-}$): R_f (22 min.) = 0.83; R_f (25.5 min.) = 0.84; R_f (DTT) = 0.83. HPLC (Method III): R_t (DTT) = 22 min. [Method III; HPLC \Results\cofact.separ3\RP2.005\1].

Adenine is present *in vitro*

The peak at 14 min. was collected, solvent evaporated and resuspended in methanol and analyzed by TLC. TLC (silica, chloroform/methanol/formic acid (17/3/0.2) visualized under UV); R_f (14 min.) = 0.16; R_f (adenine) = 0.16. HPLC (Method III): R_t (adenine) = 13 min. [Method III; HPLC\ Results\added\rp1.210\9].

DOA is present *in vitro*

The peak at 16 min. was collected, solvent evaporated and resuspended in methanol and analyzed by TLC. TLC (silica, H_20/methanol (30/70), visualized under UV); R_f (16 min.) = 0.75; R_f (DOA) = 0.77. HPLC (Method III): R_t (DOA) = 16 min. [Method III; HPLC\Results\inh8\RP2.004\3].

Biotin and DTB are present *in vitro*

The peaks at 26.5 and 28.5 were collected, solvent evaporated and resuspended in methanol and analyzed by TLC. TLC (silica, chloroform/methanol/formic acid (17/3/0.2), visualized with p-DACA); R_f (26.5 min.) = 0.58; R_f (biotin) = 0.59); R_f (28.5 min.) = 0.72; R_f (DTB) = 0.72. HPLC (Method III): R_t (biotin) = 26.5 min.; R_t (DTB) = 28.5 min.; [Method III; HPLC\ Results\ dtb.biotin1\2-6].

8.5 Experimental for Chapter Five

8.5.1 Purification of IscS from pET24a:IscS/ BL-21(DE3)

Medium scale cell cultures (Section 8.2.2; 5 L) afforded 30 g of cell paste. A cell-free lysate was prepared following Method 2 (Section 8.2.1) using buffer A. The protein solution was applied to a Q-Sepharose FF column (130 ml; Pharmacia) which had previously been equilibrated with buffer A. Protein was eluted with a 0 to 100 % gradient of buffer C over 5 column volumes at a flow rate of 10 ml/min. Fractions containing IscS, as judged by SDS-PAGE, were pooled and concentrated by ultafiltration using an Amicon pressure cell with a PM30 membrane to approximately 60 mg/ml. The concentrate was applied to a Sepharose 200 column (20 mm ID X 850 mm; Pharmacia) column equilibrated with buffer A at 3 ml/min. Protein was eluted isocratically with buffer A at 3 ml/min and eluted from 110 to 230 min. Fractions containing IscS were pooled and applied to a Blue Dye Affinity column (35 ml; Pharmacia) with a flow rate of 3 ml/min, which had previously been equilibrated with buffer C and buffer A. Protein was eluted with a linear gradient of 0 % to 100 % buffer A over five column volumes. Fractions containing IscS, as judged by SDS-PAGE, were pooled and concentrated by ultafiltration using an Amicon pressure cell with a PM30 membrane to approximately 40 mg/ml. The concentrate was applied to a Sepharose 200 column (20 mm ID X 850 mm; Pharmacia) column equilibrated with buffer A at 3 ml/min. Protein was eluted isocratically with buffer A at 3 ml/min and eluted from 110 to 230 min. The purest fractions, as judged by SDS-PAGE, were combined, concentrated by ultafiltration using an Amicon pressure cell with a PM30 membrane to approximately 50 mg/ml and stored at -80°C.

8.5.2 Purification of IscU from pET24a:IscU/ BL-21(DE3)

Medium scale cell cultures (Section 8.2.2; 5 L) afforded 35 g of cell paste. A cell-free lysate was prepared following Method 2 (Section 8.2.1) using buffer A. The protein solution was applied to a Q-Sepharose FF column (130 ml; Pharmacia) which had previously been equilibrated with buffer A. Protein was eluted with a 0 to 100 % gradient of buffer C over 5 column volumes at a flow rate of 10 ml/min. Fractions containing IscS, as judged by SDS-PAGE, were pooled and concentrated by ultafiltration using an Amicon pressure cell with a PM10 membrane to approximately 60 mg/ml. The concentrate was applied to a Sephadex 75 column (20 mm ID X 850 mm; Pharmacia) equilibrated with buffer A at 3 ml/min. Protein was eluted isocratically with buffer A at 3 ml/min and eluted from 150 to 250 min. The purest fractions, as judged by SDS-PAGE, were combined, concentrated by ultafiltration using an Amicon pressure cell with a PM10 membrane to approximately 50 mg/ml and stored at -80°C.

8.5.3 Purification of His_6-IscA from pQiscA-55 /Bl-21(DE3)

A cell-free lysate using 17 g of cell paste was prepared following Method 1 (Section 8.2.1). The protein solution was applied to a chelating Sepharose column (35 ml; Pharmacia), which was charged with $NiSO_4$ (0.2 M; 50 ml) and equilibrated with buffer D (0.5 M imidazole and 0.5 M NaCl added to buffer A). Protein was eluted with a 0 to 50 % gradient of buffer D over 10 column volumes at a flow rate of 6 ml/min. The purest fractions, as judged by SDS-PAGE, were combined, desalted and concentrated following Method II (Section 8.2.3).

8.5.4 Purification of Hsc20, Hsc66 and ferredoxin

Construction of pET24d:HscF

Detailed experimental procedures for the construction of plasmids are given below (Section 8.7). Medium scale cell cultures (Section 8.2.2; 5 L) afforded 40 g of cell paste. A cell-free lysate was prepared following Method 1 (see 8.2.1) using buffer A. The protein solution was applied to a Q-Sepharose FF column (130 ml; Pharmacia) which had previously been equilibrated with buffer A and C. Protein was eluted with a 0 to 100 % gradient of buffer C over 5 column volumes at a flow rate of 10 ml/min. Fractions

containing Hsc20 and Hsc66, as judged by SDS-PAGE, were pooled and concentrated by ultafiltration using an Amicon pressure cell with a PM30 membrane to approximately 70 mg/ml. The concentrate was applied to a Sepharose 200 column (20 mm ID X 850 mm; Pharmacia) column equilibrated with buffer A at 3 ml/min. Protein was eluted isocratically with buffer A at 3 ml/min and eluted from 110 to 230 min. The purest fractions of Hsc20 were combined, concentrated by ultafiltration using an Amicon pressure cell with a PM30 membrane to approximately 50 mg/ml and stored at -80°C.

Fractions containing Hsc66 were pooled and applied to a Phenyl Resource (35 ml; Pharmacia) column with a flow rate of 5 ml/min, which had previously been equilibrated with buffer B (1 M ammonium sulphate added to buffer A) and buffer A. Protein was eluted with a linear gradient of 0 % to 100 % buffer A over five column volumes. The purest fractions, as judged by SDS-PAGE, were combined, desalted and concentrated following Method II (Section 8.2.3.3).

Fractions containing ferredoxin, as judged by SDS-PAGE, were pooled and concentrated by ultafiltration using an Amicon pressure cell with a PM30 membrane to approximately 70 mg/ml. The concentrate was applied to a Sephadex 75 gel filtration column (20 mm ID X 850 mm; Pharmacia) equilibrated with buffer A at 3 ml/min. Protein was eluted isocratically with buffer A at 3 ml/min and eluted from 110 to 230 min.

8.6 Experimental for Chapter Six

8.6.1 Removal of small molecules from standard assay

The assay volume was scaled up to 5 ml and biotin formation proceeded for 180 min. After 180 min. the assay mixture was split into 2 X 2.5 ml, each was applied to a Slide-A-Lyzer 10K (Pierce) and dialysed against Tris-HCl buffer (50 mM, pH 8.1) overnight at 4°C. After overnight dialysis the assay mixture contained exclusively proteins. The protein mixture was concentrated with a MWCO membrane filter (0.5 ml, >5K, Millipore), split into aliquots (200 µl) and small molecules were added to their usual concentration in the assay (Table 3.2). Biotin formation was allowed to proceed for 90 min., after which it was halted by removing the protein fraction using MWCO membrane filter (0.5 ml, >5K, Millipore). Samples were then analysed for biotin formation by HPLC.

8.6.2 Inhibition experiments

Sinefungin was a kind gift of Prof. Baldwin (Oxford University). If not otherwise stated the inhibitior (1 mg) was dissolved in Tris-HCl buffer (1 ml, 50 mM, pH 8.1). A typical assay series to investigate the inhibition of BioB activity involved 18 samples. The inhibitor was diluted to its final concentration in a final volume of 50 µl assay buffer in 0.5 ml Eppendorf tubes. All the assay components, except DTB, were added to a final volume of 4 ml. 190 µl were aliquoted into the 0.5 ml Eppendorf tubes containing the inhibitor. Biotin formation was initiated by the addition of DTB.

8.6.3 Purification of His_6-PFS

A cell-free lysate using 30 g of cell paste was prepared following Method 1 (Section 8.2.1) using buffer A. The protein solution was applied to a chelating sepharose column (35 ml; Pharmacia), which was charged with $NiSO_4$ (0.2 M; 50 ml) and equilibrated with buffer D. Protein was eluted with a 0 to 50 % gradient of buffer D (0.5 M imidazole and 0.5 M NaCl added to buffer A) over 10 column volumes at a flow rate of 6 ml/min. Fractions containing purified His_6-PFS, as judged by SDS-PAGE were desalted and concentrated using Method I or II (Section 8.2.3.3).

Standard curves for DOA and adenine (260 nm)

DOA (1 mg) or adenine (1 mg) was dissolved in 1 ml of buffer A. Serial standard solution for the concentration range of interest were prepared and analysed by HPLC. A standard curve for the measurement of unknown concentration was calculated using linear regression (Figure 8.6 and 8.7).

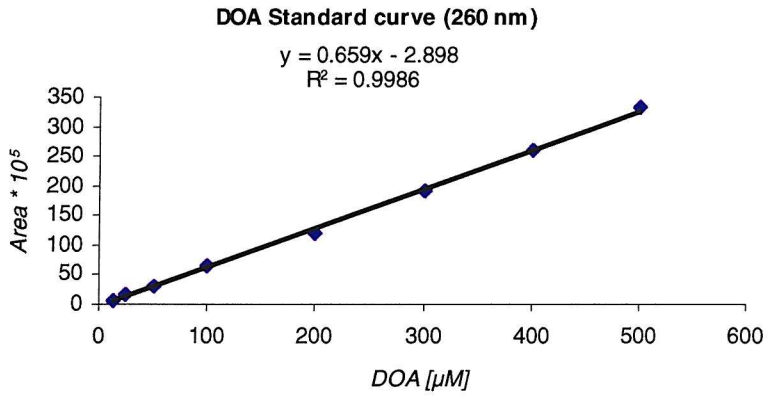

Figure 8.6: Standard curve for DOA recorded at 260 nm (σ: 0.23). [Method II; HPLC\Results\added\rp15\2-15].

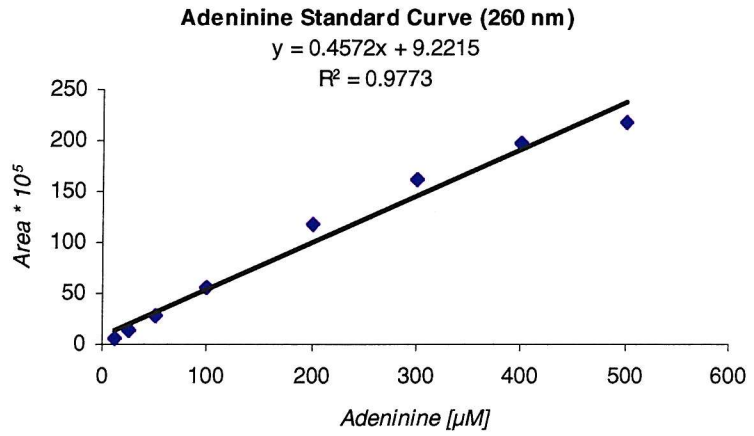

Figure 8.7: Standard curve for adenine recorded at 260 nm (σ: 0.41). [Method II; HPLC\Results\added\rp15\10-17].

Determination of the K_m for PFS

The rate of the reaction was determined for different substrate concentration (Table 8.1, Table 8.2).

DOA [µM]	Adenine I (Area) *10^5	Adenine II (Area) *10^5	Adenine III (Area) *10^5	Adenine I [µM]	Adenine II [µM]	Adenine III [µM]
12.5	0.35	5.87	5.58	0	0	0
25	12.21	12.16	11.77	6.55	6.42	5.57
50	21.25	20.86	20.79	26.30	25.46	25.31
100	32.21	33.90	33.31	50.28	53.98	52.68
200	49.00	47.70	48.31	86.99	84.16	85.49
300	58.39	57.21	58.62	107.53	104.96	108.05
400	63.41	63.92	65.14	118.53	119.65	122.31
500	70.03	69.50	69.79	132.99	131.85	132.48

Table 8.4: Conversion of DOA to adenine catalysed by 1 µM PFS/ 2 min.; I, II and III represent triplicate assays; [Method II; HPLC\Results\added\rp14\1-21].

$Adenine_{total}$ [µM]	$Error_{calc}$	DOA [µM]	v (nmol/ min)	1/v * 10^6	1/S * 10^3
0.00	0.00	12.5	0.00	0.0	80.0
6.18	0.43	25	7.72	129.5	40.0
25.69	0.44	50	32.11	31.1	20.0
52.31	1.53	100	65.39	15.3	10.0
85.55	1.16	200	106.93	9.4	5.0
106.85	1.35	300	133.56	7.5	3.3
120.16	1.58	400	150.20	6.7	2.5
132.44	0.47	500	165.55	6.0	2.0

Table 8.4: Values for the determination of K_m and specific activity [Method II; HPLC\Results\added\rp14\1-21].

The K_m of PFS was determined to be 462 µM and the specific activity was found to be 47 µmol/ min/ mg (Section 6.8.3).

NMR spectroscopy

NMR spectroscopy was carried out on a Bruker DPX400 spectrometer. PFS (1 mg /ml) was diluted in H_2O (2.5 ml), the protein was applied to a PD-10 column (Pharmacia), which had been previously equilibrated with H_2O (10 ml, pH 7.2). PFS was eluted with H_2O (3.5 ml, pH 7.2). 10 µl were added to a freshly prepared DOA solution (1 mg in H_2O, 1 ml, pH 7.2), and the reaction monitored by TLC. TLC (silica, propanol/ethylacetate (30/70), visualized with $KMnO^{4-}$): R_f (adenine) = 0.73; R_f (5'-deoxyribose) = 0.69.

After 60 min. the reaction was halted by removing the protein fraction with MWCO membrane filter (4 ml, >10K, Millipore). The flow through containing the small molecules was freeze-dried using a Modulyo freeze dryer (0°C, 10^{-2} mbar; Edwards), resuspended in 0.5 ml CD_3OD (purity: 99 %) and submitted to NMR spectroscopy.

8.6.4 Purification of MetK from pK8/BL-21(DE3)

Medium scale cell cultures (Section 8.2.2; 5 L) afforded 35 g of cell paste. A cell-free lysate was prepared following Method 1 (Section 8.2.1) using buffer A. The protein solution was applied to a Q-Sepharose FF column (130 ml; Pharmacia) which had previously been equilibrated with buffer A. Protein was eluted with a 0 to 100 % gradient of buffer C over 5 column volumes at a flow rate of 10 ml/min. Fractions containing MetK, as judged by SDS-PAGE, were pooled and concentrated by ultafiltration using an Amicon pressure cell with a PM30 membrane to approximately 70 mg/ml. The concentrate was applied to a Sepharose 200 column (20 mm ID X 850 mm; Pharmacia) column equilibrated with buffer A at 3 ml/min. Protein was eluted isocratically with buffer A at 3 ml/min and eluted from 120 to 230 min. The purest fractions, as judged by SDS-PAGE, were combined, concentrated by ultafiltration using an Amicon pressure cell with a PM30 membrane to approximately 50 mg/ml and stored at -80°C.

8.7 Experimental for Chapter Seven

8.7.1 PCR amplification of genes from genomic DNA (*E. coli*)

Depending on the gene of interest *Pfu* or *Taq* DNA polymerase were used. Table 8.5 and 8.6 show the reaction conditions used.

Component	Stock concentration	Volume (µl)	Final Concentration
H_2O (sterile)		120	
Enzyme Buffer	10 X	20	1 X
DMSO	100%	20	6%
NTP mix	10 mM each	10	500 µM each
Forward and Reverse Primer	20 µM each	10	1 µM each
Pfu DNA Polymerase	10 U/ 20 µl	20	10 U

Table 8.5: Conditions for four PCR amplification reactions using *Pfu* DNA polymerase, DNA template (1 µl; *E. coli*) was added to single amplification reaction at various concentrations ranging from 0.1 µg/ml to 0.1 ng/ml (Final volume of stock solution: 200 µl).

Component	Stock concentration	Volume (µl)	Final Concentration
H_2O (sterile)		124	
Enzyme Buffer	10 X	20	1 X
Mg^{2+}	2.5 mM	16	200 µM
NTP mix	10 mM each	10	500 µM each
Forward and Reverse Primer	20 µM each	10	1 µM each
Taq DNA Polymerase	5 U/ 20 µl	20	5 U

Table 8.6: Conditions for four PCR amplification reactions using *Taq* DNA polymerase, 1 µl of DNA template (*E. coli*) was added to single amplification reaction at various concentrations ranging from 0.1 µg/ml to 0.1 ng/ml (Final volume of stock solution: 200 µl).

The template consisted of genomic DNA of *E. coli,* previously isolated from Dr. P. Roach. There are two methodologies to start PCR amplifications termed "Hot Start" and

"Cold Start". For a "Cold Start", a stock solution excluding DNA template was prepared (Table 8.5 and 8.6). 45 to 50 µl were aliquoted into PCR tubes (0.2 ml; Radleighs) and had DNA template (1 µl) at various concentrations added. The tubes were transferred into a Progene Thermal Cycler (Techne) and the PCR amplifications were carried out using specific reaction conditions (Table 8.7). For a "Hot Start", a stock solution excluding DNA template and DNA polymerase was prepared (Table 8.5 and 8.6). 45 to 50 µl were aliquoted into PCR tubes (0.2 ml; Radleighs) and had DNA template (1 µl) at various concentrations added. The tubes were transferred into a Progene Thermal Cycler (Techne) and the PCR amplifications were carried out using specific reaction conditions (Table 8.7). After the initial denaturing step of five minutes DNA polymerase (5 µl) was added to each single tube and the PCR amplification was allowed to proceed.

Step	**Temperature**	**Time**
Denaturation	94°C	4 min.
Annealing	55°C	30 sec. to 2 min.
Extension	72°C	30 sec. to 5 min.

Table 8.7: PCR amplification reaction cycle conditions using a Progene Thermal Cycler (Techne). PCR amplifications were allowed to proceed from 25 to 35 cycles. After the last reaction cycle had completed, a final reaction cycle incubated the reaction mixture for 10 min. at 72°C, followed by storage at 4°C until removal.

8.7.2 PCR amplification of genes of interest

PCR amplifications were carried out as described in 8.7.1. Primers used are shown in Table 8.8.

Primer ID	Gene ID	Sequence (5' – 3')
Bio 1 (F)	*bio*BFD	CATATGGCTCACCGCCCACGCTGGACATTGTCG
Bio 2 (R)	*bio*BFD	AAGCTTCTCTCCTTCTACAACAAGGCAAGGTTTATGTA
Bio 3 (F)	*bio*A	AAGCTTATGACAACGGACGATCTTGCCTTT
Bio 4 (R)	*bio*A	GAATTCTTCTCCTTATTGGCAAAAAAATGT TTCATC
Bio 5 (R)	*bio*Start	TCGCGAGGCGCTGCGCCT
Bio 6 (F)	*bio*End	ACCGGTCGCCTCTGGCAG
Mio 1 (F)	*mio*C	GGGCCCGGATCCGGATGGCAGATATCACTCTT
Mio 2 (R)	*mio*C	GGGCCCGGTACCCTCCTTTTATTTGAGTAAATTAAC
Flav 1 (F)	*fpr*	GGGCCCGGTACCGGATGGCTATCACTGGCATC
Flav 2 (R)	*fpr*	GGGCCCGAGCTCCTCCTTTCAGGCATTGAGAAT TTC
Flr 1 (F)	*fld*A	GGGCCCGAGCTCGGATGGCTGATTGGGTAACA
Flr 2 (R)	*fld*A	GGGCCCGCGGCCGCTTACCAGTAATGCTCCGC
BioB 1 (F)	*bio*B	GGGCCCCATATGGCTCACCGCCCACGCTGG
BioB 1 (R)	*bio*B	GCGCGCGGATCCATCTCCTTCTCATAATGCTGCCGC
Isc 1 (F)	*isc*RSUA	CCCGGGCATATGAGACTGACATCTAAAGGG
Isc 2 (R)	*isc*RSUA	GCGCGCGGATCCATCTCCTTCTCAAACGTGGAAGCTTT CCGG
Hsc 1 (F)	*hsc*AB	CCC GGG GGA TCC ATG GAT TAC TTC ACC CTC
Hsc 2 (R)	*hsc*AB	GCGCGCCCTCAGGATCTCCTTCTTATTCGGCCTCGTC
BioD 1 (F)	*bio*D	b-CCCGGGCATATGAGTAAACGTTATTTTGTC
BioD 1(R)	*bio*D	b-GCGCGCGGATCCTTATGTACTTTCCGGTTG
Pfs (F)	*pfs*	CCCGGGGGATCCATGAAAATCGGCATC
Pfs (R)	*pfs*	ATCGATGGTACCTTCCTCCTGTTAGCCATGTGCAAG

Table 8.8: Primer design for PCR amplifications; F: forward primer, R: reverse primer; b: biotinylated.

PCR amplification of the biotin operon genes

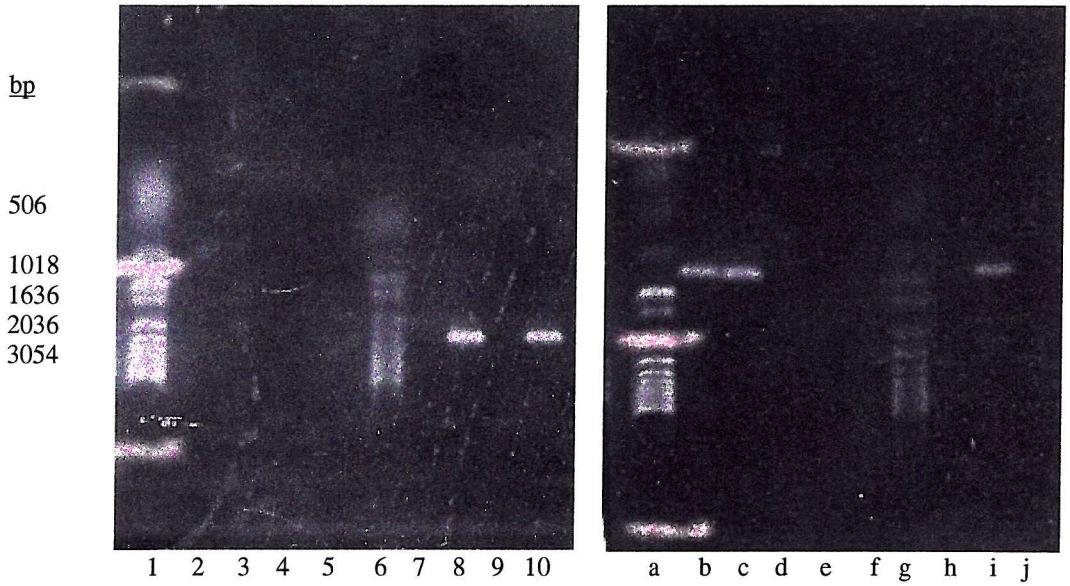

Figure 8.10: (1,6) Marker, (2-5) PCR amplification of *bio*BFD at various template concentrations, (7-10) plus DMSO; (a,g) Marker, (b-e) PCR amplification of *bio*A at various template concentrations plus DMSO, (f,h-j) minus DMSO.

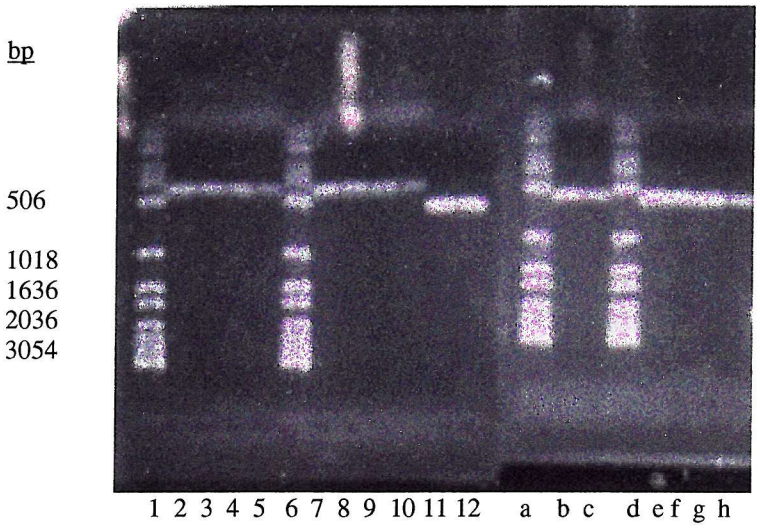

Figure 8.11: (1,6) Marker, (2-5, 7-10) PCR amplification of *bio*Start using Taq DNA polymerase at various template concentrations; (a,d) Marker, (11,12,b,c,d-h) PCR amplification of *bio*End using Taq DNA polymerase at various template concentrations.

PCR amplification of *fld*A, *fpr*, *mio*C and *bio*B

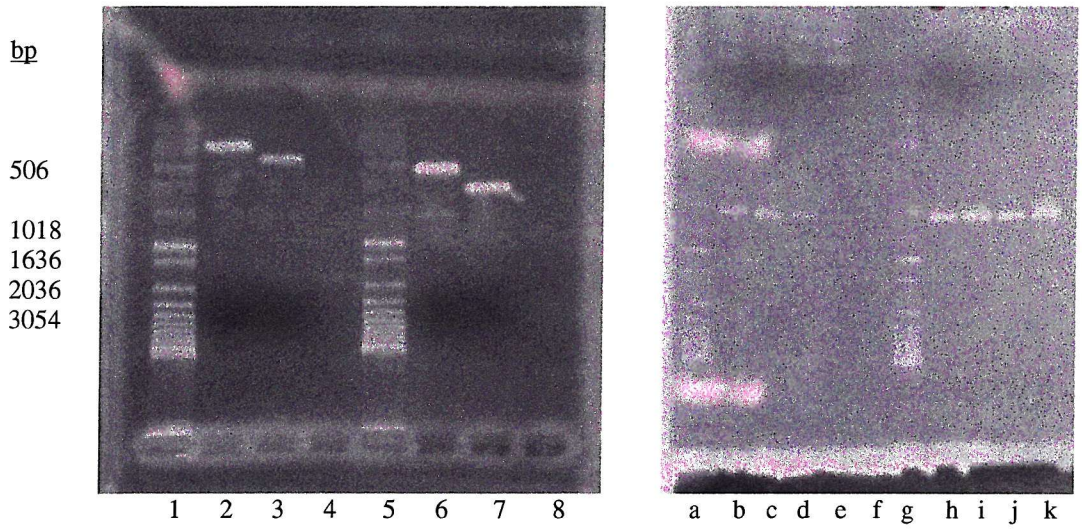

Figure 8.12: (1,5) Marker, purified PCR product of (2) *mio*C, (3,6) *fld*A, (7) *fpr*, (4,8) blank; (a,g) Marker, (b-f) PCR amplification of *bio*B at various template concentrations, (h-k) plus DMSO.

PCR amplification of the *isc* operon genes

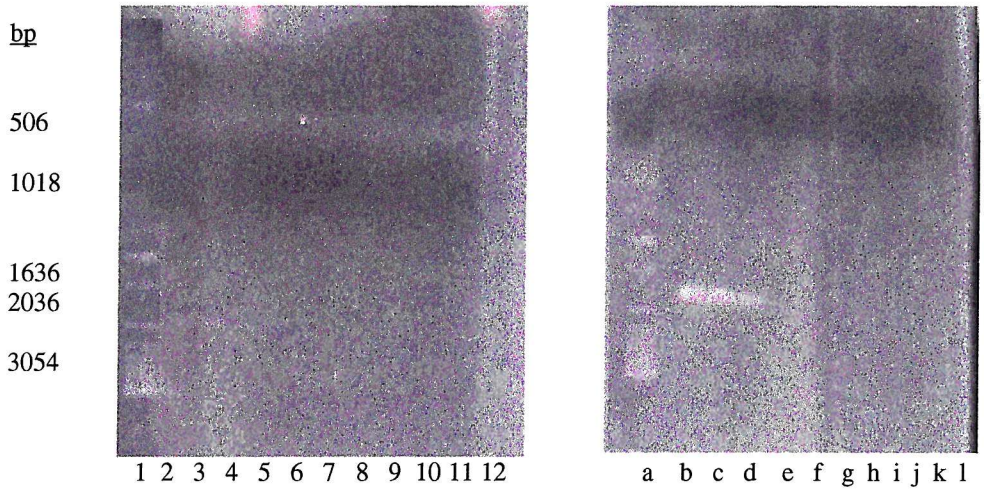

Figure 8.13: (1) Marker, (2-5) PCR amplification of *isc*HSC at various template concentrations plus DMSO, (7-10) minus DMSO, (11,12) blank; (a) Marker, (b-e) PCR amplification of *isc*SUA at various template concentrations plus DMSO, (f-j) minus DMSO, (k,l) blank.

PCR amplification of *pfs* and *bio*D

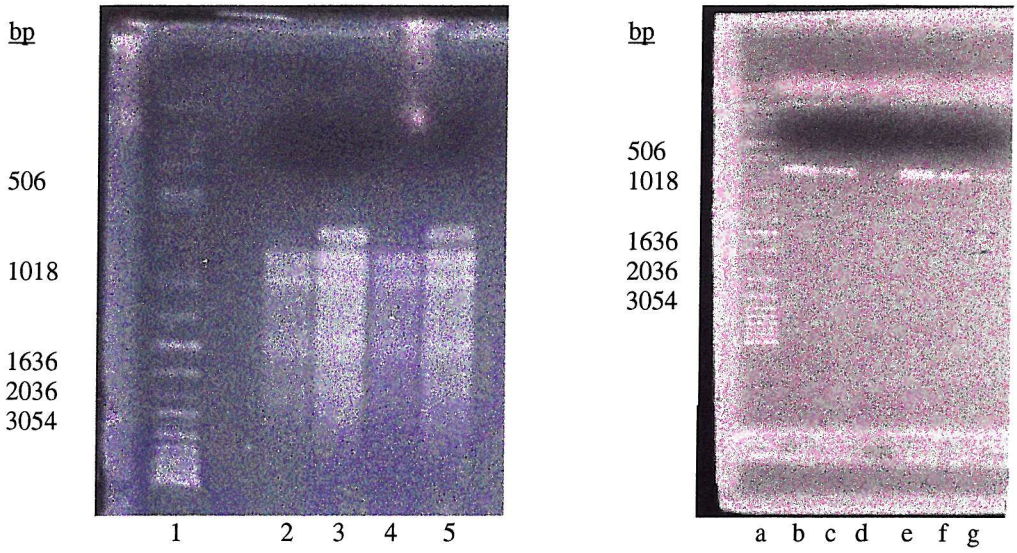

Figure 8.14: (1) Marker, (2,4) purified PCR product of *bio*D, streptavidin added, no restriction enzymes added, (3,5) purified PCR product of *bio*D, streptavidin added, restriction enzymes added; (a) Marker, (b-d) PCR amplification of *bio*B at various template concentrations, (e-g) plus DMSO.

8.7.3 Ligation of PCR products into appropriate vectors

The PCR product was purified from the reaction mixture with the Wizard PCR Preps DNA Purification System (Promega). After the purification the concentration was estimated in comparison to a 1 kb ladder (500 ng) by gel electrophoresis. Various methods were used to ligate the PCR product into the appropriate cloning or expression vector.

Method A: A pET vector was restricted with the appropriate enzymes. The PCR fragment was restricted with the same enzymes (Table 8.8).

Component	Stock Concentration	Volume (µl)	Final Concentration
H_2O (sterile)		5	
Vector or PCR fragment	~ 0.1 µg/µl	10	~ 1 µg
Compatible restriction enzyme buffer	10 X	2	1 X
BSA	1 mg/ml	2	0.1 mg/ml
Restriction enzymes	10 U/µl	0.5	0.5 U

Table 8.8: Restriction digest conditions

Both reaction mixtures were analysed on a 1% low melting agarose gel by gel electrophoresis. They were gel purified using Geneclean III Kit (Anachem) according to the manufacture instructions and ligated. The pET vector and the cut PCR fragment were incubated at an approximate molar ratio of 3:1, 1:1 and 1:3 in a final volume of 10 µl. T4 ligase (3 U) and T4 ligase buffer (1 X; 1 µl) were added. The reaction mixture was maintained at 4°C overnight.

Method B: *Pfu* DNA polymerase does not add a single deoxyadenosine to the 3' ends of the amplified fragments. The purified PCR product is A-tailed to allow subcloning into the pGEM-T vector, which has a 3' deoxythymidine residue added to both ends (Table 8.9). This step was unnecessary if *Taq* DNA polymerase was used.

Component	Stock concentration	Volume (µl)	Final Concentration
purified PCR fragment	5 ng/µl – 500 ng/µl	1 – 3	
H_2O (sterile)		0 - 2	
Enzyme Buffer	10 X	1	1 X
Mg^{2+}	2 mM	1	200 µM
ATP	1 mM	2	200 µM each
pGEM- T vector	50 ng/µl	1	5 U
Taq DNA Polymerase	1.25 U/µl	2	3 U

Table 8.9: An A-tailing procedure for blunt-ended PCR fragments

The pGEM-T vector and the purified, A-tailed PCR fragment were incubated at an approximate molar ratio of 3:1, 1:1 and 1:3 in a final volume of 10 µl. T4 ligase (3 U) and T4 ligase buffer (1 X; 1 µl) were added. The reaction mixture was maintained at 4°C overnight.

Method C: By addition of streptavidin, a protein that binds strongly to biotin, a gel shift assay could be performed. Direct digestion of the PCR fragment, followed by addition of streptavidin gave retarded, undigested PCR product and unretarded, digested PCR product (Figure 8.14). To use this direct cloning strategy, all the primer were 5' biotinylated.

Method D: The pBAD-TOPO vector and the A-tailed PCR fragment were incubated at an approximate molar ratio of 3:1, 1:1 and 1:3 (Table 8.10).

Component	Volume (µl)
H_2O (sterile)	added to a final volume of 5 µl
A-tailed PCR product	0.5 – 4
Salt solution	1
pBAD-TOPO vector	1

Table 8.10: pBAD-TOPO cloning reaction (Ligation time: 1 to 5 min.).

8.7.4 Screening for insertion of PCR fragments

The whole ligation reaction was used to transform chemically competent XL1-Blue (Stratagene). Bacteria were made chemically competent following literature procedures (139). From the resultant culture, 100 µl – 900 µl were spread onto a LB plate containing the appropriate resistance marker. If the pGEM-T vector was used, plates were prepared containing ampicillin (60 µg/ml), IPTG (0.5 mM) and X-Gal. Screening for insertion was done under the same conditions as PCR amplification. Instead of genomic DNA, one white coloured (pGEM-T) or normal coloured colony (pET, pBAD-TOPO) was picked from the plate and pippeted into the reaction mixture. The tip was transferred to Eppendorf tubes (1.5 ml) containing 2 TY (600 µl) with the appropriate resistance marker added to allow the isolation of positive clones.

The forward primer for the PCR amplification was designed to anneal to the promotor sequence of the vector. The reverse primer is the same used for amplification of this PCR product. This screening protocol identifies colonies containing the required PCR fragment and the direction of insertion. The PCR screen was checked by gel electrophoresis. Positive colonies were transferred into 2 YT medium (5 ml) and incubated overnight in a Shaker at 225 rpm and 37°C. The DNA was isolated by using Wizard *Plus* Minipreps Purification System (Promega) and characterised by restriction digestion and gel electrophoresis. Further subcloning followed the earlier protocols (Table 8.8).

References

1. Kogl, F. (1935) *Ber. Deut. Chem. Ges.* **68**, A16
2. Kogl, F., and Tonnis, B. (1936) *Z. Physiol. Chem.* **242**, 43
3. Bateman, W. G. (1916) *J. Biol. Chem.* **26**, 263
4. Boas, M. A. (1927) *Biochem. J.* **21**, 712
5. Gyorgy, P. (1931) *Z. Aerztl. Fortbild.* **28**, 377
6. Gyorgy, P., Melville, D. B., and du Vigneaud, V. (1941) *Science* **91**, 243
7. Hofmann, K., Melville, D. B., and du Vigneaud, V. (1941) *J. Biol. Chem.* **141**, 207
8. Hofmann, K., Kilmer, G. W., Melville, D. B., and du Vigneaud, V. (1942) *J. Biol. Chem.* **145**, 403
9. du Vigneaud, V., Hofmann, K., and Melville, D. B. (1942) *J. Am. Chem. Soc.* **64**, 188189
10. Harris, S. A., Wolf, D. E., Mozingo, R., and Folkers, K. (1943) *Science* **97**, 447
11. Harris, S. A., Wolf, D. E., Mozingo, R., Anderson, R. C., Arth, G. E., Arth, G. E., Easton, N. R., Heyl, D., Wilson, A. N., and Folkers, K. (1944) *J. Am. Chem. Soc.* **66**, 1756-1757
12. Knowles, J. R. (1989) *Annu. Rev. Biochem.* **58**, 195-221
13. Eisenberg, M., Prakash, O., and Hsiung, S. C. (1982) *J. Biol. Chem.* **257**, 15167-15173
14. Lane, M. D., Rominger, K. L., Young, D. L., and Lynen, F. (1964) *J. Biol. Chem.* **239**, 2865-2871
15. Bugg, T. (1997) *An Introduction to Enzyme and Coenzyme Chemistry*, 1st Ed., Blackwell Science, Oxford, UK
16. Eisenberg, M. (1973) *Adv. Enzymol.* **38**, 317-371
17. Otsuka, A. J., Buoncristiani, M. R., Howard, P. K., Flamm, J., Johnson, C., Yamanoto, R., Uchida, K., Cook, C., Ruppert, J., and Matsuzaki, J. (1988) *J. Biol. Chem.* **263**, 19577-19585
18. Gloeckler, R., Ohsawa, I., Speck, D., Ledoux, C., Bernard, S., Zinsius, M., Villeval, D., Kisou, T., Kamogawa, K., and Lemoine, Y. (1990) *Gene* **87**, 63-70

19. Bower, S., Perkins, J. B., Yocum, R. R., Howitt, C. L., Rahaim, P., and Pero, J. (1996) *J. Bacteriol.* **178**, 4122-4130
20. Phalip, V., Kuhn, I., Lemoine, Y., and Jeltsch, J. M. (1999) *Gene* **232**, 43-51
21. Baldet, P., Gerbling, H., Axiotis, S., and Douce, R. (1993) *Eur. J. Biochem.* **217**, 479-485
22. Abbot, J., and Beckett, D. (1993) *Biochemistry* **32**, 9649-9656
23. Cronan, J. E., Jr. (1989) *Cell* **58**, 427-429
24. Ploux, O., Soularue, A., Marquet, A., Gloeckler, R., and Lemoine, Y. (1992) *Biochem. J.* **187**, 685-690
25. Ifuku, O., Miyaoka, H., Koga, N., Kishimoto, J., Haze, S., Wachi, Y., and Kajiwara, M. (1994) *Eur. J. Biochem.* **220**, 585-591
26. Sanyal, I., Lee, S. L., and Flint, D. (1994) *J. Am. Chem. Soc.* **116**, 2637-2638
27. Alexeev, D., Alexeeva, M., Baxter, R. L., Campopiano, D. J., Webster, S. P., and Sawyer, L. (1998) *J. Mol. Biol.* **284**, 401-419
28. Ploux, O., Breyne, O., and Carillon, S. (1999) *Eur. J. Biochem.* **259**, 64-70
29. Ploux, O., and Marquet, A. (1996) *Eur. J. Biochem.* **236**, 301-308
30. Webster, S. P., Alexeev, D., Campopiano, D. J., Watt, R. M., Alexeeva, M., Sawyer, L., and Baxter, R. L. (2000) *Biochemistry* **39**, 516-528
31. Stoner, G. L., and Eisenberg, M. A. (1975) *J. Biol. Chem.* **250**, 4037-4043
32. Käck, H., Gibson, K. J., Gatenby, A. A., Schneider, G., and Lindqvist, Y. (1998) *Acta Crystallogr. D Biol. Crystallogr.* **D 54**, 1397-1398
33. Käck, H., Sandmark, J., Gibson, K. J., Schneider, G., and Lindqvist, Y. (1999) *J. Mol. Biol.* **291**, 857-876
34. Huang, I., Jia, J., Gibson, K. J., Taylor, W. S., Rendina, A. R., Schneider, G., and Lindqvist, Y. (1995) *Biochemistry* **34**, 10985-10995
35. Alexeev, D., Baxter, R. L., Smekal, O., and Sawyer, L. (1995) *Structure* **3**, 1207-1215
36. Käck, H., Gibson, K. J., Lindqvist, Y., and Schneider, G. (1998) *Proc. Natl. Acad. Sci. U S A* **95**, 5495-5500
37. Käck, H., Sandmark, J., Gibson, K. J., Schneider, G., and Lindqvist, Y. (1998) *Protein Sci.* **7**, 2560-2566
38. Sandalova, T., Schneider, G., Kack, H., and Lindqvist, Y. (1999) *Acta Crystallogr. D Biol. Crystallogr.* **55**, 610-624
39. Krell, K., and Eisenberg, M. (1970) *J. Biol. Chem.* **245**, 6558-6566

40. Gibson, K. J. (1997) *Biochemistry* **36**, 8474-8478
41. Yang, G., Sandalova, T., Lohman, K., Lindqvist, Y., and Rendina, A. R. (1997) *Biochemistry* **36**, 4751-4760
42. Sanyal, I., Cohen, G., and Flint, D. H. (1994) *Biochemistry* **33**, 3625-3631
43. Birch, O. M., Fuhrmann, M., and Shaw, N. M. (1995) *J. Biol. Chem.* **270**, 19158-19165
44. Frappier, F., Guillerm, G., Salib, A. G., and Marquet, A. (1979) *Biochem. Biophys. Res. Commun.* **91**, 551-527
45. Parry, R. J., and Kunitani, M. G. (1976) *J. Am. Chem. Soc.* **98**, 4024-4026
46. Guillerm, G., Frappier, F., Gaudry, M., and Marquet, A. (1977) *Biochemie* **59**, 119-121
47. Frappier, F., Jouany, M., Marquet, A., Olesker, A., and Tabet, J. C. (1982) *J. Org. Chem.* **47**, 2257
48. Baxter, R. L., Camp, D. J., Coutts, A., and Shaw, N. (1992) *J. Chem. Soc., Perkin Trans.* **1**, 255-258
49. Marquet, A., Frappier, F., Guillerm, G., Azoulay, M., Florentin, D., and Tabet, J. C. (1993) *J. Am. Chem. Soc.* **115**, 2139-2145
50. Baldet, P., Gerbling, H., Axiotis, S., and Douce, R. (1993) *Eur. J. Biochem.* **217**, 479-485
51. Shaw, N. M., Birch, O. M., Tinschert, A., Venetz, V., Dietrich, R., and Savoy, L. A. (1998) *Biochem. J.* **330**, 1079-1085
52. Marti, F. B. (1983) *E.T.H Diss. (Zürich)* Nr 7236
53. Guianvarch, D., Florentin, D., Bui, B. T. S., Nunzi, F., and Marquet, A. (1997) *Biochem. Biophys. Res. Commun.* **236**, 402-406
54. Escalettes, F., Florentin, D., Bui, B. T. S., Lesage, D., and Marquet, A. (1999) *J. Am. Chem. Soc.* **121**, 3571-3578
55. Sofia, H. J., Chen, G., Hetzler, B. G., Reyes-Spindola, J. F., and Miller, N. E. (2001) *Nucleic Acids Res.* **29**, 1097-1106.
56. Mulliez, E., Fontecave, M., Gaillard, J., and Reichard, P. (1993) *J. Biol. Chem.* **268**, 2296-2299
57. Wagner, A. F., Frey, M., Neugebauer, F. A., Schafer, W., and Knappe, J. (1992) *Proc. Natl. Acad. Sci. U S A* **89**, 996-1000
58. Birch, O. M., Hewitson, K. S., Fuhrmann, M., Burgdorf, K., Baldwin, J. E., Roach, P. L., and Shaw, N. M. (2000) *J. Biol. Chem.* **275**, 32277-32280

59. Bui, B. T. S., Florentin, D., Fournier, F., Ploux, O., Mejean, A., and Marquet, A. (1998) *FEBS Lett.* **440**, 226-230

60. Gibson, K. J., Pelletier, D. A., and Turner, I. M., Sr. (1999) *Biochem. Biophys. Res. Commun.* **254**, 632-635

61. McIver, L., Baxter, R. L., and Campopiano, D. J. (2000) *J. Biol. Chem.* **275**, 13888-13894.

62. Hewitson, K. S., Ollagnier-de Choudens, S., Sanakis, Y., Shaw, N. M., Baldwin, J. E., Münck, E., Roach, P. L., and Fontecave, M. (2002) *J. Biol. Inorg. Chem.* **7**, 83-93.

63. Ugulava, N. B., Sacanell, C. J., and Jarrett, J. T. (2001) *Biochemistry* **40**, 8352-8358.

64. Ugulava, N. B., Gibney, B. R., and Jarrett, J. T. (2001) *Biochemistry* **40**, 8343-8351.

65. Ollagnier-de-Choudens, S., Sanakis, Y., Hewitson, K. S., Roach, P. L., Baldwin, J. E., Münck, E., and Fontecave, M. (2000) *Biochemistry* **39**, 4165-4173

66. Shaw, N. M., Lehner, B., Fuhrmann, M., Kulla, H. G., Brass, J. M., Birch, O. M., Tinschert, A., Venetz, D., Venetz, V., Sanchez, J. C., Tonella, L., and Hochstrasser, D. F. (1999) *J. Ind. Micro. Biotech.* **22**, 590-599

67. Pai, C. H., and Lichtenstein, H. C. (1965) *Biochem. Biophys. Acta* **100**, 28-35

68. Pai, C. H. (1972) *J. Bacteriol.* **112**, 1280-1287

69. Kanzaki, N., Kawamoto, T., Matsui, J., Nakahama, K., and Ifuku, O. (1997) *in US Patent* 793119

70. Levy-Schil, S., Debusche, L., Rigault, S., Soubrier, F., Baccette, F., Lagneaux, D., Schleuniger, J., Blanche, F., Crouzet, J., and Mayaux, J. F. (1993) *Appl. Microbiol. Biotechnol.* **38**, 755-762

71. van Arsdell, S., Pero, J., Perkins, J., and Yocum, R. (1999) *in EU Patent* 0892066

72. Reichard, P. (1998) *Science* **260**, 1773-1777

73. Reichard, P. (2002) *Arch. Biochem. Biophys.* **397**, 149-155.

74. Ollagnier-de Choudens, S., Mulliez, E., Gaillard, J., Eliasson, R., Fontecave, M., and Reichard, P. (1996) *J. Biol. Chem.* **271**, 9410-9416

75. Sun, X., Eliasson, R., Pontis, E., Andersson, J., Buist, G., Sjoberg, B. M., and Reichard, P. (1995) *J. Biol. Chem.* **270**, 2443-2446

76. Ollagnier-de Choudens, S., Meier, C., Mulliez, E., Gaillard, J., Schünemann, V., Trautwein, A., Mattioli, T., Lutz, M., and Fontecave, M. (1999) *J. Am. Chem. Soc.* **121**, 6344-6350

77. Bianchi, V., Eliasson, R., Fontecave, M., Mulliez, E., Hoover, D. M., Matthews, R. G., and Reichard, P. (1993) *Biochem. Biophys. Res. Commun.* **197**, 792-797

78. Bianchi, V., Reichard, P., Eliasson, R., Pontis, E., Krook, M., Jornvall, H., and Lindqvist, Y. (1993) *J. Bacteriol.* **175**, 1590-1595

79. Ollagnier-de Choudens, S., Mulliez, E., Schmidt, P. P., Eliasson, R., Gaillard, J., Deronzier, C., Bergman, T., Graslund, A., Reichard, P., and Fontecave, M. (1997) *J. Biol. Chem.* **272**, 24216-24223

80. Sun, X., Ollagnier-de Choudens, S., Schmidt, P. P., Atta, M., Mulliez, E., Lepape, L., Eliasson, R., Graslund, A., Fontecave, M., Reichard, P., and Sjoberg, B. M. (1996) *J. Biol. Chem.* **271**, 6827-6831

81. Logan, D. T., Andersson, J., Sjoberg, B. M., and Nordlund, P. (1999) *Science* **283**, 6827-6831

82. Stubbe, J., and van der Donk, W. A. (1998) *Chem. Rev.* **98**, 705-762

83. Knappe, J., and Sawers, G. (1990) *FEMS Microbiol. Rev.* **6**, 383-398

84. Knappe, J., Schacht, J., Mockel, W., Hopner, T., Vetter, H., Jr., and Edenharder, R. (1969) *Eur. J. Biochem.* **11**, 316-327

85. Knappe, J., and Blaschkowski, H. P. (1975) *Methods Enzymol.* **41**, 508-518

86. Wong, K. K., Murray, B. W., Lewisch, S. A., Baxter, M. K., Ridky, T. W., Ulissi-DeMario, L., and Kozarich, J. W. (1993) *Biochemistry* **32**, 14102-14110

87. Knappe, J., Neugebauer, F. A., Blaschkowski, H. P., and Ganzler, M. (1984) *Proc. Natl. Acad. Sci. U S A* **81**, 1332-1335

88. Knappe, J., Elbert, S., Frey, M., and Wagner, A. F. (1993) *Biochem. Soc. Trans.* **21**, 731-734

89. Broderick, J. B., Henshaw, T. F., Cheek, J., Wojtuszewski, K., Smith, S. R., Trojan, M. R., McGhan, R. M., Kopf, A., Kibbey, M., and Broderick, W. E. (2000) *Biochem. Biophys. Res. Commun.* **269**, 451-456

90. Knappe, J., and Wagner, A. F. (1995) *Methods Enzymol.* **258**, 343-362

91. Vanden Boom, T. J., Reed, K. E., and Cronan, J. E., Jr. (1991) *J. Bacteriol.* **173**, 6411-6420

92. Miller, J. R., Busby, R. W., Jordan, S. W., Cheek, J., Henshaw, T. F., Ashley, G. W., Broderick, J. B., Cronan, J. E., Jr., and Marletta, M. A. (2000) *Biochemistry* **39**, 15166-15178
93. Busby, R. W., Schelvis, J. P. M., Yu, D. S., Babcock, G. T., and Marletta, M. A. (1999) *J. Am. Chem. Soc.* **121**, 4706-4707
94. Ollagnier-de-Choudens, S., and Fontecave, M. (1999) *FEBS Lett.* **453**, 25-28
95. Jordan, S. W., and Cronan, J. E., Jr. (1997) *Methods Enzymol.* **279**, 176-183
96. Hewitson, K. S., Baldwin, J. E., Shaw, N. M., and Roach, P. L. (2000) *FEBS Lett.* **466**, 372-376
97. Chong, S., Montello, G. E., Zhang, A., Cantor, E. J., Liao, W., Xu, M., and Benner, J. (1998) *Nucleic Acids Res.* **26**, 5109-5115
98. Duin, E. C., Lafferty, M. E., Crouse, B. R., Allen, R. M., Sanyal, I., Flint, D. H., and Johnson, M. K. (1997) *Biochemistry* **36**, 11811-11820
99. Sanyal, I., Gibson, K. J., and Flint, D. (1994) *Biochemistry* **33**, 3625-3631
100. Izumi, Y., Osakai, M., and Yamada, H. (1987) *J. Microbiol. Methods* **6**, 237-246
101. Bui, B. T., Escalettes, F., Chottard, G., Florentin, D., and Marquet, A. (2000) *Eur. J. Biochem.* **267**, 2688-2694.
102. Beinert, H., Holm, R. H., and Münck, E. (1997) *Science* **277**, 653-659
103. Bian, S. M., and Cowan, J. A. (1999) *Coord. Chem. Rev.* **192**, 1049-1066
104. Zheng, L. M., and Dean, D. R. (1994) *J. Biol. Chem.* **269**, 18723-18726
105. White, R. H. (1983) *Biochem. Biophys. Res. Commun.* **112**, 66-72
106. Yuvaniyama, P., Agar, J. N., Cash, V. L., Johnson, M. K., and Dean, D. R. (2000) *Proc. Natl. Acad. Sci. U S A* **97**, 599-604.
107. Flint, D. H. (1996) *J. Biol. Chem.* **271**, 16068-16074
108. Nakai, Y., Yoshirara, Y., Hayashi, H., and Kagamiyama, H. (1998) *FEBS Lett.* **433**, 143-148
109. Kredich, N. M., Foote, L. J., and Keenan, B. S. (1973) *J. Biol. Chem.* **248**, 6187-6196
110. Garland, S. A., Hoff, K., Vickery, L. E., and Culotta, V. C. (1999) *J. Mol. Biol.* **294**, 897-907
111. Fujii, T., Maeda, M., Mihara, H., Kurihara, T., Esaki, N., and Hata, Y. (2000) *Biochemistry* **39**, 1263-1273

112. Kaiser, J. T., Clausen, T., Bourenkow, G. P., Bartunik, H. D., Steinbacher, S., and Huber, R. (2000) *J. Mol. Biol.* **297**, 451-464

113. Agar, J. N., Krebs, C., Frazzon, J., Huynh, B. H., Dean, D. R., and Johnson, M. K. (2000) *Biochemistry* **39**, 7856-7862.

114. Ollagnier-de-Choudens, S., Mattioli, T., Takahashi, Y., and Fontecave, M. (2001) *J. Biol. Chem.* **276**, 22604-22607.

115. Krebs, C., Agar, J. N., Smith, A. D., Frazzon, J., Dean, D. R., Boi, H. H., and Johnson, M. K. (2001) *Biochemistry* **40**, 14069-14080

116. Schwartz, C. J., Giel, J. L., Patschkowski, T., Luther, C., Ruzicka, F. J., Beinert, H., and Kiley, P. J. (2001) *Proc. Natl. Acad. Sci. U S A* **98**, 14895-14900

117. Vickery, L. E., Silberg, J. J., and Ta, D. T. (1997) *Protein Sci.* **6**, 1047-1056.

118. Silberg, J. J., Hoff, K. G., and Vickery, L. E. (1998) *J. Bacteriol.* **180**, 6617-6624.

119. Silberg, J. J., Hoff, K. G., Tapley, T. L., and Vickery, L. E. (2001) *J. Biol. Chem.* **276**, 1696-1700

120. Ollagnier-de Choudens, S., Mattioli, T., Takahashi, Y., and Fontecave, M. (2001) *J. Biol. Chem.* **276**, 22604-22607

121. Ta, D. T., and Vickery, L. E. (1992) *J. Biol. Chem.* **267**, 11120-11125

122. Silberg, J. J., and Vickery, L. E. (2000) *J. Biol. Chem.* **275**, 7779-7786

123. Ollagnier-de Choudens, S., Mulliez, E., Hewitson, K. S., and Fontecave, M. (2002) *Biochemistry* **41**, 9145-9152

124. Kiyasu, T., Asakura, A., Nagahashi, Y., and Hoshino, T. (2000) *J. Bacteriol.* **182**, 2879-2885.

125. Goldberg, B., Rattendi, D., Yarlett, N., Llyoyd, D., and Bacchi, C. J. (1997) *J. Euk. Micro.* **44**, 352-358

126. Paolantonacci, P., Lawrence, F., Nolan, L. L., and Robert-Gero, M. (1987) *Biochem. Pharm.* **36**, 2813-2820

127. Riscoe, M. K., Schwamborn, J., Ferro, A. J., Olson, K. D., and Fitchen, J. H. (1987) *Cancer Res.* **47**, 3830-3834

128. Pugh, C. S. G., Borchart, R. T., and Stone, H. O. (1977) *Biochemistry* **16**, 3928

129. Duerre, J. A. (1962) *J. Biol. Chem.* **237**, 3737-3741

130. Cornell, K. A., and Riscoe, M. K. (1998) *Biochem. Biophys. Acta* **1396**, 8-14

131. Knappe, J., and Schmitt, T. (1976) *Biochem. Biophys. Res. Commun.* **71**, 1110-1117

132. Lee, J. E., Cornell, K. A., Riscoe, M. K., and Howell, P. L. (2000) *Acta Crystallographica Section D* **57**, 150-152

133. Hadwiger, P., and Stütz, A. E. (1998) *J. Carbohydr. Chem.* **17**, 1259–1267

134. Greene, R. C., Hunter, J. S., and Coch, E. H. (1973) *J. Bacteriol.* **115**, 57-67

135. Markham, G. D., DeParasis, J., and Gatmaitan, J. (1984) *J. Biol. Chem.* **259**, 14505-14507

136. Park, J., Tai, J., Roessner, C. A., and Scott, A. I. (1996) *Bioorg. Med. Chem.* **4**, 2179-2185

137. Saiki, R. K., Scharf, S., Faloona, F., Mullis, K. B., Hom, G. T., Erlich, H. A., and Arnheim, N. (1985) *Science* **230**, 1350-1354

138. Bradford, M. M. (1976) *Anal. Biochem.* **72**, 248-254

139. Sambrook, J., Fritsch, E. F., and Maniatis, T. (1989) *Molecular Cloning: A Laboratory Manual*, 2nd Ed., Cold Spring Harbor Laboratory Press, Cold Spring Harbor, NY

140. Laemmli, U. K. (1970) *Nature* **227**, 680-685

141. Fish, W.W. (1988) *Methods Enzymol.* **158**, 357-364

142. McCormick, D. B., and Roth, J. A. (1970) *Anal. Biochem.* **34**, 226-236

143. Ollagnier-de-Choudens, S., Mulliez, E., Fontecave, M. (2002) *FEBS Lett.* **532**, 465-468

144. Tomczyk, N. H., Nettleship, J. E., Baxter, R. L., Chrichton, H. J., Webster, S.P., Campopiano, D. J. (2002) *FEBS Lett.* **513**, 299-304